



N°d'ordre NNT : 2024ISAL0026

**THESE de DOCTORAT DE L'INSA LYON,
membre de l'Université de Lyon**

**Ecole Doctorale N° ED206
(Ecole Doctorale de Chimie de Lyon)**

Spécialité/ discipline de doctorat : Chimie

Soutenue publiquement le 03/04/2024, par :
Jingjing JIANG

**5-Hydroxymethylfurfural (HMF) in fine
chemistry: multicomponent reactions
towards 1,5-benzodiazepines and 1,4-
dihydropyridines**

**5-Hydroxymethylfurfural (HMF) en
chimie fine: reactions
multicomposantes vers les 1,5-
benzodiazepines et les 1,4-
dihydropyridines**

Devant le jury composé de :

M. BONNEVIOT Laurent, Professeur des Universités, Ecole Normale Supérieure de Lyon
Mme LUBIN-GERMAIN Nadège, Professeure des Universités, CY Cergy Paris Université
Mme DE OLIVEIRA VIGIER Karine, Professeure des Universités, Université de Poitiers
M. XAVIER Nuno Manuel, Assistant Professor, Université de Lisbonne
M. QUENEAU Yves, Directeur de Recherche au CNRS, Université de Lyon
Mme POPOWYCZ Florence, Professeure des Universités, INSA-Lyon

Président
Rapporteure
Rapporteure
Examineur
Directeur de thèse
Co-directrice de thèse

Département FEDORA - INSA Lyon - Ecoles Doctorales

SIGLE	ECOLE DOCTORALE	NOM ET COORDONNEES DU RESPONSABLE
ED 206 CHIMIE	CHIMIE DE LYON https://www.edchimie-lyon.fr Sec. : Renée EL MELHEM Bât. Blaise PASCAL, 3e étage secretariat@edchimie-lyon.fr	M. Stéphane DANIELE C2P2-CPE LYON-UMR 5265 Bâtiment F308, BP 2077 43 Boulevard du 11 novembre 1918 69616 Villeurbanne directeur@edchimie-lyon.fr
ED 341 E2M2	ÉVOLUTION, ÉCOSYSTÈME, MICROBIOLOGIE, MODÉLISATION http://e2m2.universite-lyon.fr Sec. : Bénédicte LANZA Bât. Atrium, UCB Lyon 1 Tél : 04.72.44.83.62 secretariat.e2m2@univ-lyon1.fr	Mme Sandrine CHARLES Université Claude Bernard Lyon 1 UFR Biosciences Bâtiment Mendel 43, boulevard du 11 Novembre 1918 69622 Villeurbanne CEDEX e2m2.codir@listes.univ-lyon1.fr
ED 205 EDISS	INTERDISCIPLINAIRE SCIENCES-SANTÉ http://ediss.universite-lyon.fr Sec. : Bénédicte LANZA Bât. Atrium, UCB Lyon 1 Tél : 04.72.44.83.62 secretariat.ediss@univ-lyon1.fr	Mme Sylvie RICARD-BLUM Laboratoire ICBMS - UMR 5246 CNRS - Université Lyon 1 Bâtiment Raulin - 2ème étage Nord 43 Boulevard du 11 novembre 1918 69622 Villeurbanne Cedex Tél : +33(0)4 72 44 82 32 sylvie.ricard-blum@univ-lyon1.fr
ED 34 EDML	MATÉRIAUX DE LYON http://ed34.universite-lyon.fr Sec. : Yann DE ORDENANA Tél : 04.72.18.62.44 yann.de-ordenana@ec-lyon.fr	M. Stéphane BENAYOUN Ecole Centrale de Lyon Laboratoire LTDS 36 avenue Guy de Collongue 69134 Ecully CEDEX Tél : 04.72.18.64.37 stephane.benayoun@ec-lyon.fr
ED 160 EEA	ÉLECTRONIQUE, ÉLECTROTECHNIQUE, AUTOMATIQUE https://edeea.universite-lyon.fr Sec. : Philomène TRE COURT Bâtiment Direction INSA Lyon Tél : 04.72.43.71.70 secretariat.edeea@insa-lyon.fr	M. Philippe DELACHARTRE INSA LYON Laboratoire CREATIS Bâtiment Blaise Pascal, 7 avenue Jean Capelle 69621 Villeurbanne CEDEX Tél : 04.72.43.88.63 philippe.delachartre@insa-lyon.fr
ED 512 INFOMATHS	INFORMATIQUE ET MATHÉMATIQUES http://edinfomaths.universite-lyon.fr Sec. : Renée EL MELHEM Bât. Blaise PASCAL, 3e étage Tél : 04.72.43.80.46 infomaths@univ-lyon1.fr	M. Hamama che KHEDDOUCI Université Claude Bernard Lyon 1 Bât. Nautibus 43, Boulevard du 11 novembre 1918 69 622 Villeurbanne Cedex France Tél : 04.72.44.83.69 direction.infomaths@listes.univ-lyon1.fr
ED 162 MEGA	MÉCANIQUE, ÉNERGÉTIQUE, GÉNIE CIVIL, ACOUSTIQUE http://edmega.universite-lyon.fr Sec. : Philomène TRE COURT Tél : 04.72.43.71.70 Bâtiment Direction INSA Lyon mega@insa-lyon.fr	M. Etienne PARIZET INSA Lyon Laboratoire LVA Bâtiment St. Exupéry 25 bis av. Jean Capelle 69621 Villeurbanne CEDEX etienne.parizet@insa-lyon.fr
ED 483 ScSo	ScSo¹ https://edsciencesociales.universite-lyon.fr Sec. : Mélina FAVETON Tél : 04.78.69.77.79 melina.faveton@univ-lyon2.fr	M. Bruno MILLY (INSA : J.Y. TOUSSAINT) Univ. Lyon 2 Campus Berges du Rhône 18, quai Claude Bernard 69365 LYON CEDEX 07 Bureau BEL 319 bruno.milly@univ-lyon2.fr

¹ ScSo : Histoire, Géographie, Aménagement, Urbanisme, Archéologie, Science politique, Sociologie, Anthropologie

Acknowledgement

Studying in a foreign country during a special period is a journey full of challenges, growth, and many valuable gains. On this journey, first and foremost, I would like to express my deepest gratitude to my supervisors, Dr. Yves Queneau and Prof. Florence Popowycz. My fate with COB Laboratory began in 2019. The choices of Yves Queneau and Florence Popowycz laid the foundation for my CSC application. In the past three years, their patient guidance, rigorous attitude, and professional knowledge played an important role in my entire research process, which enabled me to improve my thinking habits, paper writing skills and academic communication.

I would like to thank the faculty and staff of the Université de Lyon, INSA-Lyon, and Université Claude Bernard Lyon1 for providing convenience for my registration and study during my PhD period. Thanks to my colleagues, Mrs. Alexia Moulin, Mrs. Malvina Larduinat, Mrs. Sonia Mion, Mrs. Lucie Grand, Dr. Sylvie Moebs, Dr. Maïwenn Jacolot, Dr. Mohammed Ahmar, Dr. Stéphane Chambert, Dr. Laurent Soulère, Dr. Pauline Pacquet, Dr. Eman Dokmak, Dr. Xiaoyang Yue, Dr. Weigang Fan, Dr. Lianjie Wang, Dr. Qiang Zhang, Dr. Thibaut Barbier, Dr. Jordan Francois and ICBMS researchers who provided indispensable help throughout my PhD and the completion of this thesis.

Special thanks to Prof. Catherine Pinel (IRCELYON) and Prof. Bruno Andrioletti (Université Claude Bernard Lyon1) for being members of my annual "comité de suivi de thèse". Their feedback and guidance have provided great help in improving my research content. I would also like to express my gratitude to my jury members: Prof. Nadège Lubin-Germain (Université de Cergy-Pontoise), Prof Karine De Oliveira Vigier (Université de Poitiers), Prof. Laurent Bonneviot (Ecole Normale Supérieure de Lyon), Assistant Prof. Nuno Manuel Xavier (University of Lisbon) who agreed to serve as reviewers and defense committee members.

I am grateful to my family especially Mr. Guozheng Li for giving me full encouragement and trust, to China Scholarship Council (CSC) for providing me with financial support to study in France, and to the development of my motherland for giving me the confidence to move forward to see and embrace a broader world.

Finally, I would like to express my gratitude to all those whose names are not mentioned here, but whose contributions have left an indelible mark on my PhD period.

List of Abbreviations

BZD	Benzodiazepine
CMF	5-Chloromethylfurfural
DABCO	1,4-Diazabicyclo[2.2.2]octane
DAMF	2,5-Diaminomethylfuran
DCM	Dichloromethane
DFF	2,5-Diformylfuran
DHMF	2,5-Dihydroxymethylfurfural
DHMTFH	Tetrahydrofuran-2,5-dimethanol
DHP	Dihydropyridine
DMTHF	2,5-Dimethyltetrahydrofuran
DMSO	Dimethyl sulfoxide
DMF	2,5-Dimethylfuran
EMF	Ethoxymethylfuran
FDCA	2,5-Furandicarboxylic acid
FFCA	5-Formyl-2-furancarboxylic acid
GABA	γ -Aminobutyric acid
GVL	γ -Valerolactone
HCPN	3-(Hydroxymethyl)cyclopentanone
HHD	1-Hydroxyhexane-2,5-dione
HMFA	5-Hydroxymethyl-2-furanoic acid
5-HMF (HMF)	5-Hydroxymethylfurfural
5-HMTFFF	5-Hydroxymethyltetrahydro-2-furaldehyde
LA	Levulinic acid
MCR	Multi-component reaction
MCP	2-Hydroxy-3-methylcyclopent-2-enone
2-MeTHF	2-Methyl tetrahydrofuran
MIBK	Methyl isobutyl ketone

MTHFA	(5-Methyltetrahydrofuran-2-yl)methanol
OBMF	5,5'-Oxy(bis-methylene)-2-furfural
PTSA	<i>p</i> -Toluenesulfonic acid
S-F	Solvent-free
THF	Tetrahydrofuran
TLC	Thin-Layer Chromatography
TfOH	Trifluoromethanesulfonic acid
TsOH	4-Methylbenzenesulfonic acid

Abstract & Résumé

Contents

General Introduction

Abstract

Green chemistry practices are the pathway toward more sustainable and safer chemical processes and products. As the consumption of fossil resources and their impact on the environment are gradually being taken seriously, renewable biomass resources, which are the most abundant renewable carbon resource in nature, has attracted extensive attention from academia and industry. Complex biomass can be simplified through biorefinery, selectively retaining existing chemical functions that can be used for synthetic purposes and producing abundant bio-based platform molecules.

Today, research on converting biomass resources into biofuels, polymers and solvents has made certain progress through the bio-based platform molecules, whereas their application to the design of more complex fine chemicals remains limited. Carbohydrate-based furanic platform molecules offer original building blocks for the design of novel chemical architectures. Among them, 5-hydroxymethylfurfural (5-HMF) has attracted our attention due to its rich chemical reactivity and easy availability from sugars.

In this thesis, I focused on exploiting the aldehydic group of bio-based furanic platform molecules, especially 5-HMF, in the construction of nitrogen-containing heterocycles 1,5-benzodiazepines and 1,4-dihydropyridines which include the furyl building block arising from HMF as a substituent. The strategy relies on the use of multi-component reactions which exhibit advantageous atom economy. A critical issue is to find the appropriate conditions which are compatible with 5-HMF specific reactivity and known sensitivity to harsh conditions.

Within my project dedicated to new strategies able to build complex structures in very short sequences from 5-HMF, a first part has been the application of a multicomponent [4+2+1] cycloaddition reaction approach towards cyclic 1,5-benzodiazepines. 1,5-Benzodiazepines are an important branch of benzodiazepines which exhibit anti-inflammatory, anti-convulsive, anti-anxiety, and anti-depressant effects, especially in the treatment of mental illness. The

[4+2+1] cycloaddition reaction combined 5-HMF (or derivatives) with *o*-phenylenediamines and alkynones under novel reaction conditions, leading to the targeted 1,5-benzodiazepines under the promotion of ammonium acetate. Its application to a wide scope of substrates led to a library of variously substituted benzodiazepines that are now available to be included in the ICBMS chemical library for further biological and biochemical assays.

The second part of this thesis has concerned the use of 5-HMF in the Hantzsch dihydropyridine reaction, an important multi-component reaction involving aldehydes, ammonia and β -dicarbonyls with high atom economy, and only H₂O as by-product. The 1,4-dihydropyridine skeleton is also an important nitrogen-containing heterocyclic scaffold, widely found in hypertensive, cardiovascular and cerebrovascular drugs. The use of 5-HMF in the Hantzsch dihydropyridine synthesis has been studied using NH₄OAc as both the nitrogen source and a mild promoter. First, symmetrical 1,4-dihydropyridines were prepared by reaction of 5-HMF with two molecules of β -dicarbonyls and ammonium acetate under solvent-free conditions in excellent yields in the absence of any additional catalyst. The reaction scope was extended to a variety of β -ketoesters and β -diketones. In a second stage, we addressed the possibility to selectively reach unsymmetrical 1,4-dihydropyridines by replacing one of the two molecules of starting β -ketoester by 5,5-dimethyl-1,3-cyclohexanedione. This four-component reaction (4CR) protocol proceeded nicely in ethanol or neat conditions.

Overall, by applying this reaction to diverse substrates, a series of novel symmetrical and unsymmetrical 1,4-dihydropyridines bearing a furyl moiety as substituent was prepared. The new compounds will be involved in biological assays in the frame of the projects developed by the ICBMS chemical library.

Key words: biomass, 5-hydroxymethylfurfural (5-HMF), multi-component reaction (MCR), nitrogen-containing heterocycle, ammonium acetate, [4+2+1] cycloaddition, 1,5-benzodiazepines, Hantzsch dihydropyridine reaction.

Résumé

La pratique de la chimie verte est la voie vers des processus et des produits chimiques plus durables et plus sûrs. Alors que la consommation des ressources fossiles et leur impact sur l'environnement retiennent de plus en plus l'attention, l'utilisation de la biomasse, en tant que ressources de carbone renouvelables abondantes dans la nature, attire une grande attention de la part des cercles universitaires et industriels partout dans le monde. La biomasse complexe peut être transformée en molécules plateformes à grande échelle grâce à la bioraffinerie. Ces molécules plus simples conservent de manière sélective certaines fonctionnalités chimiques qui peuvent être exploitées pour construire ensuite des molécules biosourcées plus complexes.

Aujourd'hui, grâce au développement des molécules plateformes biosourcées, des progrès ont été réalisés dans la conversion des ressources de la biomasse dans les domaines des biocarburants, des polymères et des solvants, mais leur application dans la conception des produits plus complexes de la chimie fine reste limitée. Les molécules plateformes furaniques issus des glucides peuvent être intégrées dans la conception de nouvelles structures chimiques, conduisant ainsi à de nouvelles molécules aux propriétés originales. Parmi les molécules de la plateforme furannique renouvelable biosourcée, le 5-HMF (5-hydroxyméthylfurfural) a retenu notre attention en raison de sa riche réactivité chimique et de son accès facile à partir de sucres.

Dans cette thèse, je me suis concentrée sur l'utilisation de molécules furaniques issues de la biomasse, en particulier le 5-HMF, comme molécule plateforme pour construire des hétérocycles azotés comme les 1,5-benzodiazépines et les 1,4-dihydropyridines, par le biais de réactions à plusieurs composants qui présentent une économie d'atome avantageuse. Un problème clé est de trouver des conditions appropriées qui correspondent à la réactivité spécifique du 5-HMF et à sa sensibilité connue aux conditions difficiles.

Dans ce projet dédié à la recherche de nouvelles stratégies capables de construire des structures complexes en séquences très courtes à partir du 5-HMF, une première approche a été l'application d'une cycloaddition multicomposante [4+2+1] dans la construction des 1,5-benzodiazépines cycliques. Les 1,5-benzodiazépines sont une branche importante des benzodiazépines qui ont des effets anti-inflammatoires, anticonvulsifs, anti-anxiogènes et antidépresseurs, notamment dans le traitement des maladies mentales. Utilisant de nouvelles conditions réactionnelles, cette réaction économe en atome combine le 5-HMF (ou ses dérivés) avec des *o*-phénylènediamines et des alcynones en présence d'acétate d'ammonium. L'application de ce protocole à un large éventail de substrats a conduit à une bibliothèque de benzodiazépines diversement substituées qui sont désormais disponibles pour être intégrées dans la chimiothèque de l'ICBMS pour de futures évaluations biologiques et biochimiques.

La deuxième partie de cette thèse a concerné l'utilisation du 5-HMF dans la synthèse de dihydropyridine de Hantzsch, une importante réaction à plusieurs composants impliquant des aldéhydes, de l'ammoniac et des β -cétoesters, remarquable pour son économie d'atome, et ne consommant que de l'eau comme sous-produit. Le squelette 1,4-dihydropyridine est également un important échafaudage hétérocyclique contenant de l'azote, largement présent dans les médicaments contre l'hypertension et utilisés dans les traitements des maladies cardiovasculaires et cérébrovasculaires. Nous avons étudié l'utilisation du 5-HMF dans la synthèse des dihydropyridines de Hantzsch en utilisant NH_4OAc à la fois comme source d'azote et comme promoteur doux. Tout d'abord, des 1,4-dihydropyridines symétriques ont été préparées par réaction de 5-HMF, de deux molécules de β -cétoesters et d'acétate d'ammonium dans des conditions sans solvant avec d'excellents rendements en l'absence de tout catalyseur supplémentaire. Le champ de la réaction a été étendu à une variété de β -cétoesters et de β -dicétones. Par la suite, nous avons étudié une version à quatre composants visant la formation sélective d'1,4-dihydropyridines dissymétriques, en remplaçant les 2 équivalents de β -cétoester par 1 équivalent de β -cétoester et un équivalent de 5,5-diméthyl-1,3-cyclohexanedione. Ce processus à quatre composants (4CR) s'est révélé efficace soit sans solvant soit dans l'éthanol. Ainsi, l'application de cette réaction à divers substrats a conduit à

une série de nouvelles 1,4-dihydropyridines symétriques ou dissymétriques comportant une entité furyl comme substituant qui seront intégrées dans des évaluations biologiques et biochimiques dans le cadre des projets développés par la chimiothèque de l'ICBMS.

Mots clés : biomasse, (5-hydroxyméthylfurfural) 5-HMF, réaction multi-composants (MCR), hétérocycle azoté, acétate d'ammonium, cycloaddition [4+2+1], 1,5-benzodiazepines réaction de Hantzsch dihydropyridine.

Contents

Acknowledgement	- 1 -
List of Abbreviations	- 3 -
Abstract	- 7 -
Résumé	- 9 -
Contents	- 13 -
General Introduction	- 17 -
Chapter I Bibliography	- 21 -
1.1 Biobased chemistry in the context of green chemistry	- 21 -
1.2 General aspects of C ₂ -C ₆ bio-based platforms	- 24 -
1.2.1 Strategies of biomass conversion	- 26 -
1.2.2 Bioethanol	- 28 -
1.2.3 Bio-based acids	- 29 -
1.2.3.1 Lactic acid and 3-hydroxypropionic acid	- 29 -
1.2.3.2 Succinic acid	- 32 -
1.2.3.3 Levulinic acid	- 33 -
1.2.4 Bio-based aldehydes	- 37 -
1.3 A focus on 5-hydroxymethylfurfural (5-HMF)	- 41 -
1.3.1 Introduction	- 41 -
1.3.1.1 Market and industrial production of 5-HMF	- 42 -
1.3.1.2 Reported pathways towards 5-HMF	- 42 -
1.3.1.3 Stability of 5-HMF	- 44 -
1.3.2 Main reactions of 5-HMF	- 47 -
1.3.2.1 Reactions involving the CH ₂ OH group	- 48 -
1.3.2.2 Reactions involving the furan ring	- 52 -
1.3.2.3 Reactions involving the aldehyde functional group	- 57 -
1.3.3 Focus on multi-component reactions involving 5-HMF	- 63 -
1.3.3.1 State of the art on MCRs	- 63 -
1.3.3.2 MCRs involving 5-HMF	- 64 -
1.4 Conclusion and objectives of the thesis	- 69 -

Chapter II. The [4+2+1] cycloaddition involving 5-HMF towards 1,5-benzodiazepines ...	- 73 -
2.1 Introduction	- 73 -
2.1.1. Interest of benzodiazepines	- 74 -
2.1.2 Synthetic routes towards 1,5-benzodiazepines	- 76 -
2.1.2.1 Strategies and mechanism	- 76 -
2.1.2.2 Reaction conditions	- 80 -
2.1.2.3 Directions for our investigation	- 81 -
2.2 Synthesis of 5-HMF derived 1,5-benzodiazepines	- 82 -
2.2.1 Identification of target products and by-products	- 82 -
2.2.2 Influence of reaction conditions	- 88 -
2.2.2.1 Influence of the catalysts	- 88 -
2.2.2.2 Other reaction parameters	- 92 -
2.2.3 Structural scope of substrates	- 95 -
2.2.3.1 Scope of diamines	- 95 -
2.2.3.2 Scope of alkynones and alkyl alkynoates	- 96 -
2.2.3.3 Scope of HMF derived substrates	- 99 -
2.2.4 Mechanistic study	- 101 -
2.3 Conclusion	- 106 -
Chapter III. The Hantzsch dihydropyridine synthesis involving 5-HMF	- 109 -
3.1 Background	- 109 -
3.1.1 Introduction	- 109 -
3.1.2 The Hantzsch reaction	- 110 -
3.1.2.1 Mechanism of the Hantzsch reaction	- 110 -
3.1.2.2 Catalysts in Hantzsch reaction	- 112 -
3.1.2.3 Hantzsch-like reactions	- 114 -
3.1.3. Plan of our study	- 115 -
3.2 Synthesis of 5-HMF derived 1,4-dihydropyridines	- 116 -
3.2.1 Three-component approach towards symmetrical 1,4-dihydropyridines	- 118 -
3.2.1.1 Identification of target product and analytical protocols	- 118 -
3.2.1.2 Influence of reaction parameters	- 121 -
3.2.1.3 Structural scope	- 127 -

3.2.2 Four-component approach towards unsymmetrical 1,4-dihydropyridines	130 -
3.2.2.1 Identification of products	131 -
3.2.2.2 Optimization of the reaction conditions	132 -
3.2.2.3 Structural scope	134 -
3.2.3 Mechanistic considerations	135 -
3.2.3.1. Three-component reaction	135 -
3.2.3.2. Four-component reaction	138 -
3.3 Conclusion	139 -
General conclusions and perspectives	143 -
Experimental section	149 -
References	245 -

General Introduction

The contemporary field of chemical science is undergoing a transformative shift towards sustainability and environmental awareness, giving rise to the concept of green chemistry. Green Chemistry is dedicated to the design, development and implementation of sustainable chemical processes that minimize environmental impact, reduce waste and utilize renewable resources. Exploring biomass as a viable and renewable alternative to traditional petrochemical feedstocks is at the heart of this revolution.

Biomass is a sustainable resource consisting of organic material derived from plants, wood and agricultural residues. In contrast to the finite nature of fossil fuels, biomass represents an extensive and replenishable reservoir of carbon. Traditional petrochemistry relies on the extraction and processing of fossil fuels to produce a variety of chemicals and has been the cornerstone of the chemical industry. In contrast, biobased platform molecules derived from renewable biomass sources embody the potential for sustainable development as building blocks for the synthesis of a wide range of chemicals, materials, and fuels. This shift towards bio-based alternatives from petrochemicals contributes to a more sustainable and circular economy.

Platform molecules are a particular type of biobased intermediates which possess one or more reactive centers and are readily produced from raw biomass. A major example is 5-HMF, produced from extremely available C₆ carbohydrates. Platform molecules play an important role in the development of biobased chemistry, attracting interest either on the way they are synthesized and manufactured, or on the way they are used for the synthesis of more complex derivatives. In this respect, a powerful strategy aligning with the atom-economic principle of green chemistry is the utilization of multicomponent reactions (MCRs). MCRs represents an efficient class of synthetic methods that brings together multiple reactants/reagents in a single reaction vessel, a strategy that simplifies the synthetic route, minimizes the need for intermediate steps, and increases overall synthetic efficiency.

This thesis aims to address how these two important aspects of green chemistry, namely the use of biobased platform molecules, and the development of atom-economical processes, can be combined together by exploring multicomponent reactions involving the 5-HMF platform. The targets have been chosen among, nitrogen-containing heterocycles, which play a key role in pharmaceuticals, agrochemicals and materials science and, like all chemicals, require green and sustainable synthetic methods. In particular, the work has focused on the access to novel 1,5-benzodiazepines and 1,4-dihydropyridines, as developed in the following chapters after a bibliographic introduction.

Chapter I

Bibliography

Chapter I Bibliography

1.1 Biobased chemistry in the context of green chemistry

The 20th century saw the rise and establishment of the petroleum industry, providing a low-cost and continuous supply of hydrocarbons for chemical manufacturing, allowing the preparation of high added-value molecules ranging from fuels, functional materials to pharmaceuticals. However, with the development of industry, the irreversible impact of industrial processes on the environment and the energy crisis caused by the rapid consumption of petroleum resources have become issues of global concern. In general perception, the chemical industry is often associated with high energy consumption, pollution, and environmentally harmful evaluations. The desire of the modern chemical industry to provide useful compounds and materials through methods that are not harmful to the environment has led to the establishment and development of a discipline known as "sustainable chemistry" or "green chemistry" in order to effectively bridge this gap.¹

With green chemistry beginning as a specialized field of research in the early 1990s, the establishment of green chemistry research centers has increased exponentially, and governments have also provided substantial funding for the establishment of the discipline. Green chemistry is defined by the Environmental Protection Agency as “the design of chemical products that reduce or eliminate the use of hazardous substances”. The Twelve Principles of Green Chemistry were first introduced in 1998 by Paul Anastas and John Warner in their book titled "Green Chemistry: Theory and Practice".² From these 12 principles shown in Figure 1, we see that the issue of the resource is an important one, preferring renewable than fossil resources, requiring efficiency in their use and limiting the wastes, avoiding the use of toxic and/or hazardous solvents and reagents.

12

Principles of Green Chemistry

Waste prevention	Atom economy	Less hazardous chemical synthesis	Designing safer products
Safe solvents and auxiliaries	Design for energy efficiency	Use of renewable feedstocks	Reduce derivatives
Catalysis	Design for degradation	Real-time analysis for pollution prevention	Inherently safer processes

Figure 1. Twelve principles of green chemistry

It is important to note that the principles cover the complete cycle, from the cradle to the grave, meaning from the feedstocks themselves and their extraction from biomass, to all steps of their transformation which must be efficient and safe, and to synthesized products which must be non-toxic and biodegradable. This philosophy will help chemists to achieving both innovation in molecular design and sustainable goals.

Developing efficient and economically viable methods for the large-scale conversion of low value biomass into industrially relevant chemicals with low environmental impact is an important research challenge and chance for green chemistry. A review of advances in green and sustainable biomass chemical manufacturing was reported in 2014 by Roger A. Sheldon,³ a recognized authority in the field of green chemistry, presenting the valuable applications and huge potential for converting renewable biomass into already commercially available chemicals or new innovative chemicals with industrial prospect. Typical biomass resources are shown in Figure 2.

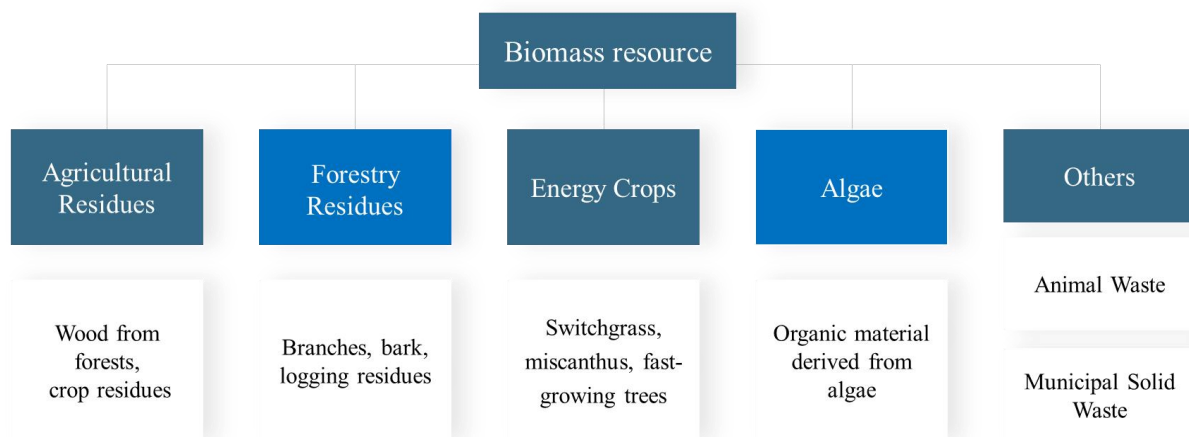


Figure 2. Main types of biomass resources

Biomass and petroleum are two distinct feedstocks used in various industrial processes. They differ significantly in terms of origin, composition, environmental impact and sustainability. In contrast to the low reactivity, hydrophobicity, high volatility and moderate to high thermal stability of petroleum feedstocks, biomass-derived platform molecules generally exhibit high reactivity, variable polarity (high for carbohydrate-derived compounds, low for fats and oils) thus variable solubility in polar or non polar solvents, low volatility and low thermal stability (Figure 3). Therefore, existing petrochemical technologies cannot be directly used to process biomass-derived compounds. The developed technologies for transformation of biomass-derived platform molecules have now been reported in some reviews, such as catalytic aqueous-phase processing from high added-value chemicals to fuels.⁴



 <div>Biomass feeds</div>	 <div>Petroleum feeds</div>
<ul style="list-style-type: none"> • Renewable resource • High oxygen content • Lower carbon footprint, carbon-neutral • High reactivity • Variable polarity • Low volatility • Low thermal stability 	<ul style="list-style-type: none"> • Non-renewable resource • Primarily hydrocarbons • Releases greenhouse gases • Low reactivity • Hydrophobic • High volatility • Moderate to high thermal stability

Figure 3. Comparison of biomass feeds and petroleum feeds

In terms of chemical conversion, petroleum feedstocks and biomass feedstocks currently have their own advantages. On the one hand, the low oxygen content and low degree of functionalization of petroleum feedstocks favor the preparation of hydrocarbon compounds and liquid hydrocarbon fuels. The vast petrochemical industry is essentially a chemical industry based on a small number of molecules (benzene, toluene, xylene, ethylene, propylene, butadiene) as the main raw materials. These molecules form the cornerstones of the production of a variety of chemicals and specialty products.⁴ In contrast, most biomass-derived platform molecules have high oxygen content that can undergo more complex reactions such as dehydration, decarboxylation, and C-O hydrogenolysis to reduce oxygen content. However, in another important aspect, more functionalized substrates derived from biomass offer easier routes to prepare a more diverse range of chemicals.⁵

Biomass is currently the only foreseeable sustainable source of chemicals and organic fuels. Biomass feedstocks for energy production can generally be divided into four categories: i) lignocellulosic biomass; ii) starch-rich crops; iii) sucrose-rich crops, and iv) oil crops. Since edible biomass feedstocks (such as starch, sugar and vegetable oil) compete with food for land, the development of biomass resources is obviously inclined towards more abundant non-edible biomass (represented by lignocellulosic biomass), to achieve more sustainable development of valuable chemicals.^{6,7}

1.2 General aspects of C₂-C₆ bio-based platforms

The U.S. Department of Energy (DOE) published in 2014 a list of highly efficient biobased platform molecules that can be converted into high-value chemicals.⁸ These platform molecules involved are mainly acids such as levulinic acid, succinic acid, aspartic acid, fumaric acid, glutamic acid, itaconic acid, 2,5-furandicarboxylic acid, or alcohols (or hydroxyacids) such as 3-hydroxypropionic acid, malic acid, glucaric acid, 3-hydroxybutyrolactone, glycerol, sorbitol, arabinitol and xylitol. In 2010, Bozell and Petersen updated the original list,⁹ with the addition of bioethanol, lactic acid and two important

furanic molecules, furfural and 5-HMF. Several molecules in the original list were retained in the updated list, as shown in Table 1. The new list included the most promising platform molecules from C₂ to C₆, most of them arising from carbohydrates with the exception of glycerol, which is a by-product of the fats and oil hydrolysis process. Among them, bio-hydrocarbons refer to hydrocarbon compounds derived from renewable biomass sources such as bio-based olefins produced by dehydration of alcohols or decarboxylation of fatty acids. These two lists have inspired research on bio-based platform molecules in multiple fields. Figure 4 shows explicitly the structures of all these platform molecules.

Table 1. Promising bio-based platform molecules

Bio-based platform molecules published by DOE in 2004	
3-Hydroxypropionic acid	Itaconic acid
Aspartic acid	2,5-Furandicarboxylic acid
Succinic, Fumaric, Malic acid	3-Hydroxybutyrolactone
Glycerol	Glucaric acid
Glutamic acid	Sorbitol
Levulinic acid	Xylitol and arabinitol
Bio-based platform molecules revisited by Bozell and Petersen in 2010 (Chemicals updated are shown in bold)	
Ethanol	Bio-hydrocarbons
Lactic acid	Furfural
5-Hydroxymethyl furfural	3-Hydroxypropanoic acid
Glycerol	2,5-Furandicarboxylic acid
Succinic acid	Levulinic acid
Sorbitol	Xylitol

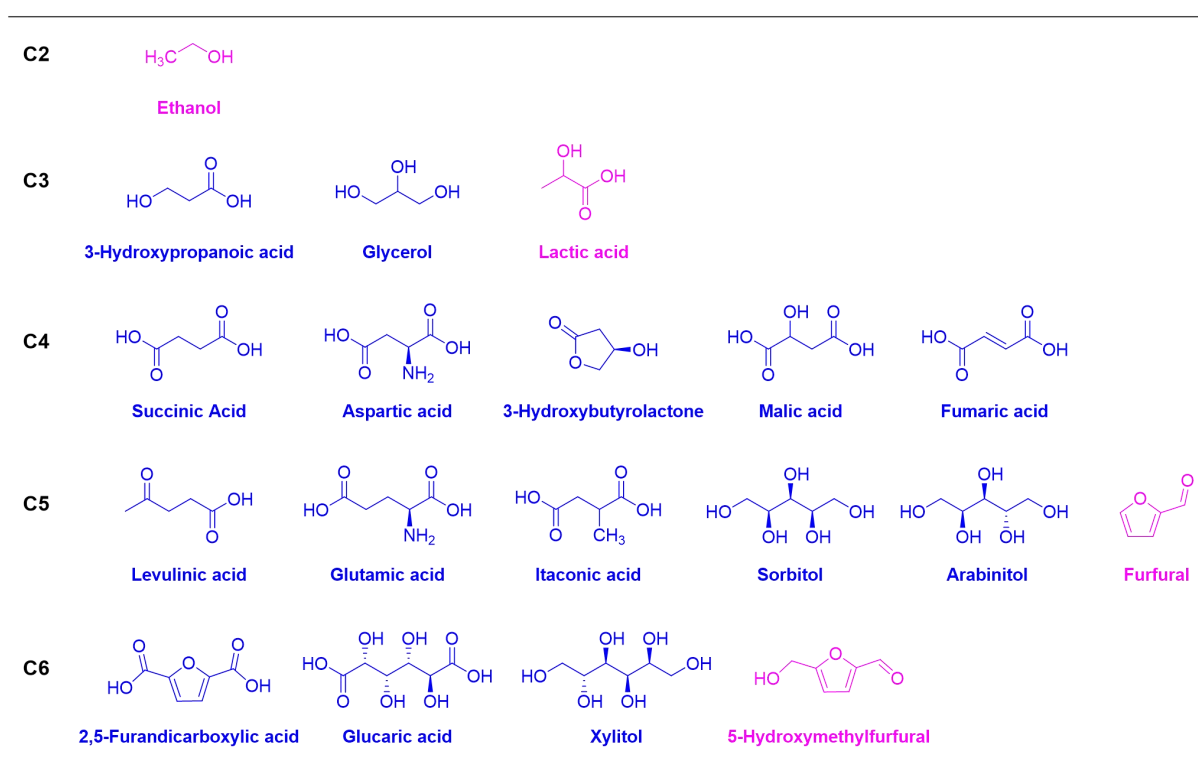


Figure 4. C₂-C₆ biobased platform molecules (in blue the 2004 compounds, in pink, those added in 2010)

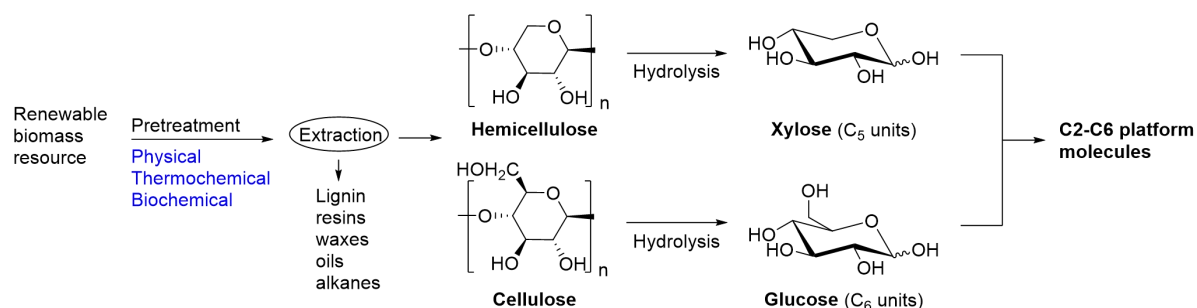
1.2.1 Strategies of biomass conversion

Lignocellulose is the most abundant cellulosic biomass produced annually in the world. Cellulose and hemicellulose are the main components of lignocellulose (accounting for about 75%) and are also the most abundant forms of carbohydrates. In recent years, research groups in multiple fields have focused their attention on the development of more efficient and environmentally friendly methods for synthesizing valuable chemicals from biomass feedstocks, especially lignocellulose.^{10, 11}

An important part of the current research on cellulose is aimed at deconstructing the biopolymer to produce fermentable sugars. Due to the high structural complexity of biomass, its conversion often involves a combination of multiple catalytic processes. Biomass conversion pretreatment can be broadly categorized into several main types: i) physical pretreatment, involving mechanical action or physical processes to change the structure of

biomass, such as reducing size, helping to increase the surface area of biomass particles; ii) thermochemical, primarily utilizing heat and pressure to break down biomass components; iii) biochemical, commonly including acid hydrolysis, alkaline hydrolysis, organic solvent pretreatment to destroy the structure of biomass materials, uses microorganisms such as fungi, bacteria or enzymes to degrade lignin, cellulose and hemicellulose. These pretreatment methods can be used sequentially or in combination, depending on various factors such as biomass feedstock type, desired products, treatment costs and more.¹²⁻¹⁴

Overall, biomass undergoes pretreatment processes such as distillation or liquid-liquid extraction techniques to remove other components such as lignin and increase the accessibility of cellulose and hemicelluloses. Acid-catalyzed hydrolysis or enzymatic hydrolysis is used to break down the polysaccharides (hemicellulose and cellulose) in biomass into monomeric sugars, typically xylose and glucose. Finally, C₅ and C₆ sugars are converted into C₂-C₆ bio-platform chemicals and biofuels through microbial fermentation or chemical conversion (Scheme 1).^{3, 15}



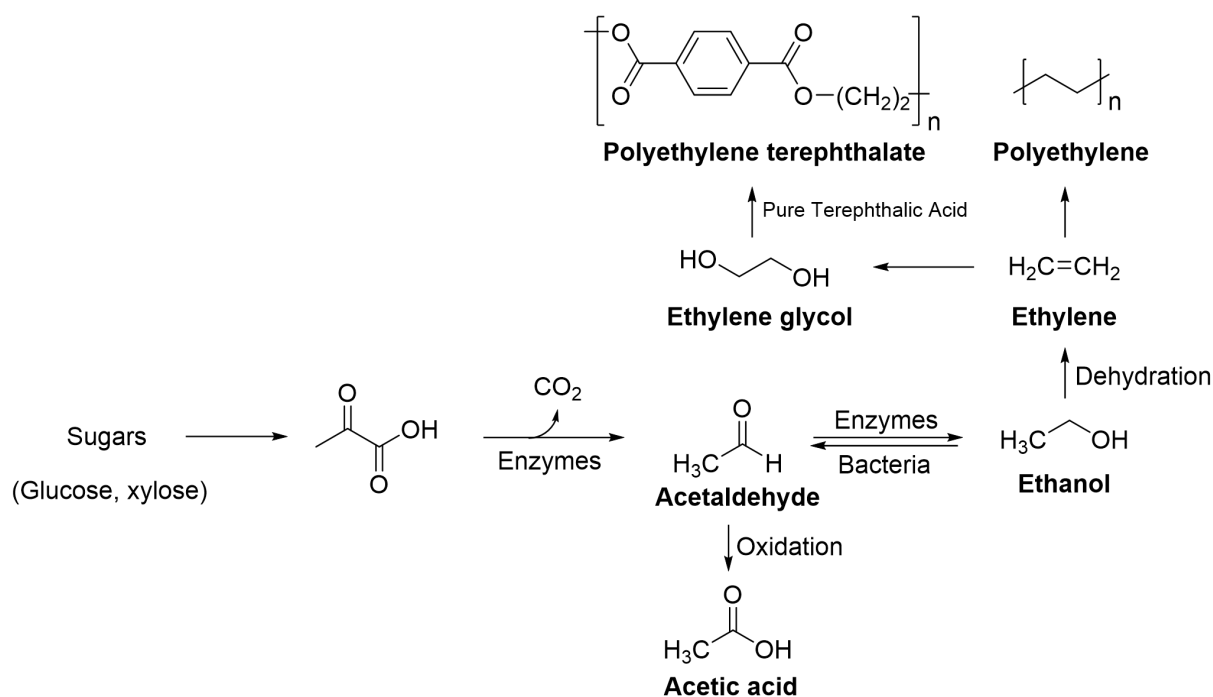
Scheme 1. Conversion steps from biomass to C₂-C₆ platform molecules

Biomass-derived products presently include mainly biofuels, bio-based platform molecules and bio-based materials. A representative biofuel is bioethanol produced through the fermentation of sugars. Bio-based platform molecules mainly include alcohols, aldehydes, organic acids and heterocycles. Bio-based materials include polymers, solvents, textiles, composites and other valuable chemicals derived from bio-based platform molecules.¹⁵⁻¹⁸ This chapter cannot comprehensively cover the rapidly developing biomass platform products at

both academic and industrial scales. In this chapter, we will only briefly introduce several representative C₂-C₅ bio-based platform molecules, namely ethanol, lactic acid and 3-hydroxypropionic acid, succinic acid, levulinic acid, furfural, and finally conduct an overview of the C₆ platform molecule 5-hydroxymethylfurfural.

1.2.2 Bioethanol

Bioethanol is C₂ bio-based platform molecule produced through the fermentation of sugars (such as glucose and xylose) derived from biomass. It can be used as a transportation fuel or as an additive to conventional gasoline, making it a renewable alternative to fossil fuels.^{19, 20} Bioethanol can also be used in various industrial processes, such as solvent extraction and as a precursor in the production of chemicals. Ethylene, and ethylene glycol derived from it, are not only widely used in petrochemical industry production (of propylene, benzene, toluene), but can also be used as structure unit compound for the production of polyethylene and polyethylene terephthalate. In addition, fermentation of sugar into ethanol and then microbial oxidation into acetic acid has become the main method of producing acetic acid since the end of the 19th century (Scheme 2).^{21, 22}



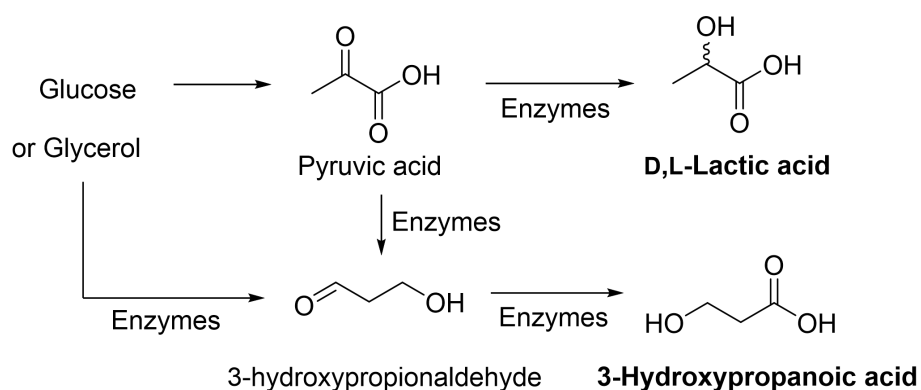
Scheme 2. Representative pathways for the production of bioethanol and derivatives

Ethanol is separated from water and other components by distilling the ethanol-rich fermentation broth. To circumvent the existing debate about edible feedstocks and bioethanol, non-food feedstocks (e.g., corn stover, wheat straw, switchgrass, miscanthus) and other lignocellulosic biomass are being explored to address issues related to conventional bioethanol production.

1.2.3 Bio-based acids

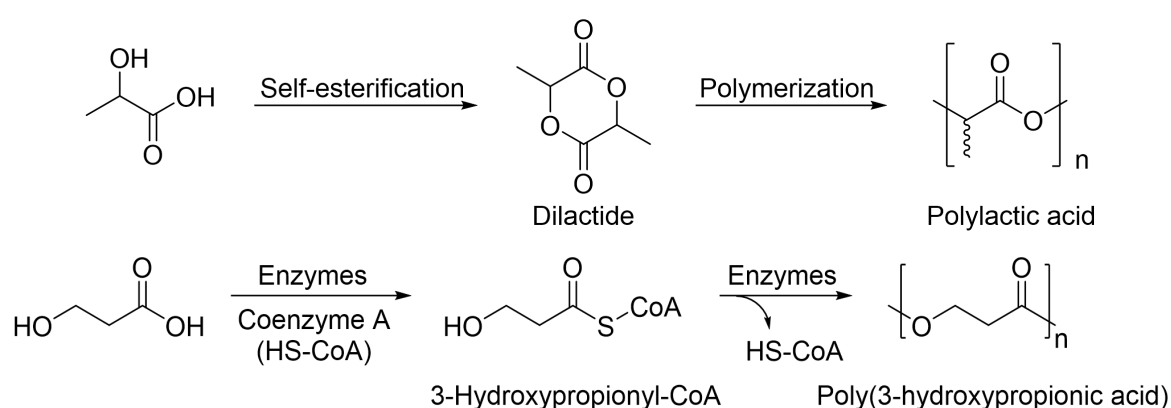
1.2.3.1 Lactic acid and 3-hydroxypropionic acid

Lactic acid and 3-hydroxypropionic acid are both C₃ platform molecules containing one hydroxyl group and one carboxyl group. Lactic acid is a naturally occurring organic acid that can exist as two optical isomers: L-lactic acid and D-lactic acid. Lactic acid is produced by the fermentation of sugar (usually glucose or lactose) by lactic acid bacteria, which are microorganisms in nature.^{23, 24} Currently, about 90% of global lactic acid production relies on the fermentation process. The central intermediate produced by glucose metabolism, pyruvic acid, is a key precursor to the production of lactic acid, although there is still a small amount of lactic acid produced through chemical synthesis using acrylonitrile, acetaldehyde and propylene from petrochemical sources as starting material. In recent years, integrated biorefinery approaches have been explored, where lactic acid is produced alongside other valuable products, creating a more sustainable and economically viable process. 3-Hydroxypropionic acid, an isomer of lactic acid with the hydroxyl at C₃ arises mainly from the enzymatic transformation of glycerol, one of the top biobased platform molecules recognized by the U.S. DOE, available either from the hydrolysis of vegetable oils or from carbohydrate sources through microbial fermentation processes.^{25, 26} The conversion process typically involves enzymatic reactions from glycerol to 3-hydroxypropionaldehyde, followed by oxidation to 3-hydroxypropionic acid, for example under the action of lactate dehydrogenase (Scheme 3).



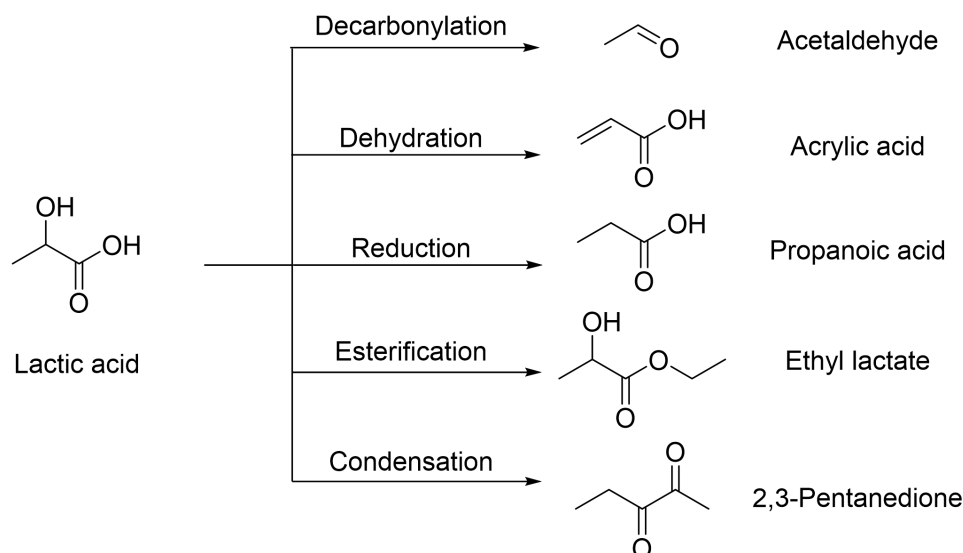
Scheme 3. Bio-pathways for the production of D,L-lactic acid and 3-hydroxypropionic acid

Lactic acid and 3-hydroxypropionic acid are universal block compounds suitable for the production of biodegradable polymers, such as polylactic acid and poly(3-hydroxypropionic acid). Polylactic acid is a bioactive thermoplastic material and produced by the polymerization of dilactide derived from the self-esterification of lactic acid. Poly(3-hydroxypropionic acid) belongs to the polyhydroxyalkanoates family and can be produced through microbial fermentation using engineered microorganisms (Scheme 4). They have gained popularity as an eco-friendly and sustainable alternative to traditional petroleum-based plastics and finds applications in packaging, textiles, agriculture and biomedicine.^{27, 28}



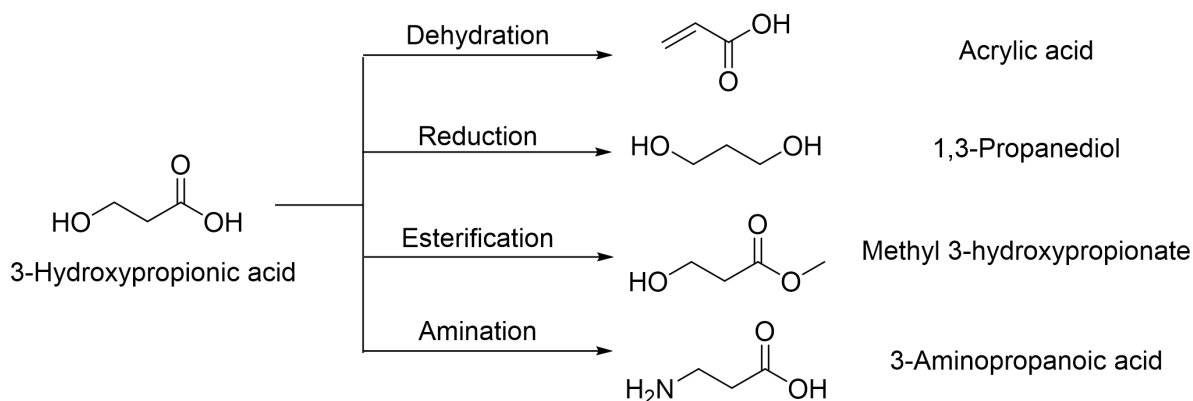
Scheme 4. Pathways for the production of polyesters from Lactic acid and 3-hydroxypropionic acid

The bifunctional nature of lactic acid allows conversion into a variety of useful products such as acetaldehyde, acrylic acid, propionic acid, ethyl lactate and 2, 3-pentanedione (Scheme 5).²⁹ Among them, ethyl lactate is considered a green solvent and is used in many industries due to its low toxicity, low volatility, versatility and biodegradability.³⁰



Scheme 5. Important chemicals derived from various transformations of lactic acid

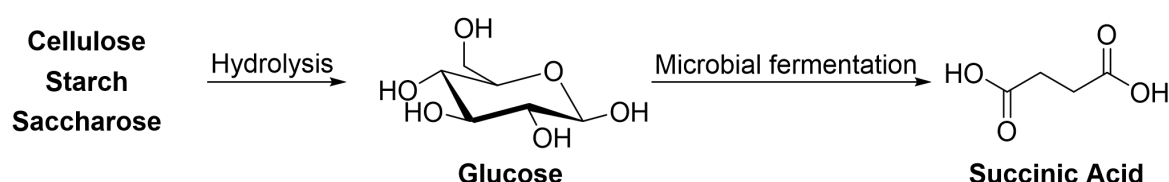
3-Hydroxypropionic acid can undergo various chemical transformations to introduce specific functional groups or chemical moieties. Including dehydration to acrylic acid, selective reduction to 1,3-propanediol, esterification to methyl 3-hydroxypropionate, amination to 3-aminopropanoic acid etc. (Scheme 6). Its derivatives can also serve as versatile intermediates for the synthesis of various specialty chemicals, and the choice of transformation pathway depends on the target application of the final product.³¹



Scheme 6. Important chemicals derived from various transformations of 3-hydroxypropionic acid

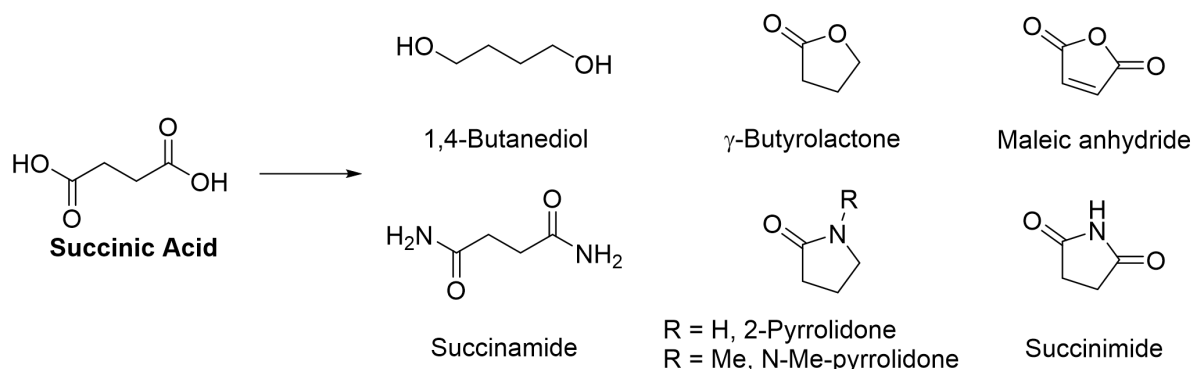
1.2.3.2 Succinic acid

Succinic acid is a C₄ dicarboxylic acid. It is a naturally occurring acid that plays an important role in tricarboxylic acid cycle of cellular metabolic processes. Traditional chemical methods for preparing succinic acid involve the catalytic hydrogenation of maleic anhydride produced by the oxidation of butane or butadiene. However, since 2010, technological advances in carbohydrate fermentation and purification have made biobased succinic acid economically attractive.³² Succinic acid can be produced through a two-step process, in the first step, cellulose is hydrolyzed into glucose, and in the second step, glucose is fermented to produce succinic acid (Scheme 7).³³ The company Roquette S.p.A. has achieved industrial-scale production of biobased succinic acid. Purification technology based on distillation-crystallization enables succinic acid purity to reach over 99%.³⁴



Scheme 7. Fermentation of sugars to form succinic acid

In recent years, succinic acid has gained attention for the production of various chemicals. It can be used as an intermediate for the synthesis of a series of C₄ building blocks such as 1,4-butanediol, γ -butyrolactone, maleic anhydride, succinamide, 2-pyrrolidone, *N*-methyl pyrrolidone and succinimide (Scheme 8).³⁵ In addition, succinic acid is also a key structural unit in the production of biodegradable polymers such as polybutylene succinate.^{35, 36}

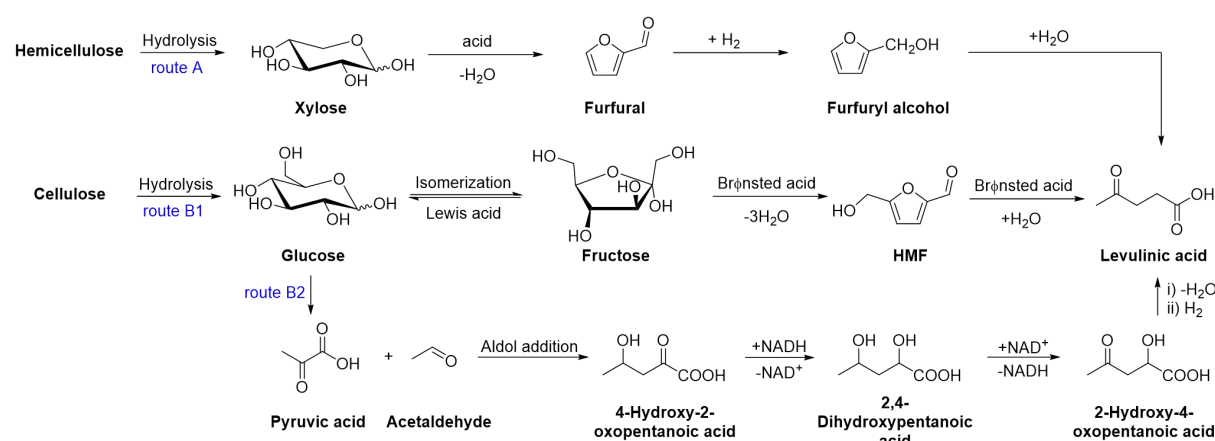


Scheme 8. Succinic acid derived C₄ chemicals

Different applications of succinic acid and its derivatives were also investigated. For example, it is used as acidity regulator, flavor enhancer and dietary supplement in food or investigated as an electrolyte additive for lithium-ion batteries and so on.³⁷

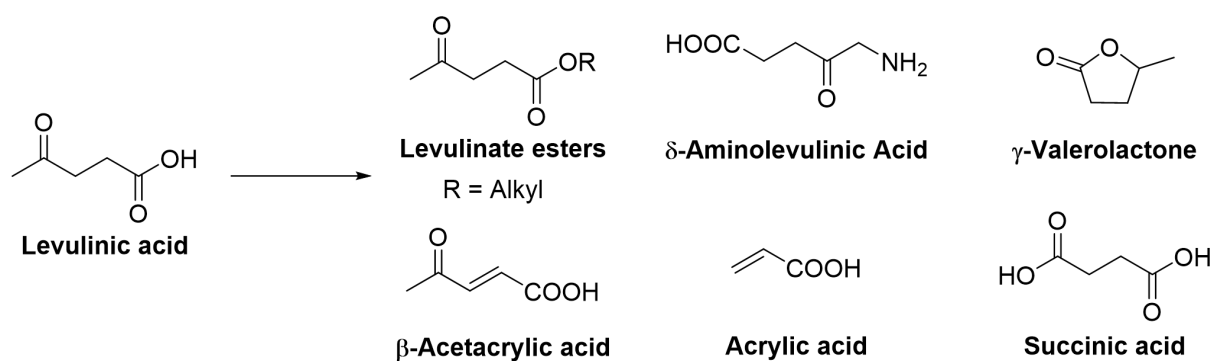
1.2.3.3 Levulinic acid

Levulinic acid is a biodegradable C₅ carboxylic acid. Its preparation from biomass involves several different possible pathways. One starts from hemicelluloses which undergoes acid hydrolysis to obtain C₅ sugars (such as xylose). The furfural obtained after dehydration of C₅ sugar is converted into furfuryl alcohol and subsequently to levulinic acid. However, considering raw material costs, process efficiency, market demand and other aspects, this method is not economically favorable for the time being (Scheme 9, route A). The most important route is the acid-catalyzed multi-step conversion of polysaccharides into C₆ monosaccharides (glucose and fructose), followed by dehydration to 5-HMF, and then rehydration into levulinic acid (Scheme 9, route B1). In addition, C₆ monosaccharides can also be fermented to produce pyruvic acid and acetaldehyde as key intermediates to prepare levulinic acid (Scheme 9, route B2).^{38, 39}

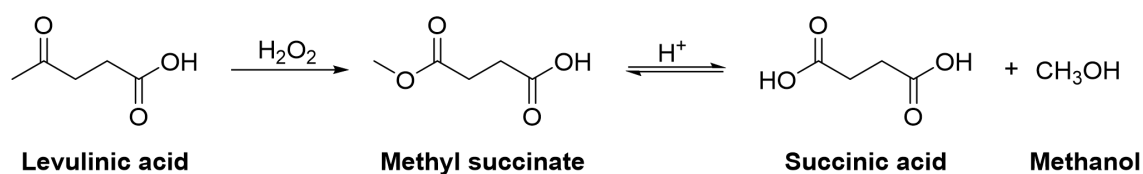


Scheme 9. Preparation of levulinic acid from C₅ or C₆ route

Levulinic acid can be converted into various derivatives, such as esters, amides, lactones, acrylic acid etc. (Scheme 10).^{40, 41} The versatility of the chemistry of levulinic acid and its derivatives offers a wide range of possible applications. Levulinic acid is a key intermediate in the synthesis of various chemicals including pharmaceuticals, agrochemicals and other specialty chemicals,^{42, 43} its derived levulinate esters can be used as a solvent in a variety of applications.^{44, 45}

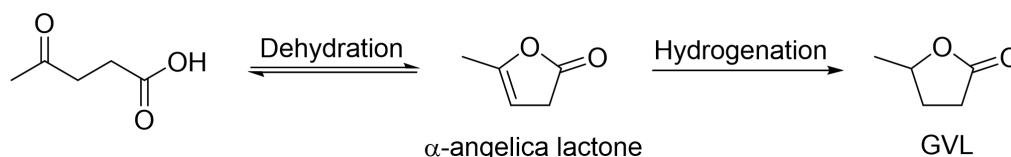


Levulinic acid can be converted into succinic acid under certain conditions. For example, in the presence of hydrogen peroxide, levulinic acid undergoes Baeyer-Villiger oxidation to add an oxygen atom to convert the ketone into an ester, forming methyl succinate, which is subsequently cleaved into succinic acid and methanol under acidic conditions (Scheme 11).⁴⁶



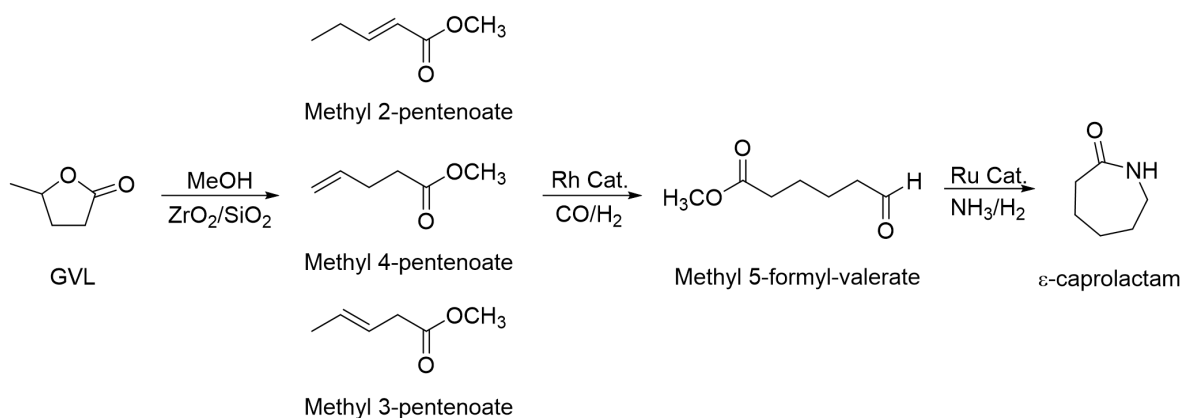
γ -Valerolactone (GVL) is a representative cyclic ester derived from levulinic acid that is commonly used as a green solvent and chemical platform in various industrial applications. Catalytic production of GVL from levulinic acid *via* an α -angelica lactone intermediate has been a hot topic in the past decade (Scheme 12).^{47, 48} Studies have showed that acidic sites and

metal sites of the catalysts are important for the dehydration and hydrogenation steps in the conversion of levulinic acid to GVL. Many novel efficient catalytic strategies have been reported, mainly including Raney nickel, noble metal catalysts (such as palladium or ruthenium) or other supported metal catalysts.^{47, 49}



Scheme 12. Preparation of GVL from levulinic acid by dehydration and hydrogenation

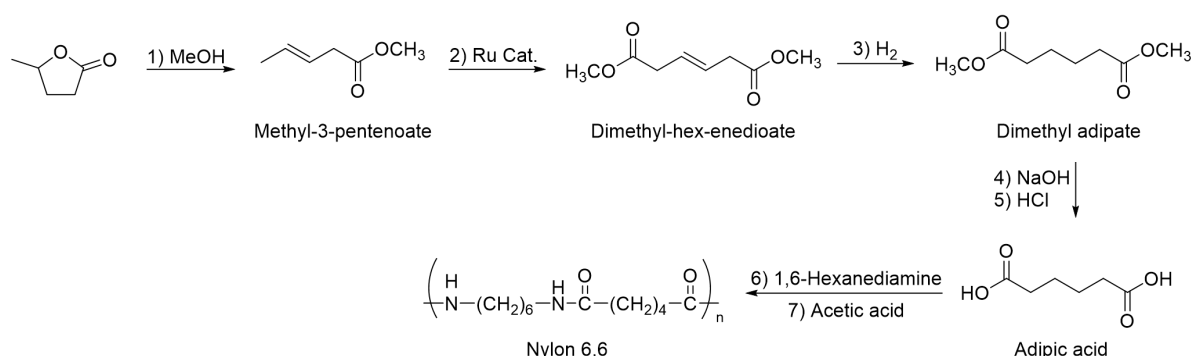
GVL is a useful building block for the synthesis of polyesters and other polymers. Johannes G. de Vries et al. reported the ring opening of GVL with methanol in the gas phase and obtained over 95% selectivity of methyl 2-, 3-, and 4-pentenoate over $\text{ZrO}_2/\text{SiO}_2$ catalyst. Among them, methyl 4-pentenoate accounted for 81% converted into methyl 5-formyl-valerate with 90% selectivity, which was reported to generate ϵ -caprolactam as the monomer of nylon 6 *via* reductive amination and ring closure (Scheme 13).⁵⁰



Scheme 13. Synthesis of ϵ -caprolactam from GVL ring opening

Choi et al. developed a protocol for the synthesis of nylon 6,6 from GVL. The steps involved in this transformation include the esterification of GVL to methyl-3-pentenoate, metathesis of methyl-3-pentenoate to dimethyl-hex-enedioate, hydrogenation of dimethyl-hex-enedioate to

dimethyl adipate, hydrolysis of dimethyl adipate to adipic acid, and polymerization of adipic acid to Nylon 6,6 (Scheme 14).⁵¹

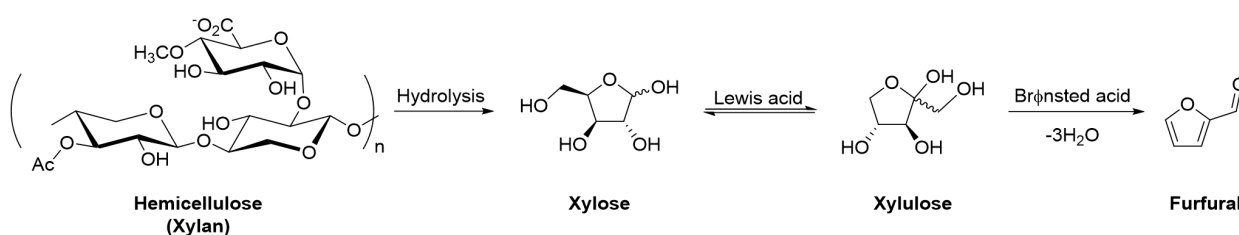


Scheme 14. Multi-steps synthesis of nylon 6,6 from GVL

In 2021, Florian Kerkel et al. conducted a detailed study on the toxicity and biodegradability of GVL as a solvent. GVL used as a solvent was proven to be readily biodegradable and exhibited low acute toxicity towards aquatic organisms. The solvent properties of GVL were compared with those of classical organic solvents based on the Hansen solubility parameter (HSP), which refers to fundamental parameters that categorizes the solubility behavior of substances. GVL exhibits a very high polar HSP of $\delta_p = 14.0 \text{ MPa}^{1/2}$, and a relatively low hydrogen bonding HSP of $\delta_h = 8.0 \text{ MPa}^{1/2}$. Therefore, it is too polar to match solvents like ethyl acetate ($\delta_p = 5.3 \text{ MPa}^{1/2}$, $\delta_h = 7.2 \text{ MPa}^{1/2}$) or ethers, while its ability to form hydrogen bonds is too low to match the HSP of polar alcohols such as methanol ($\delta_p = 12.3 \text{ MPa}^{1/2}$, $\delta_h = 22.3 \text{ MPa}^{1/2}$). However, it is worth noting that according to the 3D Hansen space with GVL and 45 kinds of classical solvents discussed by Prat et al., the solvent N-methyl-2-pyrrolidone, dimethylacetamide, methylformamide, *N,N'*-dimethylpropylurea, acetone and dimethyl sulfoxide (DMSO) are considered to have similar solvent properties with GVL because they were identified to have a distance in Hansen space of $R_a < 5 \text{ MPa}^{1/2}$ to GVL. Therefore, GVL can be further classified as a highly dipolar aprotic solvent.⁵²

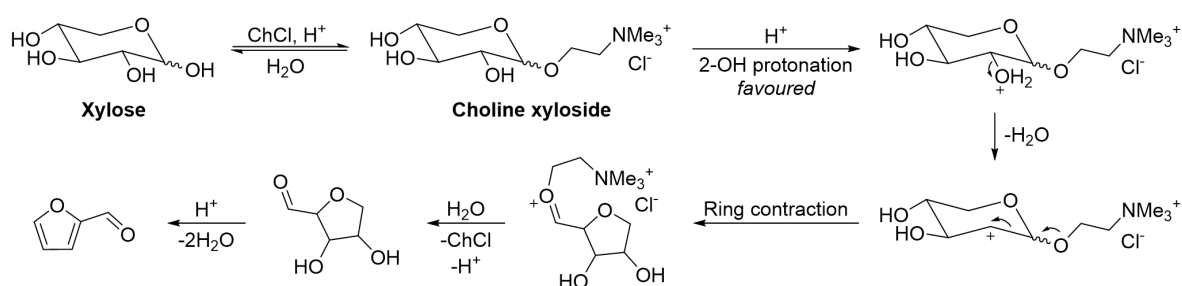
1.2.4 Bio-based aldehydes

Furfural is a versatile bio-based top C₅ platform molecule which plays an important role in the biorefining industry. Several reviews have been published on the production of furfural from biomass lignocellulosic and sugars.⁵³⁻⁵⁷ In recent years, furfural is produced on an industrial scale in batch or continuous reactors from lignocellulosic biomass such as bagasse, corncobs, stalks, switchgrass and hardwoods. Selective dissolution and depolymerization of hemicellulose allow the transformation of biomass into pentose sugars. The hydrolysis and dehydration process of hemicellulose can be accomplished in water or in aqueous-based biphasic systems in the presence of mineral acids (such as H₂SO₄, HCl) and organic acids (such as HCOOH, CH₃SO₃H). It is proposed in the literature that the dehydration step first involves the isomerization of xylose into xylulose under the catalysis of Lewis acid sites, and then the dehydration of xylulose into furfural under the catalysis of Brønsted acid sites (scheme 15).⁵⁸



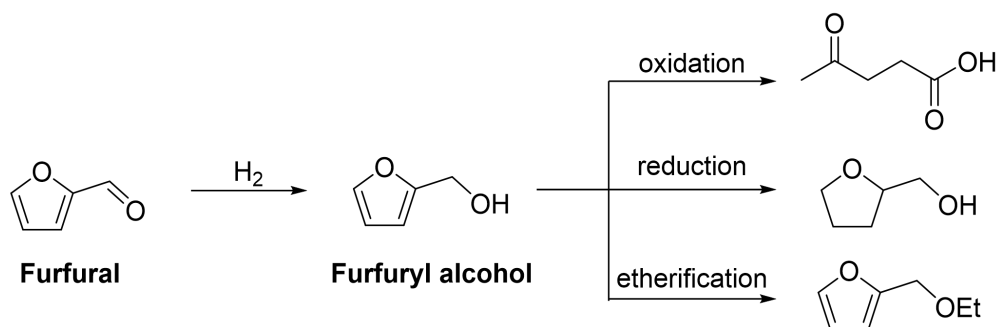
Scheme 15. Production route of furfural from hemicellulose

De Oliveira Vigier and colleagues have recently shown that the addition of choline chloride is beneficial to the transformation of xylose to furfural in presence of HCl (Scheme 16). The faster furfural formation rate is due to the formation of an intermediate choline xyloside which undergoes easier dehydration than xylose itself. This protocol allows efficient furfural synthesis even using concentrated starting xylose solution, compared to other processes leading to significant formation of by products such as humins.⁵⁹



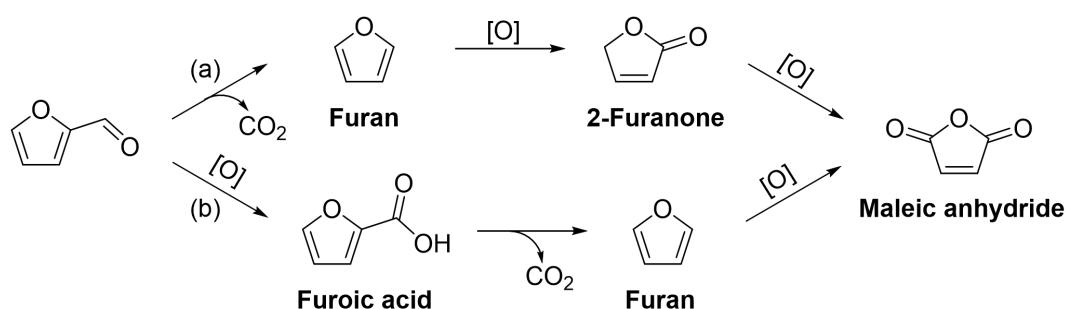
Scheme 16. Mechanism for xylose dehydration to furfural through choline xyloside intermediate

One of the most important transformations of furfural is hydrogenation to produce furfuryl alcohol. Furfuryl alcohol is a versatile intermediate that can be used in the production of resins, coatings, polymers and used as a solvent. It can also be converted into other chemicals through reactions such as oxidation, reduction and etherification etc. (Scheme 17).⁶⁰



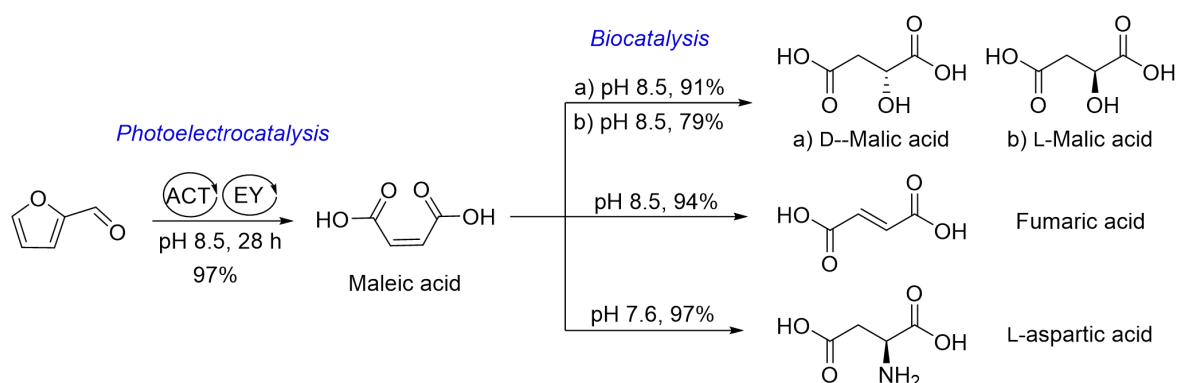
Scheme 17. Conversion of furfural to furfuryl alcohol and its derivatives

Currently, the direct oxidation of furfural to maleic anhydride under aerobic conditions has been reported. A possible mechanism involved the oxidative decarboxylation of furfural to furan, the oxidation of furan to furanone, and the final oxidation of furanone to maleic anhydride was proposed by Manuel Ojeda et al. by detecting the presence of the main reaction product when using $\text{VO}_x/\text{Al}_2\text{O}_3$ catalysts (Scheme 18a).⁶¹ In reports on the gas-phase oxidation of furfural to maleic anhydride using a vanadium phosphorus oxide catalyst (VPO), another possible mechanism was proposed, suggesting furoic acid to be the key intermediate (Scheme 18b).⁶²



Scheme 18. Proposed $\text{VO}_x/\text{Al}_2\text{O}_3$ or VPO catalyzed conversion of furfural to maleic anhydride

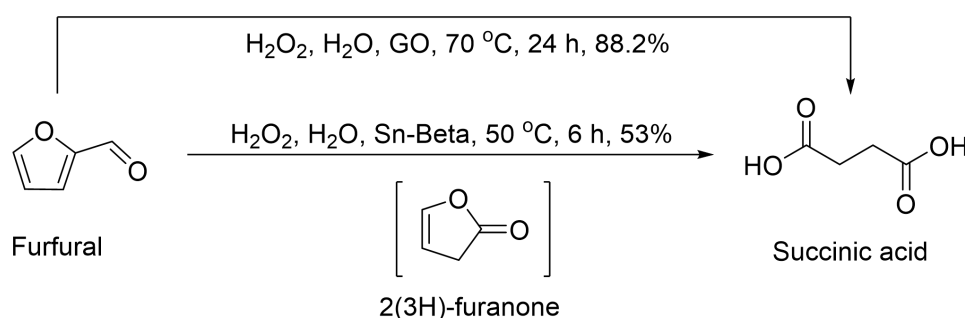
A combined electro-, photo-, and biocatalytic approach was used for the one-pot selective conversion of furfural to several C_4 chemicals, including maleic acid, D-malic acid, L-malic acid, fumaric acid and L-aspartic acid (Scheme 19). Through the electrochemical oxidation with 4-acetamido-2,2,6,6-tetramethylpiperidine-*N*-oxyl (ACT) and the photo-oxygenation with eosin Y (EY), maleic acid was produced in 97% yield from furfural. It was then selectively converted to D-malic acid, L-malic acid, fumaric acid and L-aspartic acid by biocatalysis in 91%, 79%, 94%, 97% yield in the presence of different enzymes include maleate hydratase, maleate *cis-trans* isomerase, fumarase or L-aspartase.⁶³



Scheme 19. Electro-, photo-, and biocatalysis for one-pot selective conversion of furfural into C_4 chemicals

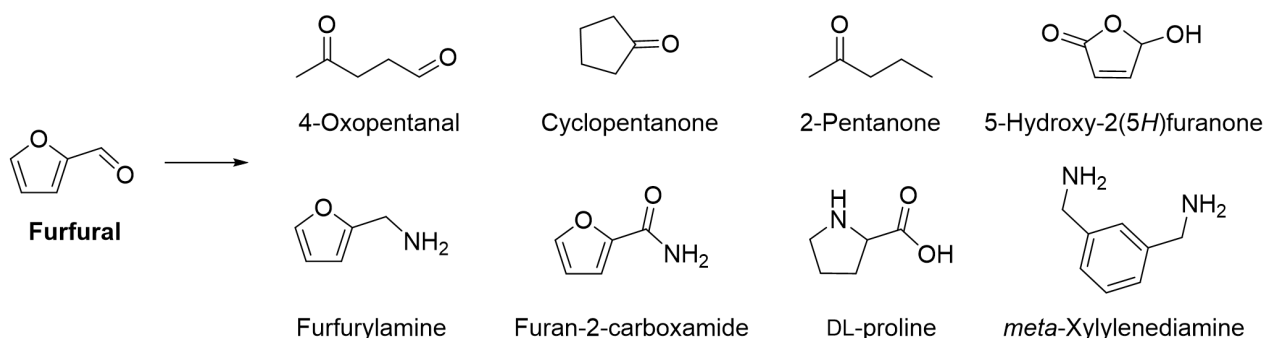
The oxidation of furfural to succinic acid over acidic metal-free graphene oxide was reported by Lv et al. Using modified hydrophilic graphene oxide as solid acid catalyst, and H_2O_2 as an oxidant, furfural was converted into succinic acid in 88% yield under mild conditions. The -

SO₃H group on the graphene oxide support is a crucial catalytic site for furfural oxidation, with suitable acidity essential for the selectivity of the reaction.⁶⁴ Lewis acidic Sn-Beta was also reported for the selective oxidation of furfural to succinic acid in water when using H₂O₂ as an oxidant. Contrary to other Lewis acids such as HBeta-38 and TS-1 which have an activating effect on H₂O₂ and promote the generation of maleic acid, Sn-Beta accelerated the Baeyer-Villiger oxidation of furfural to 2(3*H*)-furanone intermediate by activating furfural, and provide succinic acid in the yield of 53% (Scheme 20).⁶⁵



Scheme 20. Conversion of furfural to succinic acid

In addition, furfural can also be converted into other chemicals such as 4-oxopentanal, cyclopentanone, 2-pentanone, 5-hydroxy-2(5*H*)furanone, furfurylamine, furan-2-carboxamide, DL-proline and *meta*-xylylenediamine which are useful intermediates in agriculture, pharmaceutical and other fields (Scheme 21).^{66, 67}



Scheme 21. Other furfural derived chemicals

1.3 A focus on 5-hydroxymethylfurfural (5-HMF)

1.3.1 Introduction

5-HMF was added to the updated “Top potential value-added chemicals” list in 2010 by Joseph J. Bozell and Gene R. Petersen.⁹ 5-HMF is a C₆ biobased platform molecule derived from starch and cellulose raw materials, and is certainly the most studied thermal degradation product of sugars. 5-HMF contains one aldehyde group and one alcohol group attached to a furan ring. It can undergo various structural reorganizations through chemical transformation leading to a large number of applications in fine chemistry.^{68, 69} 5-HMF and its derivatives are known as the "sleeping giant" of renewable chemicals due to their huge market potential. In recent years, the production and transformation of HMF have been widely investigated. In the past decade (2014-2023), the number of related reports has continued to grow, as shown in Figure 5. In this section, we will try to depict the most representative aspects of the production, stability and conversion of HMF.

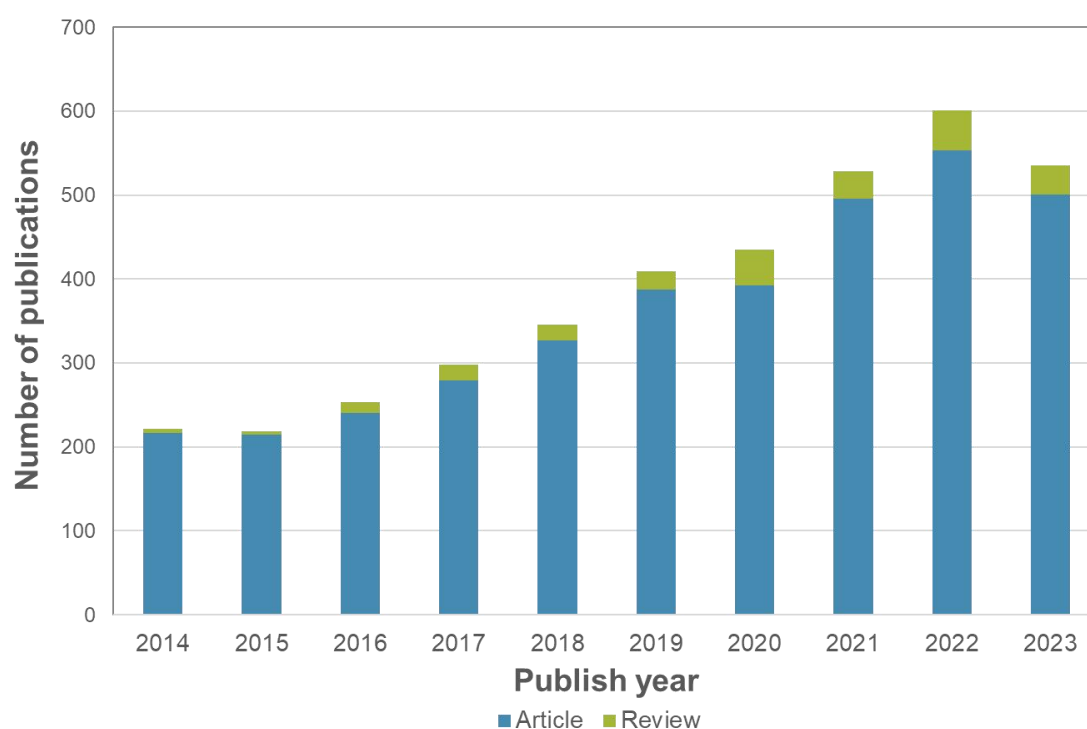


Figure 5. Number of publications per year on HMF (2014-2023) Source: Web of Science (keyword: 5-hydroxymethylfurfural (Fields: Abstract))

1.3.1.1 Market and industrial production of 5-HMF

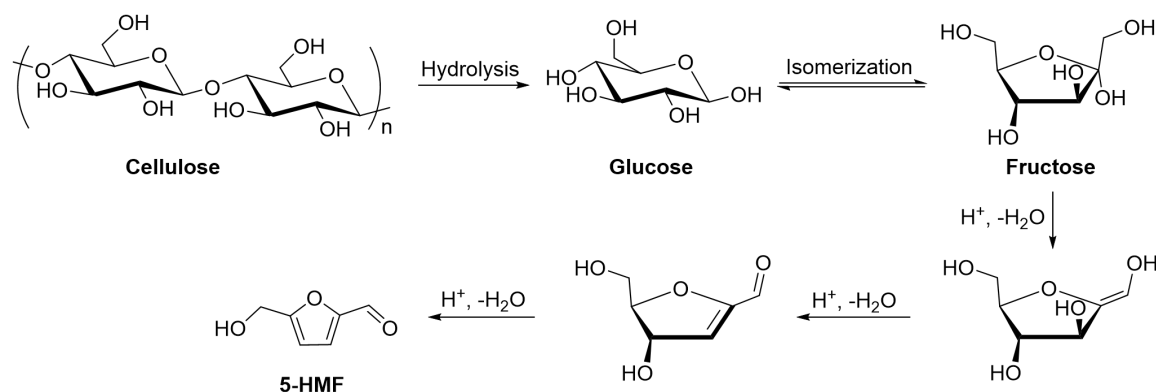
The minimum selling price of HMF was estimated to be 930.6 USD/ton.⁷⁰ According to a recent share report, the 5-HMF market is expected to grow strongly at a compound annual growth rate of 1.3% during the period of 2023 to 2029.⁷¹ Currently, the 5-HMF production in Europe is the highest in the world, and its export volume ranks also first. In terms of 5-HMF market share, China accounts for more than 60% of the Asia-Pacific region. Some of the leading manufacturers and suppliers of 5-HMF include Merck, AVA Biochem, Zhejiang sugar energy technology et al. The factory of the AVA Biochem company located in Switzerland has been the first to produce 5-HMF in 2014. Its production is based on an innovative water-based hydrothermal process, providing 5-HMF with a purity up to 99.9% from industrial sugars.

An important derivative of 5-HMF is 2,5-furandicarboxylic acid (FDCA), prepared after oxidation of 5-HMF. FDCA can be used as a precursor for polyethylene furan-2,5-dicarboxylate, which is considered as a next-generation polyester and a bioreplacement for polyethylene terephthalate, produced on a commercial scale by companies such as Synvina, AVA Biochem and Sulzer.⁷² Another important application of 5-HMF is the industrial production of 2,5-dimethylfuran (DMF) as the most valuable biofuel candidate through catalytic hydrogenolysis.⁷³ Besides, 5-HMF is a natural, non-toxic formaldehyde alternative used in the synthesis of various types of adhesives by Avalon industries, such as 5-HMF-based phenolic, melamine and urea resins. Other applications for 5-HMF currently being developed by Avalon include agrochemicals, pharmaceutical active ingredients, wood composites, paints and coatings.

1.3.1.2 Reported pathways towards 5-HMF

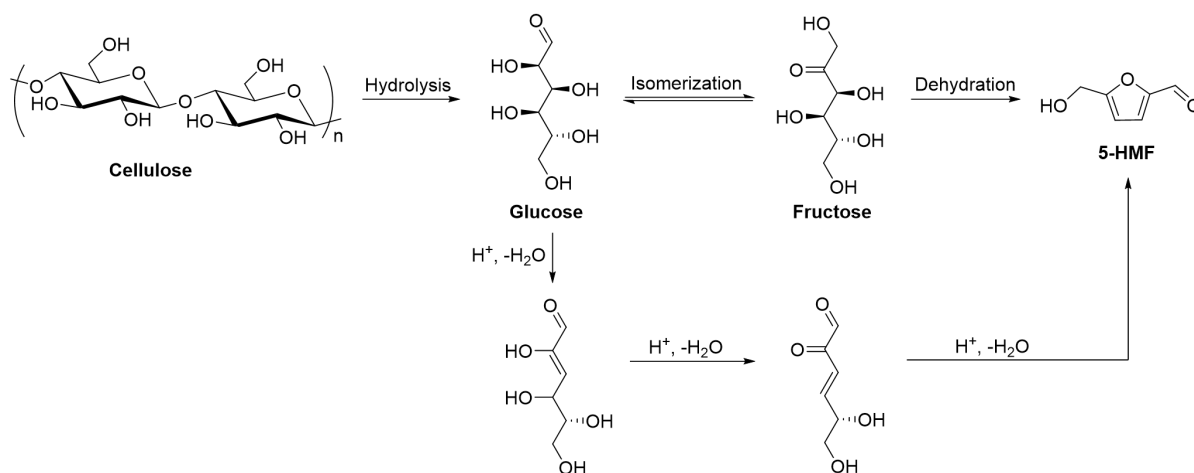
Several mechanisms either cyclic or acyclic have been proposed for the reaction of C₆ sugars to 5-HMF. It is worth noting that almost all mechanisms proposed so far are based on studies of processes performed in aqueous medium. The most reported method is the direct formation

of HMF from hexoses under acid catalysis and the sequential removal of three molecules of water. The mechanism of the cyclic pathway involves the formation of cyclic furanose intermediates. It is speculated that the hemiacetal generated from dehydration of fructose undergoes two consecutive β -dehydrations in the ring to form 5-HMF (Scheme 22).⁶⁷



Scheme 22. Cyclic pathways of cellulose to 5-HMF

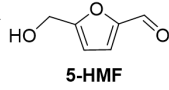
In the acyclic pathway, possible mechanisms have also been proposed. Dehydration of glucose lead to the formation of the key enol intermediate (3-deoxyglucose-2-ene), followed by two consecutive β -dehydrations and ring closure, ultimately yielding 5-HMF. It is noteworthy that fructose is generally reported to be much more selective for HMF than glucose. Kuster proposed an explanation that the more stable ring structure of glucose hinders the ability to form acyclic enediol intermediates in an acyclic mechanism (Scheme 23).⁷⁴



Scheme 23. Acyclic pathway of cellulose to 5-HMF

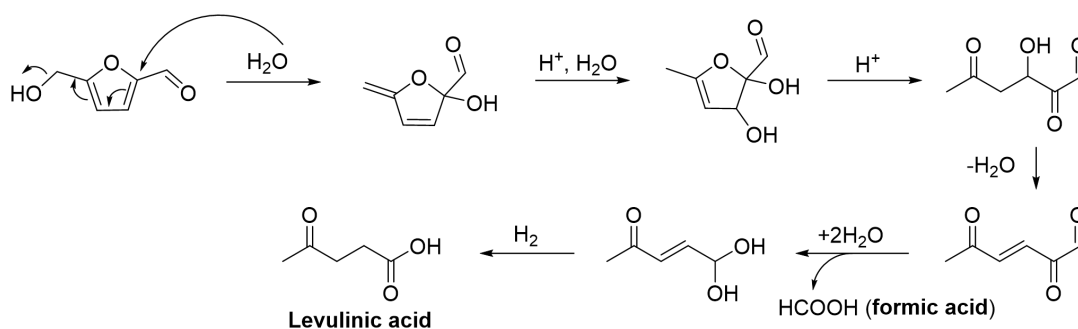
Being a promising bio-based platform molecule, the preparation of 5-HMF has been a rapidly growing research field in the past 20 years.⁷⁵ Early research on the dehydration of monosaccharides (hexoses) to prepare 5-HMF mainly performed in water using mineral acids as catalysts (mainly Brønsted acids such as sulfuric or hydrochloric acid).⁷⁶ Since HMF has poor stability under acidic aqueous solution conditions, it is likely to further evolve to levulinic acid and formic acid, which is an important factor leading to the lower yield of 5-HMF. A large number of processes have subsequently been developed to facilitate the production of HMF from biomass feedstocks, from initially simple aqueous systems, to organic solvent systems, biphasic systems and ionic liquid systems. The main advantages and drawbacks in different production processes are summarized in Table 2. It is worth noting that conversions in various reaction media generally involve the use of acidic catalysts.

Table 2. HMF production process development

Acidic conditions		 5-HMF
Solution systems	Features	
Aqueous systems	Good solubility of raw material; Low conversion or/and low selectivity.	
Organic solvents DMSO, DMF, DMA	Good solubility of raw material; Higher conversion and selectivity; Solvent is difficult to separate and remove.	
Other organic solvents	Low conversion or/and low selectivity.	
Biphasic systems Organic solvents/aqueous	MIBK, 2-BuOH as extraction solvents; Higher conversion and higher selectivity.	
Ionic liquid-based systems	Higher selectivity and yields. High cost, difficult to separate and recycle.	

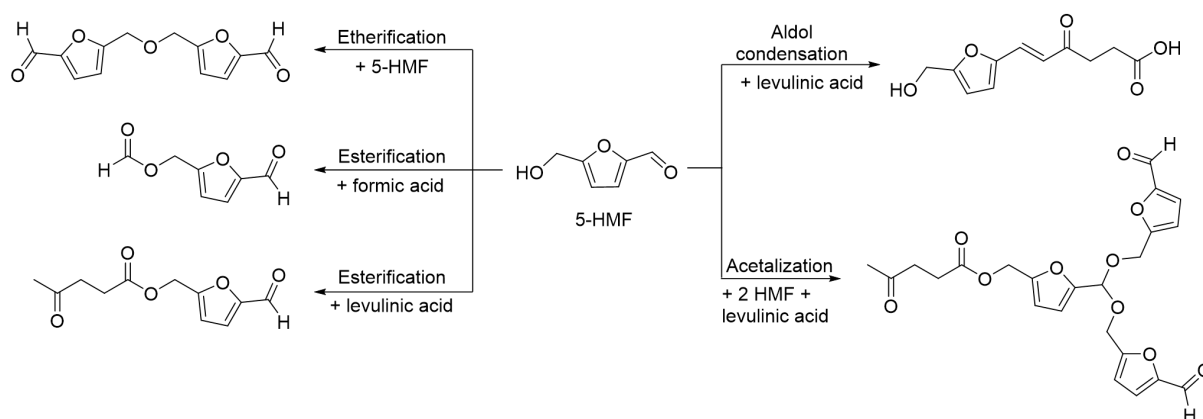
1.3.1.3 Stability of 5-HMF

The complex reactivity of HMF is due to the combination of functional groups which make it susceptible to undergo different types of reactions. The chemical stability of HMF, way lower to that of furfural, has been mentioned in many reports. Exposure of HMF to acidic conditions can lead to the formation of levulinic acid and formic acid as rehydration products following the possible mechanism proposed by Horvat (Scheme 24).⁷⁷



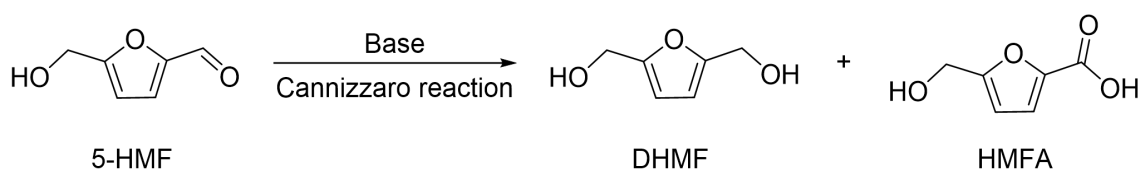
Scheme 24. The rehydration mechanism of HMF to levulinic acid and formic acid under acidic conditions

Complex mixtures of insoluble dark brown viscous liquids or solids, commonly known as humins, are produced under acidic or alkaline conditions. In 2020, Shen and Liu et al. used HMF as a model molecule to explore the chemical structure and formation mechanism of HMF derived humins under acidic conditions.⁷⁸ By capturing key intermediates at low temperature (around 20 °C), the structural evolution process towards humins has been demonstrated. The dimer product 5,5'-oxy(bis-methylene)-2-furfural (OBMF) obtained by the self-etherification reaction of HMF was isolated by column chromatography. ¹H NMR spectrum showed the presence of levulinic acid and formic acid. HPLC-MS/MS and column chromatography revealed the formation of two esterification intermediates, HMF formate and HMF levulinate, as well as the acetalization product of HMF levulinate with 2 molecules of HMF. Furthermore, the aldol condensation product of HMF and levulinic acid were also observed and characterized to be (*E*)-6-[5-(hydroxymethyl)furan-2-yl]-hex-4-oxo-5-enoic acid. It was confirmed that many different reactions can take place when the HMF is exposed to an acidic process. It is worth noting that in addition to the characterized structures, there are still many complex polyfuranic compounds generated through polymerization or/and polycondensation reactions that are difficult to characterize so far. For example, HMF also participates in complex aldol condensation and polymerization reactions under alkaline conditions.⁷⁹ A formation approach of HMF derived by-products/humins is shown in Scheme 25. The formation of humin-like materials has also been observed during the production of furfural from pentose sugars.



Scheme 25. The formation of HMF derived humins under acidic conditions

Finally, other undesired by-products can be formed when alkaline conditions are reached, for example through aldol condensation, isomerization, polymerization or like in the reported Cannizzaro reaction leading to 2,5-dihydroxymethylfurfural (DHMF) and 5-hydroxymethyl-2-furanoic acid (HMFA) (Scheme 26).⁸⁰⁻⁸²



Scheme 26. The Cannizzaro reaction of HMF towards DHMF and HMFA

In conclusion, the chemical stability of HMF is highly dependent on the reaction conditions, particularly the pH of the reaction medium. Acidic conditions generally favor transformations that involve the furan ring. Under acidic conditions, HMF is prone to hydrolysis, isomerization and dehydration reactions, resulting in the formation of levulinic acid, formic acid and derivatized complex molecules. On the other hand, under alkaline conditions, aldol condensation, base-catalyzed isomerization, polymerization and the formation of carboxylates can be observed. These reactions lead to the production of larger molecules, such as dimers, polymers and carboxylate ions. In general, the reactivity of HMF in both acidic and alkaline environments brings challenges and opportunities to the conversion of HMF.

1.3.2 Main reactions of 5-HMF

The reactivity of HMF stems from its unique molecular structure, featuring a furan ring, an aldehyde and a hydroxyl functional groups. Biobased HMF has up to now been essentially applied to the preparation of bio-based chemicals, solvents, polymers or fuels, but becomes recently an attractive candidate for fine chemistry applications. As shown in Figure 6, HMF is an important intermediate in the production of many molecules which can be used in polymer, biofuel and other chemical transformation fields, such as 2,5-diformylfuran (DFF), 2,5-furandicarboxylic acid (FDCA), 2,5-dihydroxymethylfuran (DHMF), 2,5-dimethylfuran (2,5-DMF), 2,5-diaminomethylfuran (DAMF), ethoxymethylfuran (EMF), levulinic acid (LA) and caprolactone, etc. In addition, HMF can also be used as a starting material for the preparation of more complex chemicals with various properties.

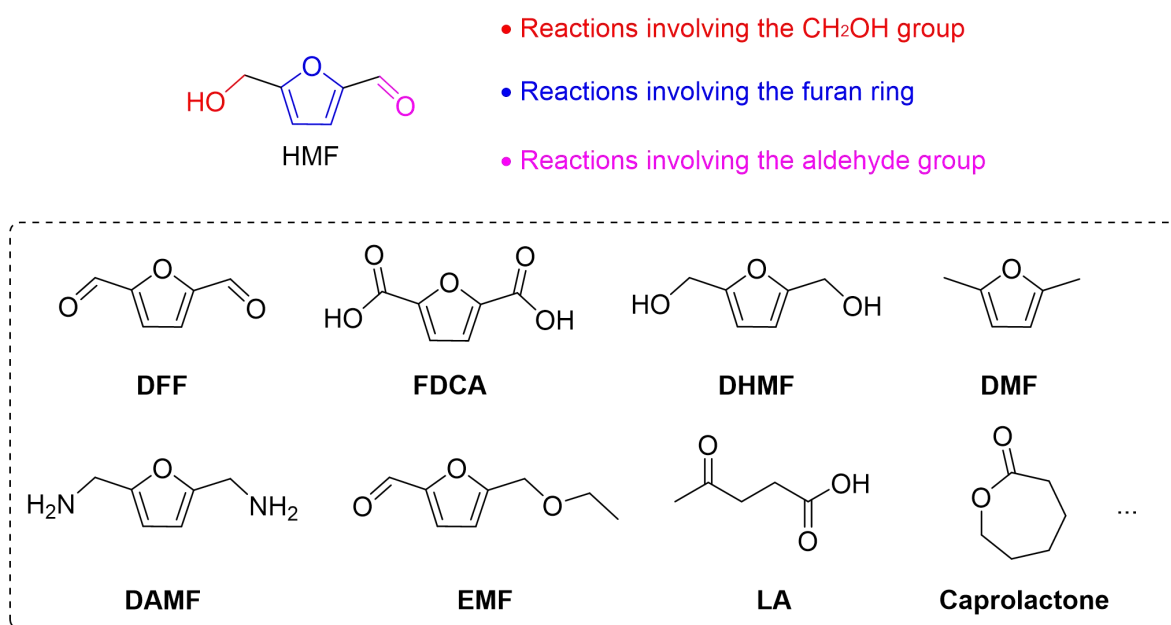


Figure 6. Presentative industrially valuable chemicals prepared from HMF

In this section, I will outline the representative chemical transformation of HMF starting with the hydroxyl group, the furan ring, and the aldehyde group respectively. First, we discuss the modification of hydroxy group, including oxidation, halogenation, esterification, and etherification reactions. Reactions involving the furan ring are then discussed, including ring opening, ring rearrangement, furan-ring hydrogenation and Diels-Alder reactions. Finally,

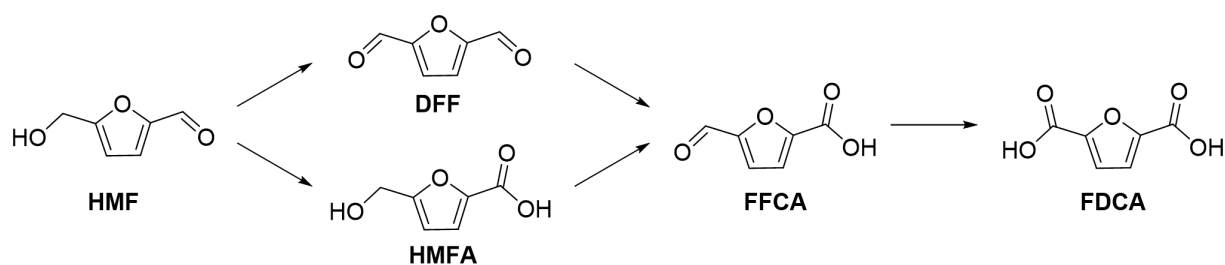
transformations of aldehyde group are shown, including reduction, amination, condensation and Morita-Baylis-Hillman reactions.

1.3.2.1 Reactions involving the CH₂OH group

The reactivity of the hydroxymethyl group in HMF, being a primary alcohol close to an aromatic moiety, is related to that of a benzyl alcohol. The reactivity of the hydroxyl group in the 5-HMF molecule allows the synthesis of a series of derivatives with different functional groups, depending on the reaction conditions and the presence of specific catalysts. Some common reactions involving hydroxyl groups in 5-HMF include oxidation, halogenation, esterification and etherification.

1.3.2.1.1 Oxidation of CH₂OH groups

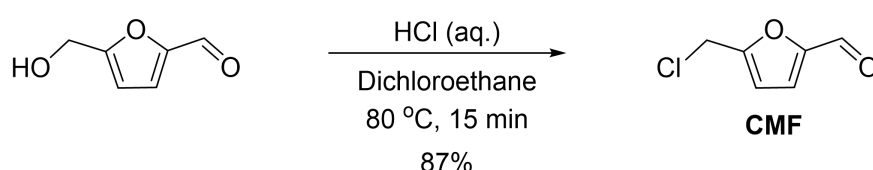
2,5-Diformylfuran (DFF) is a multifunctional platform molecule with broad application prospects in pharmaceuticals and polymers. The selective oxidation of HMF to DFF is an ongoing challenge because the varying reactivity of multiple reaction sites can lead to the formation of other oxidation products such as 5-hydroxymethyl-2-furanoic acid (HMFA), or to the formation of further oxidation carboxylic acid products like 5-formyl-2-furancarboxylic acid (FFCA) and FDCA (Scheme 27). The activation and selective oxidation of the hydroxyl group to a carbonyl group are key factors when achieving the reaction from HMF to DFF. Various catalysts (include noble metal, non-noble metal, photocatalysts) in organic solvent or water to selectively convert HMF to DFF in 90-99% yield by using air, oxygen or hydroperoxide as oxidants have been reported.⁸³ The catalyst loading generally has an important impact on the oxidation depth.



Scheme 27. Representative oxidation pathways of HMF

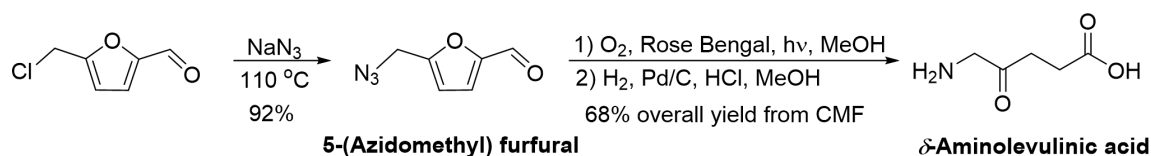
1.3.2.1.2 Halogenation of CH₂OH groups

HMF can undergo halogen substitution and be converted into 5-halomethylfurfural. An important example is 5-chloromethylfurfural (CMF). A series of classic halogenation reagents (HCl/SOCl₂/Me₃SiCl/POCl₃) can be successfully applied for the halogenation of HMF (Scheme 28). In general, hydroxyl groups in primary alcohols are not very reactive toward halogen substitution, but in HMF, the high reactivity of the methylene hydroxyl group is attributed to the electron-withdrawing properties of the furan ring. In fact, CMF is also a valuable bio-based platform molecule that can be prepared directly from C₆ sugars.^{84, 85}



Scheme 28. The formation of 5-halomethylfurfural

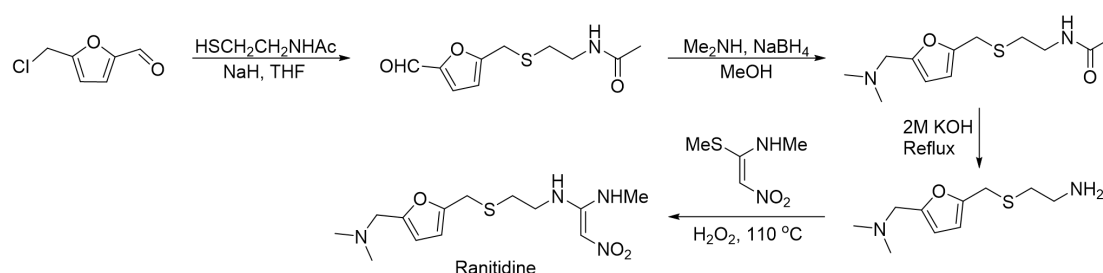
CMF serves as starting material for a singlet oxygen-mediated δ -aminolevulinic acid synthesis. δ -Aminolevulinic acid is a highly active agricultural and pharmaceutical intermediate and a natural herbicide. It is also used in photodynamic therapy as protoporphyrin precursor. The reaction of CMF and NaN₃ led to the formation of 5-(azidomethyl) furfural, and then singlet oxygen was added to the furan ring through photooxidation under oxygen, finally leading to δ -aminolevulinic acid in 68% yield after catalytic hydrogenation (Scheme 29).⁸⁶



Scheme 29. Synthesis of natural herbicide δ -aminolevulinic acid from CMF

Ranitidine was reported to be produced from CMF in four steps. Ranitidine is a medication that belongs to a class of drugs known as histamine H₂-receptor antagonists, commonly used

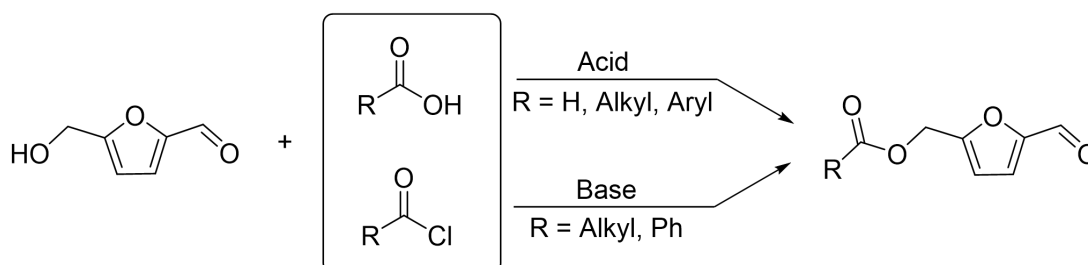
to treat conditions related to excess stomach acid production. Its synthesis from CMF involves four steps, the active chloromethyl functionality of CMF was used to form sulfide bond and the (dimethylamino)methyl group was introduced through reductive amination of aldehyde group. Ranitidine was finally obtained from CMF in overall 68% yield with an average yield of 91% per step, further proving the huge development potential of CMF as a biomass-derived platform chemical in green synthesis of drugs (Scheme 30).⁸⁷



Scheme 30. Four steps synthesis of Ranitidine drug from CMF

1.3.2.1.3 Esterification of CH₂OH groups

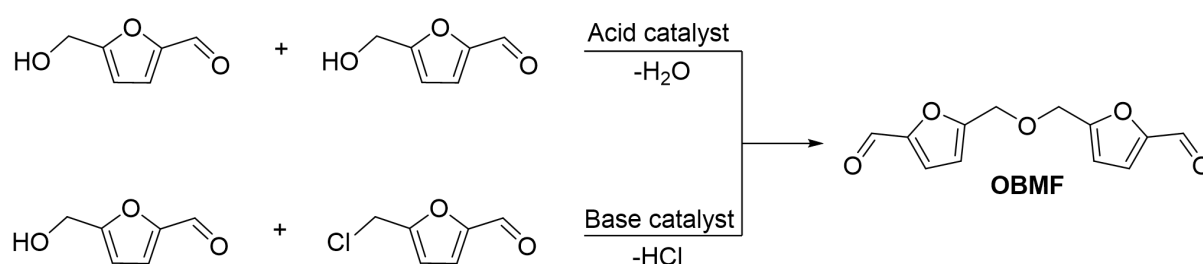
HMF esters are available from two main routes (Scheme 31). One is the classical reaction of HMF with carboxylic acids in the presence of an acid catalyst. For example, Fernandes et al. reported the acetylation of HMF with acetic acid using *p*-sulfonic acid calix[4]arene (1 mol%) as catalyst under microwaves (80 °C) led to the formation of 5-acetoxymethylfurfural in 99% yield.⁸⁸ A second one is the reaction of HMF with acid chloride under basic conditions, like the example shown by Bogna et al. in 1987, who treated HMF in pyridine with benzoyl chloride to give 5-benzoyloxymethyl-2-furaldehyde in 84 % yield.⁸⁹



Scheme 31. The preparation of HMF esters from HMF with carboxylic acids or acid chloride

1.3.2.1.4 Etherification of CH₂OH groups

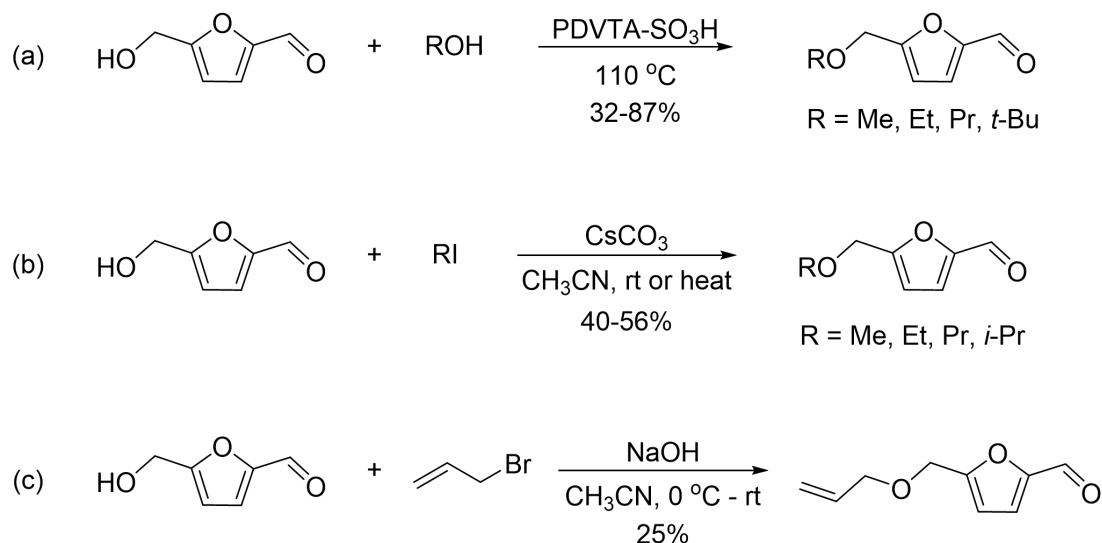
In acidic conditions, self-etherification of HMF leads to the formation of OBMF by S_N2 displacement of a water molecule after *in-situ* formation of an oxonium ion. The use of homogeneous organic acids (*p*-toluenesulfonic acid, trifluoromethanesulfonic acid),^{90,91} Lewis acid (ytterbium triflate, ferrous sulfate),⁹² or heterogeneous acid (Amberlyst 15, ZSM-5 (HPZ), oxide graphene)^{93, 94, 95, 96} has been reported. In a few papers, OBMF can also be obtained through the Williamson reaction of one HMF molecule and one CMF molecule in the presence of a base such as NaOH (Scheme 32).⁹⁶



Scheme 32. The formation of OBMF from HMF

The etherification of the CH₂OH group of HMF can be achieved in multiple ways (Scheme 33). The reaction of HMF with linear alcohols can produce alkoxy methylfurfurals. Commonly reported alcohols include methanol, ethanol, propanol and butanol.⁹⁷⁻¹⁰² For example, 32-87% yield of alkoxy methylfurfurals were prepared in the presence of a functionalized porous organic polymer bearing sulfonic acid groups (PDVTA-SO₃H) catalyst (Scheme 33a).⁹⁹ The esterification of long-chain alkyl alcohols, phenol, benzyl alcohol or propargyl alcohol with HMF under acidic conditions have also been studied by Maria J. Climent and Avelino Corma et al.^{103-105,106} Another method is to prepare alkoxy methylfurfural by reacting HMF with alkyl halide. For example, Martin K. Safo et al. prepared methoxy-, ethoxy-, propoxy-, isopropoxy methylfurfural in 40-56% yield *via* Williamson ether synthesis of HMF and alkyl iodides in the presence of Cs₂CO₃ (Scheme 33b).^{107,108} In a work published by David R. Spring et al., they prepared 25% yield of 5-((allyloxy)methyl)furan-2-carbaldehyde by adding finely ground sodium hydroxide to a

stirred solution of HMF in acetonitrile, followed by dropwise addition of allyl bromide (Scheme 33c).¹⁰⁷



Scheme 33. The etherification of HMF with alcohol, alkyl and allyl halides

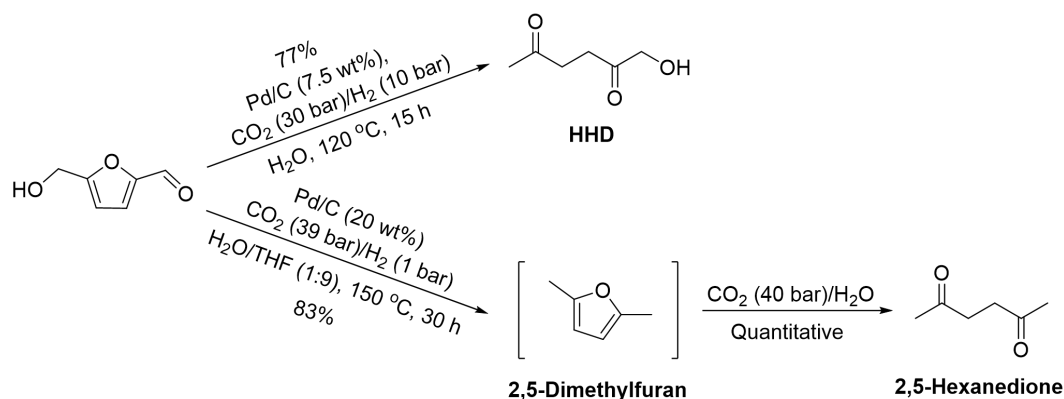
1.3.2.2 Reactions involving the furan ring

The furan ring in HMF contains reactive sites that can undergo various chemical transformations, leading to the formation of different products. Compared with the hydroxyl groups and aldehyde groups on HMF, reactions involving the furan ring of HMF are not so many. A major one is the hydrolysis of the furan ring under acidic conditions leading to the generation of levulinic acid through the cleavage of the ether bond, mentioned in the stability of HMF section. In this section, we will outline the other reactions on the furan ring of HMF, notably the ring-opening, ring rearrangement, ring reduction and Diels-Alder reaction of HMF.

1.3.2.2.1 Ring opening of 5-HMF

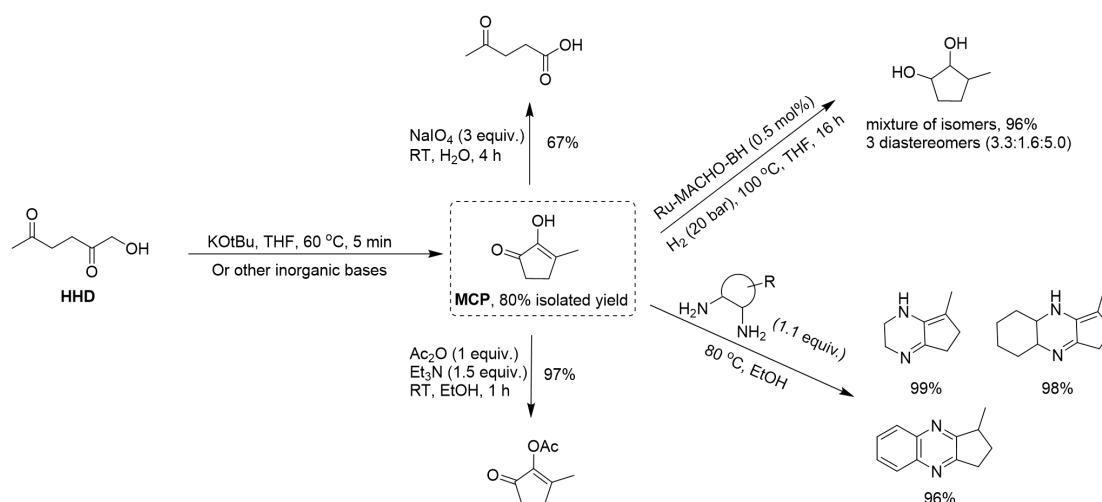
The ring-opening reaction of HMF can afford new C₆ linear ketones, such as 1-hydroxyhexane-2,5-dione (HHD) and 2,5-hexanedione, which may involve multiple steps such as oxidation, rearrangement, and selective functional group transformation. One of the

earliest examples by Liu et al. in 2014 proposed the Pd/C-catalyzed hydrogenation of HMF in CO₂/H₂O system which afforded HHD with up to 77% yield. Another emerging molecule 2,5-hexanedione was first obtained in high yield *via* DMF intermediate after optimization of the reaction conditions, notably changing the solvent to a mixture of H₂O and tetrahydrofuran (THF) (Scheme 34).¹⁰⁹



Scheme 34. Pd/C-CO₂/H₂O cooperative catalysis for the production of HHD and 2,5-hexanedione

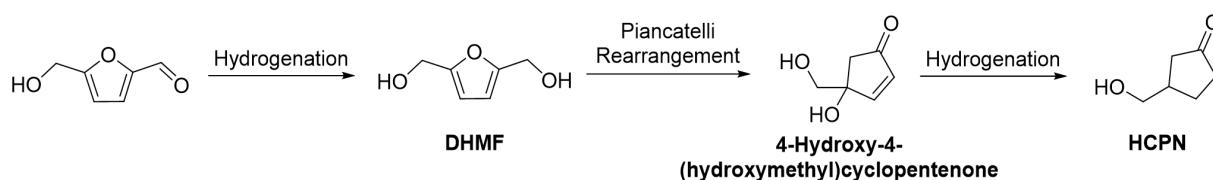
HHD can be further converted into 2-hydroxy-3-methylcyclopent-2-enone (MCP) *via* intramolecular aldol reaction. In 2018, Johannes G. de Vries et al. developed an efficient bases-catalyzed strategy for the conversion of HHD into MCP. MCP is a hub chemical which can be further transformed into levulinic acid, enol acetate, diol and *N*-heterocyclic compounds through oxidative ring cleavage, acetylation, hydrogenation and condensation reaction, respectively (Scheme 35).¹¹⁰



Scheme 35. Intramolecular aldol condensation of HHD to MCP as a hub to valuable chemicals

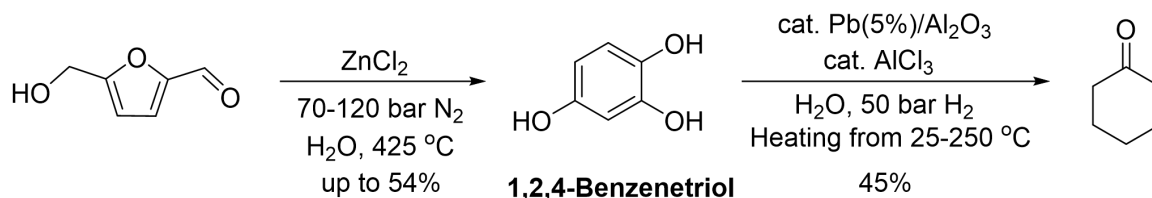
1.3.2.2.2 Ring rearrangement of 5-HMF

3-(Hydroxymethyl)cyclopentanone (HCPN) can be obtained from HMF, usually involving the hydrogenation of HMF to DHMF, which undergoes Piancatelli rearrangement to 4-hydroxy-4-(hydroxymethyl)cyclopentenone, followed by hydrogenation to give HCPN (Scheme 36). The conversion of HMF to HCPN was first reported in 2014, using metal oxide-supported Au nanoparticles as the catalyst.¹¹¹ Subsequently, several examples of supported metal-catalyzed conversions from 5-HMF to HCPN under hydrogen pressure in water have been reported. Most of them resulted in almost full conversion of HMF with selectivity toward HCPN ranging from 80% to 94%.¹¹²



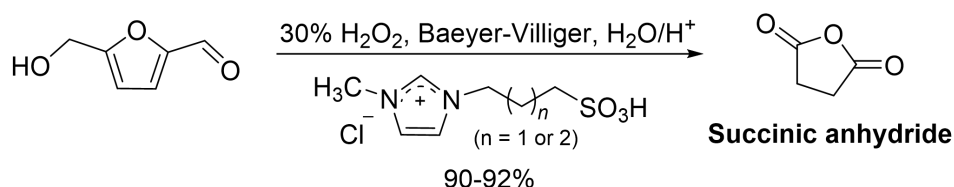
Scheme 36. Preparation of HCPN from HMF ring rearrangement

1,2,4-Benzenetriol can be prepared from HMF catalyzed by soft Lewis acids such as ZnCl_2 , $\text{Zn}(\text{OTf})_2$ and $\text{Fe}(\text{OTf})_2$. When using ZnCl_2 as catalyst, up to 54 mol% yield of 1,2,4-benzenetriol was achieved with 89% conversion of HMF at 70-120 bar N_2 atmosphere in water. After catalytic hydrodeoxygenation of 1,2,4-benzenetriol, 45 mol% cyclohexanone was provided over 5 wt% Pd on Al_2O_3 combined with AlCl_3 catalyst, as an important raw material for polymer products (Scheme 37).¹¹³



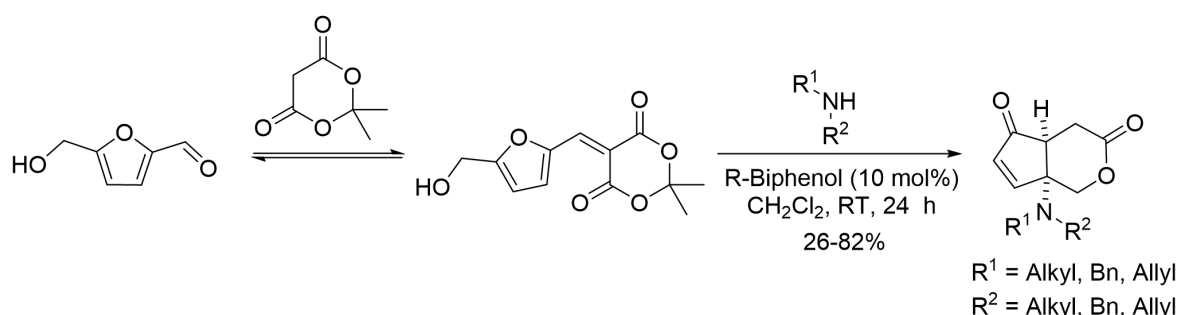
Scheme 37. Preparation of 1,2,4-benzenetriol from HMF as a novel biobased intermediate

The conversion of HMF to succinic anhydride was carried out under 1-(3-alkylsulfonic)-3-methylimidazolium chloride Brønsted acidic ionic liquid catalysis and hydrogen peroxide oxidation. The succinic acid obtained after two Bayer-Villiger oxidation steps is dehydrated under strong acidic ionic liquid to give succinic anhydride in 90-92% yield (Scheme 38).¹¹⁴



Scheme 38. Conversion of HMF to succinic anhydride

Novel aminated fused lactone-cyclopenten-2-ones were prepared by reaction of the Knoevenagel product arising from Meldrum's acid and HMF with a wide range of secondary amines. Through the furan ring-opening-cyclization-lactonization cascade process, highly functionalized δ -lactone fused cyclopenten-2-ones were formed in 26-82% yields under the promotion of (R)-Biphenol which act as a weak Brønsted acid (Scheme 39).¹¹⁵

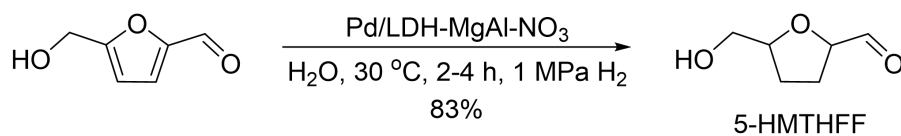


Scheme 39. Production of δ -lactone fused cyclopenten-2-ones from HMF

1.3.2.2.3 Hydrogenation of 5-HMF furan ring

The Han group achieved the hydrogenation of the furanyl ring of HMF while keeping the C=O of aldehyde group intact for the first time. 5-Hydroxymethyltetrahydro-2-furaldehyde (5-HMTHFF) were prepared from HMF over Pd/LDH-MgAl-NO₃ catalyst (LDH: Layered double hydroxide, a tunable heterogeneous catalyst support), the selectivity reached 83% with

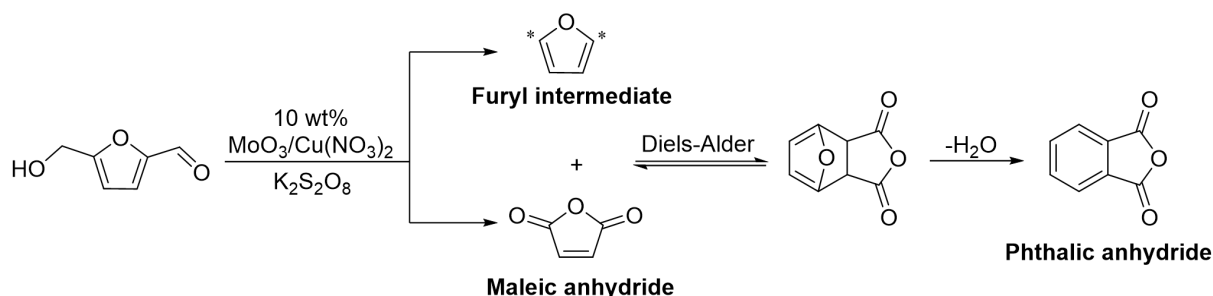
near full conversion of HMF (Scheme 43). This strategy is also applicable to furfural. The use of water as solvent and the special properties of LDH-MgAl-NO₃ are beneficial to inhibit the hydrogenation of C=O groups.¹¹⁶



Scheme 43. Selective conversion of HMF to 5-HMTHFF

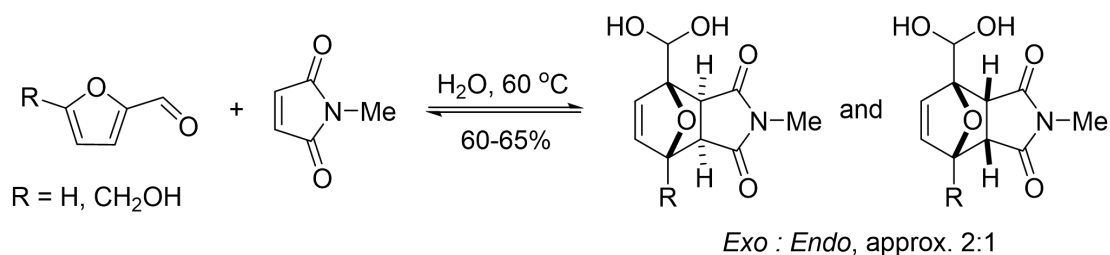
1.3.2.2.4 Diels-Alder cycloaddition of 5-HMF

Lu Lin et al. reported the one-pot synthesis of phthalic anhydride from HMF. MoO₃ and Cu(NO₃)₂ catalysts have a strong synergy in this reaction, promoting the decarbonylation of HMF to an active furyl intermediate, and the oxidation of HMF to maleic anhydride. Diels-Alder cycloaddition of active furyl intermediate with maleic anhydride and subsequent dehydration in one pot, providing phthalic anhydride in the yield of 63% (Scheme 40).¹¹⁷



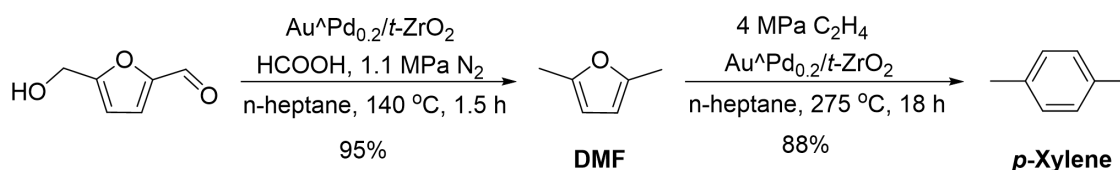
Scheme 40. Pathway of the one-pot conversion of HMF into phthalic anhydride

Bruijninx et al. reported a direct Diels-Alder coupling of HMF or furfural with *N*-methyl maleimide in aqueous media to produce geminal diol products in 60 to 65% yield. The main role of water is thought to be to pull the equilibrium toward the product side by chemically trapping the partially Diels-Alder adducts (Scheme 41).¹¹⁸



Scheme 41. Novel Diels-Alder adducts from HMF or furfural with N-methyl maleimide

A conversion of HMF and ethylene to *p*-xylene was reported by Lei Tao et al. The multifunctional 1% Au⁰Pd_{0.2}/t-ZrO₂ catalyst shows a promoting effect on the rapid formation of DMF, and the dehydration aromatization of DMF and ethylene to produce *p*-xylene, provides over 80% yield of *p*-xylene (Scheme 42).¹¹⁹ It is worth noting that although *p*-xylene has important industrial applications, its toxicity and the adverse effects on human health and environment cannot be ignored.



Scheme 42. Production of renewable *p*-xylene from HMF and ethylene

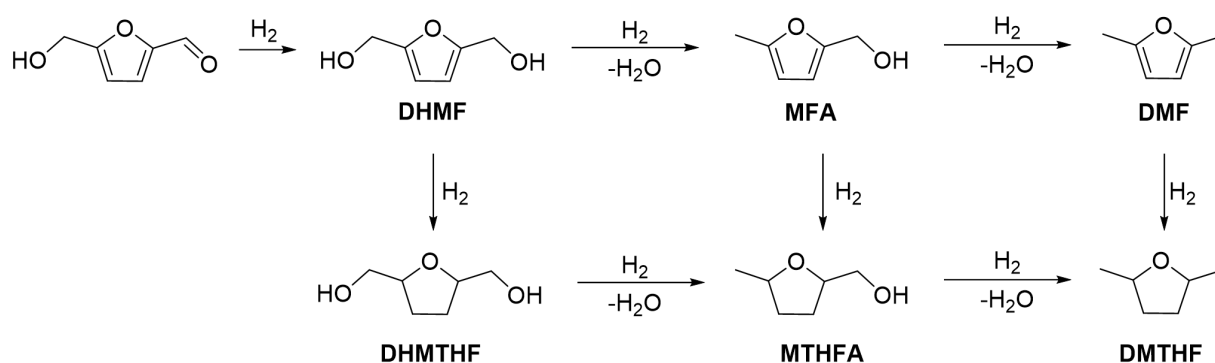
1.3.2.3 Reactions involving the aldehyde functional group

The reactivity of the aldehyde group is attributed to the electrophilic nature of the carbon atom in the carbonyl group. A series of common reactions involving the aldehyde functional groups of HMF will be mentioned in this section, such as reduction, amination, condensation and Morita-Baylis-Hillman reaction.

1.3.2.3.1 Reduction of 5-HMF aldehyde group

The reduction of HMF is an important reaction for converting HMF into valuable chemical intermediates or products with applications in polymers, fuels and other industries. The choice of reducing agents, as well as reaction conditions, will determine the selectivity and yield of

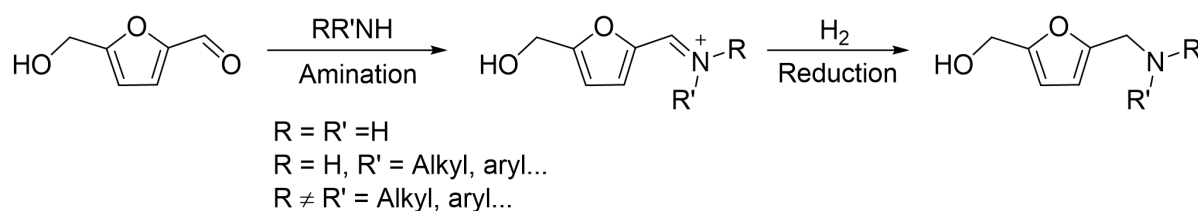
the desired products. The initial reduction of the aldehyde group of HMF leads to the formation of 2,5-bis(hydroxymethyl)furan (DHMF). Further hydrogenation can yield tetrahydrofuran-2,5-dimethanol (DHMTHF), 5-methylfurfuryl alcohol (MFA), (5-methyltetrahydrofuran-2-yl)methanol (MTHFA), 2,5-dimethylfuran (DMF), 2,5-dimethyltetrahydrofuran (DMTHF) etc. (Scheme 44).¹²⁰



Scheme 44. Representative reduction pathways of HMF

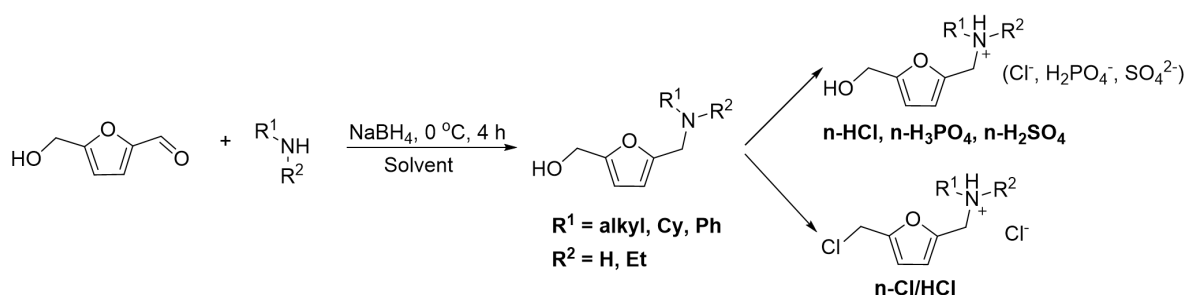
1.3.2.3.2 Amination of 5-HMF aldehyde group

Aldehydes can easily react with ammonia/amines to form imines. The nitrogen atom of ammonia or amines first attacks the carbonyl carbon in HMF, leading to a nucleophilic addition product which then forms an imine intermediate after removal of water. This imine intermediate can be further reduced to primary amines, secondary amines or even tertiary amines (Scheme 45). It is found that under the action of some heterogeneous monometallic (Ni, Co, Ru, Pd, Pt, Rh) and bimetallic (Ni-Cu, Ni-Mn) catalysts, the reaction can provide excellent yields.^{121, 122} As reported by Queen et al., a palladium functionalized MOF/polymer composite (UiO-67/PpPDA/Pd) was employed in the reductive amination of HMF under 5 bar H₂ at 50 °C to provide the amines with good to excellent yields (68-96%).¹²³



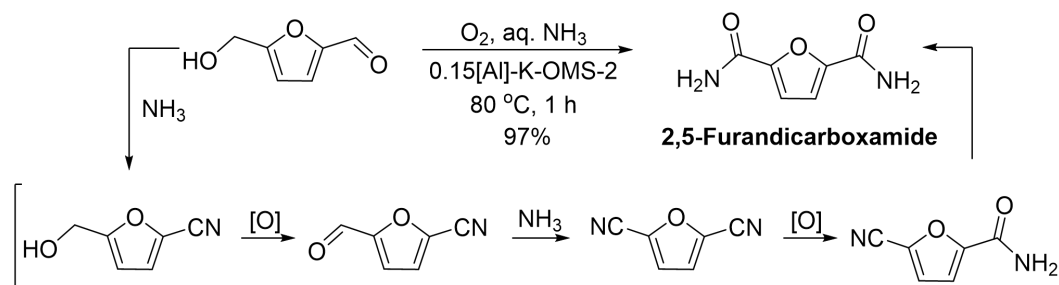
Scheme 45. Reductive amination of HMF and ammonia or amines

The Ananikov group synthesized a series of multifunctional protic ammonium ionic liquids with various inorganic anions from HMF and inorganic acids *via* a carbon-neutral pathway (Scheme 46). The products were studied with respect to their solvent properties as well as their biological ones. The ionic liquids containing sulfate anions have the ability to dissolve cellulose. The introduction of a chlorine atom into the side chain of the furfural unit is beneficial to the bactericidal effect. Physicochemical properties study indicated that most of these ionic liquids were stable when stored for more than six months.¹²⁴



Scheme 46. Synthesis of HMF-derived ionic liquids

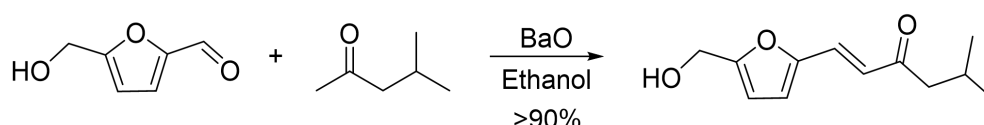
Jie Xu group studied the performance of a series of metal-cation-doped (In^{3+} , Cr^{3+} , Co^{2+} , Ni^{2+} , Cu^{2+} , Zn^{2+} , Al^{3+}) cryptomelanes ($[\text{M}]\text{-K-OMS-2}$) as catalysts in the aerobic ammoxidation-hydration tandem reaction of HMF to 2,5-furandicarboxamide. Among them, the 0.15[Al]-K-OMS-2 catalyst has high activity for alcohol oxidation and nitrile hydration. Al-doping increased the reactivity of lattice oxygen and the strength of strong acid sites, resulting in 97% yield of 2,5-furancarboxamide (Scheme 47).¹²⁵



Scheme 47. Preparation of 2,5-furancarboxamide from HMF

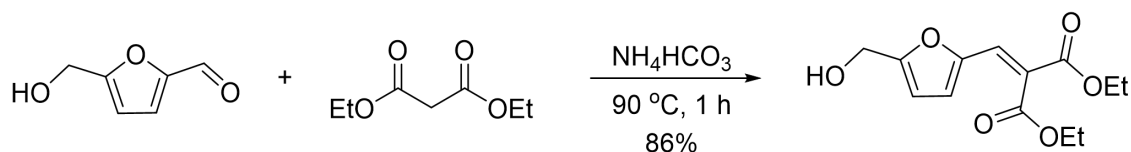
1.3.2.3.3 Condensation involving the 5-HMF aldehyde group

Ketones with enolizable α -H atom can be coupled with HMF to form new C-C bonds *via* cross-aldol condensation reaction in alkaline medium. Examples include the use of alkyl ketones, cycloalkanones and α,β -unsaturated ketones. Recently, Vigier et al. used an efficient alkaline metal oxide catalyst (BaO) to promote the conversion of HMF and methyl isobutyl ketone (MIBK) into 1-(5-(Hydroxymethyl)furan-2-yl)-5-methylhex-1-en-3-one through aldol condensation, with the yield exceeds 90% (Scheme 48).¹²⁶



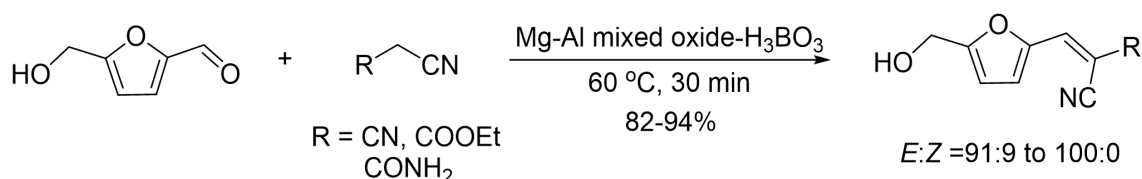
Scheme 48. BaO catalyzed aldol condensation of HMF and MIBK

Schijndel et al. reported the Knoevenagel condensation of furan aldehydes and diethyl malonate in the presence of ammonium salts. A 86% yield of HMF derived condensation product was obtained when ammonium bicarbonate was used as a catalyst (Scheme 49).¹²⁷



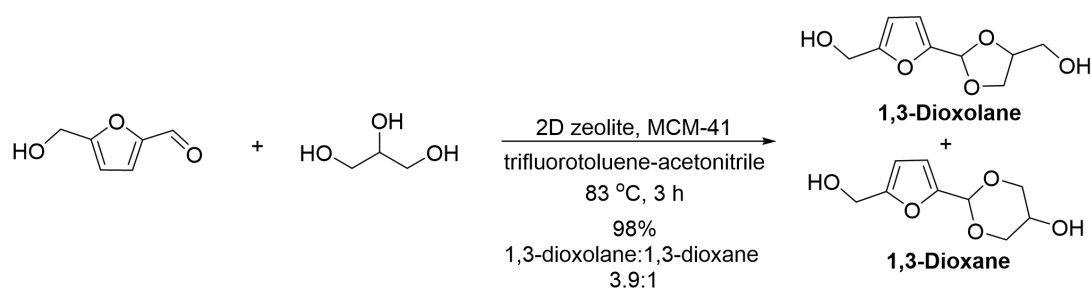
Scheme 49. Condensation of HMF and diethyl malonate

Mancipe et al. reported the boric acid deposited on hydrotalcite catalyzed Knoevenagel condensation of HMF and active methylene compounds to afford a series of HMF derivatives containing an acrylonitrile moiety. The acid-base sites associated with the catalyst can accelerate the reaction leading to high yields (82-94%) and high (*E*)-isomer selectivity (91:9 to 100:0) of condensation products (Scheme 50).¹²⁸



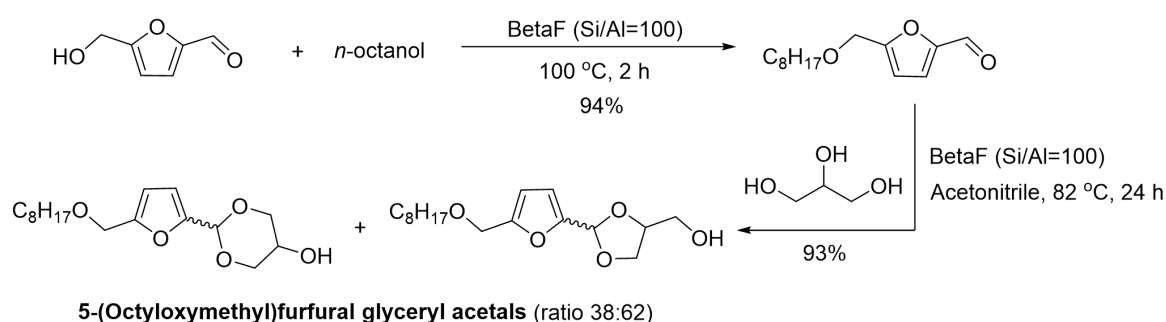
Scheme 50. Condensation of HMF and active methylene nitrile

In 2018, a protocol was developed by Corma et al. to prepare diols (which are potential monomers) from HMF and glycerol by acetalization reaction under acid-catalyzed conditions (Scheme 51). A 2D zeolite (ITQ-2) and a structured mesoporous material (MCM-41) with mild Bronsted acid sites exhibited excellent selectivity for the reaction. The use of zeolite favors to the stabilization of the carbocations formed from the protonated hemiacetal. The secondary hydroxyl group or one primary hydroxyl group of glycerol attacks the carbocation to obtain either a 1,3-dioxolane or a 1,3-dioxane.¹²⁹



Scheme 51. Valuation of HMF and glycerol into diol monomers

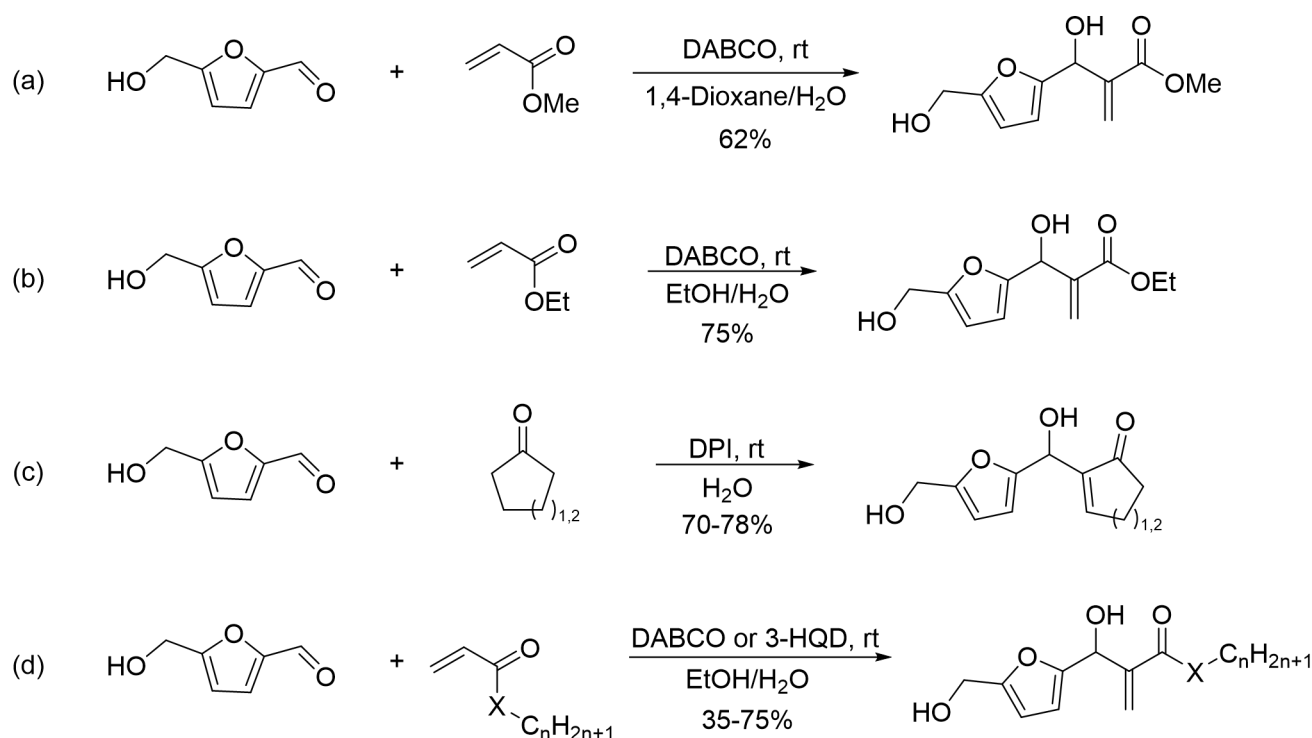
In the same year, Corma group developed another protocol targeting biomass-derived non-ionic surfactants from HMF, fatty alcohols and glycerol *via* etherification and acetalization reactions under acid-catalyzed conditions. 5-Octyloxymethylfurfural is obtained by etherification of HMF and *n*-octanol, and then the aldehyde of 5-octyloxymethylfurfural is attacked by glycerol in the presence of BetaF zeolite, leading to the 5-(octyloxymethyl)furfural glycerol acetal was finally obtained (Scheme 52).¹⁰⁵



Scheme 52. Valuation of HMF, *n*-octanol and glycerol into biobased surfactants

1.3.2.3.4 Morita-Baylis-Hillman reaction of 5-HMF

HMF has been used as substrate in Morita-Baylis-Hillman reaction (MBH) reaction for the first time in 2001, using DABCO as stoichiometric base, leading to 62% of corresponding product after 36 h in 1,4-dioxane/H₂O (1:1, v/v) (Scheme 53a).¹³⁰ In 2015, Tan et al reported the MBH reaction of HMF (and furfural) and its derivatives using a combination of bio-based solvents such as EtOH/H₂O (1:1, v/v) to replace traditional solvents, with yields up to 90% in the presence of DABCO after 24 h (Scheme 53b).¹³¹ In 2019, Tan et al. developed a series novel functionalized scaffolds from HMF, glycosyloxymethylfurfural with cycloalkenones *via* the MBH reaction in pure water with yields in the 70-78% range after 30 h when using 6,7-dihydro-7-hydroxy-5*H*-pyrrolo[1,2-*a*]imidazole (DPI) as catalyst (Scheme 53c).¹³² In 2021, the strategy was applied to the preparation of original biobased amphiphiles from hydrophobic alkenes. These amphiphiles were shown to emulsify both polar and apolar oils, providing W/O and O/W emulsions, which means that could be used as relevant alternatives to traditional petroleum-based polyethoxylated surfactants (Scheme 53d).¹³³



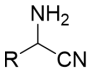
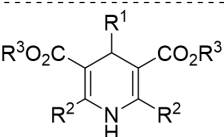
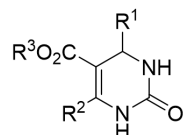
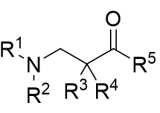
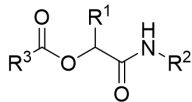
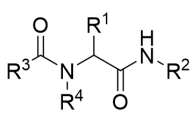
Scheme 53. MBH Reaction involving HMF

1.3.3 Focus on multi-component reactions involving 5-HMF

1.3.3.1 State of the art on MCRs

Multi-component reactions (MCRs) continue to be a vibrant and evolving field in organic synthesis. MCRs offer an efficient and atom-economic approach for the construction of complex molecules by combining three or more reactants/reagents in a single reaction vessel and usually involves the formation of multiple new bonds, such as C-C, C-N, C-S bond. They have gained significant attention for their potential in streamlining synthesis processes and improving overall efficiency.¹³⁴ The ability of aldehydes to act as electrophiles and form new bonds makes them valuable components in MCRs, allowing the construction of complex molecules efficiently. Classic name reactions include the Strecker, Hantzsch, Biginelli, Mannich, Passerini and Ugi multi-component reaction discovered earlier, all of them involving the participation of an aldehyde as one of the substrates (Table 3).

Table 3. Classical multi-component reactions involving aldehydes

$RCHO + NH_3 + HCN \longrightarrow$		Strecker, 1850
$R^1CHO + NH_3 + R^2C(=O)CH_2COOR^3 \longrightarrow$		Hantzsch, 1882
$R^1CHO + H_2N-C(=O)-NH_2 + R^2C(=O)CH_2COOR^3 \longrightarrow$		Biginelli, 1891
$HCHO + R^1-NH-R^2 + R^3C(=O)CH_2R^4 \longrightarrow$		Mannich, 1912
$R^1CHO + R^2NC + R^3COOH \longrightarrow$		Passerini, 1921
$R^1CHO + R^2NC + R^3COOH + R^4NH_2 \longrightarrow$		Ugi, 1959

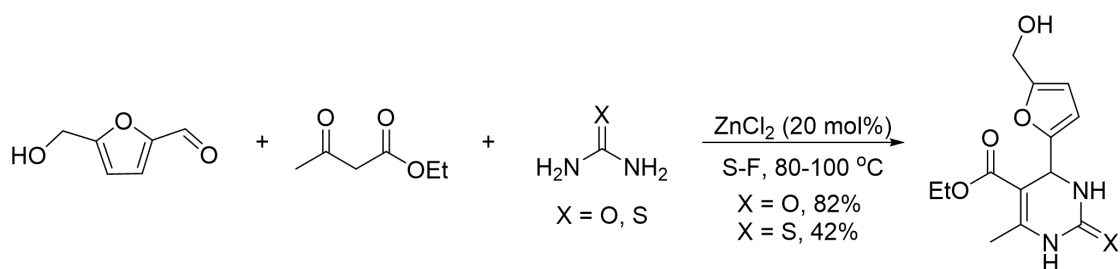
MCRs have been recognized as the preferred method for designing and discovering bioactive compounds. The scaffolds derived from the MCRs can be considered as a novel synthetic hub with enormous diversity, from which further synthetic steps can lead to the synthesis of libraries of advanced drug-like compounds. Reviews on the use of MCRs in terms of synthesis, structure and biological activity of derived molecules show the importance of the field, with the emergence of new reactions making a wider range of organic scaffolds becoming available.¹³⁴

1.3.3.2 MCRs involving 5-HMF

Multicomponent reactions encourage one-pot synthesis processes towards target molecules aiming at avoiding energy consumption and resource waste in trivial purification processes. In such reactions, the factors that need to be addressed are notably the availability of starting materials, the reaction selectivity and the tolerance and environmental impact of the substrates. MCRs based on carbonyl condensation are the most common strategy to construct complex molecules. In this section, we will focus on the use of HMF or analogs as carbonyl substrate in multi-component reactions.

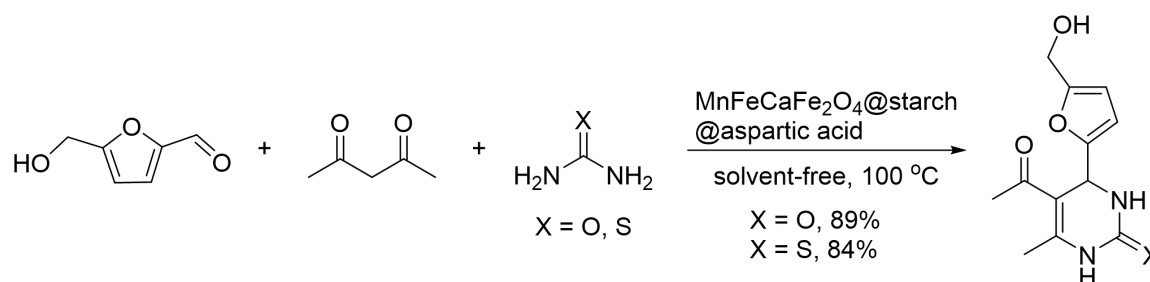
1.3.3.2.1 5-HMF in Biginelli reaction

Fan et al. investigated the reactivity of HMF in Biginelli reaction, preparing a series of functionalized dihydropyrimidinones in 30-86% yields. For example, reaction of HMF with ethyl acetoacetate and urea or thiourea at 80-100 °C using Lewis acid ZnCl_2 (20 mol%) as a catalyst, yielding 82% and 42% corresponding dihydropyrimidinones after 16 h and 24 h, respectively (Scheme 54).¹³⁵



Scheme 54. Lewis acid catalyzed Biginelli Reaction involving HMF

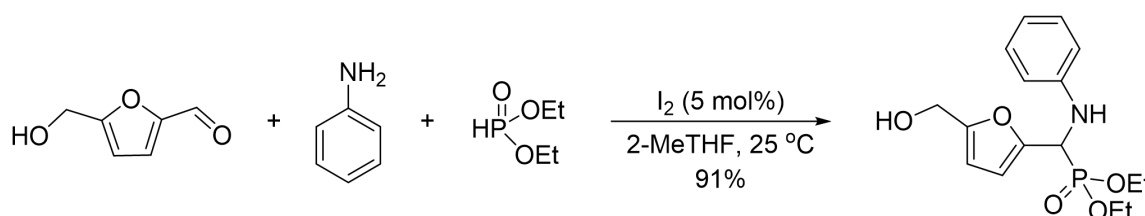
Afradi et al. designed a nanocatalyst aspartic-acid-loaded starch-functionalized Mn-Fe-Ca ferrite magnetic nanoparticles for the efficient synthesis of dihydropyrimidine derivatives in solvent-free conditions. HMF was explored as one of the substrates, reacting with acetylacetone, urea or thiourea for 15 min at 100 °C to yield 89% and 84% of the dihydropyrimidine product, respectively (Scheme 55).¹³⁶



Scheme 55. Nanocatalyst catalyzed Biginelli Reaction involving HMF.

1.3.3.2.2 5-HMF in Kabachnik-Fields reaction

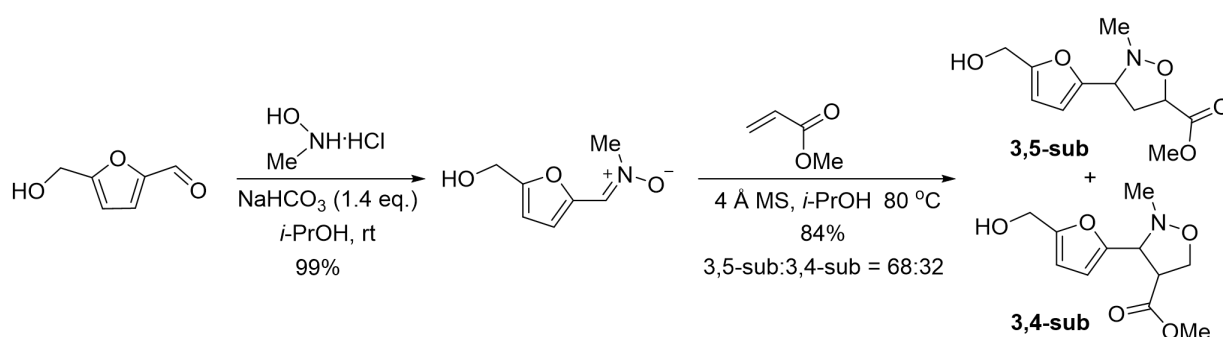
Fan et al. investigated the use of biomass-derived HMF in a one-pot Kabachnik-Fields reaction for the first time. A variety of furan-based α -amino phosphonates were prepared in moderate to excellent yields (31-91%) with iodine as the catalyst and biobased 2-methyltetrahydrofuran (2-MeTHF) as the solvent. Aliphatic and aromatic amines, dialkyl phosphites are well tolerated in this reaction. As an example, the reaction of HMF, aniline and diethyl phosphite resulted in the formation of 91% of target α -amino phosphonate product (Scheme 56).¹³⁷



Scheme 56. Kabachnik-Fields reaction involving HMF

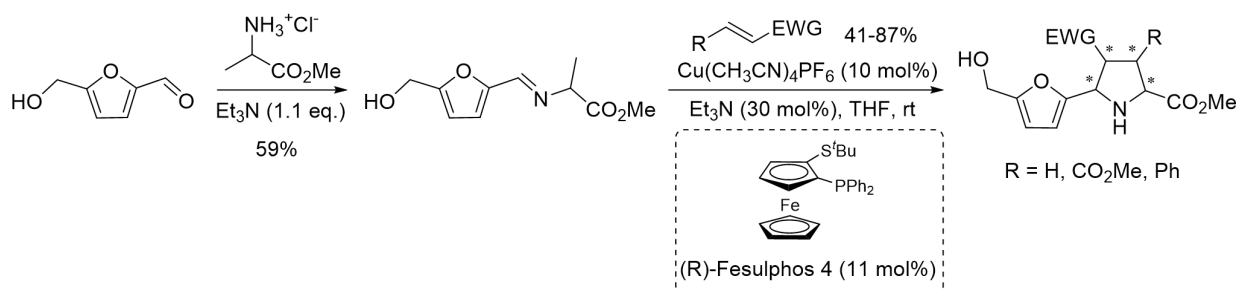
1.3.3.2.3 5-HMF in dipolar cycloaddition reactions

Wang et al investigated the synthesis of 3-furanyl isoxazolidines from the dipolar cycloaddition of HMF-based nitrones with electro-deficient olefins. Up to 84% and 75% combined isomer yields were provided in stepwise and one-step reactions, respectively. For example, commercially available *N*-methyl hydroxylamine hydrochloride and HMF are condensed in isopropanol to obtain HMF-based nitron, sodium bicarbonate is used to neutralize excess hydrochloride. The isolated nitron was subsequently undergo a cycloaddition with methyl acrylate in isopropanol to provide 84% yield of 3,5-sub and 3,4-sub regioisomers mixture (Scheme 57).¹³⁸



Scheme 57. Dipolar cycloadditions of HMF

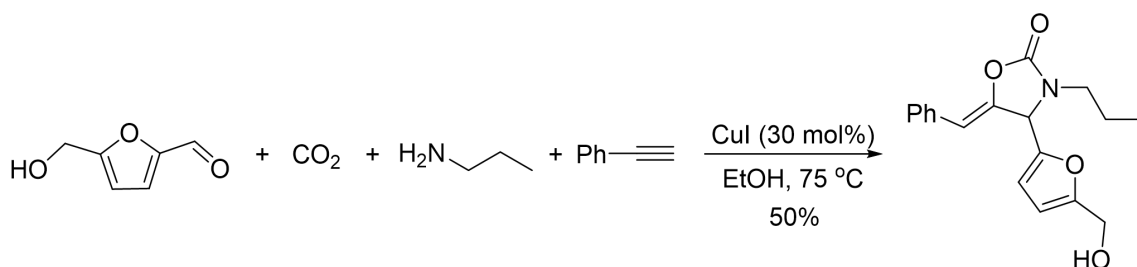
The catalytic asymmetric 1,3-dipolar cycloaddition was reported by Cristobal et al. The condensation of HMF with commercially available alanine methyl ester hydrochloride first led to the formation of HMF-derived iminoesters using Et₃N as base. By using (*R*)-Fesulphos/Cu(CH₃CN)₄PF₆ complex as catalyst, the subsequently cycloaddition of HMF-derived iminoesters with activated alkenes provides enantiomerically enriched heterocyclic scaffolds in 41-87% yield with high enantioselectivity (79-99% ee) (Scheme 58).¹³⁹



Scheme 58. Asymmetric dipolar cycloadditions of HMF

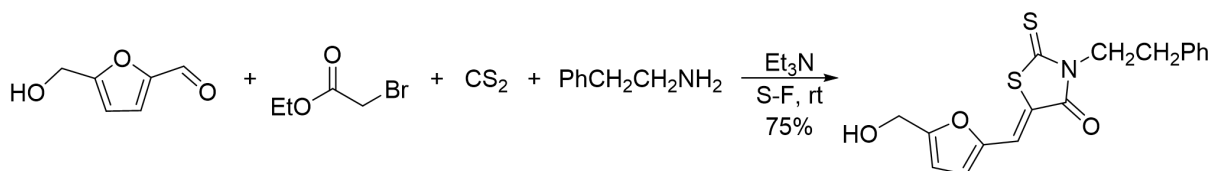
1.3.3.2.4 Other MCRs involving 5-HMF

In 2018, Wu et al. reported a Cu-catalyzed four-component coupling of furanic aldehydes with CO₂, terminal aromatic alkynes and primary aliphatic amines to construct oxazolidinones, using ethanol as solvent. A series of 1,3-oxazolidin-2-ones were obtained in 17-84% yield when CuI was used as catalyst. In most cases, the yield of the target product in this reaction is low. As an example, 50% yield of 1,3-oxazolidin-2-one product was provided by the reaction of HMF, CO₂, propylamine and phenylacetylene (Scheme 59). The low yield from furanic aldehydes can presumably be attributed to the instability of the furan ring which is possible led to a series of side reactions such as furan ring-opening, furan ring polymerization, and polymeric humins formation.¹⁴⁰



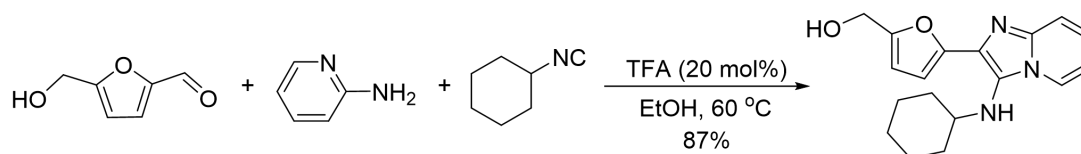
Scheme 59. Construction of oxazolidinones from HMF or furfural

Rhodanine-furan hybrids were synthesized *via* one pot stereoselective reaction in solvent-free (S-F) conditions by Sabahi-Agabager et al. The reaction of bio-based furanic aldehydes (HMF, CMF, furfural) with ethyl bromoacetate, carbon disulfide and primary amines (phenethylamine, benzylamine and 2-methoxyethylamine) give 45-75% yield of rhodamine-furan hybrids at room temperature in the presence of Et₃N (Scheme 60).¹⁴¹



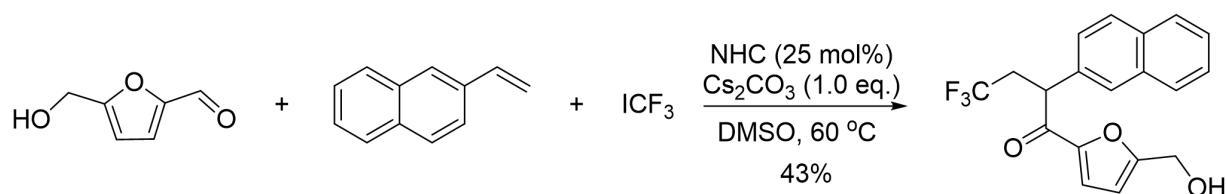
Scheme 60. Construction of rhodamine-furan hybrids from furfural, HMF and CMF

Victoria de la Sovera et al. investigated the reactivity of HMF in a three-component Groebke Blackburn-Bienaymé reaction. The reaction of HMF with cyclic amidines (5- or 6-membered) and isocyanides afforded a new imidazoheterocycles library in the presence of 20 mol% of trifluoroacetic acid (TFA). The maximum yield of 87% was obtained using 2-aminopyridine and isocyanocyclohexane as starting materials react with HMF at 60 °C (Scheme 61)..¹⁴²



Scheme 61. Groebke Blackburn-Bienaymé Reaction involving HMF

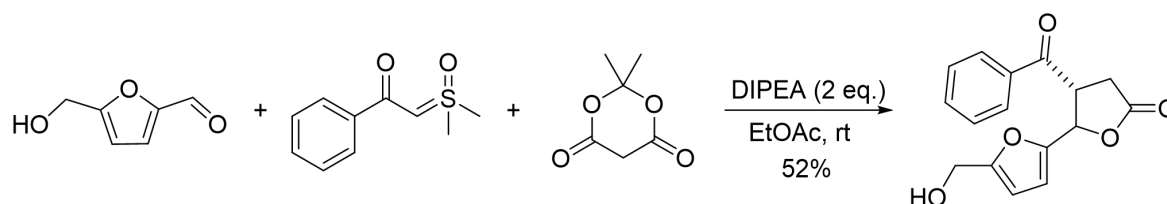
HMF reactivity was investigated in several other MCRs. Yang et al. employed a strategy of biomimetic *N*-heterocyclic carbene catalysis to assemble HMF with an alkene, for example vinyl naphthalene, and a perfluoroalkyl reagent such as trifluoriodomethane in the presence of Cs_2CO_3 , providing access to the corresponding α -aryl- β -perfluoroalkyl ketone as shown in Scheme 62 in 43% yield. Compared to the benzaldehyde (81%) and furfural (75%) substrates, the low yield of HMF substrate is most likely attributed to the sensitivity of the hydroxyl group present in HMF.¹⁴³



Scheme 62. Synthesis of fluorinated analogues of α -aryl ketones

Another multi-component reaction of aldehydes, sulfoxonium ylides and Meldrum's acid was conducted by Peng et al in the presence of *N,N*-diisopropylethylamine (DIPEA), the reaction of electron-rich aromatic aldehydes with Meldrum's acid and sulfoxonium ylides produced trans- β,γ -disubstituted- γ -butyrolactones (relative configuration was assigned based on X-ray diffraction of a representative example) in good yields (65-98%). However, HMF led to a

lower 52% yield of the corresponding product possibly due to competitive reaction of the free hydroxyl group in HMF with Meldrum's acid causing side reactions (Scheme 63).¹⁴⁴



Scheme 63. Synthesis of HMF derived disubstituted γ -butyrolactone

1.4 Conclusion and objectives of the thesis

Biomass-derived platform chemicals play a crucial role in the development of sustainable and eco-friendly chemical processes. These chemicals are obtained from renewable biomass resources, such as agricultural residues, forest biomass, and dedicated energy crops, providing an alternative to finite fossil resources. Biomass feedstocks capture carbon dioxide during their growth, helping to mitigate the overall carbon footprint of chemical production. Biomass-derived platform chemicals serve as building blocks for the production of a wide range of chemical products, including biofuels, bioplastics, and biochemicals. Their importance extends beyond chemical production to impact energy, agriculture, and environmental conservation, contributing to the overall transition toward a more sustainable and resilient future.

HMF contains multiple functional groups, including an aldehyde, a hydroxyl group, and an aromatic ring. These functional groups provide various reaction sites, allowing their simultaneous incorporation in target molecules *via* MCRs. The hydroxyl group in HMF can participate in various reactions, providing additional avenues for introducing diversity in the product. The conjugated system in the furan ring of HMF enhances its reactivity and makes it amenable to various reactions involving π electrons. The aldehyde group in HMF is highly reactive, making it a versatile electrophile in MCRs. HMF can be transformed into a variety of derivatives through different reaction pathways. This versatility makes it valuable in the

synthesis of diverse products in a single step or a sequence of steps within an MCR, including those with potential applications in drug discovery and medicinal chemistry.

Overall, the sustainable nature of HMF derived from biomass increases its attractiveness as a precursor for the production of fine chemicals, in line with the principles of green chemistry and renewable resources. The combination of functional group diversity, reactivity, and sustainability makes HMF a suitable and attractive substrate for multicomponent reactions, providing a versatile platform for the synthesis of a variety of compounds.

In order to investigate how the specific reactivity of HMF could be combined with the efficiency of some multicomponent reactions, we have chosen nitrogen-containing heterocycles as targets. Such compounds are widely studied in natural products chemistry and pharmaceutical sciences, due to their widely dispersed biological activities such as antimalarial, antibacterial, antihypertensive, etc. The use of different combinations of substrates to construct new diversely functionalized heterocycles will expand the structural scope of such complex molecules. The aim here is to investigate how HMF, with its unique structural features and reactivity, can be included as a pertinent aldehyde in multi-component synthetic schemes toward nitrogen-containing heterocycles. The results of our investigations on the synthesis of HMF derived 1,5-benzodiazepines and 1,4-dihydropyridines are detailed in the next two chapters.

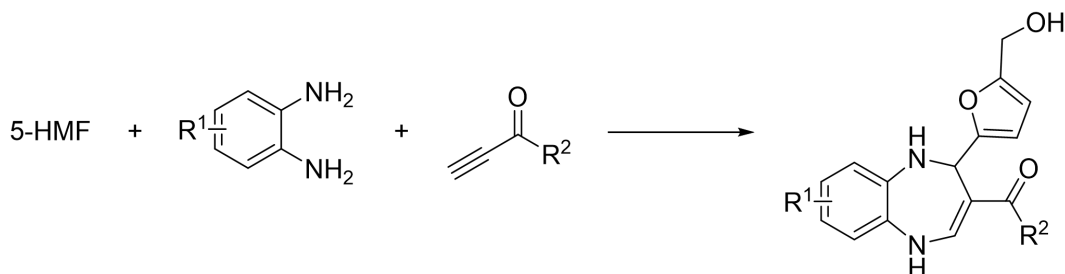
Chapter II

The [4+2+1] cycloaddition involving 5-HMF towards 1,5-benzodiazepines

Chapter II. The [4+2+1] cycloaddition involving 5-HMF towards 1,5-benzodiazepines

2.1 Introduction

In the late sections of the bibliographic chapter we have reviewed the early results related to the application of the renewable platform molecule 5-HMF towards fine chemicals in one-pot MCRs. In the first part of my thesis, we have developed this strategy using another reaction, that is the [4+2+1] cycloaddition of 5-HMF with a diamine and an alkynone to generate the seven-membered 1,5-BZD scaffold (Scheme 64).



Scheme 64. Reaction of HMF, diamines and alkynones towards 1,5-BZDs

In this chapter, we will first describe the results of our detailed methodological investigation of the [4+2+1] cycloaddition reaction of 5-HMF with *o*-phenylenediamine and but-3-yn-2-one. The study focuses first on the search for the most appropriate catalyst-solvent couple, before evaluating the structural scope of the reaction using diversely substituted diamines, alkynones or alkyl alkynoates and 5-HMF derivatives. Before that, we provide a brief overview of the interest and synthesis of 1,5-benzodiazepines.

Benzodiazepines (BZDs) are important heterocyclic compounds due to their rich biological and pharmacological activities.^{145, 146} An historic review reported in 1968 by Archer and Sternbach, gave a relatively comprehensive summary of the early chemistry towards BZDs.¹⁴⁷ Over subsequent decades, important research work on the biological viewpoint gradually confirmed the interest of BZDs. Still now, considering their great potential in the

pharmaceutical field, this expanding family of molecules continues to attract the attention of chemists for diversifying the structures and developing efficient synthetic schemes. The six representative basic ring structures of BZDs (1,2; 1,3; 1,4; 1,5; 2,3; 2,4-BZDs, with numbering starting from the N side closest to the benzene ring) are shown in Figure 7.

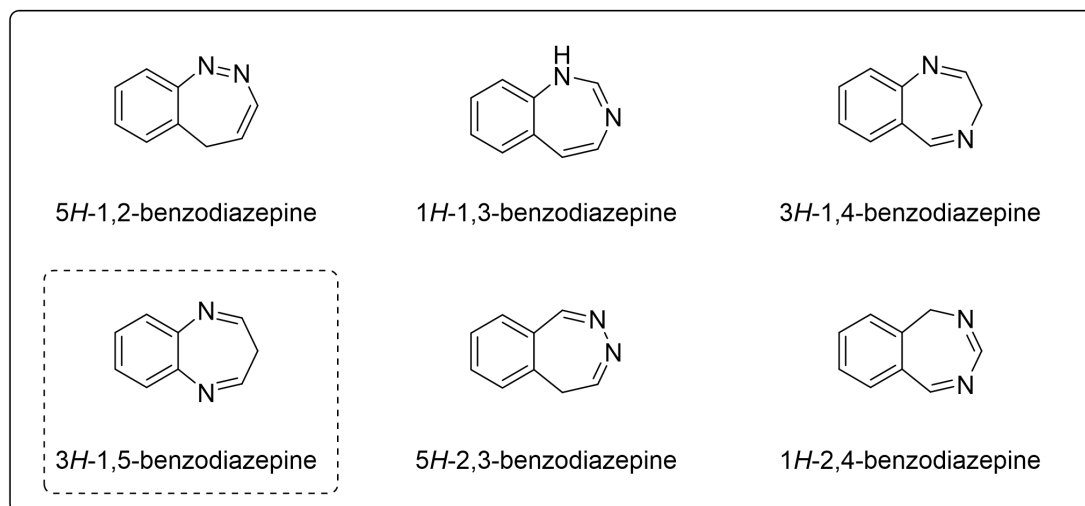


Figure 7. Basic ring structures of benzodiazepines

2.1.1. Interest of benzodiazepines

Benzodiazepines are bicyclic benzene-fused seven-membered ring compounds containing two nitrogen atoms on the seven-membered ring. They are widely used as sedatives, hypnotics, anti-anxiety and anticonvulsants by facilitating the actions of the natural brain neurotransmitter γ -aminobutyric acid (GABA) to decrease the excitability of neurons. Since the pharmacology of BZDs is influenced by differences in affinity for specific GABA_A (γ -aminobutyric acid type A) receptor subtypes, constructing BZDs is a promising avenue to explore differential pharmacological activities.¹⁴⁸

The 1,5-BZDs class, are the most studied BZDs. They have their two nitrogen atoms at positions 1 and 5 of the seven-membered ring and can also be considered as a 2, 3-benzo annelated derivatives of 1, 4-diazepines. 1,5-BZDs are depicted either in the form of imines (diimine and monoimine) or enamines (Figure 8).^{147, 149}

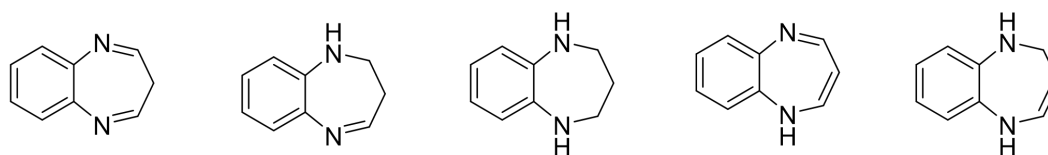


Figure 8. Different forms on the seven-membered ring of 1,5-benzodiazepines

The family of 1,5-BZDs is an important class of psychotropic pharmacophores particularly as sedatives and antiepileptic agents.^{150, 151} Some 1,5-BZDs are also reported to be non-nucleoside inhibitors of HIV-1 reverse transcriptase.¹⁵² Several typical marketed examples are presented in Figure 9.^{153, 154, 155, 156} Among them, Clozapine is an atypical antipsychotic drug and has been on the market since 1972. Arfendazam, synthesized in the 1970s, is a partial agonist at GABA_A receptors and therefore has relatively mild sedative effects. Clobazam is an important long-acting 1,5-BZD that was originally developed in the early 1970s as an anxiolytic and is currently marketed as an adjunctive treatment for epilepsy and anxiety disorders. Nevirapine is an acquired immunodeficiency syndrome (AIDS) prevention drug, especially for HIV-1 infection and was approved for medical use in the United States in 1996. In addition to these activities, 1,5-BZDs are also reported to possess analgesic, anti-inflammatory, antimicrobial, anticonvulsant and other activities.^{157, 158}

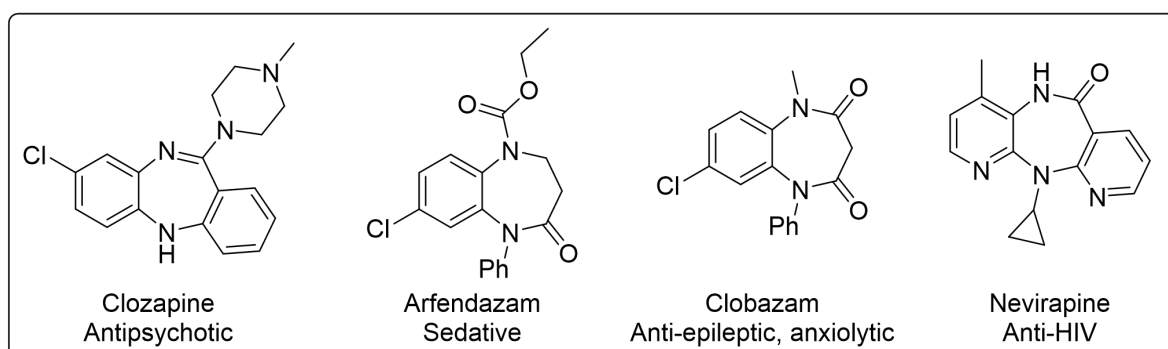


Figure 9. Marketed molecules possessing the 1,5-diazepine skeleton

2.1.2 Synthetic routes towards 1,5-benzodiazepines

2.1.2.1 Strategies and mechanism

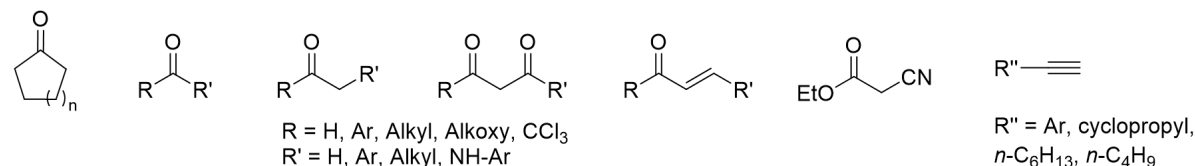
The 1,5-BZD skeleton can be accessed by different methods through a classical sequence involving only two components, namely *o*-phenylenediamine and an electrophilic partner, or *via* multi-component protocols when more than one electrophilic partner is used.^{159, 160} With respect to the amine substrate, multi-component strategies still essentially use substituted *o*-phenylenediamines to provide the aromatic ring and the two nitrogen atoms on the seven-membered ring. More diversely functionalized 1,5-BZDs can be synthesized through multi-component reactions. Actually, most examples of three-component reactions are based on a 4+2+1 combination for building the seven-membered ring, however a few four-component approaches based on a 4+1+1+1 construction have also been reported.

Significant diversity can arise from the electrophilic partners, including different substituted ketones or alkynes (Scheme 65). The most popular methods involve the condensation of *o*-phenylenediamine and a ketone, followed by cyclization. In three-component strategies, reactions of β -dicarbonyl compounds with benzaldehydes generally exhibit satisfactory efficiency. In some cases, substituted heterocyclic aldehydes such as thiophene, furan, thiazole, pyridine aldehydes and aliphatic aldehydes were also used in the reaction.¹⁶¹⁻¹⁶⁷ The combination of aldehydes with 3-butyne-2-one has also been reported once.¹⁶⁷ The use of combinations of two couples of electrophilic components, such as α -diketone and 1,3-cyclodione, α -diketone and α,β -unsaturated carbonyl compounds have also been reported for the access to 1,5-BZDs.¹⁶⁸⁻¹⁷¹ One-pot multiple step 4-component towards 1,5-BZDs, examples involving a *N,N*-dimethylformamide dimethyl acetal as a one-carbon building block reacting in ethanol with *o*-phenylenediamines, aldehyde derivatives/isatin and aromatic ketones have been reported.^{170, 171}

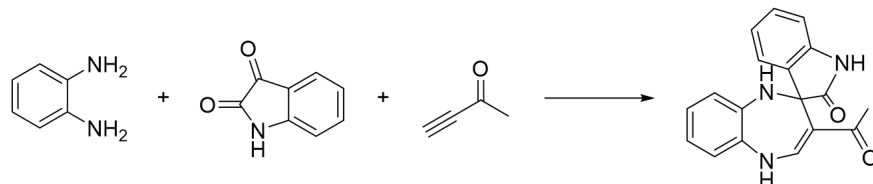
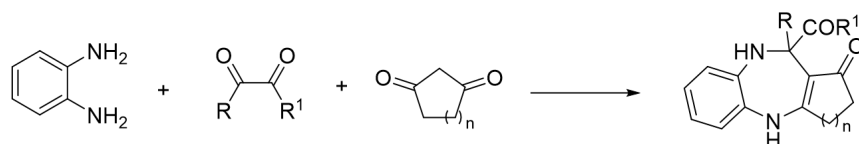
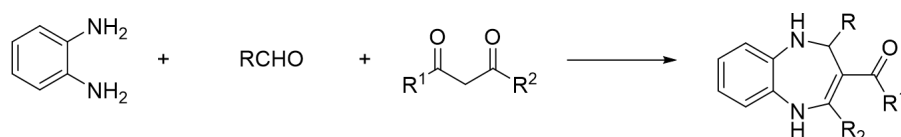
Two component reaction access to 1,5-benzodiazepines:



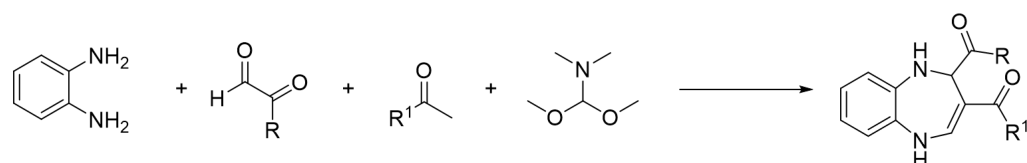
Electrophilic partners:



Three-component reaction access to 1,5-benzodiazepines:



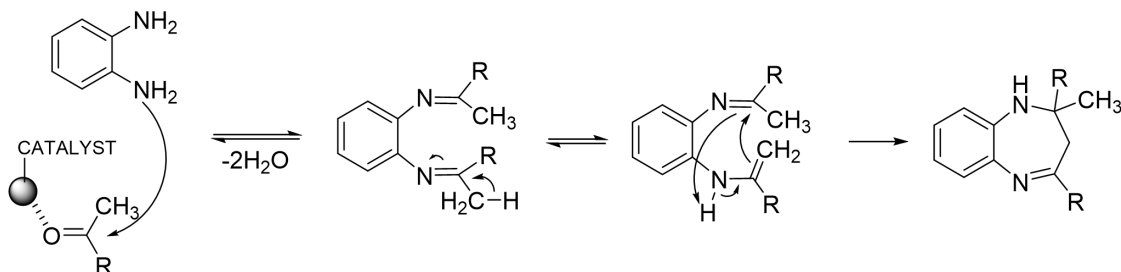
Four component reaction access to 1,5-benzodiazepines:



Scheme 65. Synthetic routes towards 1,5-benzodiazepines

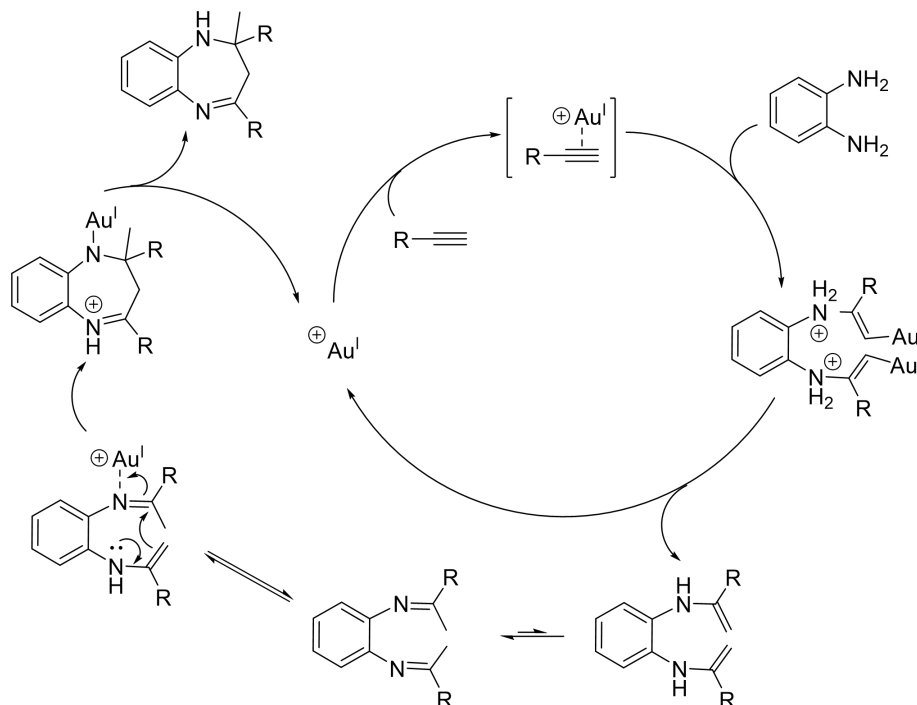
The classic pathway involves the coupling of the diamine with an electrophilic ketone most often α,β -unsaturated carbonyl compounds, β -diketones and β -ketoesters. The role of the catalyst in this reaction is to enhance the electrophilicity of the carbonyl carbon by activating the oxygen atom of the carbonyl group, thereby promoting the nucleophilic attack of *o*-phenylenediamine on the ketones to generate the imine intermediates (also called the Schiff

base intermediates). Then, the isomerization of the imine to the enamine is achieved through hydrogen transfer, before the final cyclization giving rise to the 1,5-BZD scaffold. A general mechanism involving *o*-phenylenediamine and ketones is demonstrated in Scheme 66.



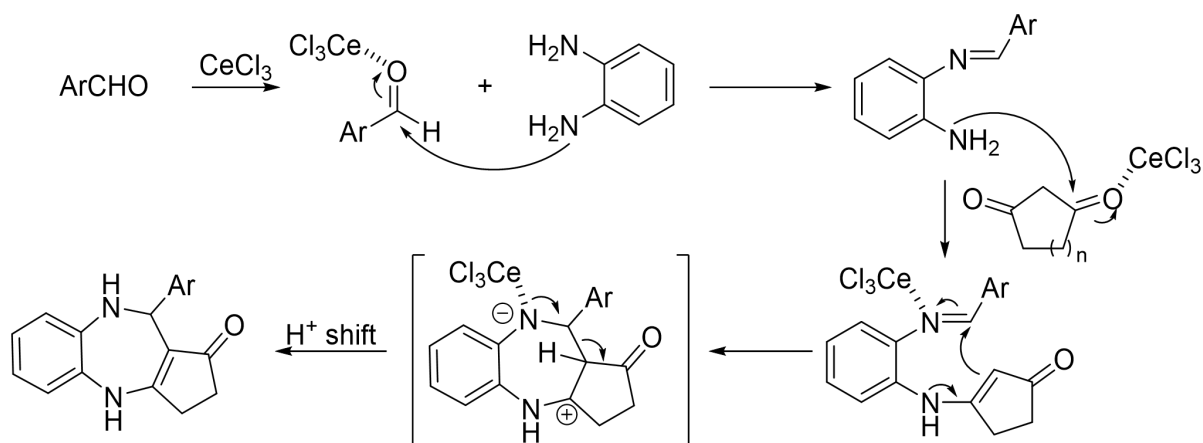
Scheme 66. General mechanism for the synthesis of 1,5-BZDs involving *o*-phenylenediamine and ketones

In the case of terminal alkynes used as electrophilic substrate, a gold(I)-catalyzed tandem amination/cyclization mechanism was proposed by Liu et al.¹⁷² Once the gold catalyst activates the alkyne, reaction of *o*-phenylenediamine with two molecules of alkynes forms the *bis*-enamine, which then undergoes isomerization *via* hydrogen atom transfer to form the *bis*-imine. Finally, this intermediate *bis*-imine undergoes intramolecular cyclization to provide the 1,5-BZD, as depicted in Scheme 67.



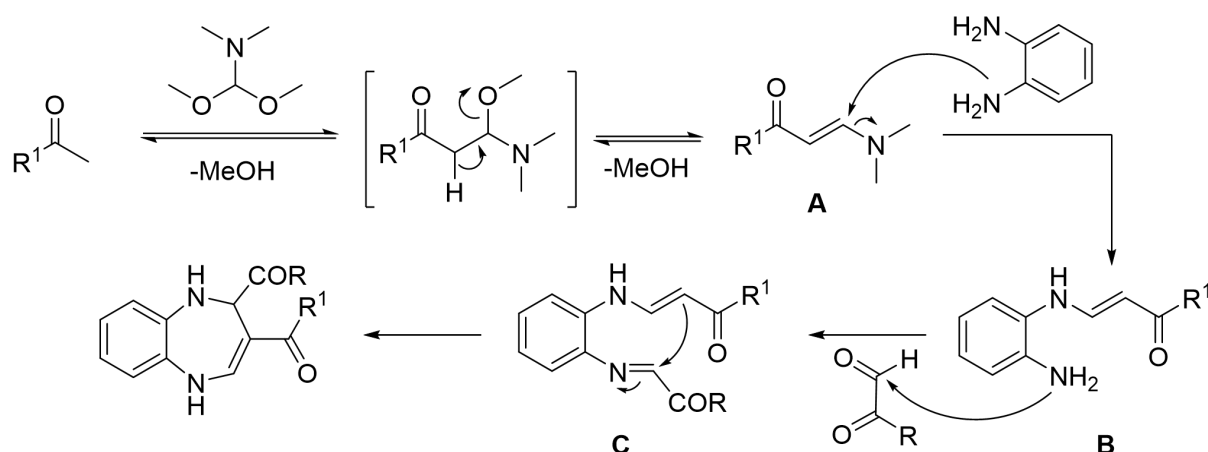
Scheme 67. Gold catalyzed tandem amination/cyclization of alkynes and *o*-phenylenediamine

When two different electrophilic partners are used, more diversely functionalized 1,5-BZDs can be synthesized. For example, Wang et al. reported the synthesis of a 1,5-BZD from *o*-phenylenediamine, 1,3-cyclodione and some aldehydes under Lewis acid catalysis (the Lewis acid here refers to cerium(III) chloride) for which they proposed the mechanism depicted in Scheme 68.¹⁶³



Scheme 68. An example of the three-component reaction mechanism towards 1,5-BZDs

For the other type of four-component reaction involving the dimethylformamide dimethyl acetal as one-carbon fragment. Wang et al. proposed a plausible mechanism shown in Scheme 69.¹⁷⁰ First, a nucleophilic substitution reaction occurs between the enolized aromatic ketone and *N,N*-dimethylformamide dimethyl acetal to give a chalcone intermediate A with removal of two molecules of methanol. Then, nucleophilic addition of one amino group of *o*-phenylenediamine onto the chalcone intermediate A leads to the formation of enamine intermediate B. Subsequently, the remaining amino group in intermediate B attacks the electrophilic carbonyl carbon of the α -diketone substrate, leading to the corresponding intermediate C through a nucleophilic addition-dehydration reaction. Finally, intermediate C undergoes intramolecular cyclization and proton transfer to give the 1,5-BZD product.



Scheme 69. Mechanism of four component reaction towards 1,5-BZDs

2.1.2.2 Reaction conditions

In terms of catalysis, Lewis acids, Brønsted acids, metal-based catalysts (supported catalysts and nano-catalysts) have been shown to successfully promote the formation of 1,5-BZD.^{163, 173-175} For example, Lewis acids such as molecular iodine (I_2), silver nitrate ($AgNO_3$), metal halides including cerium chloride ($CeCl_3$), zinc chloride ($ZnCl_2$), ferric chloride ($FeCl_3$), indium chloride ($InCl_3$), indium bromide ($InBr_3$), ytterbium chloride ($YbCl_3$), lanthanide salts such as yttrium triflate ($Yb(OTf)_3$), scandium triflate ($Sc(OTf)_3$) and ceric ammonium nitrate (CAN) were reported for BZDs synthesis.

Among Brønsted acids, acetic acid, trifluoroacetic acid, *p*-nitrobenzoic acid, silica supported sulfuric acid, boric acid, sulfanilic acid, polyphosphoric acid, hydrochloric acid generated *in situ* from 2,4,6-trichloro-1,3,5-triazine, have been proved to be effective in promoting the formation of 1,5-BZD.

A few of base-catalyzed methods have also been reported, such as triethylamine and Piperidine.¹⁶⁰ Typical examples of acid, base catalysts and other catalysts that are not classified but may have Lewis acid or Brønsted acid properties are listed in **Table 4**.

Table 4. Common acid-base catalysts used in the preparation of 1,5-BZD

Lewis acids		
CeCl ₃	InCl ₃	AgNO ₃
CeCl ₃ ·7H ₂ O	InBr ₃	Yb(OTf) ₃
ZnCl ₂	YbCl ₃	Sc(OTf) ₃
FeCl ₃	I ₂	CAN
Brønsted acids		
Acetic acid	Silica sulfuric acid	Sulfanilic acid
Trifluoroacetic acid	Boric acid	Polyphosphoric acid
<i>p</i> -Nitrobenzoic Acid	2,4,6-Trichloro-1,3,5-triazine	
Base		
Triethylamine	Piperidine	
Other		
MAP, DAP or TSP	L-ascorbic acid	DABCO-diacetate
Amberlyst-15 in ionic liquid		

MAP = Mono-ammonium phosphate, DAP = Di-ammonium phosphate, TSP = triple super phosphate.

Regarding the solvent, these strategies are usually performed in alcohol (MeOH and EtOH), in solvent-free conditions or in water. In rare cases, dichloromethane (DCM), toluene and other solvents were used, depending on the reactants and catalytic system.

In some cases, additional activation was provided by the use of ultrasound for example when using DABCO-diacetate as an acidic ionic liquid/catalyst, or microwave irradiation for a reaction using acetic acid as catalyst.^{176, 177}

2.1.2.3 Directions for our investigation

First, let us mention that in many examples of MCR approaches towards 1,5-BZDs, the reported protocol involves actually a stepwise addition, first mixing two components, with subsequent addition of the third one, making the reaction more like a one-pot two-step

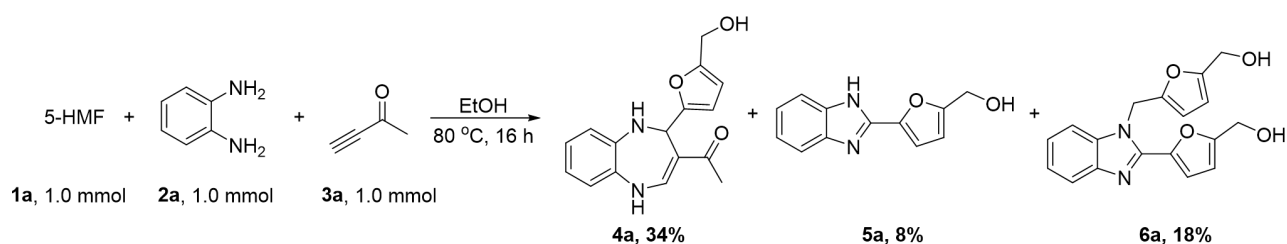
sequence than a formal MCR. In our work, we have exclusively investigated real multicomponent reactions, with all substrates present from the very beginning of the protocol.

As far as the range of aldehydes is concerned, the use of heterocyclic aldehydes has been explored only to a small extent (thiophenyl, furyl, thiazolyl, pyridyl).¹⁶¹⁻¹⁶⁷ While furfural has been used in a few cases to react with *o*-phenylenediamines and β -diketones (ethyl acetoacetate and dimedone) to prepare 1,5-BZD, 5-HMF has never been reported in any reaction for the synthesis of 1,5-BZDs, possibly attributed to the previous low availability of HMF and its known instability under acidic conditions. Considering the rich functionality provided by 5-HMF, it is good to integrate this interesting biobased platform in the scope of aldehydes for the synthesis of fine chemicals, with its peculiar reactivity and stability, very different to that of furfural. Therefore, our first project in this thesis has been to explore the use of 5-HMF in MCRs to construct diverse 1,5-BZDs under mild conditions *via* a one-pot, one-step approach.

2.2 Synthesis of 5-HMF derived 1,5-benzodiazepines

2.2.1 Identification of target products and by-products

The first experiment that we performed has been the three-component reaction of 5-HMF, *o*-phenylenediamine and but-3-yn-2-one using ethanol as the solvent at 80 °C. As the reaction progressed, TLC showed the appearance of several new spots. Once the starting material was almost completely consumed, the mixture was diluted with ethyl acetate and washed with a saturated sodium chloride solution. After drying the organic layer with anhydrous sodium sulfate, the solvent was evaporated and the residue was purified by silica gel column chromatography. Giving a pure target product **4a** in 34% yield. Besides, [5-(1H-benzo[d]imidazol-2-yl)furan-2-yl]methanol **5a** and {5-{[2-[5-(hydroxymethyl)furan-2-yl]-1H-benzo[d]imidazol-1-yl]methyl}furan-2-yl}methanol **6a** were produced in 8% and 18% yield respectively, which may arise from the condensation/cyclization sequence of 5-HMF and *o*-phenylenediamine (Scheme 70).



Scheme 70. Three-component reaction towards product and by-products involving 5-HMF

The right structure of the expected seven-membered product **4a** was identified by mass spectrometry (MS) ($MH^+ = 285.1$) and NMR spectra (1H , ^{13}C , DEPT 135, 1H - 1H COSY, HSQC and HMBC). By-products **5a** and **6a** were also observed in the crude spectra and detected in MS with $MH^+ = 215.1$ (**5a**) and $MH^+ = 325.1$ (**6a**), as shown in Figure 10.

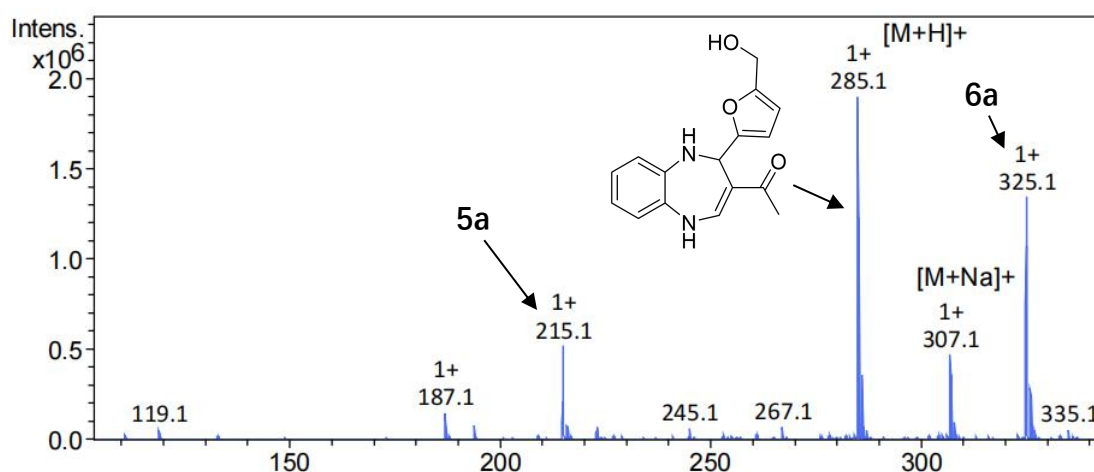


Figure 10. Crude mass spectrometry containing 1,5-BZD **4a** and by-products **5a**, **6a**

In the 1H NMR spectrum of compound **4a**, some peaks gave indications on the newly formed bonds, notably proton H_5 at δ 9.32 ppm, H_4 at δ 7.50 ppm, H_1 at δ 6.15 ppm and H_2 at δ 5.57 ppm. The 1H - 1H COSY spectrum exhibits the anticipated correlation between H_1 - H_2 and H_4 - H_5 , showing that in the newly formed bonds, H_1 and H_2 , H_4 and H_5 are in adjacent positions, respectively (Figure 11 & 12).

Among them, protons H₅ and H₁ had no associated carbons in HSQC, while the corresponding carbon signals of H₄ and H₂ were observed at δ 143.0 ppm (C₄) and δ 51.6 ppm (C₂) respectively, confirming that new C-N bonds were formed through this reaction (Figure 13). The HMBC spectrum demonstrates that the new proton H₄ interacts with nearby carbon at 51.6 δ ppm (C₂), while the new protons H₁ and H₅ interact with nearby carbon at 113.7 δ ppm (C₃). The new proton H₂ interacts with the carbon at 113.7 δ ppm and 143.0 δ ppm (C₃ and C₄), which clearly identified the formation of the new C₂-C₃ bond and ultimately determines the structure of **4a** (Figure 14).

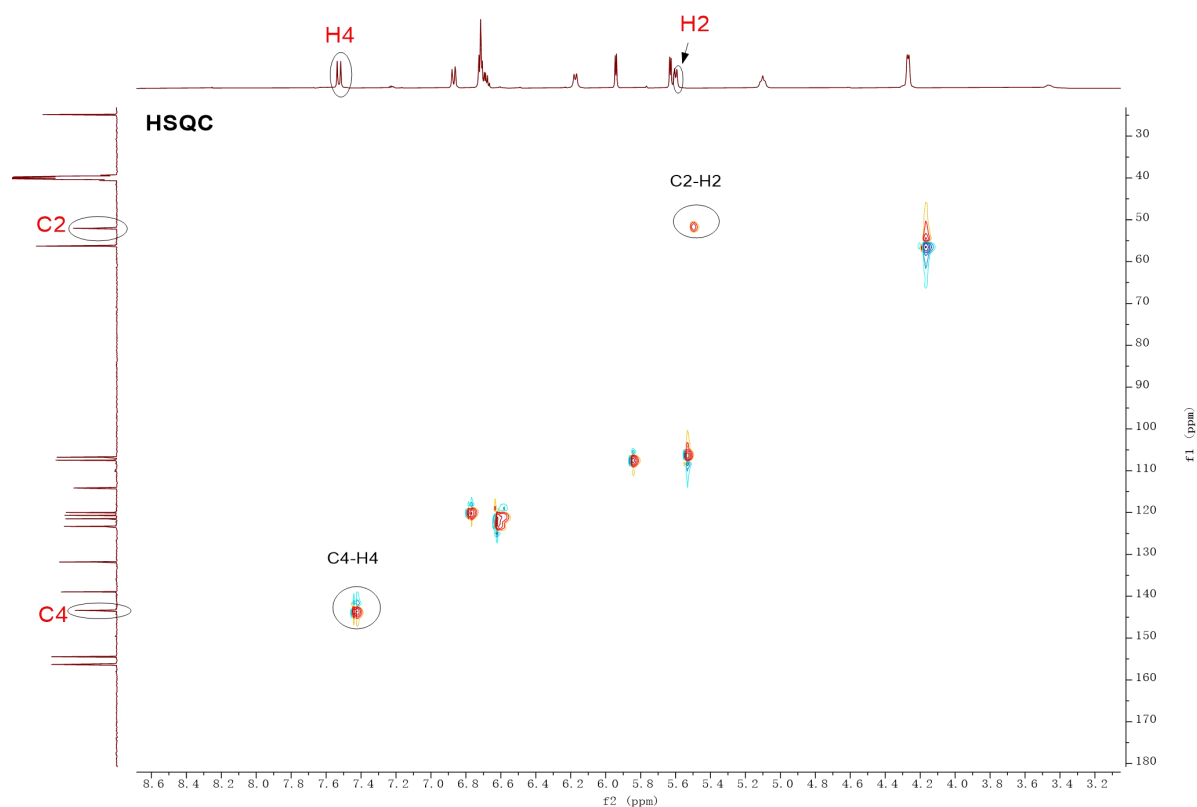


Figure 13. Confirmation of the formation of C-N bonds using HSQC NMR spectroscopy

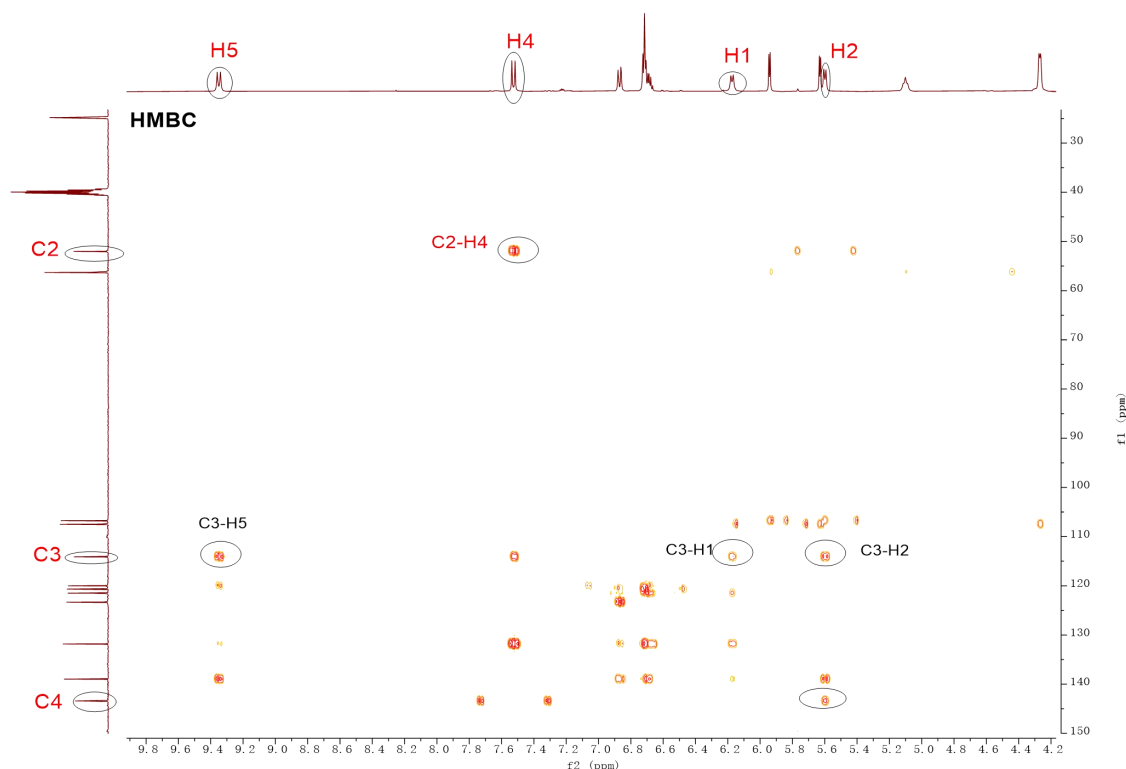
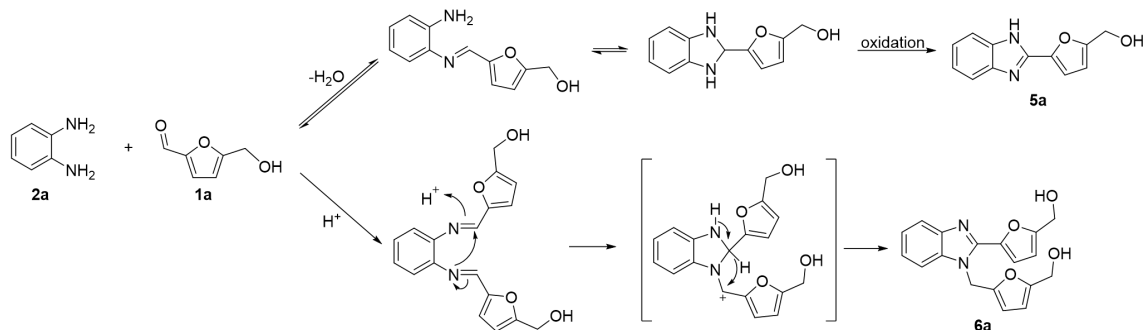


Figure 14. Confirmation of the formation of C₂-C₃ bond using HMBC NMR spectrum

By referring to literature, we know that the reaction of *o*-phenylenediamine and aromatic aldehydes can diverge towards by-products **5a** and **6a**.^{178, 179} In one case, *o*-phenylenediamine condenses with the carbonyl group of 5-HMF to form a Schiff base, which then undergoes ring-closing and oxidative dehydrogenation to provide benzimidazole **5a**. Another possibility is that two molecules of aldehyde react with the amine group on one molecule of *o*-phenylenediamine to form a double Schiff base, and then a thermodynamically stable 1,2-disubstituted benzimidazole **6a** is obtained *via* ring-closing (Scheme 71).



Scheme 71. Possible routes towards **5a** and **6a**

The benzimidazole structure of **5a** was confirmed by comparison with NMR data reported in the previous literature,¹⁸⁰ the newly formed proton peak (NH) was observed at δ 12.9 ppm. We identified the structure of **6a** by MS and NMR. A visual comparison of the ^1H NMR spectrum of by-products **5a** and **6a** is presented in Figure 15. In the ^1H NMR spectrum of **6a**, we observed multiple sets of the same type of proton peaks (as shown in the black frame), the number of furan protons, hydroxyl proton and methylene protons showed twice that of the **5a** spectrum. Another point of concern is that compared with the **5a** spectrum, the NH proton peak disappeared in **6a**. Instead, a new proton peak of N-CH₂ appeared at δ 5.78 ppm. Combined with other NMR experiments (^{13}C NMR, ^1H - ^1H COSY, DEPT, HSQC and HMBC), it was confirmed that the structure of by-product **6a** is the adduct of *o*-phenylenediamine and two molecules of 5-HMF (see detailed ^1H and ^{13}C information of **5a** and **6a** in experimental section).

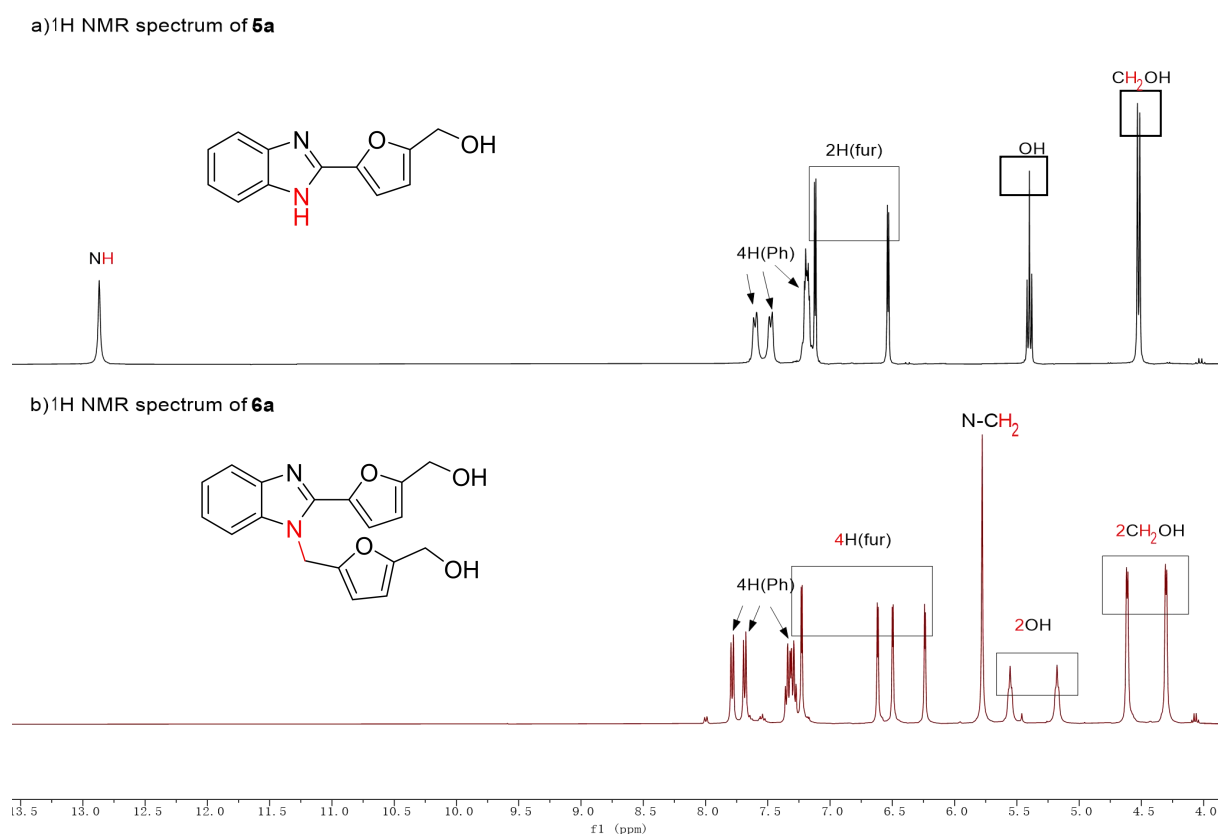


Figure 15. Comparison of ^1H NMR spectra of by-products **5a** and **6a**

Overall, we demonstrated the competition between the formation of the target product **4a** and undesired side reactions towards **5a** and **6a**. In order to conveniently evaluate the influence of the reaction parameters on the reaction outcome in subsequent experiments, we developed a method for calculating the yields by NMR in deuterated DMSO (DMSO-*d*₆), based on an internal standard (1,3,5-trimethoxybenzene) added to the obtained crude reaction mixture in 1/3 equivalent amount. 1,3,5-Trimethoxybenzene is easy to handle, solid at room temperature therefore easily weighed on the balance, and unable to react chemically with the analyzed compounds. It is thus considered as a suitable internal standard since its methyl proton peak at δ 3.70 ppm with limited overlap with peaks of raw materials, and newly formed products or intermediates. Furthermore, it has good solubility in DMSO-*d*₆.

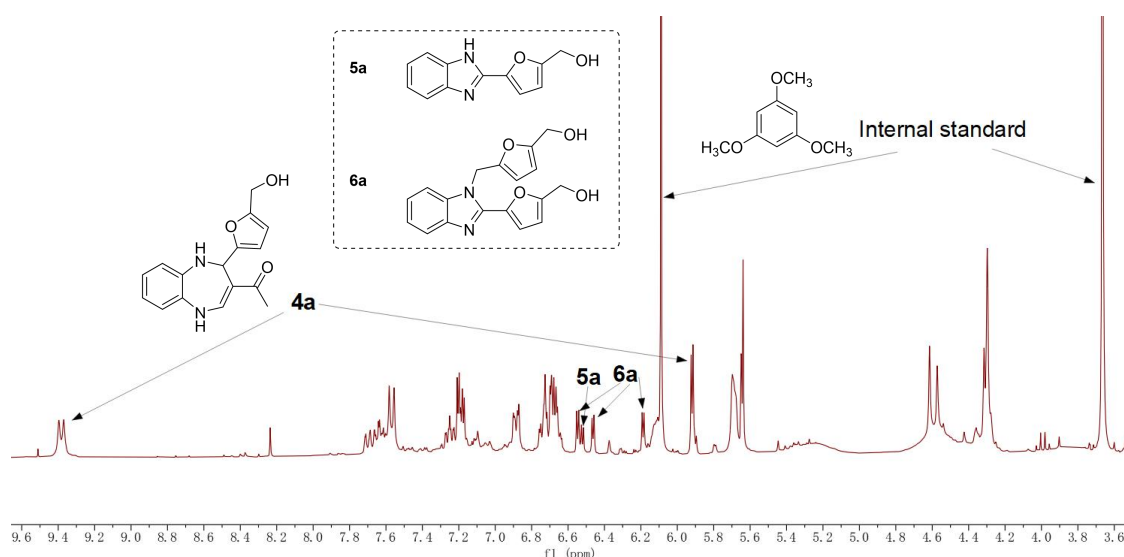


Figure 16. An example of crude reaction mixture containing internal standard and products

2.2.2 Influence of reaction conditions

2.2.2.1 Influence of the catalysts

Due to the sensitivity of 5-HMF, the investigation required an in-depth revisit of reaction parameters as compared to benchmark aldehydes. We first screened a series of catalysts including Lewis acids and Brønsted acids (Table 5). However, addition of catalytic amounts

of Lewis acids such as FeCl₃, AlCl₃, ZnCl₂ and I₂ significantly inhibited this transformation towards desired seven-membered 1,5-benzodiazepine **4a** although 5-HMF was completely consumed (entries 1-4), while CsBr provided similar yields to those under catalyst-free condition (entry 5). *p*-Toluenesulfonic acid (PTSA), acetic acid or benzoic acid did not provide better results towards **4a**. No target product was obtained in the presence of trifluoromethanesulfonic acid, a much stronger acid (entries 6-9). However, it was observed that **6a** was always present in 14-32% yield under the acidic catalyst conditions exemplified above, which is consistence with the path to by-product **6a** under acidic conditions proposed in the previous section.

Table 5. Investigation of acid catalysts in three-component 1,5-benzodiazepine synthesis

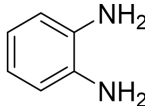
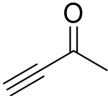
5-HMF (1.0-1.2 mmol) + o-phenylenediamine (1.0 mmol) + propargyl alcohol (1.0 mmol) $\xrightarrow[80\text{ }^{\circ}\text{C}, 16\text{ h}]{\text{EtOH (2 mL)}}$ **4a** + **5a** + **6a**

Entry ^a	Catalyst (20 mol%)	NMR Yield of 4a/5a/6a
1	FeCl ₃	2/9/23
2	AlCl ₃	trace/5/14
3	ZnCl ₂	10/9/14
4	I ₂	2/0/22
5	CsBr	38/8/17
6	Amberlyst 15	16/8/21
7	PTSA	36/trace/17
8	CH ₃ COOH	32/trace/22
9	PhCOOH	30/trace/27
10	CF ₃ SO ₃ H	0/trace/32

^a Reaction conditions: Entries 1-5, 5-HMF (1.0 mmol). entries 6-10, 5-HMF (1.2 mmol).

Some other salts were examined in this reaction (Table 6), such as the neutral salt sodium thiocyanate (NaSCN) (entry 1) and the weak basic salts sodium acetate (NaOAc) and sodium bicarbonate (NaHCO₃) (entries 2-3), both of which promoted the formation of the target product **4a** in 54%, 59% and 52% yields, respectively. Reducing the loading of NaOAc to 30 mol% and decrease the reaction time to 7 h almost had no effect on the yield (entry 4).

Table 6. Investigation of several sodium salts in three-component 1,5-benzodiazepine synthesis

5-HMF	+		+		$\xrightarrow[50\text{ }^{\circ}\text{C}, 16\text{ h}]{\text{EtOH (2 mL)}}$	4a	+	5a	+	6a
1.2 mmol		1.0 mmol		1.0 mmol						

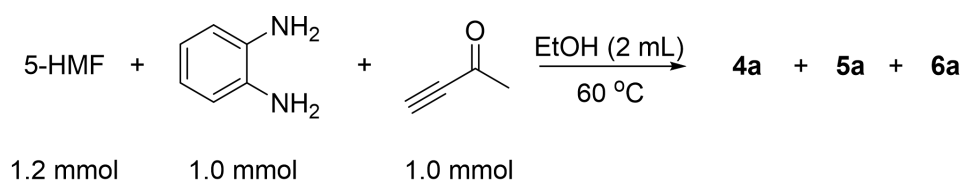
Entry	Catalyst (50 mol%)	NMR Yield of 4a/5a/6a
1	NaSCN	54/11/8
2	NaOAc	59/8/trace
3	NaHCO ₃	52/9/4
4 ^a	NaOAc (30 mol%)	61/9/4

^a Reaction time: 7 h.

Acknowledging the sensitivity of HMF to harsh conditions and considering that the reaction selectivity may be related to the pH environment, we then turned our attention to milder salts. Several ammonium salts were screened for this reaction (Table 7). Applied to the reaction of 5-HMF (1.2 mmol), *o*-phenylenediamine (1.0 mmol) and but-3-yn-2-one (1.0 mmol) at 60 °C, the presence of ammonium salts such as NH₄HCO₂, (NH₄)₂CO₃, (NH₄)₂SO₄ and NH₄OAc reduced by-product **6a** from 18% to trace amounts, which also facilitated the separation of the product (entries 1-4) since **4a** and **6a** show very similar polarities during column chromatography. NH₄Cl also resulted in an NMR yield of 54% of the target product (entry 5). Among the various ammonium salts investigated, NH₄OAc exhibited the best efficiency with 68% NMR yield of the desired product **4a** (entry 4). A 70% isolated yield was measured for

this reaction, which is consistent with the NMR yield taking into account the experimental errors and the accuracy of the measurements, showing that the separation by silica gel chromatography was easy and efficient. The ammonium sulfate was also quite effective, with an even better selectivity for the BZD vs by-product **5a**. However, there were several considerations that led us to choose ammonium acetate. First, reactions involving acetate ions tend to be milder compared to sulfate ions. Second, ammonium acetate can act as a buffer in some reactions, helping to maintain a relatively constant pH value. Third, ammonium acetate is generally more soluble in organic solvents than ammonium sulfate.

Table 7. Optimization of the three-component synthesis of 1,5-benzodiazepine



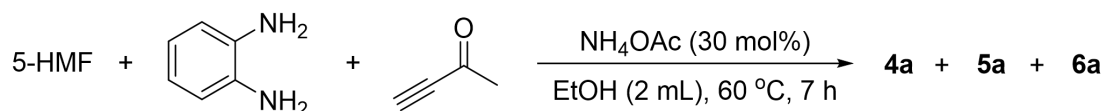
Entry	Catalyst (30 mol%)	Time	NMR Yield of 4a/5a/6a
1	NH ₄ HCO ₂	6 h	60/12/trace
2	(NH ₄) ₂ CO ₃	6 h	43/8/trace
3	(NH ₄) ₂ SO ₄	6 h	66/10/trace
4	NH ₄ OAc	7 h	68(70)/14/trace
5	NH ₄ Cl	7 h	54/messy

Ammonium acetate and ammonium sulfate have been shown to promote glucose dehydration to 5-HMF with good yields in a previous report.¹⁸¹ In that work, the authors suggested that ammonium acetate and ammonium sulfate prevented the further degradation of 5-HMF towards levulinic acid and formic acid, therefore limited acid-catalyzed degradation of HMF compared to harsher acids. The efficacy of ammonium acetate and ammonium sulfate in our MCR cycloaddition reaction can thus be attributed to its efficiency as a catalyst and for its mildness towards HMF itself.

2.2.2.2 Other reaction parameters

The stoichiometric ratio of starting materials was also taken into consideration (Table 8). Stoichiometric ratios of equal amounts or slight excesses of *o*-phenylenediamine or but-3-yn-2-one resulted in a certain decrease (7-16%) in the yield of **4a** (entries 1,3,4) compared to the ratio of 1.2:1:1 of **1a/2a/3a** (entry 2).

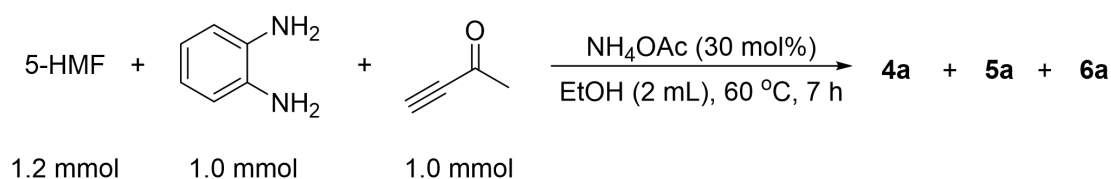
Table 8. Optimization of the three-component synthesis of 1,5-benzodiazepine



Entry	Stoichiometric of 1a:2a:3a	NMR yield of 4a/5a/6a
1	1:1:1	54/10/trace
2	1.2:1:1	68/14/trace
3	1:1.2:1	52/16/trace
4	1:1:1.2	61/10/trace

Running the same reaction with different loadings of NH₄OAc (20 mol%, 25 mol%, 35 mol%) did not provide better results than 30 mol% NH₄OAc, which was thus used in the following experiments (Table 9).

Table 9. Optimization of the three-component synthesis of 1,5-benzodiazepine



Entry	Catalyst	NMR yield of 4a/5a/6a
1	NH ₄ OAc (20 mol%)	55/11/trace
2	NH ₄ OAc (25 mol%)	62/14/trace
3	NH ₄ OAc (30 mol%)	68/14/trace
4	NH ₄ OAc (35 mol%)	63/13/trace

Other factors such as solvent and concentration were also investigated (Table 10). The NMR yield of the target product was obtained in 52% with DCM as solvent (entry 1), whereas other solvents such as MeCN, THF, 1,4-dioxane, DMSO or water provided no more than 31% yield of the target product (entries 2-6). Ethanol gave clearly the best results as compared to above mentioned set of organic solvents and water, although adjusting the ethanol volume (entries 7-8) did not further improve the reaction results.

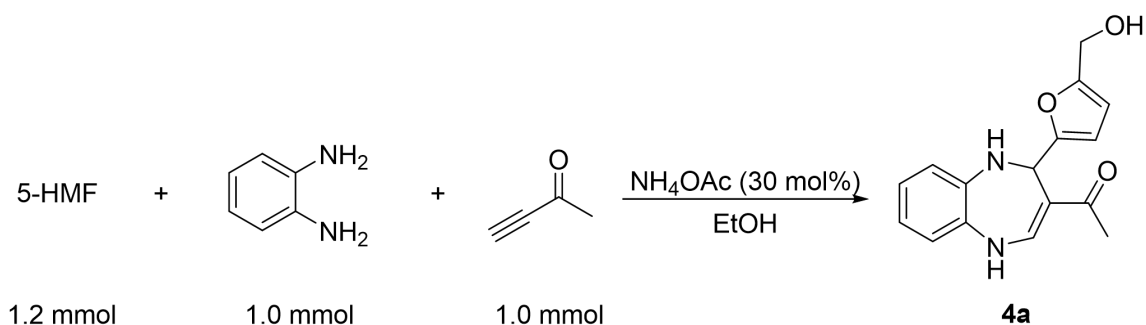
Table 10. Influence of solvents

$ \begin{array}{c} \text{5-HMF} + \text{1,2-phenylenediamine} + \text{3-penten-2-one} \xrightarrow[60\text{ }^{\circ}\text{C, 7 h}]{\text{NH}_4\text{OAc (30 mol\%)}} \text{4a} + \text{5a} + \text{6a} \\ \text{1.2 mmol} \qquad \qquad \text{1.0 mmol} \qquad \qquad \text{1.0 mmol} \end{array} $		
Entry	Solvent (2.0 mL)	NMR Yield of 4a/5a/6a
1	DCM	52/13/trace
2	MeCN	31/27/trace
3	THF	13/messy
4	1,4-Dioxane	26/messy
5	DMSO	23/messy
6	H ₂ O	19/7/trace
7	EtOH (1.5 mL)	63/15/trace
8	EtOH (2.5 mL)	66/15/trace

Finally, the influence of the reaction duration and temperature on the yield of **4a** were briefly investigated based on the optimized conditions obtained from the above experiments. As depicted in Table 11, the reaction reached a yield of 52% within 15 minutes (entry 1), increased to 60% then 64 % after 1 and 3 hours respectively, reaching a maximum yield of 68% after 7 hours (entry 5 of entries 2-6). Keeping 7 hours as constant reaction duration,

lowering the temperature to 50 °C, or elevating it to 70 °C or 80 °C led to slightly lower yields (entries 7-9). the results showed that the reaction at 60 °C provided a better yield under the current NH₄OAc/EtOH system.

Table 11. Optimization of the three-component synthesis of 1,5-benzodiazepine



Entry	Time	Temperature	NMR yield of 4a
1	1/4 h	60 °C	52
2	1 h	60 °C	60
3	3 h	60 °C	64
4	5 h	60 °C	65
5	7 h	60 °C	68
6	8 h	60 °C	67
7	7 h	50 °C	60
8	7 h	70 °C	58
9	7 h	80 °C	56

Overall, the combination of ammonium acetate and ethanol proved to be a clean and efficient couple and was applied to the three-component reaction of various diamines, alkynones and aldehydes towards diverse 1,5-benzodiazepines in the next section.

2.2.3 Structural scope of substrates

2.2.3.1 Scope of diamines

The optimized conditions (30 mol% NH₄OAc in ethanol, 60°C, sealed tube), which generated compound **4a** in 70% isolated yield were then used throughout the exploration of the substrate structural scope. Firstly, a collection of variously substituted *o*-phenylenediamines were used in the reaction (Figure 17). In general, all *o*-phenylenediamines reacted smoothly to afford the corresponding 1,5-benzodiazepines in fair yields with a good tolerance of functionalities such as alkyl, alkoxy and halo substituents. The six substituted but symmetrical *o*-phenylenediamines conducted logically to a single product (**4b-4g**). 4,5-Disubstitutedbenzene 1,2-diamine clearly lead to lower yield of 1,5-benzodiazepine together with by-product benzimidazole and various impurities. When testing 4,5-dinitrobenzene-1,2-diamine with a strong electron-withdrawing group NO₂, the yield dropped significantly to 24% (**4f**) but 36% yield of the imine intermediate (analogue of intermediate E in the mechanism section) from the condensation of HMF and 4,5-disubstitutedbenzene 1,2-diamine was observed. The reasons for low yields may involve influences from many aspects. For example, the presence of substituents cause steric hindrance, thereby affecting the reactivity of the diamine. The substituent affects the condensation reaction of diamine with α,β -unsaturated carbonyl compounds by changing the nucleophilicity of the amino group in *o*-phenylenediamine. Substituents affect the properties of the carbon atoms in the benzene ring, leading to potential side reactions. Electronic effects may also influence the intramolecular cyclization step in the formation of 1,5-benzodiazepine.

Non-symmetrical *o*-phenylenediamines led to a mixture of two regioisomers difficult to separate (**4h/h'** and **4i/i'**) but in the same range of yield (66% and 62% respectively) (Figure 18). The formation of regioisomers depends on the different sites (two amino) at which nucleophilic attack occurs during the reaction with α,β -unsaturated carbonyl compounds, where it could be affected by electronic effects.

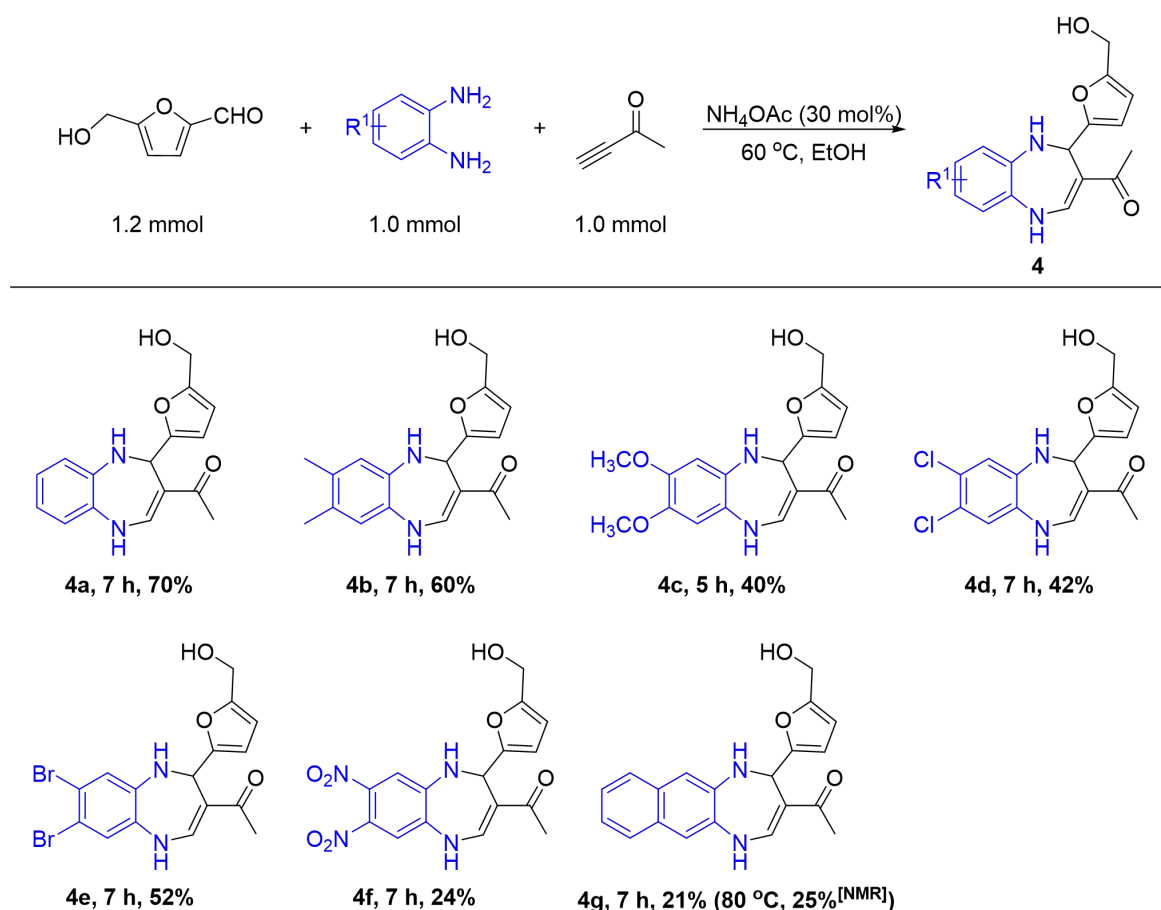


Figure 17. Scope of substituted *o*-phenylenediamine substrates

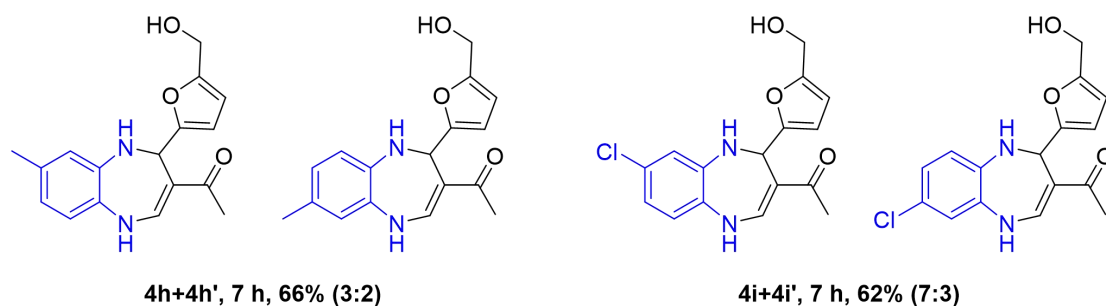


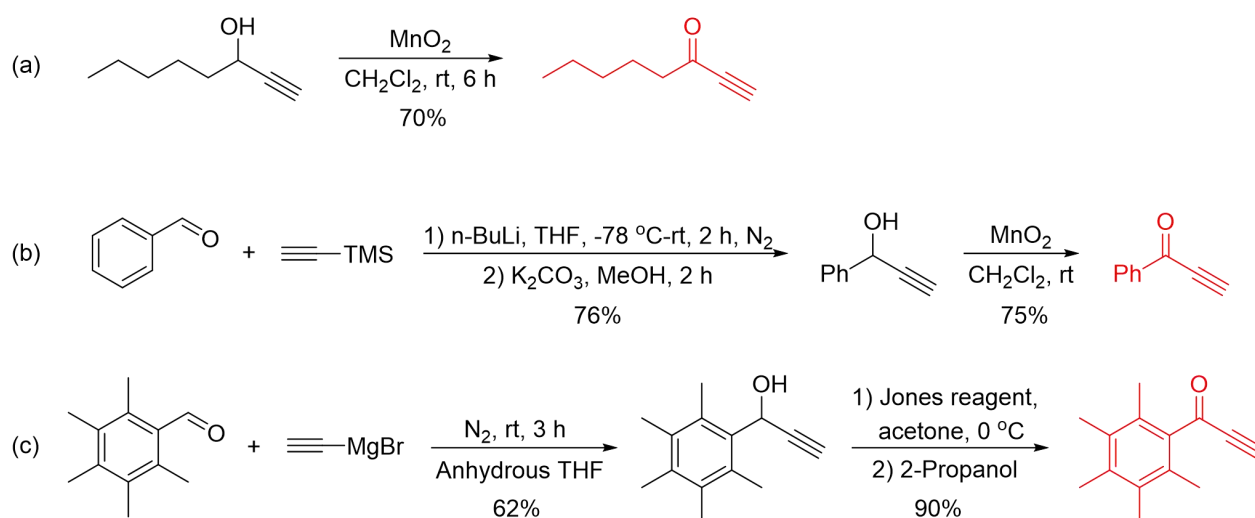
Figure 18. Scope of substituted *o*-phenylenediamine substrates

2.2.3.2 Scope of alkynones and alkyl alkynoates

The scope investigation was then extended to the alkynone reagent by using various alkynones or alkyl alkynoates. Five of the six substrates we wanted to use in this scope investigation were not commercially available, so we prepared them according to literature

procedures. We used the following synthetic sequence: i) the reaction of corresponding aldehyde and a Grignard reagent (ethynylmagnesium bromide) or trimethylsilyl acetylene to prepare the intermediate alkynols; ii) the oxidation of alkynols by manganese dioxide (MnO_2) or Jones reagent to synthesize alkynones (Scheme 72).

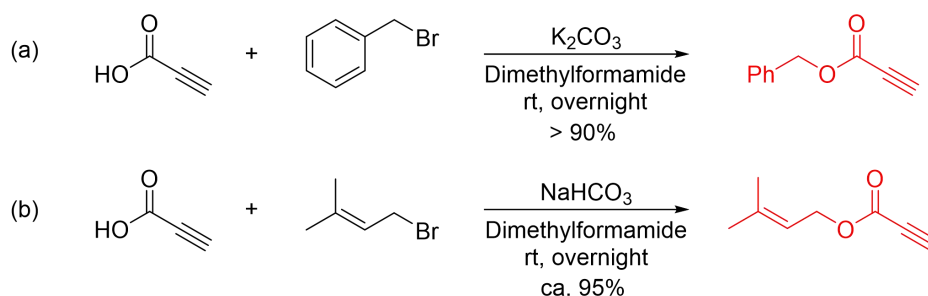
Oct-1-yn-3-one was obtained by MnO_2 oxidation of oct-1-yn-3-ol in DCM (Scheme 72a).¹⁸² To get 1-phenylprop-2-yn-1-one, the following sequence was followed: *n*-BuLi (1.6 M in hexane) reaction with trimethylsilyl acetylene in THF at -78°C , followed by reaction with benzaldehyde led to the corresponding 1-phenylprop-2-yn-1-ol, which was then oxidized to 1-phenylprop-2-yn-1-one using MnO_2 as an oxidizing agent (Scheme 72b).¹⁸² For 1-(2,3,4,5,6-pentamethylphenyl)propan-2-yn-1-one, we first performed the reaction of ethynylmagnesium bromide (0.5 M in THF) with 2,3,4,5,6-pentamethylbenzaldehyde in THF at 0°C to give 1-(2,3,4,5,6-pentamethylphenyl)prop-2-yn-1-ol, which was further oxidized using Jones reagent (Scheme 72c).^{182, 183}



Scheme 72. Preparation of alkynone substrates

For the alkyl alkynoates, we performed the nucleophilic substitution reaction of propiolic acid and alkyl bromide in the presence of base. Benzyl propiolate was obtained by reaction of propiolic acid benzyl bromide in presence of K_2CO_3 in dimethylformamide at room temperature (Scheme 73a).¹⁸⁴ Reaction of propiolic acid with 1-bromo-3-methyl-2-butene in

the presence of NaHCO₃ in dimethylformamide at room temperature led to 3-methylbut-2-en-1-yl propiolate in approximately 95% yield (Scheme 73b).¹⁸⁵



Scheme 73. Preparation of alkyl alkynoate substrates

The various alkynones and alkyl alkynoates were then used in the MCR of 5-HMF with *o*-phenylenediamines. Good yields of desired product were obtained when 1-octyn-3-one or 1-phenylprop-2-yn-1-one were used as reagents (Figure 19), giving the products **4j** and **4k** in 74% and 67% yields, respectively. Reaction with 1-(2,3,4,5,6-pentamethylphenyl)prop-2-yn-1-one required an extended reaction time to 18 hours for yielding product **4l** in 68% yield.

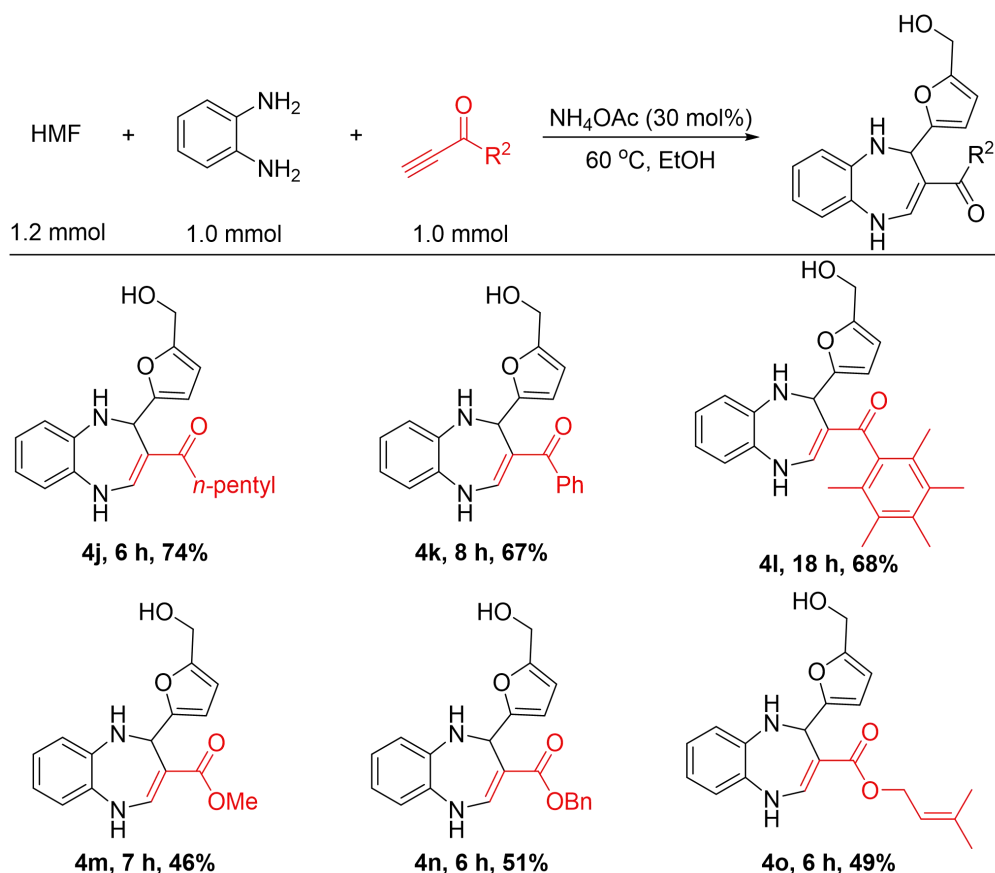
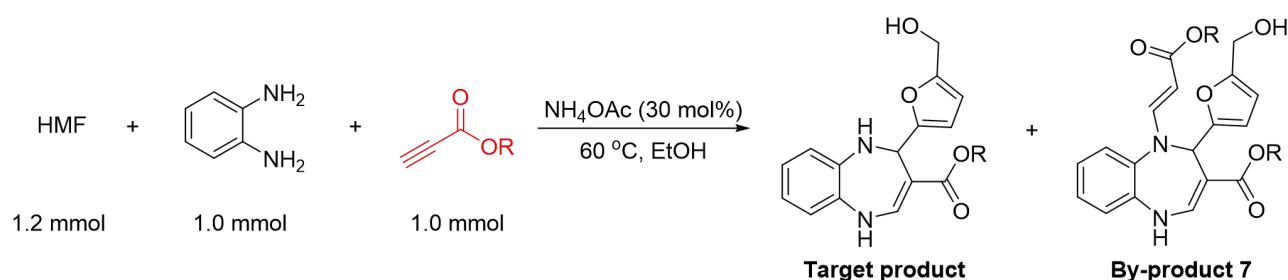


Figure 19. Scope of alkynone and alkyl alkynoate substrates

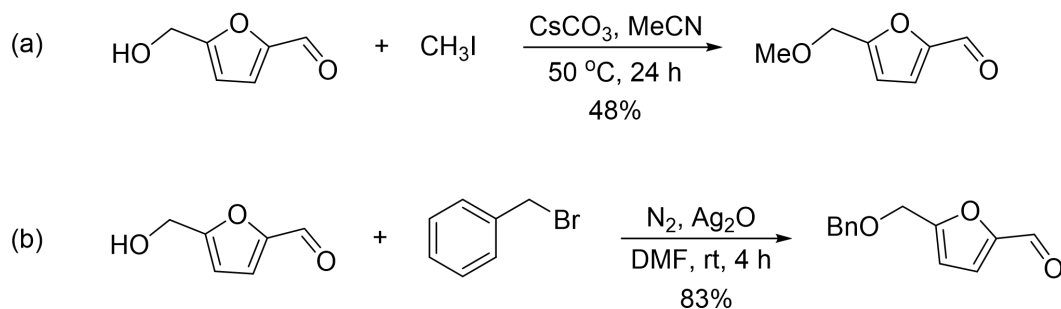
Alkyl propynoates exhibited lower yields of target products in the reaction with 5-HMF and *o*-phenylenediamine, with 1,5-benzodiazepines in 46%, 51% and 49% yields (**4m-4o**), however, the lower yield is due to the fact that when using alkyl propynoate substrates, not only the by-products **5a** (15-18%) and **6a** (6-10%) are generated, but also resulting in another by-product **7** (range 12-20% yield) (Scheme 74), which is possible to be obtained through aza-Michael addition of the target product and one molecule of alkyl propynoate, or a competitive intermediate route that is different from the formation of the target product.¹⁸⁶



Scheme 74. Alkyl propynoate substrates derived By-product 7

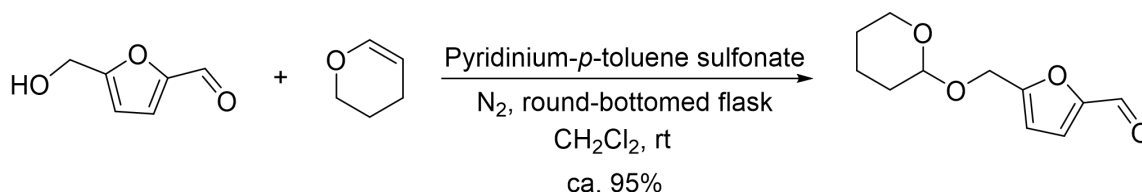
2.2.3.3 Scope of HMF derived substrates

After screening various diamines and alkynones/alkyl alkynoates for this three-component procedure, a series of substituted furfurals was investigated. Among them, several HMF derived substrates were prepared according to the reported literatures. 5-Methoxymethylfuran-2-carbaldehyde was prepared *via* the nucleophilic substitution reaction between HMF and methyl iodide (CH_3I) in the presence of Cs_2CO_3 (Scheme 75a).¹⁸⁷ 5-((Benzyloxy)methyl)furan-2-carbaldehyde was prepared from HMF and benzyl bromide under N_2 atmosphere in the presence of silver oxide (Scheme 75b).¹⁸⁸



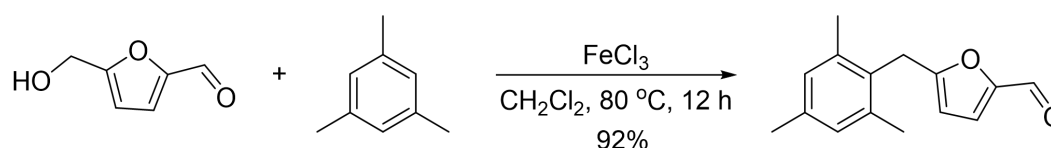
Scheme 75. Preparation of 5-methoxy- or 5-((benzyloxy)-methyl)furan-2-carbaldehyde

Under inert atmosphere (N_2), using HMF and 3,4-dihydro-2*H*-pyrane as starting material, in the presence of pyridinium *p*-toluene sulfonate, tetrahydropyranyloxymethyl-5-furfural was provided in approximately 95% yield in CH_2Cl_2 (Scheme 76).¹⁸⁹



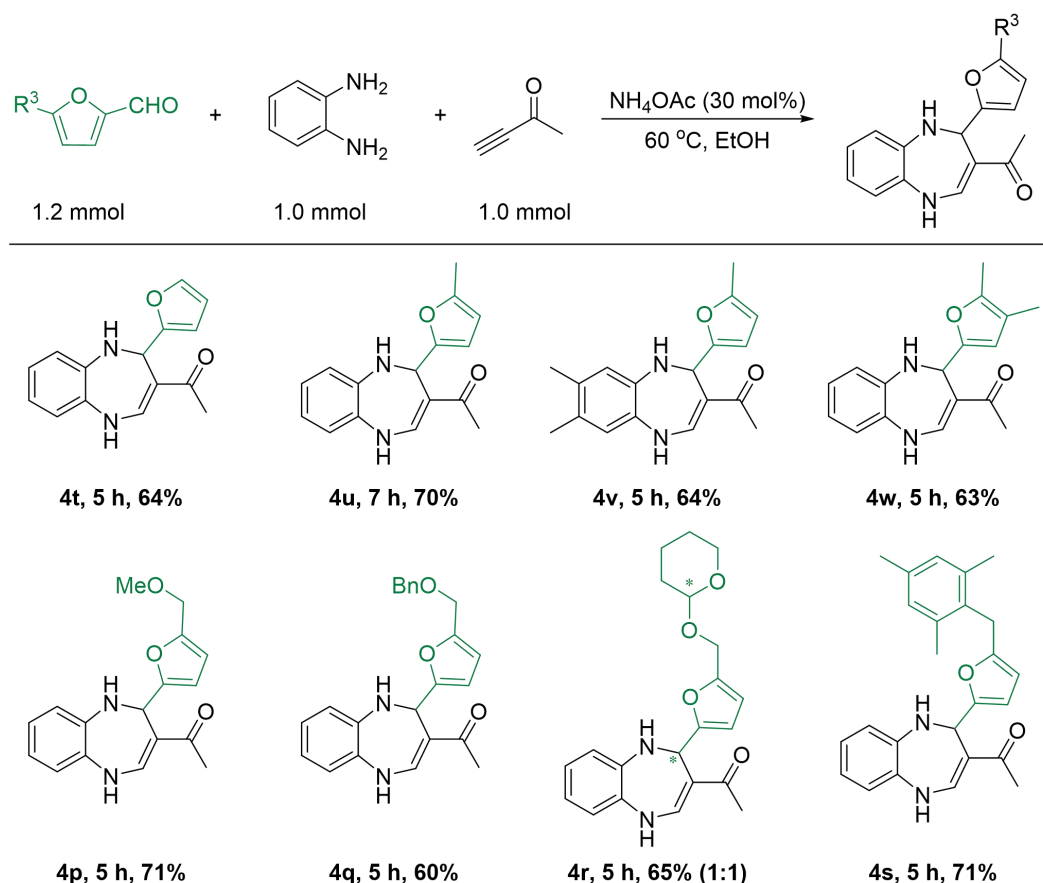
Scheme 76. Preparation of 5-(((tetrahydro-2*H*-pyran-2-yl)oxy)methyl)furan-2-carbaldehyde

Using ferric chloride ($FeCl_3$) as the catalyst, HMF and mesitylene were mixed in CH_2Cl_2 , and 5-(2,4,6-Trimethylbenzyl)furan-2-carbaldehyde was obtained in 92% yield at 80 °C through the Friedel-Crafts reaction (Scheme 77).¹⁹⁰



Scheme 77. Preparation of 5-(2,4,6-trimethylbenzyl)furan-2-carbaldehyde

The MCR reaction of these different furanic aldehydes was then investigated. Furfural and commercially available 5-methylfurfural and 4,5-dimethyl furfural react well to give the desired products in the same range of yields (63% to 70%) (**4t-4w**). The 5-HMF derived substrates, prepared from 5-HMF through known procedures as shown above, reacted smoothly under the optimized conditions affording the target products with yields of 71% (**4p**), 60% (**4q**), 65% (**4r**, as a (1:1) mixture of two diastereomers), and 71% (**4s**), respectively (Scheme 78).

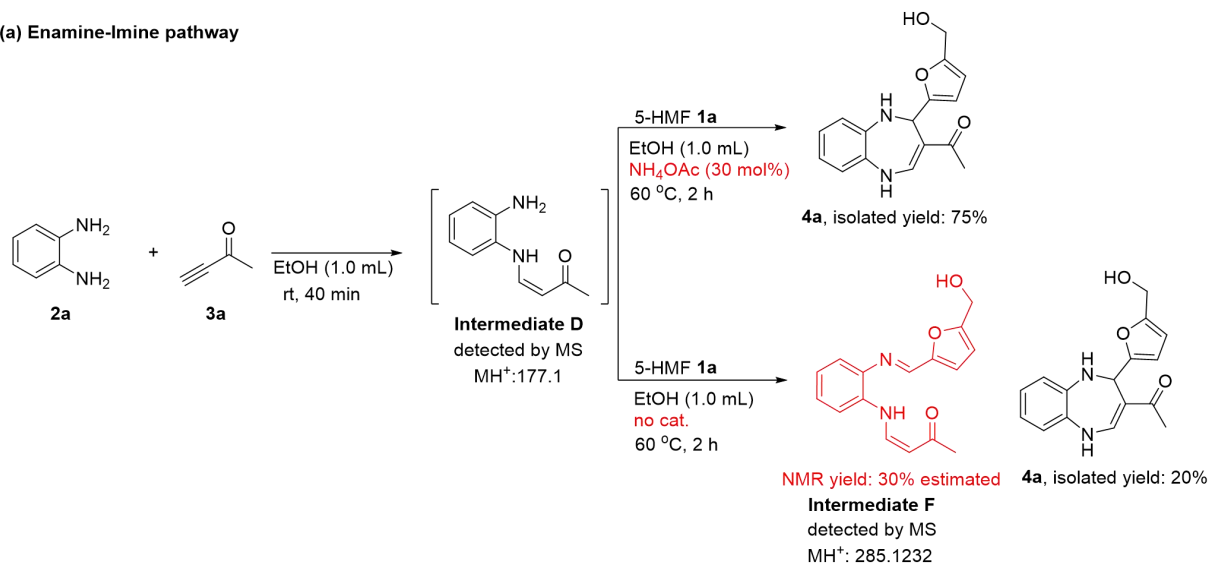


Scheme 78. Scope of 5-HMF derived aldehydes and furfurals

2.2.4 Mechanistic study

In multi-component reactions, the reaction may undergo different pathways depending in which order the substrates interact. Aiming at a better understanding of the mechanism in the present case, control experiments were conducted in the presence of only two partners amongst the three, with attempts to detect reaction intermediates by NMR or MS experiments, before adding the third partner. When mixing o-phenylenediamine and but-3-yn-2-one in ethanol for 40 minutes at room temperature, the enamine product **D** can be detected by MS (enamine plus H⁺: 177.1). Then, 5-HMF, ammonium acetate and ethanol (1 mL) were added to the solution and stirred at 60 °C for 2 hours to obtain **4a** with an isolated yield of 75% (Scheme 79a). When this second step was performed without ammonium acetate, only 20% of **4a** was obtained after 2 hours, together with a 30% estimated yield (NMR) of the uncyclized intermediate F, identified by HRMS with a MH⁺ 285.1232.

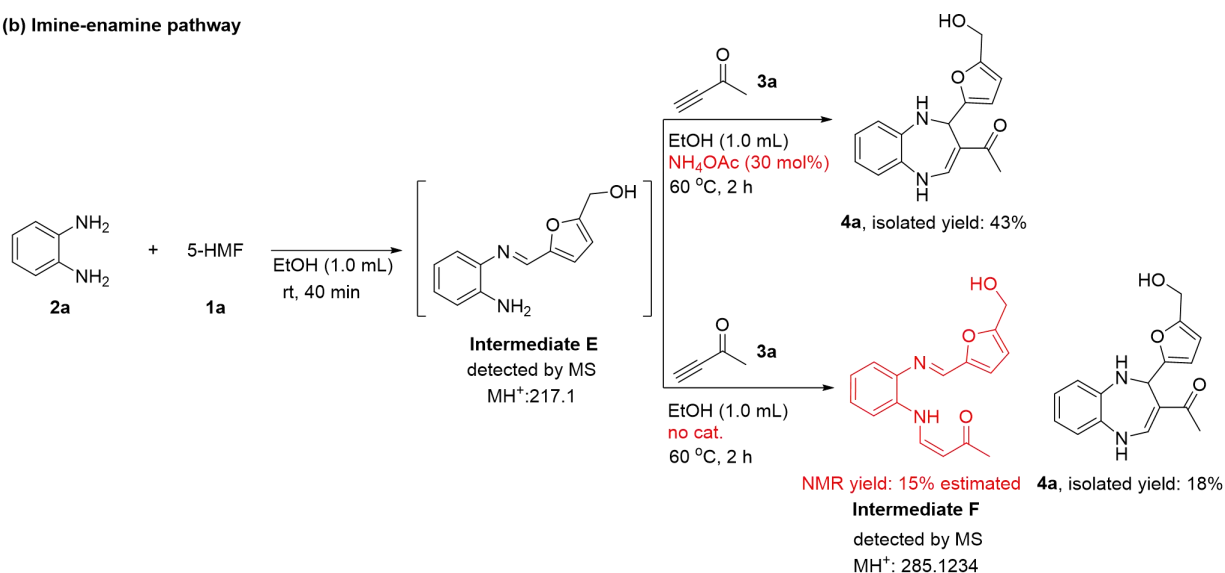
(a) Enamine-Imine pathway



Scheme 79a. Control experiments

The second way to start with two of the three reactants was to mix *o*-phenylenediamine and 5-HMF, leading to the imine product **E** detected by MS (imine plus H^+ : 217.1). Then, but-3-yn-2-one and ammonium acetate were added, yielding the target product in a lower 43% yield (Scheme 79b). Formation of intermediate **F** (MH^+ : 285.1234) was also observed when the second step was performed in the absence of any catalyst.

(b) Imine-enamine pathway



Scheme 79b. Control experiments

The structure of intermediate **F** was fully characterized by 1D (^1H NMR, ^{13}C NMR, DEPT) and 2D (^1H - ^1H COSY, HSQC and HMBC) NMR spectra, the corresponding ^1H NMR and ^{13}C NMR spectra are shown in Figures 20 and 21. The newly formed protons were found at δ 12.98 ppm (NH), δ 8.57 ppm (N=CH), δ 7.64 ppm ($\text{H}_{4''}$) and δ 5.36 ppm ($\text{H}_{3''}$) in ^1H NMR spectrum. In the ^1H - ^1H COSY spectrum (Figure 22), the correlation between the two protons $\text{H}_{4''}$ and $\text{H}_{3''}$ on the generated C=C bond of the intermediate **F** can be clearly observed. Intermediate **F** is considered to be in the *Z* configuration since the coupling constant of the hydrogen on the alkene is low ($\text{H}_{3''}$, $J = 7.8$ Hz).

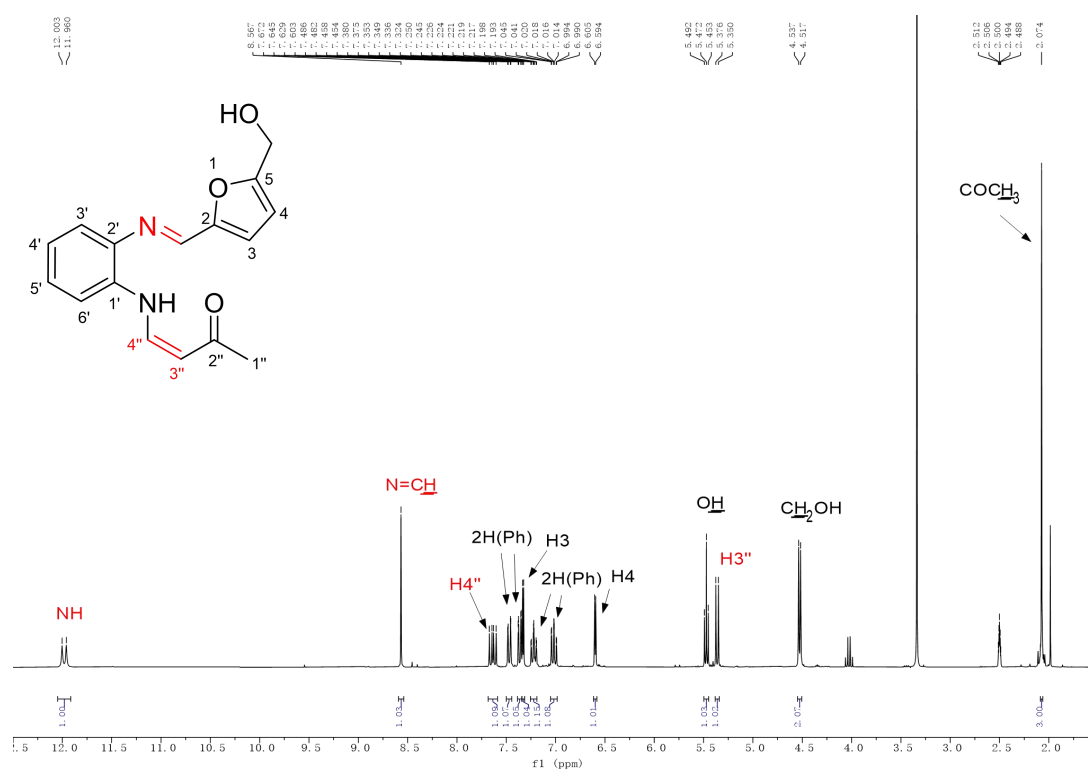


Figure 20. ^1H NMR spectrum of the intermediate **F**

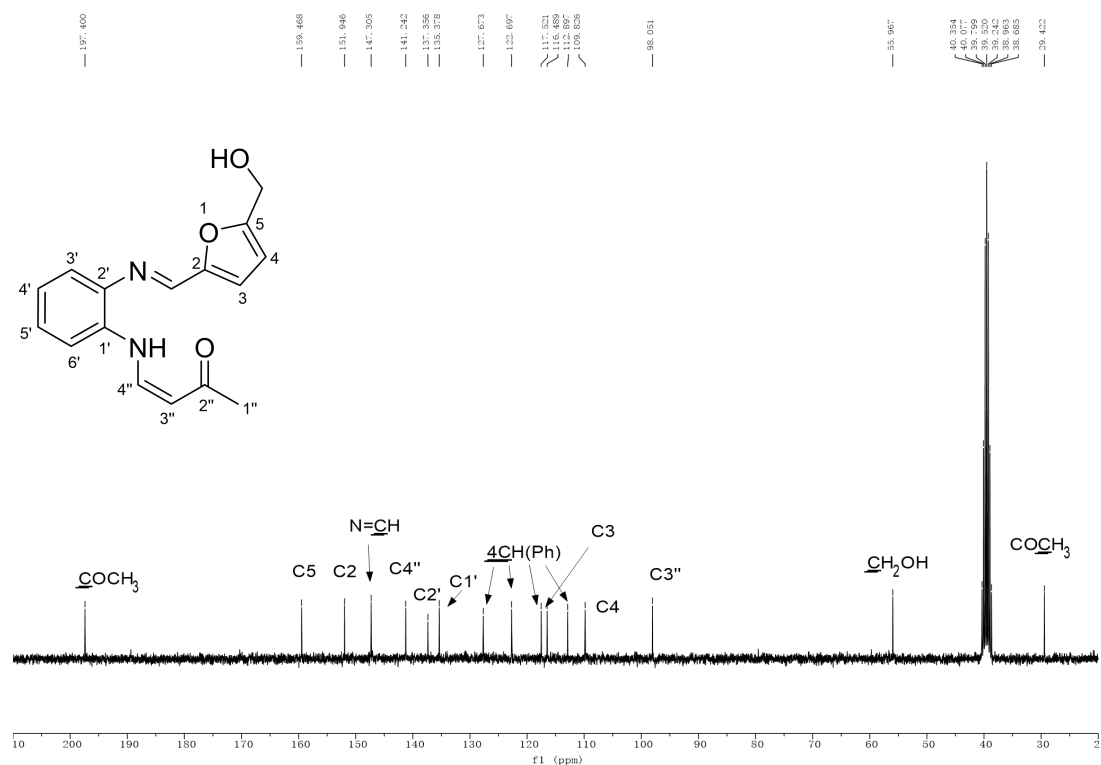


Figure 21. ^{13}C NMR spectrum of the intermediate **F**

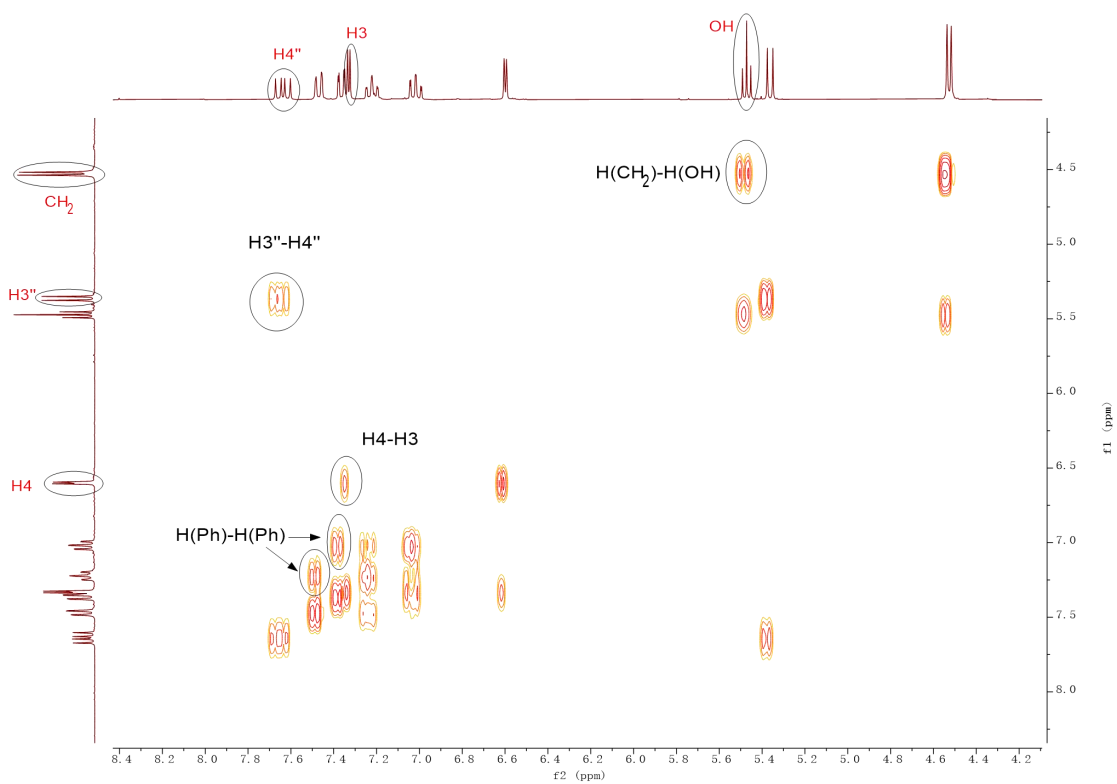
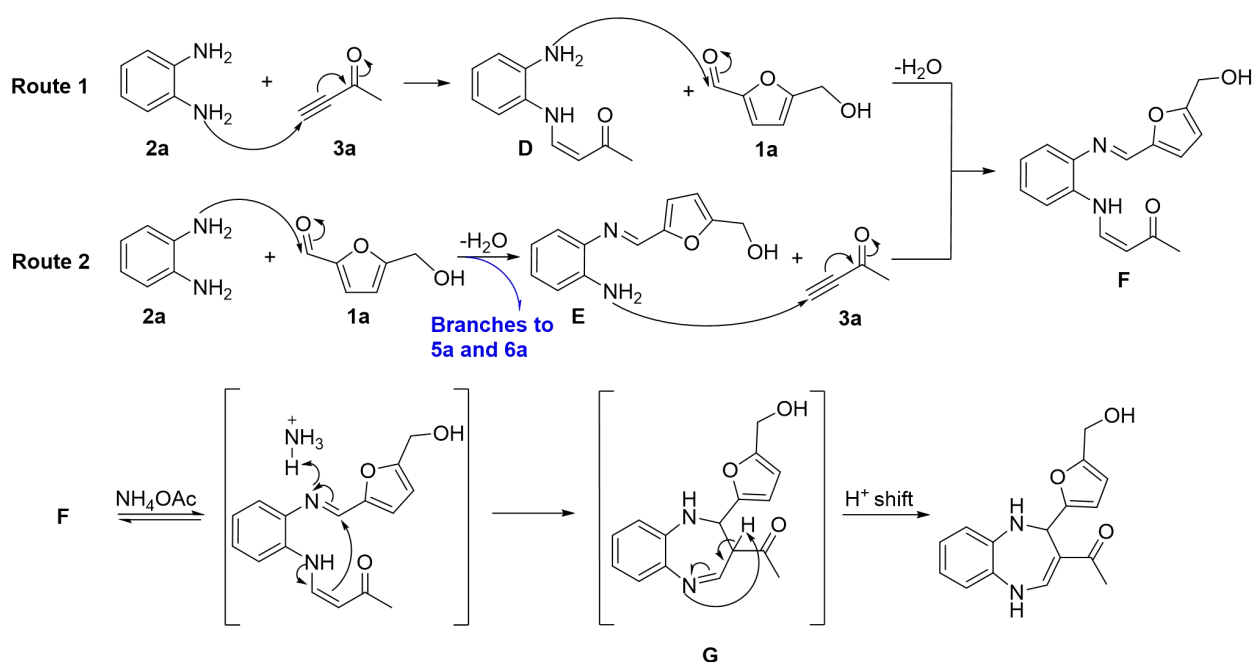


Figure 22. ^1H - ^1H COSY NMR spectrum of the intermediate **F**

On the basis of the above experimental observations and previous reports, a possible reaction mechanism is proposed. The reaction may first generate intermediate enaminoketone **A** through the addition of *o*-phenylenediamine and but-3-yn-2-one, then intermediate **F** by formation of an imine arising from the reaction of the second amino group with the carbonyl group of 5-HMF (Scheme 80, route 1). The alternative route is the formation of the imine intermediate **E** by condensation of one amino group of *o*-phenylenediamine with 5-HMF, then reaching intermediate **F** by 1,4-addition of the second amino group onto the but-3-yn-2-one (Scheme 80, route 2). Ammonium acetate could promote the intramolecular cyclization of intermediate **F** into intermediate **G**, which would undergo a proton transfer to form the most stable target product. It is also possible that ammonium acetate would activate the ketone to more reactive intermediates, either by protonation or by formation of an iminium, facilitating subsequent ring formation. As shown in Scheme 80, the reaction likely proceeds through a mixed pathway.



Scheme 80. Proposed mechanism for the [4+2+1] cycloaddition involving 5-HMF

2.3 Conclusion

In summary, we have developed the first application of the bio-based platform 5-HMF in the multi-component reaction towards 1,5-benzodiazepines. Thanks to a careful investigation of the influence of all parameters, a set of particularly mild reaction conditions, namely ammonium acetate in ethanol at 60 °C, was established. The participation of ammonium acetate is considered to improve chemoselectivity, offering an interesting, mild and clean alternative method for broadening the functionalization of 1,5-benzodiazepines. This reaction was found to be applicable to a broad range of substrates, providing a facile and efficient entry to new functionalized 1,5-benzodiazepines. This study provides a diversification of the scope the use of 5-HMF in fine chemistry.

Chapter III

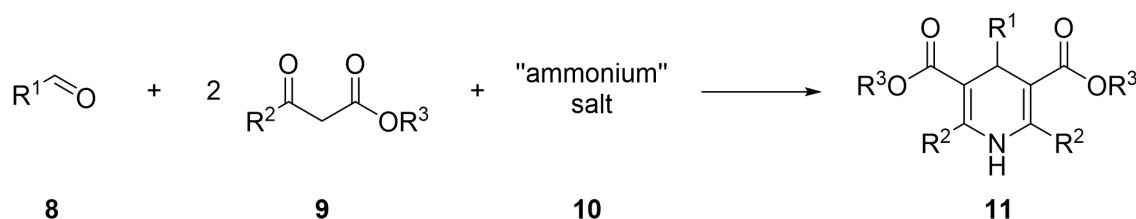
The Hantzsch dihydropyridine synthesis involving 5-HMF

Chapter III. The Hantzsch dihydropyridine synthesis involving 5-HMF

3.1 Background

3.1.1 Introduction

The previous chapter highlighted the remarkable compatibility of ammonium acetate, used as a catalyst, with HMF chemical reactivity. This led us to explore other reactions involving HMF in which ammonium acetate would be not only a catalyst or a promoter acting on the rate determining steps, but also a source of ammonia able to deliver a nitrogen atom in the target. In the second part of my thesis, I focused on the use of 5-HMF in a widely used MCR involving ammonium salts, namely, the Hantzsch synthesis of 1,4-dihydropyridines (1,4-DHPs) (Scheme 81).



Scheme 81. Hantzsch 1,4-dihydropyridines synthesis

The Hantzsch pyridine synthesis was first mentioned by Arthur Hantzsch in 1881 as a method to produce 1,4-dihydropyridine (1,4-DHP) product by condensation of acetaldehyde, ammonia and ethyl 3-oxobutanoate.¹⁹¹ It can be considered as one of the oldest MCRs. The use of 1,4-DHP by Smith Kline and Bayer as hypotensive and vasodilatory agents opened significant interest towards this scaffold from the medicinal chemistry community.^{192, 193}

1,4-DHPs are renowned for a wide range of biological properties, among them as calcium channel blocker used in cardiovascular, cerebrovascular and antihypertensive drugs by interfering with the entry of calcium ions into cells.¹⁹⁴ Figure 23 exemplifies some marketed drugs and other biologically active molecules that include symmetric or non-symmetric 1,4-

dihydropyridines with different substituents on the DHP pharmacophore. 1,4-DHPs have also been reported to exhibit other biological activities, such as antibacterial, antioxidant, antidiabetic or antihyperglycemic, lipid modulating agents, α -amylase and α -glucosidase inhibitors and insecticidal.¹⁹⁵⁻²⁰¹

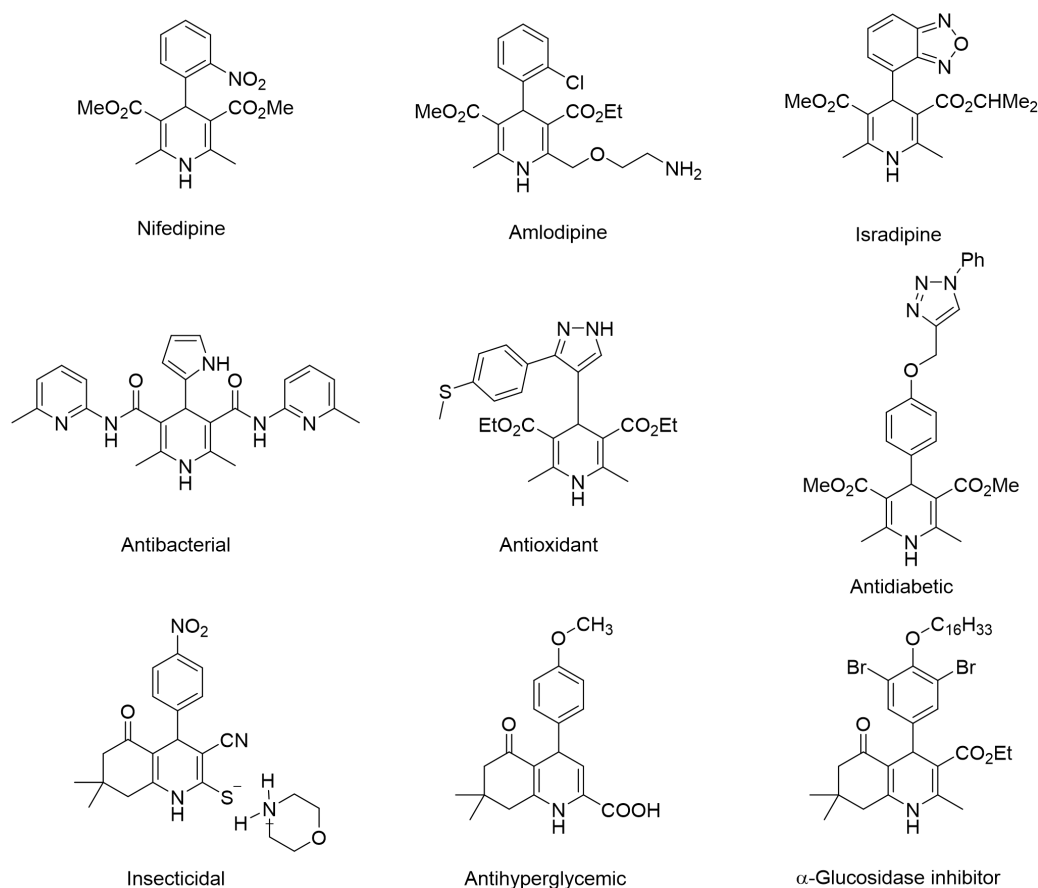


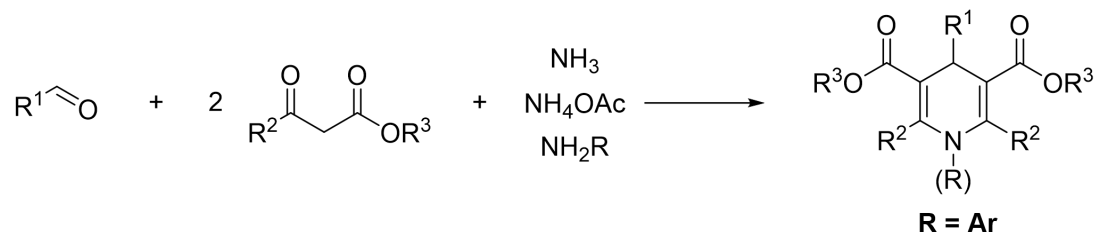
Figure 23. Some bioactive molecules containing 1,4-DHP skeleton

3.1.2 The Hantzsch reaction

3.1.2.1 Mechanism of the Hantzsch reaction

The Hantzsch reaction is one of the earliest multicomponent reactions discovered and is considered to be the most classic and attractive route to construct 1,4-DHPs until now.²⁰²⁻²⁰⁵ This MCR typically involves the reaction of an aldehyde, two molecules of β -ketoester, and a nitrogen source, as depicted in Scheme 82. It is noteworthy that ammonia used in the original Hantzsch protocol was replaced by ammonium salts especially ammonium acetate in most

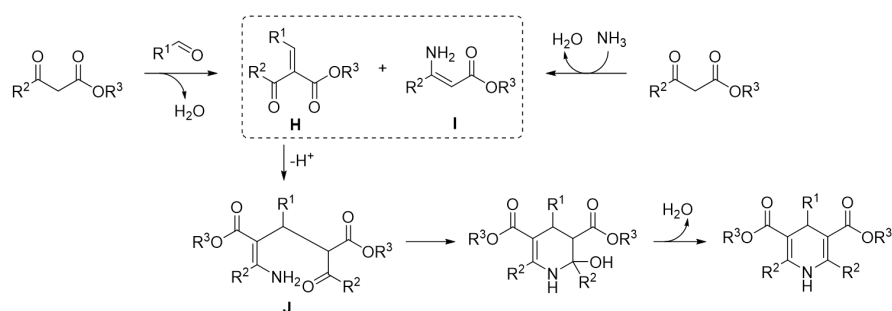
later studies, considering that ammonium acetate as an ammonium salt has practical advantages in the Hantzsch reaction, such as better control of pH and easier storage, use and handling than ammonia. Anilines can also be used to prepare N-substituted products.



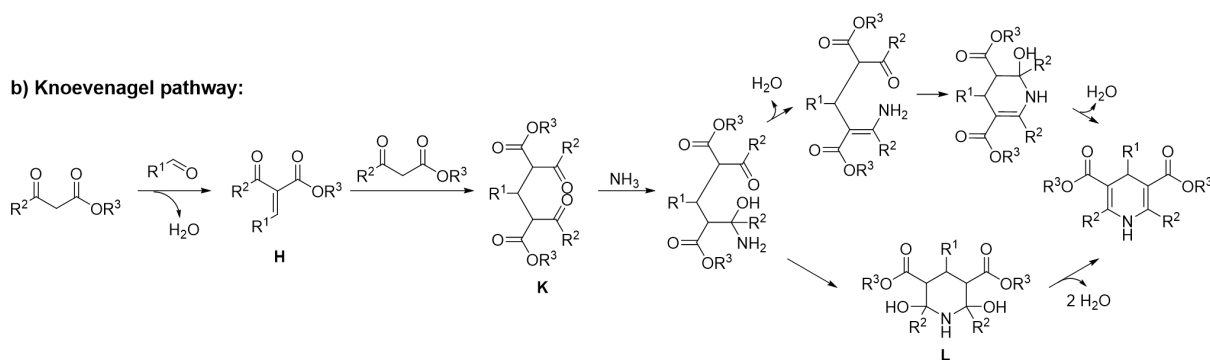
Scheme 82. Typical Hantzsch reaction

Regarding the mechanism of the Hantzsch reaction, several possible pathways have been reported, varying in which order the generated Knoevenagel and enamine intermediates are involved (Scheme 83).^{206, 207}

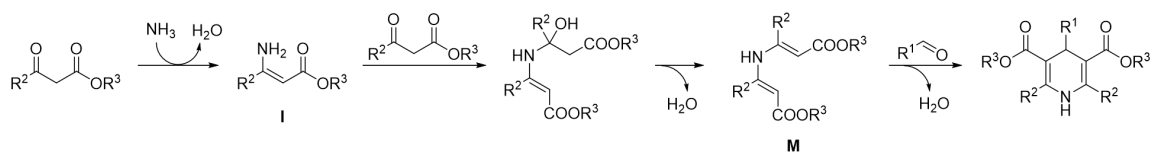
a) Knoevenagel-enamine pathway:



b) Knoevenagel pathway:



c) Dienamine pathway:



Scheme 83. Proposed mechanism of the Hantzsch reaction

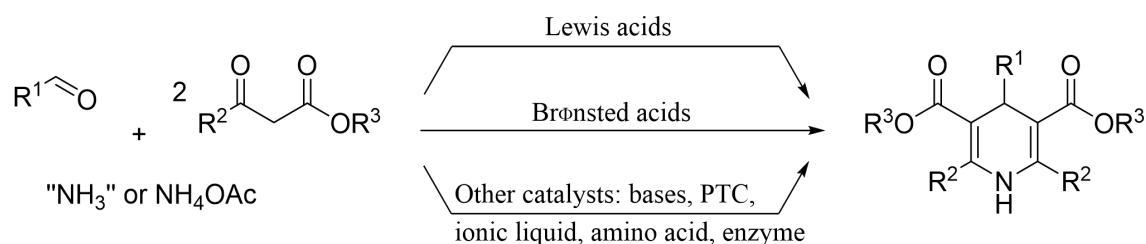
The most accepted reaction pathway, based on NMR monitoring, involves the Knoevenagel condensation between the β -ketoester and the aldehyde giving the α,β -unsaturated carbonyl intermediate **H**. In parallel, the ammonia attacks the β -carbonyl carbon of the β -ketoester, affording the enamine intermediate **I**. Compound **H** serves as a Michael acceptor to react with **I** and provide compound **J** through a 1,4-conjugate addition. Final intramolecular cyclization and dehydration starting from compound **J** provides the 1,4-DHP structure (Scheme 83a).

An alternative mechanism, referred to as the “Knoevenagel pathway”, involves an initial Knoevenagel condensation of a β -ketoester and an aldehyde giving intermediate **H**. Then, 1,4-addition of a second β -ketoester on the Knoevenagel condensation product **H** provides intermediate **K**. Nucleophilic attack of ammonia on intermediate **K**, followed by dehydration and cyclization provide the 1,4-DHP scaffold (Scheme 83b).

A third, more rarely mentioned, possibility involves the initial nucleophilic attack of ammonia on the β -carbonyl carbon of the β -ketoester to form the enamine **I**. The amino group of enamine **I** then reacts with another molecule of β -ketoester to give dienamine **M** after dehydration. Subsequently, the dienamine **M** attacks as a nucleophile to the carbonyl carbon of the aldehyde, resulting in the formation of a new carbon-carbon bond, finally yielding the 1,4-DHP product *via* intramolecular cyclization. (Scheme 83c).

3.1.2.2 Catalysts in Hantzsch reaction

In terms of catalysis, the development of the Hantzsch reaction involves the exploration of various types of catalysts, mainly Lewis acids and Brønsted acids, other catalysts such as phase transfer catalysts (PTC), ionic liquids, amino acids and enzyme catalysts have also been explored (Scheme 84).²⁰⁸ This is also right for analogous reactions using slightly different reagents, referred to as Hantzsch-like reactions (*vide infra*).



Scheme 84. Different types of catalysis reported for the Hantzsch reaction

Considering the proposed mechanism of Hantzsch reaction, compounds that can coordinate with the carbonyl oxygen atom enhance the electrophilicity of the carbonyl carbon atom and the acidity of β -dicarbonyl compounds, thereby achieving the purpose of accelerating the reaction.

The cationic part of Lewis acids is most likely to coordinate both the carbonyl oxygen of the carbonyl compound and the aldehyde which is beneficial to enhancing the electrophilicity of both carbonyl carbon atoms. The use of Lewis acids has been reported as the catalysts in the Hantzsch/Hantzsch-like dihydropyridine synthesis in a large number of publications. Metallic Lewis acids such as halides, triflate, nitrate, sulfate salts of Fe, Al, Ba, Bi, Li, Cd, Mg, Ce, Sc, Yb, Zn, K, Zr and some metal oxide nanoparticles of Zn, Ni, Cu, Mg, Fe, Ti, Zr promote this reaction.²⁰⁸⁻²¹⁰

Brønsted acids tend to promote protonation of the carbonyl oxygen of carbonyl compounds and aldehyde which is also conducive to the formation of Knoevenagel condensation product and enamine, and may even play a promoting role in the final dehydration step towards 1,4-DHPs. The original Hantzsch reaction uses acetic acid as the Brønsted acid catalyst. TsOH, TfOH, nicotinic acid have also been proved to be efficient catalysts, as well as supported Brønsted acids, for example silica or zirconia supported (SO_3H , PPA, HClO_4) catalysts.^{208, 210}

Using quaternary ammonium salts with bulky and hydrophobic substituents, such as tetrabutyl ammonium bromide, benzyl trimethylammonium fluoride hydrate and tetrabutylammonium hydrogen sulfate as phase transfer catalysts can improve the overall efficiency of the reaction by allowing better contact between the reactants. Quaternary ammonium cations can form complexes with anionic substances participating in the reaction, which enhances the nucleophilicity of the anionic substances and promotes the reaction between nucleophiles and electrophiles.

Other species such as imidazolium ionic liquids ([EMIM]OAc, [tbmim]Cl₂/AlCl₃, Silica-SO₃H-[BMIM][PF₆]), neutral covalent molecules (triphenyl phosphine and trimethyl silyl iodide), amino acid (L-Proline), enzymes (Bakers' yeast, triacyl glycerol acyl hydrolase), ordered mesoporous materials (MCM-41 materials, SBA-15 materials etc.) and bases (Et₂NH and piperidine) have also been investigated.^{207, 208, 211}

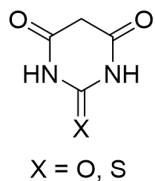
Finally, let us note that the use of ammonium acetate as the nitrogen source has been reported to provide high yields of Hantzsch products from aromatic aldehydes and β -ketoester even without the involvement of additional catalysts or under microwave conditions.^{212, 213}

3.1.2.3 Hantzsch-like reactions

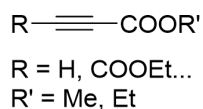
In the recent years, variations have been developed by replacing one or more components in the classical Hantzsch reaction with novel reactive building blocks, but basically following the ideas of the Hantzsch reaction, thus being referred to as "Hantzsch-like" reactions. They have greatly increased the structural diversity of 1,4-DHPs, especially the synthesis of unsymmetrical 1,4-DHPs. The alternatives mainly include the following categories: i) substituting the β -ketoester with β -amidoketone or malononitrile or alkyne; ii) using an enamine in place of the amine/ β -ketoester couple; iii) substituting the aldehyde with an enone. Several examples are depicted in Scheme 85.²¹⁴

Reactive building blocks:

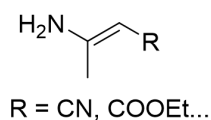
β -Amidoketones:



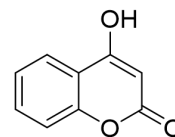
Alkynes:



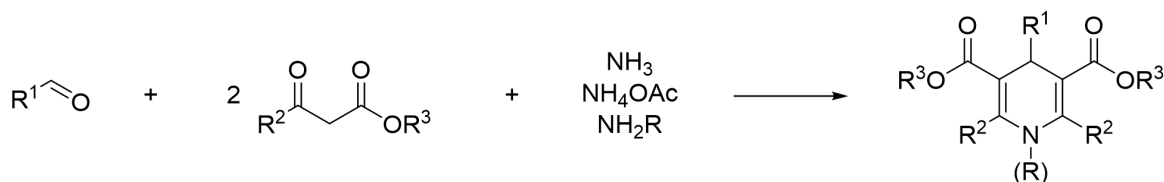
Enamines:



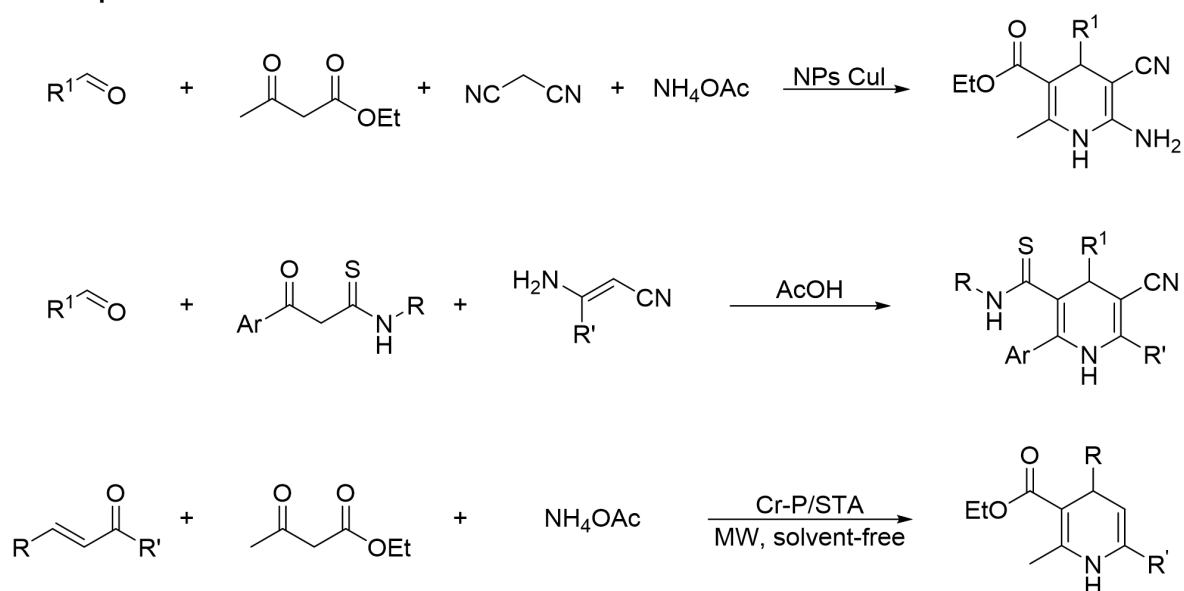
Enones:



Hantzsch reaction:



Examples of Hantzsch-like reactions:



Scheme 85. Hantzsch-like reactions using various alternative building blocks

3.1.3. Plan of our study

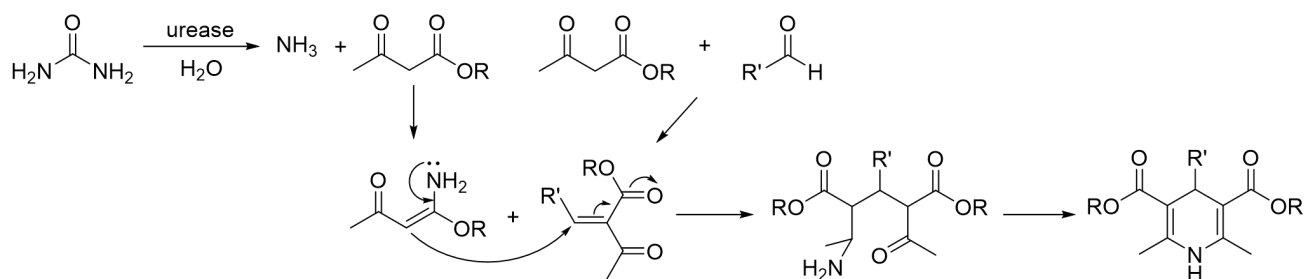
The introduction of heterocyclic substituents is an interesting structural diversification in drug design. The case of the Hantzsch reaction of 5-HMF, which exhibits very different chemical reactivity and sensitivity compared to furfural, has been only scarcely studied as substrate in the Hantzsch dihydropyridine synthesis.^{135, 215-219} Considering the rich functionality of 5-HMF,

its incorporation into a MCR strategy to prepare diverse 1,4-DHPs has been the aim of the second project of my thesis.

In this chapter, we give a detailed investigation of the use of 5-HMF in the Hantzsch dihydropyridine synthesis. First, we explored the three-component synthesis of symmetrical 1,4-DHPs from 5-HMF, a β -dicarbonyl compound and a nitrogen source, studying the influence of the nitrogen source and of the other reaction parameters to define the mildest conditions. The structural scope of the reaction using diversely substituted β -dicarbonyls was then evaluated and extended to the four-component reaction towards unsymmetrical 1,4-DHPs when two different β -dicarbonyls are used.

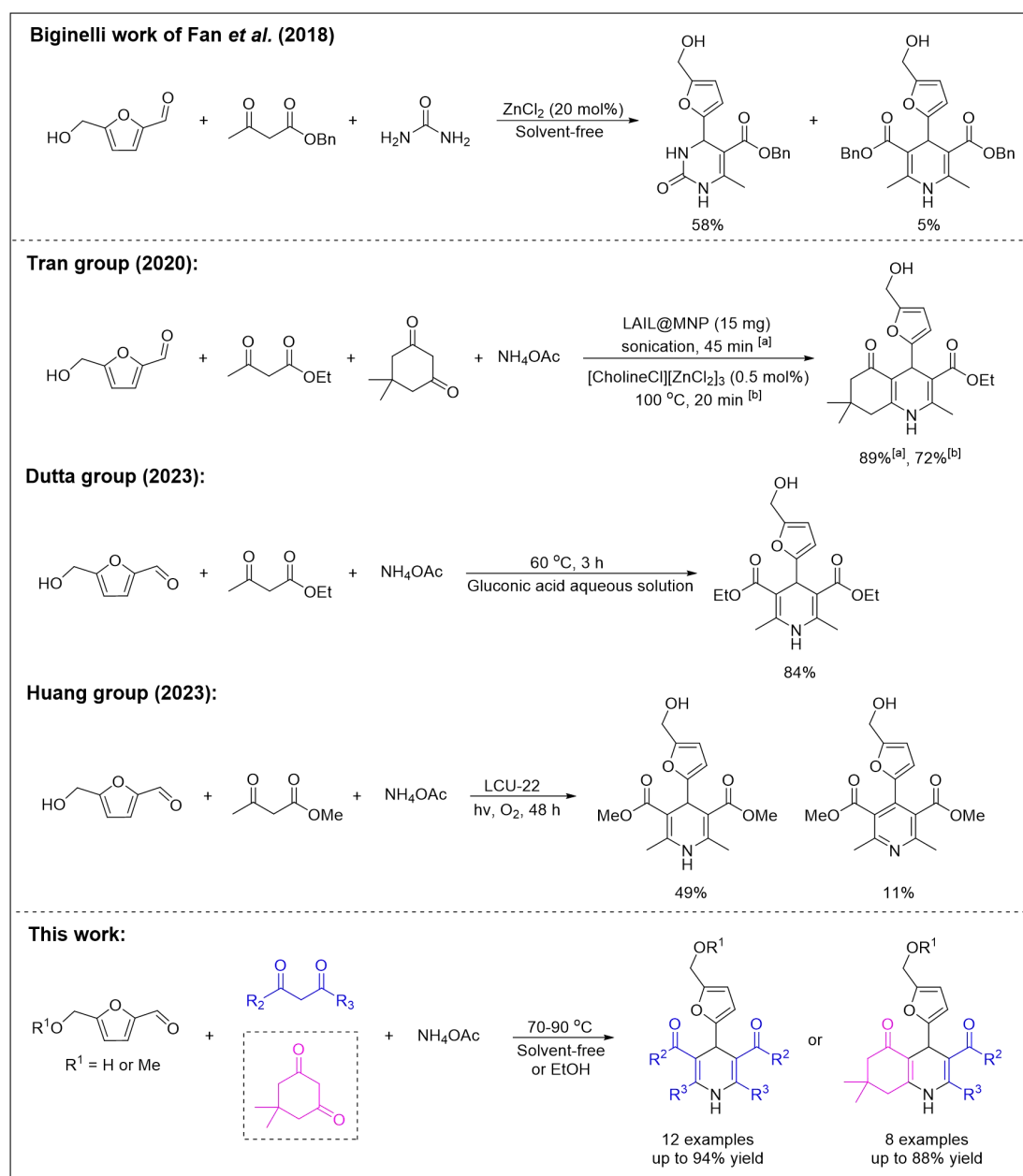
3.2 Synthesis of 5-HMF derived 1,4-dihydropyridines

The key earlier finding with respect to the use of 5-HMF in the Hantzsch reaction has been an observation by W. Fan in 2018 in our laboratory, when he investigated the Biginelli reaction towards 3,4-dihydropyrimidin-2-ones.¹³⁵ He found that in some cases, when the Biginelli reaction was sluggish, small quantities of Hantzsch dihydropyridines were obtained as by-products in the presence of the Lewis acid ZnCl_2 . This was the first mention ever of a Hantzsch product arising from HMF. This can be explained by the degradation of urea forming ammonia, triggering the possible Hantzsch pathway competing with the Biginelli one. A study of biocatalyst urease catalyzing the release of ammonia from urea to participate in the Hantzsch reaction reported by Tamaddone et al. in 2016 provides experimental support for this competitive mechanism, as shown in Scheme 86.²¹⁵



Scheme 86. Possible mechanism of urea releases ammonia for Hantzsch reaction

Since this report from our laboratory in 2018, the very few investigations on the Hantzsch dihydropyridine synthesis in which 5-HMF is mentioned as substrate have only concerned the use of complex catalysts and solvents,²¹⁶⁻²¹⁹ such as an acidic imidazolium chlorozincate (II) ionic liquid immobilized onto magnetic Fe₃O₄ catalyst requiring sonication (LAIL@MNP), deep eutectic solvents in the presence of [CholineCl][ZnCl₂]₃ or gluconic acid, or LCU-22 ([Zn(1-ipIM)₃]₂[Zn₆(AsW₉O₃₃)₂(1-ipIM)₆]₂(1-HipIM)) leading also to the oxidized pyridine (Scheme 87).



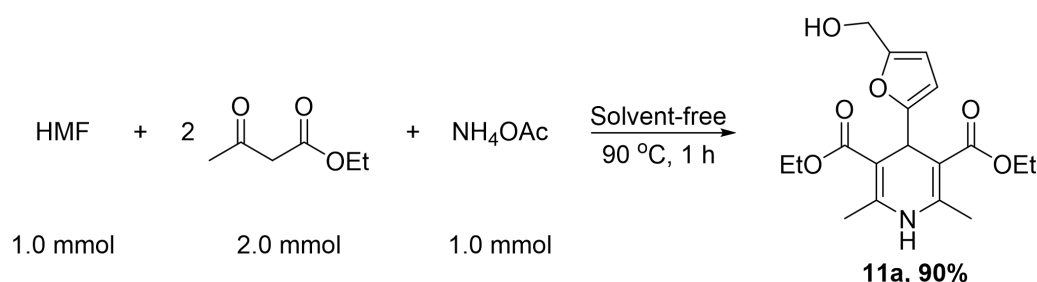
Scheme 87. Reported Hantzsch dihydropyridine synthesis of 5-HMF

Overall, very limited information was available on the use of HMF in Hantzsch reactions, and no example of reactions involving HMF in the absence of any complex catalyst or solvent was ever reported. In the next sections, we show the results of our investigation of this reaction, focusing on finding appropriate conditions for the reaction without any additional complex catalyst. Then we applied the best protocol to a range of diversely substituted β -dicarbonyls in the three and the four-component reaction towards symmetrical and unsymmetrical 1,4-DHPs.

3.2.1 Three-component approach towards symmetrical 1,4-dihydropyridines

3.2.1.1 Identification of target product and analytical protocols

We initiated our study of 5-HMF in Hantzsch reaction with the three-component protocol which leads to the symmetrical 1,4-DHPs. The first reactions were performed using ethyl acetoacetate as β -dicarbonyl compound and ammonium acetate as nitrogen source. In order to develop the cleanest and mildest conditions, we focused on systems able to play both the role of the nitrogen source and a smooth catalyst, and making possible to run the reaction under no-solvent conditions or in a solvent considered as acceptable in terms of green chemistry principles. The survey was first performed by reacting 5-HMF (1 mmol, 1 eq.), ethyl acetoacetate (2 mmol, 2 eq.) and ammonium acetate (1 mmol, 1 eq.) under solvent-free conditions at 90 °C, leading to the expected 1,4-DHP **11a** after 1 hour in 90% isolated yield after purification by silica column chromatography (Pentane : EA = 2:1) (Scheme 88).



Scheme 88. Three-component Hantzsch dihydropyridine synthesis involving 5-HMF

The structure of product **11a** could be identified by 1D NMR (¹H NMR, ¹³C NMR, DEPT) and 2D NMR (COSY, HSQC, HMBC) spectroscopies. In the ¹H NMR spectrum of **11a** (Figure 24), newly formed proton signal at δ 5.17-4.91 ppm (H₄) and δ 8.88 ppm (NH) was observed.

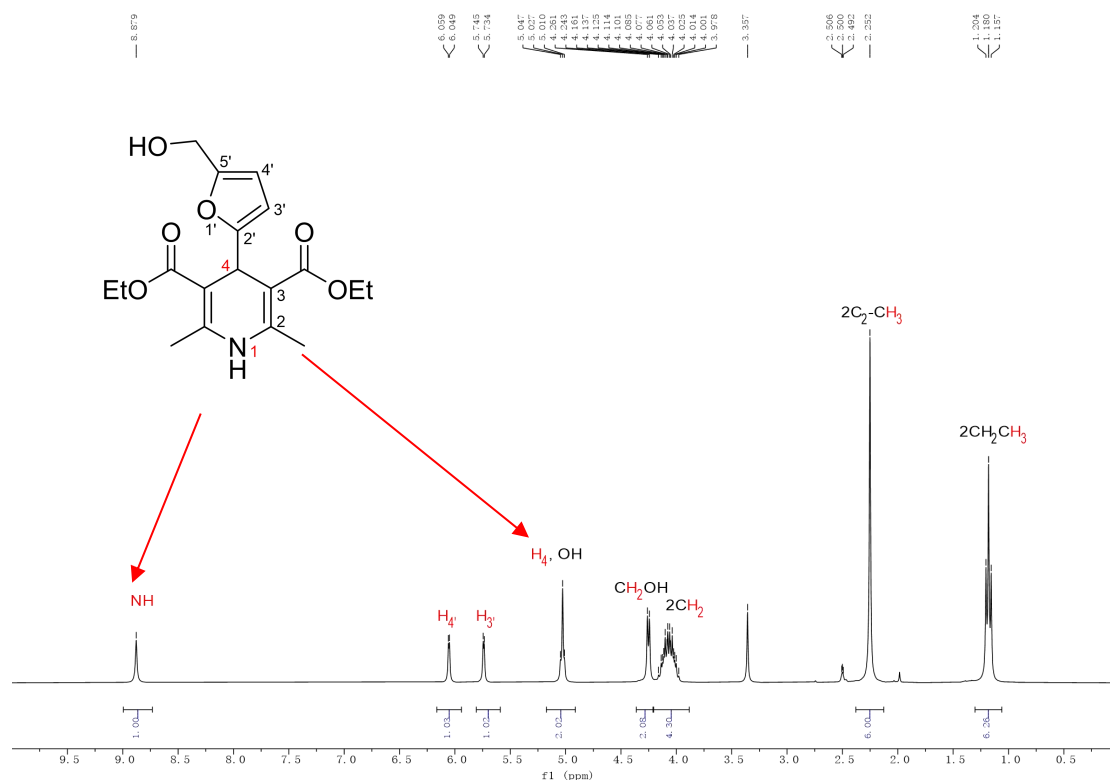


Figure 24. ^1H NMR spectrum of the 1,4-dihydropyridine **11a**

The newly formed single proton peak at δ 8.88 ppm has no relevant peak signal in the HSQC spectrum and is confirmed to be the proton peak of NH, while the one-proton signal overlapping with the OH at δ 5.17-4.91 ppm is correlated with a carbon at δ 32.9 ppm (Figure 25). In the HMBC spectrum, the correlation of $C_{3/5}$ - H_1 , ($\underline{CH_3}$ - $C_{2/6}$)- H_1 , \underline{CO} - H_4 can be observed (Figure 26). The positions of the newly formed C_4 - C_3 and C_2 - N_1 bonds were further verified, clearly indicating the formation of 1,4-DHP **11a**.

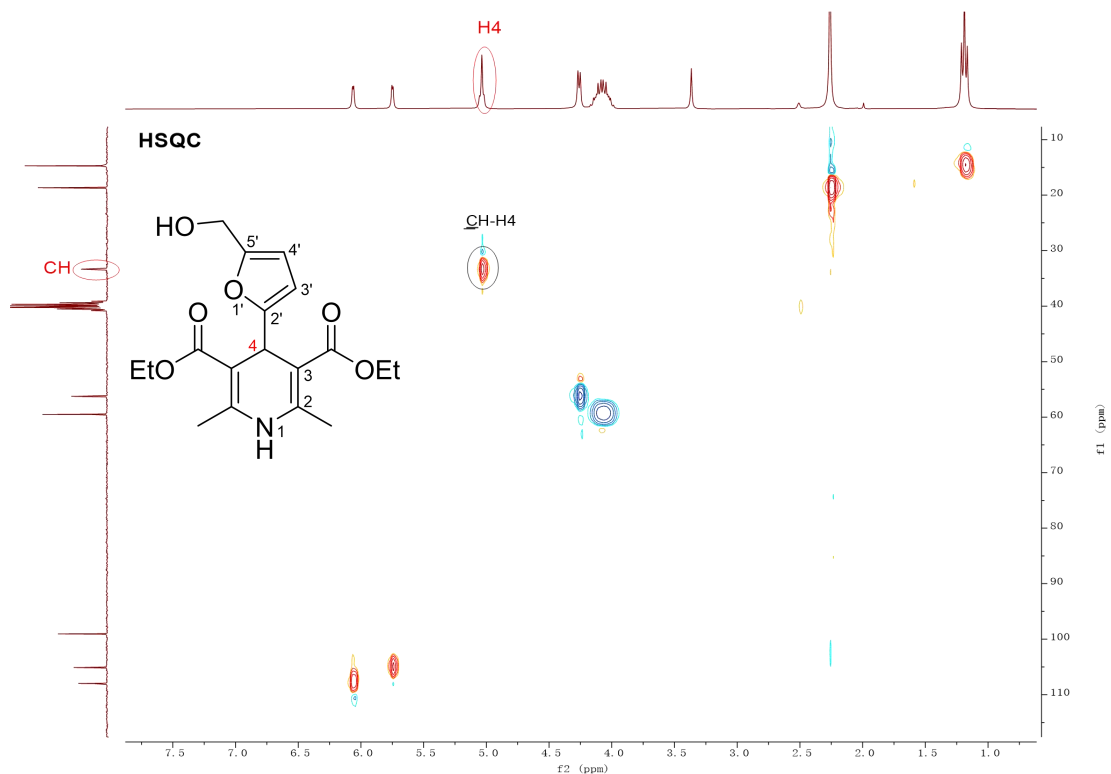


Figure 25. HSQC NMR spectrum of the 1,4-dihydropyridine **11a**

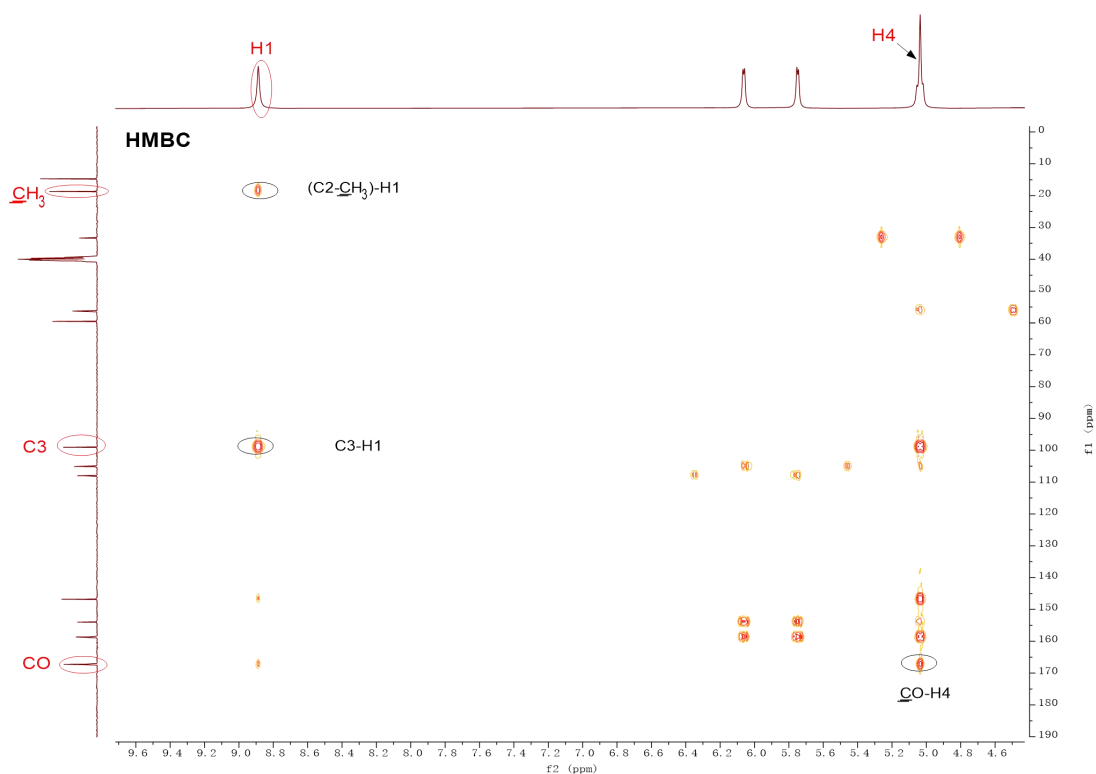


Figure 26. HMBC NMR spectrum of 1,4-dihydropyridine **11a**.

The ^1H NMR spectra of the crude reaction mixture were recorded in the presence of 1,3,5-trimethoxybenzene (1/3 equivalent, 56 mg) as internal standard, in which integration of specific peaks belonging to the starting material, Hantzsch product **11a**, the Knoevenagel intermediate **N** or other unidentified by-products, allowed to determine the proportions of these compounds. The example is shown below (Figure 27).

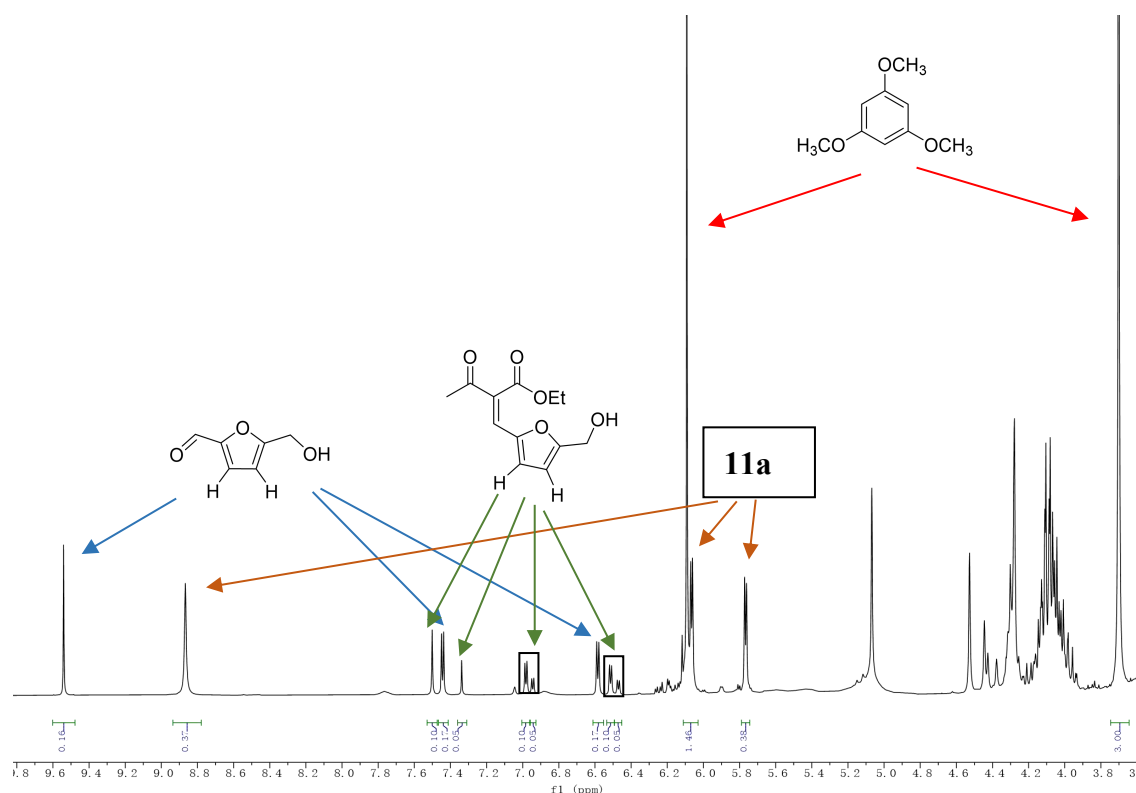
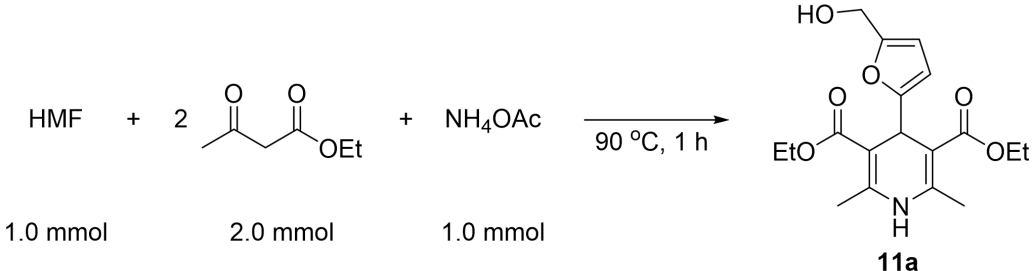


Figure 27. The selected proton signals used for estimating the NMR yield of 5-HMF, Knoevenagel intermediate **N** and **11a** (NMR spectrum of entry 1 reaction in Table 12)

3.2.1.2 Influence of reaction parameters

Having a reaction which works at 90% yield was a very good result. It was interesting to further study the relevant parameters affecting the yield of the reaction, notably with respect to the counteranion. Thus, besides ammonium acetate, several other ammonium salts and ammonia solutions were investigated in this three-component reaction. The results are summarized in Table 12.

Table 12. Screening of nitrogen sources in the three-component Hantzsch reaction of HMF

			
Entry	“N” source	Conversion of 5-HMF (%)	NMR yield of 11a (%)
1	(NH ₄) ₂ CO ₃ , solvent-free	83	37
2	NH ₄ HCO ₂ , solvent-free	100	40
3	NH ₄ I, solvent-free	43	0
4	NH ₄ Cl, solvent-free	15	0
5	NH ₄ Br, solvent-free	<10	0
6	(NH ₄) ₂ SO ₄ , solvent-free	<10	0
7	Ammonia solution (30% in H ₂ O)	100	70
8	Ammonia solution (0.5 M in dioxane)	trace	0
9	NH ₄ HCO ₂ (1 M in EtOH)	100	74
10	NH ₄ OAc, solvent-free	100	90

Using (NH₄)₂CO₃ (Table 12, entry 1) led to a significantly lower yield of 37% of target product with 83% conversion of 5-HMF and more than 20% of the starting amount ethyl acetoacetate remaining, as well as 15% yield in Knoevenagel intermediate (intermediate **N**).

The structure of the Knoevenagel intermediate **N** was identified by analyzing 1D and 2D NMR. Both the *Z* and *E* configurations of intermediate **N** were observed. In the ¹H NMR spectrum, the newly formed proton was observed at δ 7.52 ppm or δ 7.33 ppm (Figure 28). By comparing the NOSEY spectra of the two structures, it can be found that there is a correlation between *CH* (at δ 7.52 ppm) and *COCH₃* (at δ 2.34 ppm) in the NOSEY spectra of the former

(blue one), but no obvious correlation was observed in the latter (black one), so the former spectra is considered to be that of the compound with the *Z* configuration, while the latter is for the compound with the *E* configuration (Figure 29).

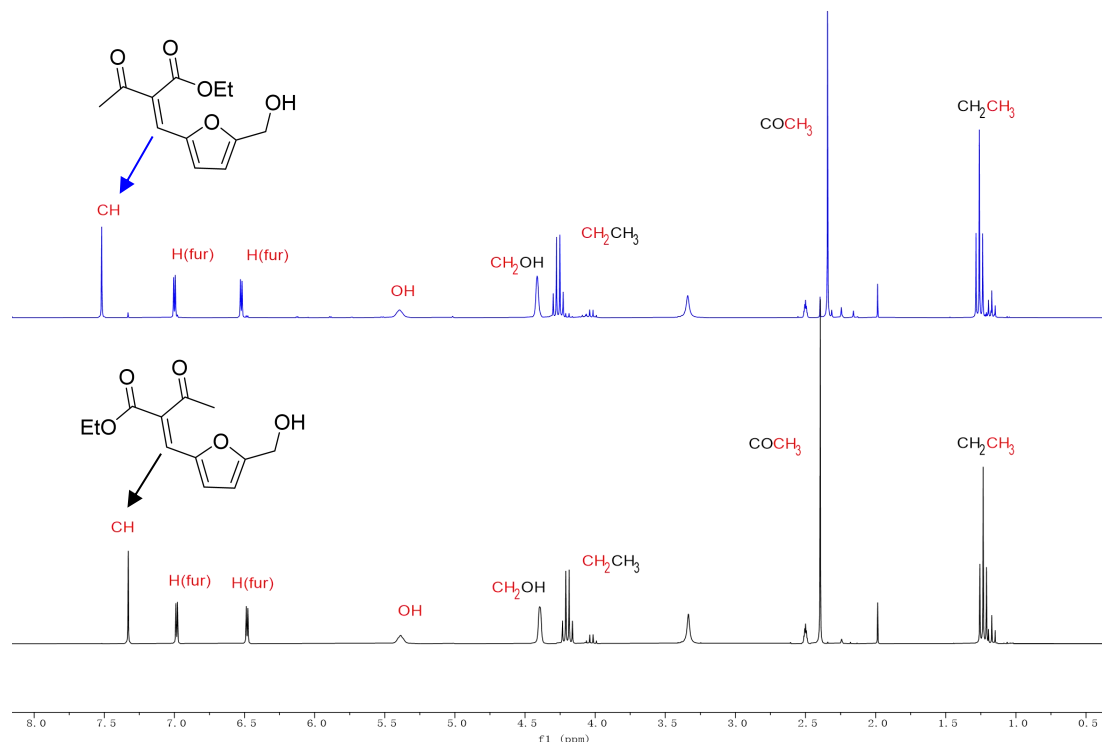


Figure 28. The ^1H NMR spectrum of Knoevenagel intermediate N

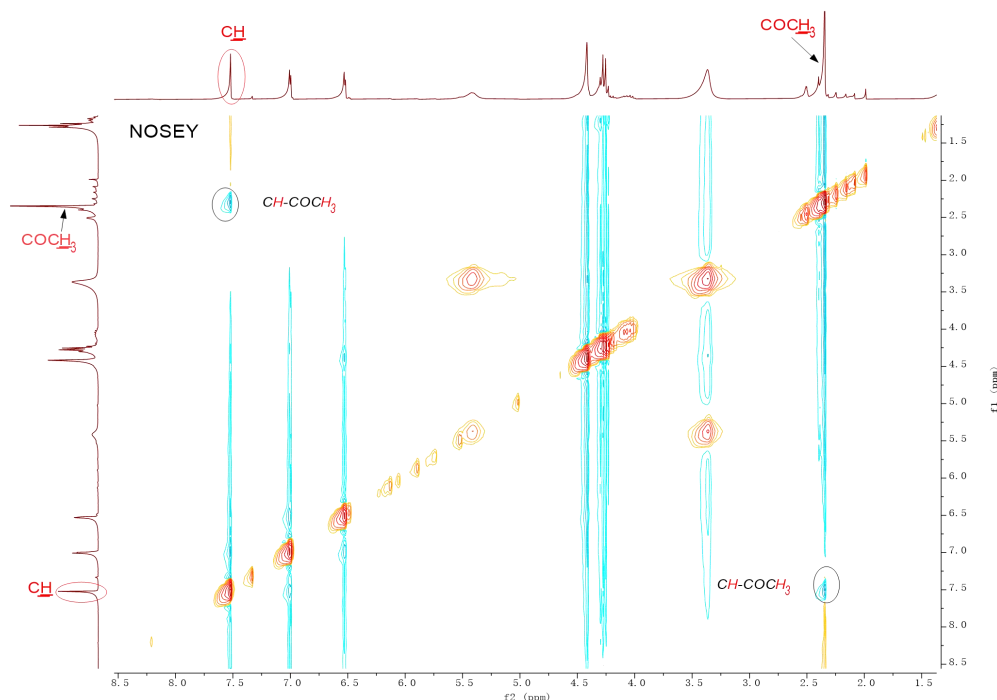


Figure 29. The NOESY NMR spectrum of Knoevenagel intermediate N

Going back to the discussing Table 12, using ammonium formate (NH_4HCO_2) under neat conditions (Table 12, entry 2) led to a messy mixture with only a 40% yield of target product together with some Knoevenagel intermediate **N** (ca. 12%) though all 5-HMF was consumed. No target product was generated either when ammonium halides (I, Cl, Br) or ammonium sulfate were tested (Table 12, entries 3-6). In these cases, NMR of the crude mixture showed essentially starting materials, except for NH_4I which gave a messy mixture of unconverted reagents, together with some unidentified by-products. A few sets of conditions using nitrogen sources which are commercially available in solution were also tested. Interestingly, a 30% ammonia solution in water led to a 70% yield of target product (Table 12, entry 7) while the ammonia solution in dioxane was ineffective (Table 12, entry 8). A solution of ammonium formate (NH_4HCO_2) in EtOH provided target product in 74% yield (Table 12, entry 9). Overall, using ammonium acetate as nitrogen source leads to the target product **11a** in the highest yield of 90% under solvent-free conditions (Table 12, entry 10).

The difference between the results using ammonium halides and ammonia solutions should be attributed to the fact that the ammonium ions in ammonium halide or ammonium sulfate is positively charged, which makes the nitrogen atom lacking nucleophilicity thus not readily available for a nucleophilic attack. In contrast, ammonia, which has neutral nitrogen atom with lone pairs of electrons, is more nucleophilic and readily undergo nucleophilic reactions with electrophiles such as β -ketoesters, thereby initiating the formation of 1,4-dihydropyridine products. Ammonium ions with weak bases counteranions appear the best balance, because the ammonia form is also present while the ammonium form can behave as the acid catalyst. Therefore, we chose NH_4OAc as the nitrogen source for the next step of the study under solvent-free conditions.

The appropriate amount of ammonium acetate was then optimized (Table 13). The reaction of 5-HMF with ethyl acetoacetate in the presence of ammonium acetate was performed at 90 °C for 1 hour. As mentioned before, an equivalent amount of ammonium acetate (1 mmol, 1eq.) provided a 90% NMR yield of **11a** (entry 1). A small increase of the yield of target 1,4-DHP

was observed when a slight excess of ammonium acetate (1.2 to 1.5 equiv.) was introduced (entries 2-3), with a maximum yield of 94% in the presence of 1.5 equivalents. Adding more ammonium acetate (1.8 equiv.) did not lead to a better yield (entry 4). Therefore, we selected 1.5 equivalents of NH₄OAc for subsequent experiments.

Table 13. Influence of the amount of ammonium acetate

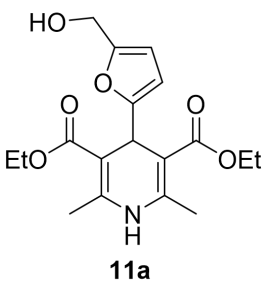
11a

Entry	NH ₄ OAc (mmol)	NMR Yield of 11a (%)
1	1.0	90
2	1.2	91
3	1.5	94
4	1.8	91

The effects of reaction temperature and reaction time were then studied and the results are shown in Table 14. Lowering the temperature to room temperature resulted in a significant decrease in the yield to 66% (entry 1). Extending the reaction time to 4 h at room temperature ended with a good 75% yield (entry 2). Further extension of the reaction time to several hours had no effect on the yield (entry 2/3). When screening reaction temperatures from 50 °C to 80 °C (entries 4-6, 8), we found that when the reaction was run for 1 hour, the yield increased slightly with increasing temperature. A slightly higher yield of 93-94% was achieved at 80 °C or 90 °C (entries 8, 11), and a similar yield of 93% was achieved at 70 °C (entry 6). At 70 °C, extension of the reaction time to several hours had no effect on the yield (entries 6/7), whereas a clear decrease in the yield was observed at 80 °C (entries 8/9). The reaction kinetics appear thus to be not strongly dependent on the reaction temperature. Actually, all

conditions used in this study resulted in high or excellent yields, in a very clean reaction allowing to run it under a wide range of temperatures.

Table 14. Influence of temperature and reaction time

$\text{HMF} + 2 \text{CH}_3\text{COCH}_2\text{CO}_2\text{Et} + \text{NH}_4\text{OAc} \xrightarrow{\text{solvent-free}}$			
1.0 mmol	2.0 mmol	1.5 mmol	 <p>11a</p>
Entry	Temperature	Time	NMR Yield of 11a (%)
1	rt	1 h	66
2	rt	4 h	75
3	rt	22 h	74
4	50 °C	1 h	84
5	60 °C	1 h	90
6	70 °C	1 h	93
7	70 °C	15 h	92
8	80 °C	1 h	94
9	80 °C	15 h	76
10	90 °C	25 min	93
11	90 °C	1 h	94

Isolation of products

Isolation of the products was achieved using silica gel column chromatography. However, for the reaction which give very high yields of target products, we checked whether it was possible to avoid the chromatography protocol and if simple aqueous washings and extractions with ethyl acetate could provide the pure final product. In Figure 30 are displayed

the ^1H NMR spectrum for the product arising from the reaction achieved under the condition in Table 14 entry 10 (90 °C, 25 min), comparing the NMR spectrum of the crude reaction mixture (a), the NMR spectrum of the product purified by column chromatography (b) and the spectrum of the product obtained after simple treatment with ice water and extraction in ethyl acetate (c). Spectrum (c) confirms that remarkably high purity can be obtained with the simple washing and extraction protocol.

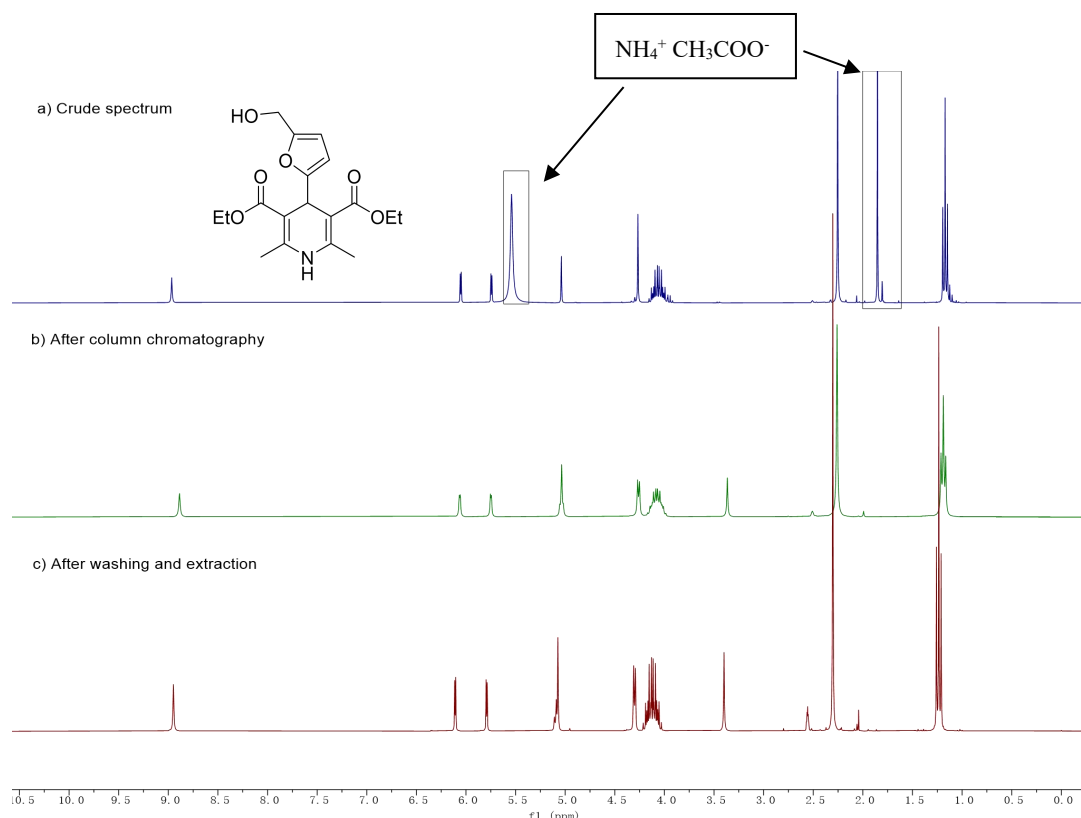


Figure 30. Comparison of the **11a** spectrum of crude reaction mixture (a), after silica gel chromatography column (b) and after washing and extraction work up (c)

3.2.1.3 Structural scope

In the structural scope section, we first investigated the generality of the Hantzsch dihydropyridine reaction of 5-HMF using nine differently substituted dicarbonyl substrates, either ketoesters including the initial ethyl acetoacetate example, or diketones (**1a-1i**).

Considering the results of the above experiments, we decided to choose the following set of conditions, 5-HMF (1.0 mmol), β -diketones (2.0 mmol), ammonium acetate (1.5 mmol), no solvent, at 70 °C during 1 hour, as standard conditions. The yields shown in the different figures are isolated yields after column chromatography unless otherwise stated.

As shown in Figure 31, we found that most of the β -ketoesters gave the corresponding 1,4-dihydropyridines in excellent yields with full conversion of HMF. The alkyl acetoacetates (ethyl, methyl and benzyl esters) provided respectively 93%, 92%, and 92% of the corresponding target products (**11a-11c**). The methoxyethyl and allyl esters also performed well, providing 93% and 84% of the targeted products (**11d-11e**), respectively. Switching to the methyl 4-methoxyacetoacetate led to a significantly reduced yield of the target product accompanied by a complex mixture of unidentified molecules (**11f** compared with **11b**).

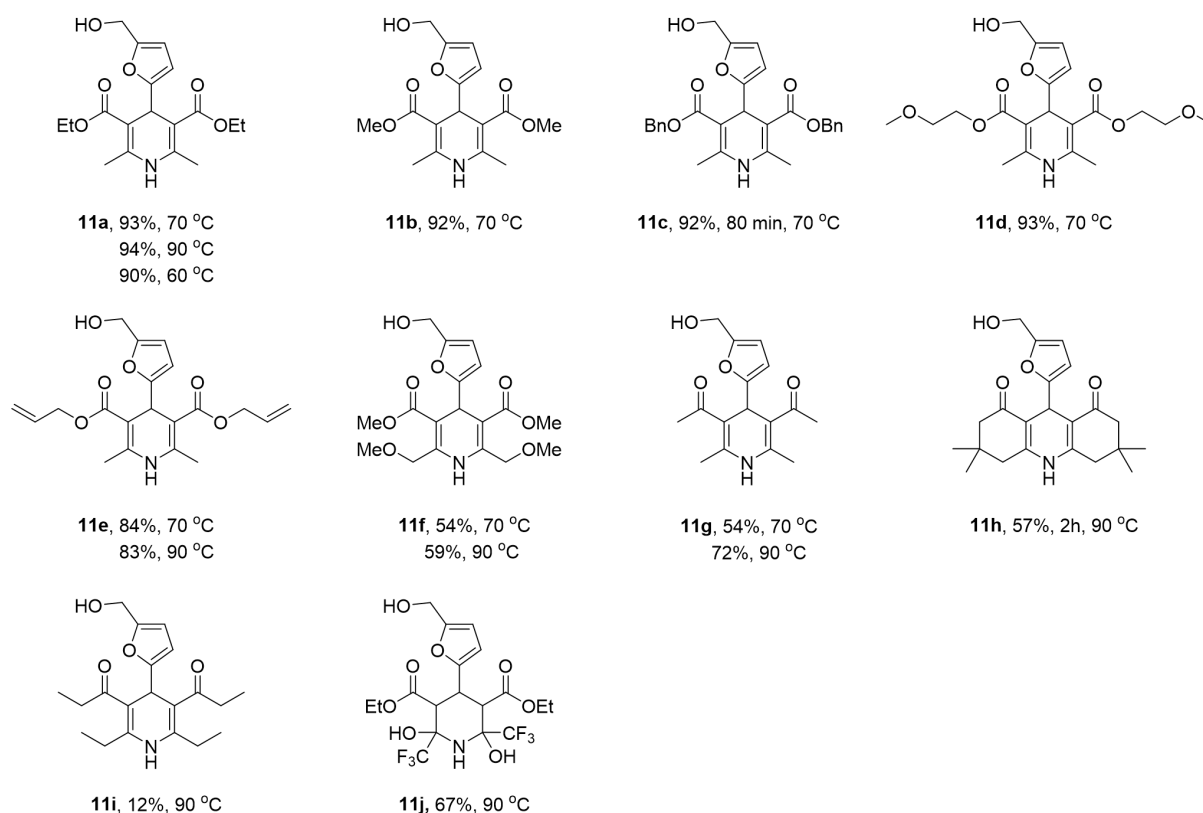


Figure 31. The Hantzsch reaction of HMF with various β -diketones

β -Diketones were also relevant substrates in the reaction though giving more complex results as compared with β -ketoesters. Acetylacetone provided product **11g** in 54% yield at 70 °C, and 72% yield upon increasing the temperature to 90 °C accompanied by approximately 8% of Knoevenagel intermediate and some unidentified impurities possibly coming from other condensations of starting materials, with complete conversion of HMF and acetylacetone. 5,5-Dimethyl-1,3-cyclohexanedione (dimedone) provided 57% of the target product **11h** at 90 °C, as well as a mixture of unidentified and difficult-to-isolate impurities, with complete conversion of HMF and dimedone, based on the furan proton peaks and possible dimedone methyl peaks observed in the crude proton spectrum of the impurity mixture, it is speculated that the generation of unidentified impurities involving increased degradation or various condensation reactions of HMF and dimedone. 3,5-Heptanedione proved much less efficient with only 12% of product **11i** at 90 °C, together with about 40% of the Knoevenagel intermediate (MH^+ : 237.2), 52% of the enamine intermediate (MH^+ : 128.2) and highly polar unidentified gummy impurity, but no HMF or 3,5-heptanedione remaining. Finally, the β -ketoester bearing a strong electron-withdrawing group CF_3 lead to the formation of the undehydrated product **11j**.

Two substituted HMF were then studied, 5-methoxymethylfurfural (prepared by ourselves like in Chapter II) and chloromethylfurfural (CMF) (Figure 32). Reaction of 5-methoxymethylfurfural with ketoesters or acetylacetone gave similar results as compared to HMF, leading to the products **11k**, **11l** and **11m** in 92%, 83%, 60% yield respectively. Oppositely, when chloromethylfurfural (CMF)⁸⁴ was used in this reaction, no obvious formation of the target Hantzsch product was observed, while complete conversion of CMF and ethyl acetoacetate was observed as well as the formation of many impurities. This behavior is likely due to the ability of the C-Cl linkage to compete as an electrophilic function, causing the reaction to proceed along different paths from that toward the target DHPs.

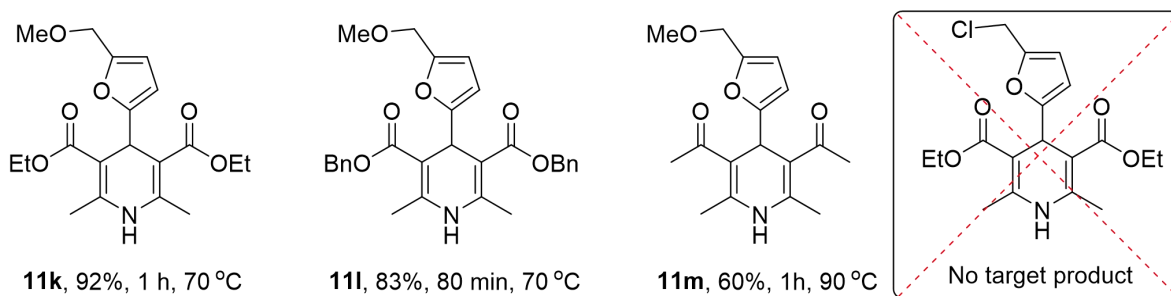
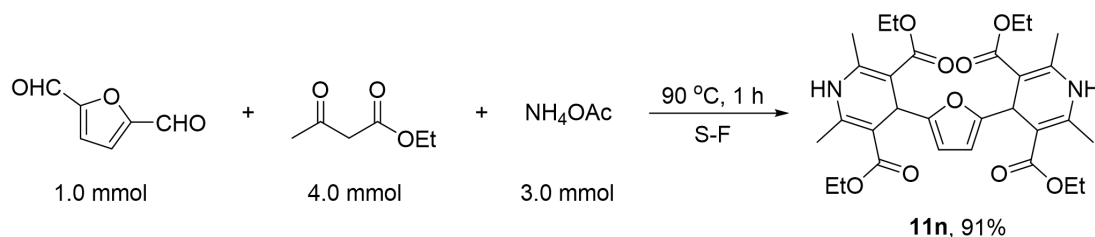


Figure 32. Synthesis of symmetrical 1,4-dihydropyridines with modulation of the 5-HMF scaffold

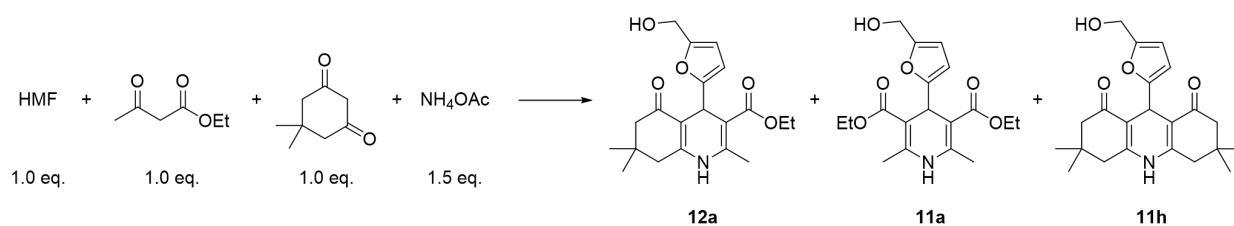
The reaction was also applied to DFF which is a bis-aldehydic molecule. Some examples of the use of bis-aldehydes in Hantzsch dihydropyridine synthesis or Hantzsch-like reactions have been reported, among them some aromatic ones like phenyl-bis-carboxaldehydes.²²⁰ We therefore tested the furanic equivalent DFF in this reaction, which led to a 91% yield of the double 1,4-dihydropyridine **11n** structure under solvent-free conditions (Scheme 89).



Scheme 89. Hantzsch double dihydropyridine synthesis involving 5-HMF

3.2.2 Four-component approach towards unsymmetrical 1,4-dihydropyridines

Reviewing the biological molecules we exemplified in the background of this chapter, we know that unsymmetrical 1,4-DHPs derived from dimedone substrate also have rich potential pharmacological activities. The study was then extended to the four-component protocol using two different dicarbonyl compounds, namely one equivalent of β -ketoester/diketone and one equivalent of dimedone. In such a case, there is a selectivity issue, since the reaction can actually provide either the unsymmetrical 1,4-dihydropyridine, or some symmetrical ones (combining either twice the ethyl acetoacetate or twice the dimedone) (Scheme 90).



Scheme 90. Four component Hantzsch protocol and possible products

In this section, we will first provide the evidence of the structure of the target product obtained by the reaction of HMF with ethyl acetoacetate, 5,5-dimethyl-1,3-cyclohexanedione and ammonium acetate. Then we report the result of our methodological investigations checking the optimal conditions in terms of solvent, NH_4OAc dosage and temperature. Finally, we describe the investigation of the substrate scope using β -dicarbonyl compounds in the four-component reaction.

3.2.2.1 Identification of products

The mass spectrometry clearly differentiated the three possible products, with MH^+ (**12a**) = 360.2, MH^+ (**11a**) = 350.2, MNa^+ (**11h**) = 392.2, respectively. In terms of NMR spectroscopy, for the symmetrical products **11a** and **11h**, we relied on samples obtained during the structural scope of the three-component reactions when using two molecules of ethyl acetoacetate or dimedone as reactant. In Figure 33, we provide a ^1H NMR spectrum of the expected newly formed product **12a** in the four-component reaction, and the ^1H NMR spectra of the symmetrical products **11a** and **11h** obtained in the three-component reaction. Several interesting points can be observed. Firstly, the chemical shift of the NH peak of **12a** is between **11a** and **11h**. Secondly, the proton peaks in **12a** from δ 0.50 ppm to δ 4.20 ppm (in the dashed box) can be regarded as a superimposition of **11a** and **11h** (methyl and ethyl protons). Finally, with respect to integration in this δ 0.50-4.20 ppm part of the spectrum, the integration of **12a** is exactly half of the sum of **11a** and **11h**. Overall, this led us to unambiguously determine the structure of unsymmetrical target product **12a**. Let us note that compound **12a** can also be considered as a polyhydroquinoline.

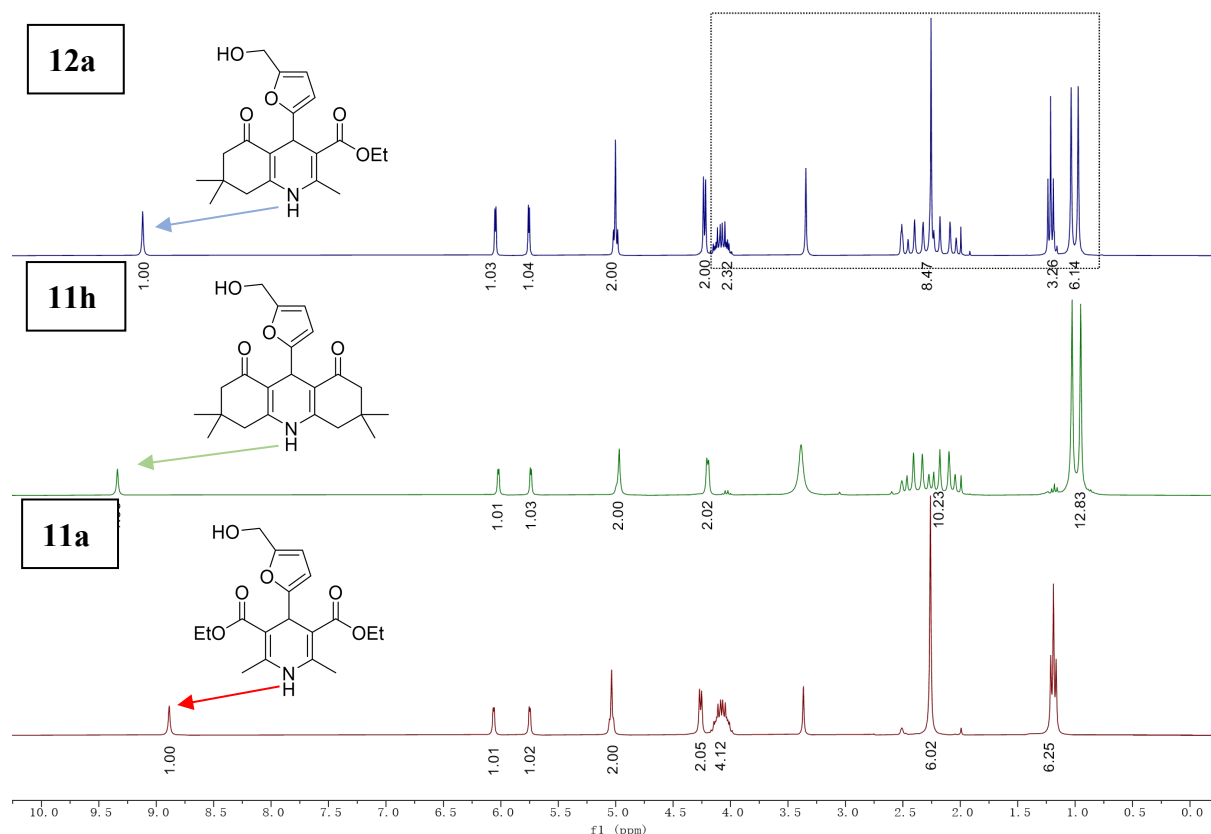


Figure 33. Pure spectrum of newly formed **12a** and known symmetrical products **11h** and **11a**

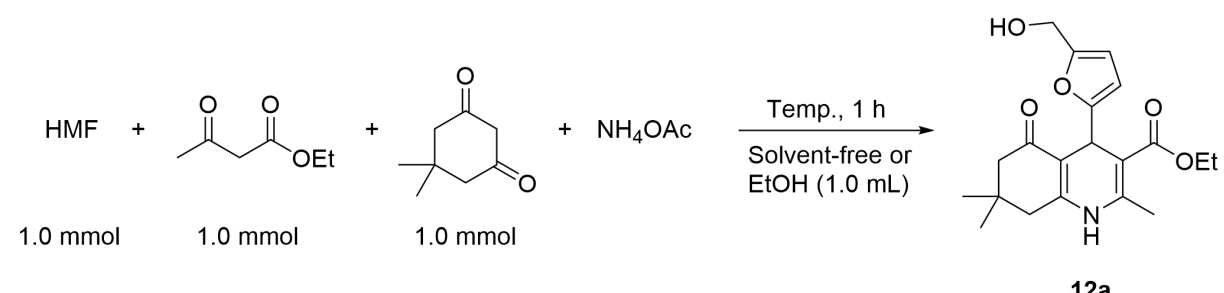
3.2.2.2 Optimization of the reaction conditions

In the four-component reaction, we first applied the no-solvent classical conditions used before and compared with the reaction in ethanol. Both were very good, however, the reaction in ethanol appeared slightly more efficient (84% vs 79%, entries 1-2), so we kept this as the standard conditions here. This slight difference can possibly arise from solubility issues for dimedone, which is a solid. In all cases, the protocol underwent very selectively toward the four-component pathway leading to compound **12a** with good to excellent yields.

Increasing the amount of ammonium acetate (1.5-2.5 equivalents) at 90 °C, also led to 84% yield of **12a** when using 1.5 equivalents of ammonium acetate. Further increasing the amount of ammonium acetate did not improve the yield or even resulted in a gradual decrease compare to the 1.5 equivalents of NH₄OAc (entries 3-6). Lowering further the reaction temperature to 70°C or 50 °C resulted in a decrease in yields, 79% and 58% respectively

(entries 7-8). Therefore, we chose 80 °C for subsequent experiments. The yields of these symmetric by-products are given in Table 15, however they must be used with precaution because they result from integration measurements of peaks which partially overlap, therefore being approximate. In most cases, a small amount of the symmetrical product **11a** involving two molecules of ethyl acetoacetate was present (6-8%), while the other symmetrical product **11h** involving two molecules of diketone was observed only as trace amounts (0-5%).

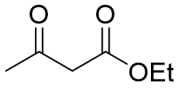
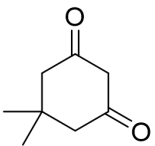
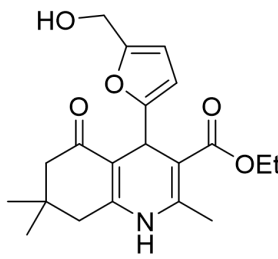
Table 15. Optimization of four-component Hantzsch 1,4-dihydropyridine synthesis

					
Entry	NH ₄ OAc (mmol)	Temperature	Solvent	NMR Yield 12a (%)	NMR Yield (11a/11h) (%)
1	1.5	80 °C	Solvent-free	79	9/<5
2	1.5	80 °C	EtOH	84	7/2
3	1.0	90 °C	EtOH	80	6/2
4	1.5	90 °C	EtOH	84	7/2
5	2.0	90 °C	EtOH	83	7/trace
6	2.5	90 °C	EtOH	81	7/trace
7	1.5	70 °C	EtOH	79	8/trace
8	1.5	50 °C	EtOH	58	11/trace

Regarding the reaction time, the reaction performed quite well even after 20 or 40 min, giving 73% and 81% target product, respectively (Table 16, entries 1-2). The yield slightly increased when prolonging the reaction time (entries 3-4). Regarding the impact of a more concentrated medium, the ethanol quantity could be halved without yield decrease (entries 3/5, 4/6). After screening various factors in this reaction, we can consider that stoichiometric ratio of

1:1:1:1.5 (among which NH_4OAc is 1.5 equivalents) in 2M ethanol (based on HMF) at 80 °C for 80 minutes as the optimal reaction conditions, with the highest yield of 88% obtained in the four-component reaction (entry 5).

Table 16. Optimization of reaction time and concentration

HMF	+		+		+	NH_4OAc	$\xrightarrow[\text{EtOH}]{80\text{ }^\circ\text{C}}$	
1.0 mmol		1.0 mmol		1.0 mmol		1.5 mmol		12a
Entry	Time	Solvent*	NMR Yield (%)					
1	20 min	EtOH (1 M)	73					
2	40 min	EtOH (1 M)	81					
3	80 min	EtOH (1 M)	84					
4	100 min	EtOH (1 M)	83					
5	80 min	EtOH (2 M)	88					
6	100 min	EtOH (2 M)	85					

* Concentration of HMF in EtOH.

3.2.2.3 Structural scope

The optimal conditions were then applied to a short structural scope in which 5-HMF and 5,5-dimethyl-1,3-cyclohexanedione were condensed with a series of β -ketoesters or 1,3-diketones, leading to a family of unsymmetrical dihydropyridines shown in Figure 34. In these reactions, both HMF and ketones are completely converted. The results are consistent with what was observed in the symmetrical examples, with acetoacetic esters working the best to afford the corresponding products in 80% to 88% yields (**12a-12e**). Methyl 4-methoxyacetoacetate led to only 45% yield of target unsymmetrical product (**12f**) with no more than 6% symmetrical by-products and some high polar impurities which are difficult to identified. When the β -

diketone acetylacetone was used, **12g** was obtained in only 61% yield, along with a total of approximately 8% symmetrical by-products, and other impurities. Replacing 5-HMF with 5-methoxymethylfurfural provided 72% of **12h**. Overall, a general preference for the formation of the unsymmetrical products was observed, with only trace amounts (0-4%) of **11h** and few (4-8%) β -ketoester symmetrical products observed.

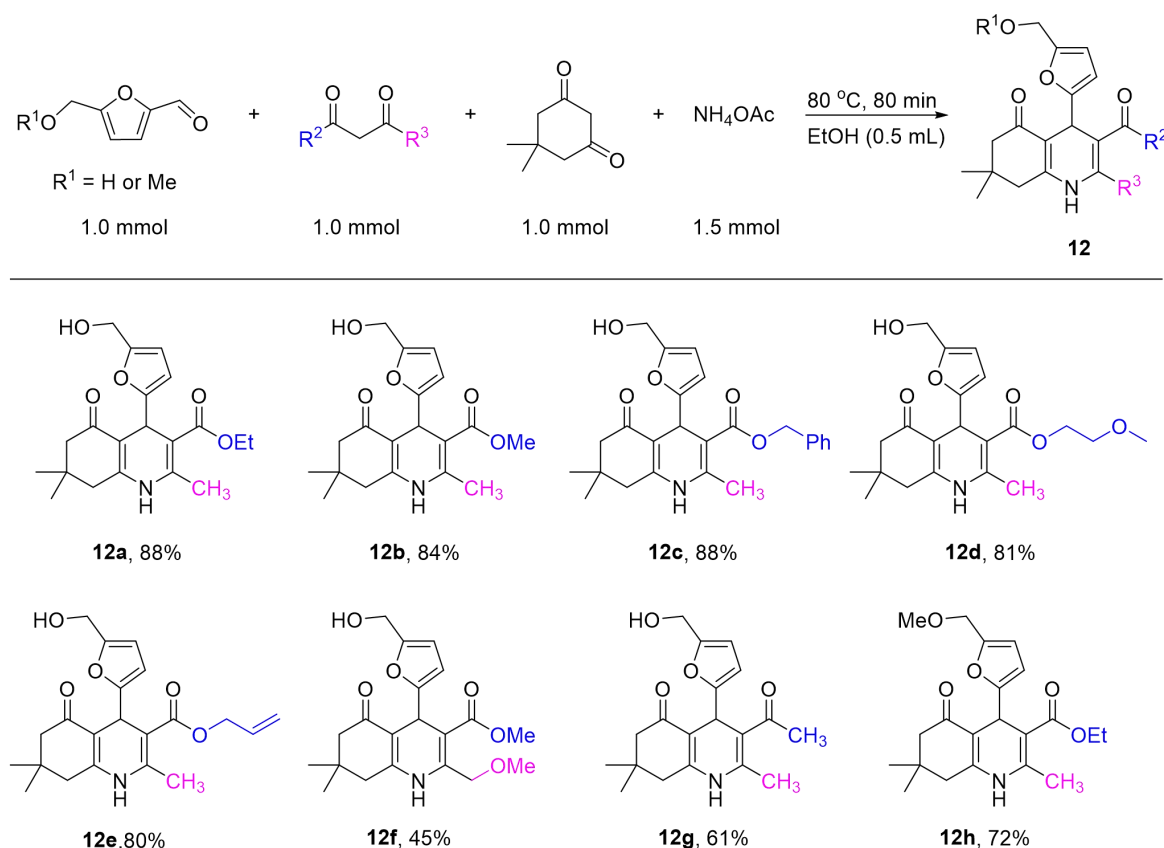


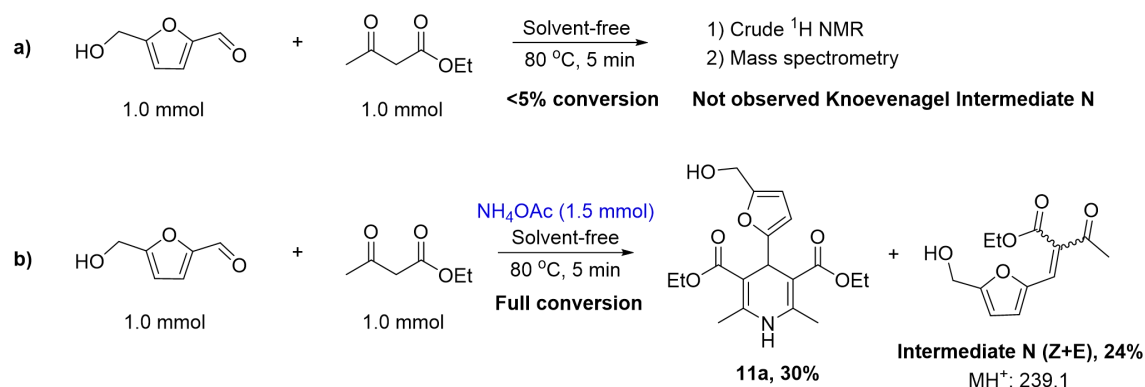
Figure 34. Synthesis of unsymmetrical 1,4-dihydropyridines

3.2.3 Mechanistic considerations

3.2.3.1. Three-component reaction

Several control experiments using only two of the three reagents have been conducted with the aim of identifying some intermediates and checking which intermediates are more or less easily formed depending on the substrates.

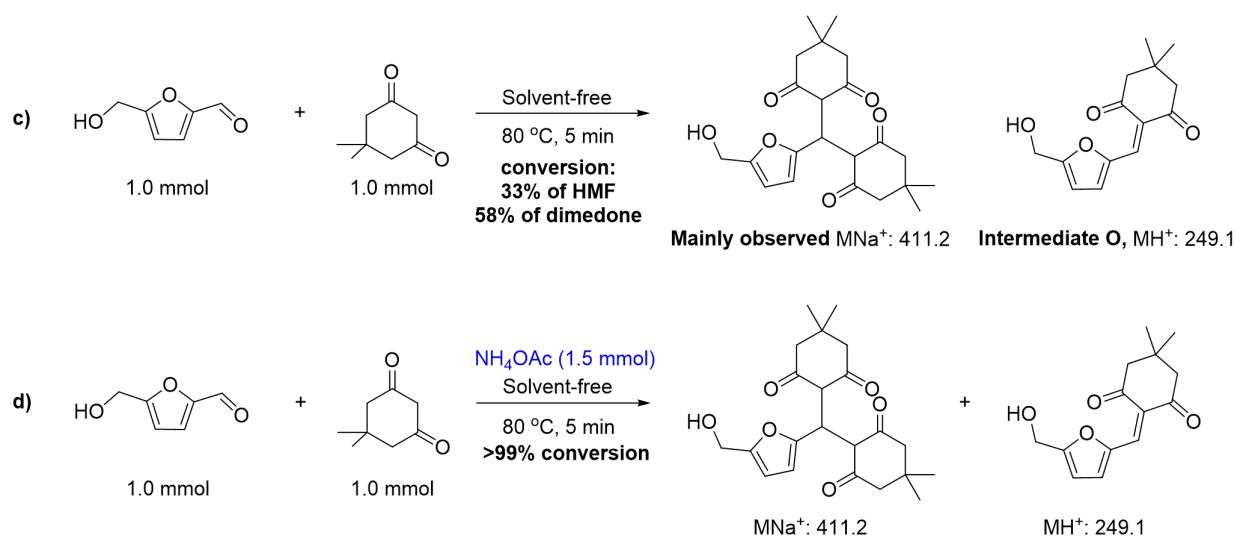
In the absence of ammonium acetate, the reaction of HMF with ethyl acetoacetate at 80 °C under solvent-free conditions (Scheme 91a) did not lead to any target product **11a** nor Knoevenagel condensation product, after 5 minutes, checked by mass and NMR spectrometry, with essentially only starting materials remaining. However, the same experiment with 1.5 equivalents of ammonium acetate led after 5 minutes to the complete conversion of the reactants and generated 30% yield of the corresponding 1,4-dihydropyridine **11a** and 24% Knoevenagel intermediate **N**. The presence of the Knoevenagel condensation intermediate **N** was clearly identified by ^1H NMR and by MS (molecular weight MH^+ : 239.1) in the crude reaction mixture (Scheme 91b). Ammonium acetate is thus clearly indispensable to the formation of the Knoevenagel intermediate between HMF and ethyl acetoacetate.



Scheme 91a and b. Checking intermediates in presence or absence of ammonium acetate

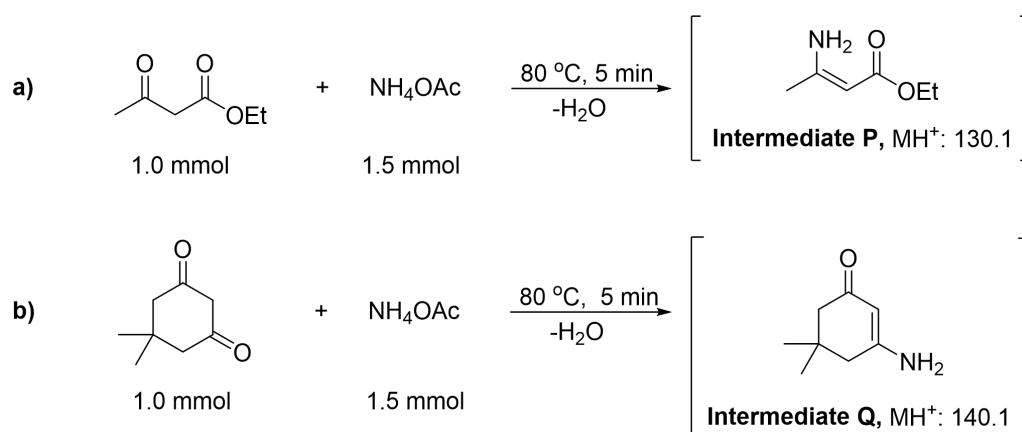
Interestingly, it was different for the reaction of HMF with dimedone (Scheme 91, c and d). Indeed, even in absence of ammonium acetate, the reaction at 80 °C led to a 33% conversion of HMF and 58% conversion of dimedone. For this reaction, the MS shows a very small peak indicating the presence of intermediate **O** (MH^+ : 249.1) in limited amount, as well as a very big one at mass [MNa^+ : 411.2] which could possibly correspond to the product of bis-addition arising from the diketone addition onto the Knoevenagel intermediate **O** of HMF and dimedone, though not isolated due to the easy reversibility of the 1,4-reaction. In the presence of ammonium acetate, the reaction mixture quickly turned into a dark viscous state and almost complete conversion of the reactants was observed after 5 minutes. In this experiment, the

mass (MNa^+ : 411.2) was observed again as the main peak by MS, while the other peak at (MH^+ : 249.1) was significantly more important than in experiment c.



Scheme 91c and d. Checking intermediates in presence or absence of ammonium acetate

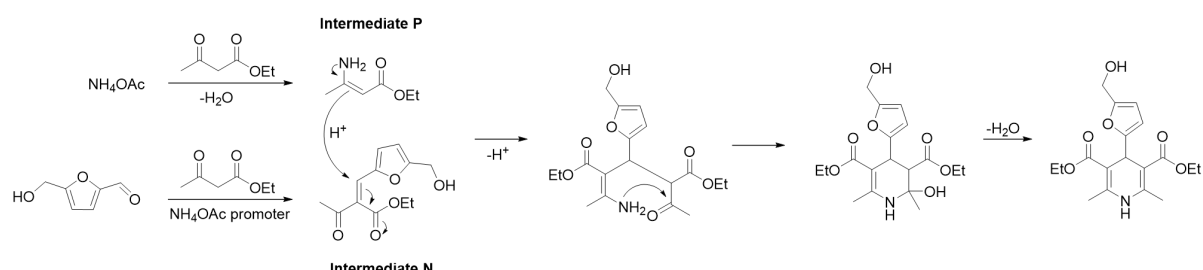
Control experiments in the absence of HMF were conducted in order to check the formation of the enamines. Both enamines **P** and **Q** arising from ethyl acetoacetate and dimedone were clearly identified by MS with masses (MH^+ : 130.1) and (MH^+ : 140.1) respectively (Scheme 92).



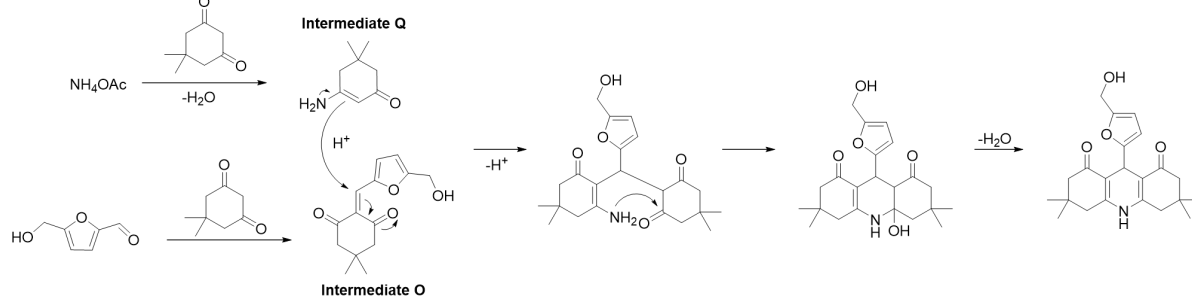
Scheme 92. Checking the formation of enamines

The overall outcome of HMF in the three-component reactions is depicted in Scheme 93. In the three-component reaction, the Knoevenagel condensation of HMF and one molecule β -ketoester or β -diketone produce intermediates **N** or **O**. Another molecule of β -ketoester or β -diketone reacts with ammonium acetate to generate the enamine intermediate **P** or **Q**. Then, intermediate **N** and **P** (**O** and **Q**) undergo Michael addition and dehydration condensation to form the target symmetrical 1,4-DHP products. Ammonium acetate plays a key role in providing an environment to promote the Knoevenagel condensation reaction.

Ketoester case:



Diketone case:

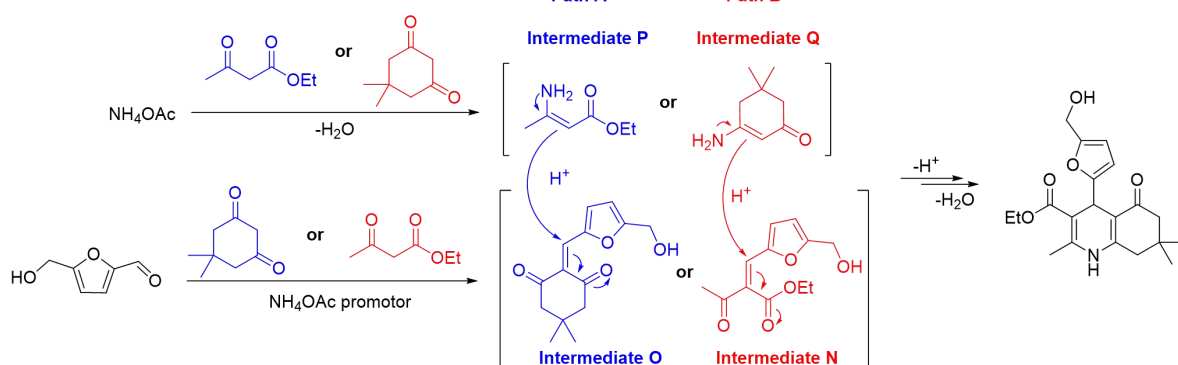


Scheme 93. Formation of the 5-HMF based symmetrical 1,4-dihydropyridines

3.2.3.2. Four-component reaction

We know from the optimization and substrate scope experiments that the four-component reaction using HMF, dimedone, ammonium acetate and a series of dicarbonyl fourth partners showed a clear preference toward unsymmetrical products. We also know from the control experiments that both Knoevenagel intermediates and enamines can be formed suggesting that the reaction could follow either one or the other between pathways A (blue route) or B (red route) depicted in Scheme 94.

Four-component case:



Scheme 94. Formation of the 5-HMF based unsymmetrical 1,4-dihydropyridine

There is an apparent paradox in the reactivity of the diketone in this reaction. Indeed, from the structural scope of the three-component reaction, we learned that yields in Hantzsch products from diketones were lower, suggesting some lower reactivity at one step of the pathway. However, we learned also from the control experiments that the Knoevenagel intermediate II (arising from dimedone) can be formed more easily than the one arising from ethyl acetoacetate, since it was observed even in the absence of ammonium acetate. The lower yields of the dimedone 3-CR reaction is therefore not due to a slower first step to the Knoevenagel intermediate, but at one of the later steps of the process, either the Michael addition, cyclization or dehydration steps. It is thus possible to suggest that the reaction selectivity towards the unsymmetrical product in the 4-CR protocol starts with the formation of the Knoevenagel product between HMF and dimedone, which undergoes addition of the enamine arising from ethyl acetoacetate and ammonium acetate, then following the final cyclization and dehydration steps towards the target 4-CR Hantzsch products.

3.3 Conclusion

We have conducted the first complete study of the use of 5-HMF in the Hantzsch dihydropyridine synthesis reaction. A wide range of novel symmetrical and unsymmetrical 5-HMF derived 1,4-DHPs were obtained for the first time in good to excellent yields using the

Hantzsch dihydropyridine synthesis in the absence of any additional catalyst or complex additive and in solvent-free or ethanolic solution conditions.

Overall, this protocol exhibits remarkable characters in terms of sustainable chemistry, combining a very atom-economical multicomponent reaction, a biobased substrate, the absence of solvent or the use of a clean, safe and biobased solvent EtOH. This study provides also an additional example of how ammonium acetate appears to be a very useful participant in the chemistry of HMF.

General conclusions and perspectives

General conclusions and perspectives

The work described in this thesis has aimed at combining several important sides of green chemistry by focusing on the utilization of biobased platform molecules in atom-economical synthetic processes, using mild and clean reaction conditions. Our exploration centered on the 5-hydroxymethylfurfural (5-HMF) platform which has become a major biobased building block with increased availability, though its applications remain limited in the design of novel fine chemicals. Multicomponent reactions (MCRs) can give access to more complex structures like those applied in pharmaceutical, agrochemical, and materials science. In this study, we specifically targeted novel nitrogen-containing heterocycles, in particular 1,5-benzodiazepines and 1,4-dihydropyridines, for which green and sustainable synthetic methods need to be investigated to develop their diversity.

We first applied our strategy towards the 1,5-benzodiazepines scaffold found in a wide range of biologically relevant structures. The point was to use HMF and its derivatives in the [4+2+1] cycloaddition reaction with *o*-phenylenediamine and 3-buten-2-one. HMF had never been used in this type of reaction. With respect to the reaction conditions, we applied the use of ammonium acetate as promoter for the first time in such a reaction. Very mild conditions, namely 30 mol% ammonium acetate at 60 °C in ethanol, were found as the most efficient conditions. The scope of the reaction was then extended to variously substituted *o*-phenylenediamines, different types of alkynone/alkyl alkynoate and a few HMF-derived furanic aldehydes, affording 23 examples of new 1,5-benzodiazepine in moderate to good yields that are now included in the ICBMS chemical library for further biological and biochemical assays.

After having noticed the interesting promoting effect of ammonium acetate and its compatibility with HMF chemical behavior in the first part of this thesis, we wanted to further explore its usability in HMF chemistry. To do so, we focused the second part of this thesis on the use of HMF in the Hantzsch dihydropyridine synthesis, which is an important

multicomponent reaction involving aldehydes, ammonia, and β -dicarbonyl substrates to synthesize 1,4-dihydropyridines, and known to proceed using ammonium acetate as a nitrogen source. Previous uses of HMF in this reaction had only been reported using complex solvents and catalysts, so our goal was to establish more environment friendly conditions.

The application of 5-HMF in the Hantzsch synthesis of dihydropyridines using NH_4OAc as a nitrogen source and mild accelerator was thus investigated. We demonstrated that much simpler and cleaner conditions than those previously reported could be used. Indeed, the reaction could proceed under solvent-free conditions without any additional catalyst, very efficiently leading to symmetrical 1,4-dihydropyridine in excellent yields when reacting HMF with two molecules of β -dicarbonyl compounds (β -ketoester/ β -diketone). The reaction using a mixture of two different β -dicarbonyl substrates proceeded also efficiently, leading selectively to unsymmetrical 1,4-dihydropyridine in a four-component protocol in the absence of solvent or in ethanol. Overall, 19 new products in this family have been prepared and are now stocked in the ICBMS chemical library.

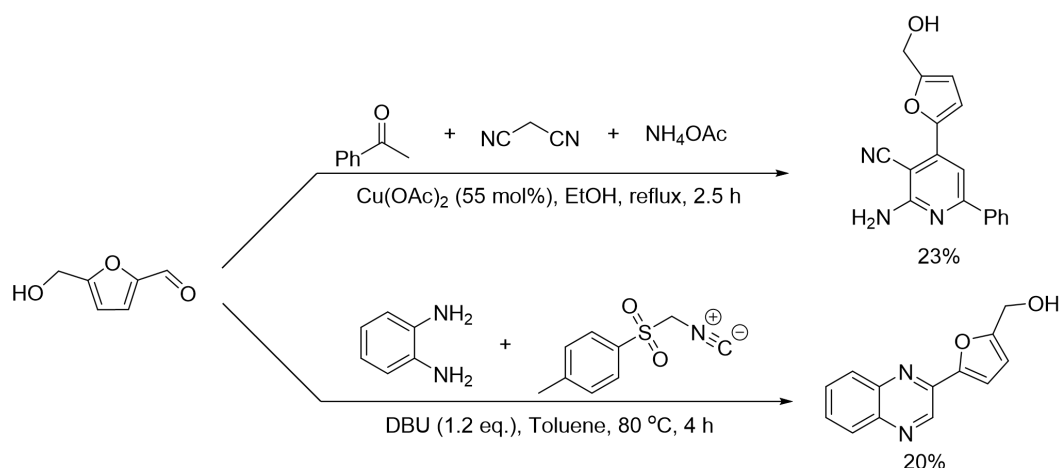
These results illustrate that it is possible to diversify HMF chemistry, by showing how this biobased building block enables the synthesis of complex chemicals across diverse fields. This work also demonstrates the power of the combination of HMF chemistry with the use of MCRs, providing a more sustainable access to diverse molecular structures, thus addressing also the chemistry of fine chemicals and pharmaceuticals. The convergence of advanced synthetic methods with the availability of HMF emphasizes a transformative approach to green and efficient chemical synthesis, in line with the development trends of modern organic chemistry.

Perspectives

The successful investigations of HMF in multi-component reactions like the Biginelli, Kabachnik-Fields reaction, nitron dipolar cycloaddition, $[4+2+1]$ cycloaddition and

Hantzsch reactions pave the way to further developments. There are many other MCRs for which solutions have not been found yet, such as typical MCRs including Strcker reaction, Mannich reaction, Passerini reaction, Ugi reaction, Yonemitsu reaction and novel MCRs involving aldehyde substrates that have only been rarely reported.

We have explored a couple of MCR that have not yet been developed in HMF chemistry. In this section, we present the results of two additional MCRs firstly the reaction of HMF with acetophenone, malononitrile and ammonium acetate aimed at constructing 2-amino-3-cyanopyridines and secondly the reaction of HMF with *o*-phenylenediamine and *p*-toluenesulfonylmethyl isocyanide towards quinoxalines (Scheme 95).



Scheme 95. Preliminarily examined MCRs involving HMF

Though uncomplete, these studies give the first insights on the way HMF behaves in these reactions. For the first one, more than 50 articles use benzaldehyde as the aldehydic substrate while no mention the use of HMF. Using copper acetate which proved to be active for the reaction with benzaldehyde, we found a 23% yield of the desired 2-amino-3-cyanopyridine product from HMF though with incomplete conversion of acetophenone. For the second one towards quinoxalines, we chose to perform a one-pot reaction with *o*-phenylenediamine and *p*-toluenesulfonylmethyl isocyanide, conditions once reported when using benzaldehyde (or furfural). In the presence of 1,8-Diazabicyclo[5.4.0]undec-7-ene (DBU), the reaction

proceeded at 80°C in toluene in 4 hours, yielding a complex mixture of products among which the desired quinoxaline, giving a 20% yield after purification.

These two results are interesting and give directions for future work, however they also show that expanding the utilization of HMF to directly access new furan-based scaffolds in other multicomponent strategies with high selectivity or high yield continues to pose a challenge worth being studied in depth, accommodating the specific reactivity of HMF.

Experimental section

Experimental section

1. General information

Unless otherwise stated in the procedure, all commercial materials and solvents were used without further purification and were supplied by Aldrich, Acros, Lancaster, Alfa Aesar, Fluka, Carlo Erba or TCI (purchased at the highest commercial quality grade). All reactions were performed in a 10 mL screw-cap tube using anhydrous solvents or without solvent. NMR spectra were recorded on a Bruker DRX-300 (^1H : 300 or 400 MHz; ^{13}C : 75 or 100.1 MHz) spectrometer using $\text{DMSO}-d_6$ or CDCl_3 . The chemical shifts (δ ppm) and coupling constants (Hz) are reported in the standard fashion. The following abbreviations are used to explain the multiplicities: s = singlet, d = doublet, t = triplet, q = quartet, m = multiplet, br = broad. Electrospray ionization (ESI) mass spectrometry (MS) experiments were performed on a Thermo Finnigan LCQ Advantage mass. High-resolution mass spectra (HRMS) were recorded on Bruker MicrOTOF-Q II XL spectrometer using ESI as ionization source. Analytical thin-layer chromatography was carried out on silica gel Merck 60 D254 (0.25 mm). Flash chromatographies were performed on Merck Si 60 silica gel (40-63 μm). Melting points were measured using a BUCHI Labortechnik AG B-540 apparatus and noted in $^{\circ}\text{C}$.

2. Experimental section of the [4+2+1] cycloaddition reaction

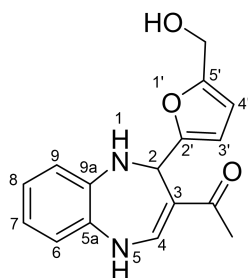
2.1 General procedure for the [4+2+1] cycloaddition reaction

General procedure: A solution of aldehydes (**1**, 1.2 mmol, 1.2 equiv.), *o*-phenylenediamine compounds (**2**, 1.0 mmol, 1.0 equiv.), alkynes or alkyl alkynoates (**3**, 1.0 mmol, 1 equiv.) and NH_4OAc (0.3 mmol, 0.3 equiv.) in ethanol (2 mL) was stirred at 60 $^{\circ}\text{C}$ for indicated hours. After cooling down to room temperature, the reaction was diluted with ethyl acetate (20 mL) and washed with saturated aqueous sodium chloride solution (20 mL). The organic layer was separated and the aqueous layer was extracted with ethyl acetate (3 \times 10 mL). The organic phases were combined and dried over Na_2SO_4 . After filtration, the residue was concentrated and purified by flash column chromatography on silica gel (n-pentane/EA=3:7 to 0:10) or

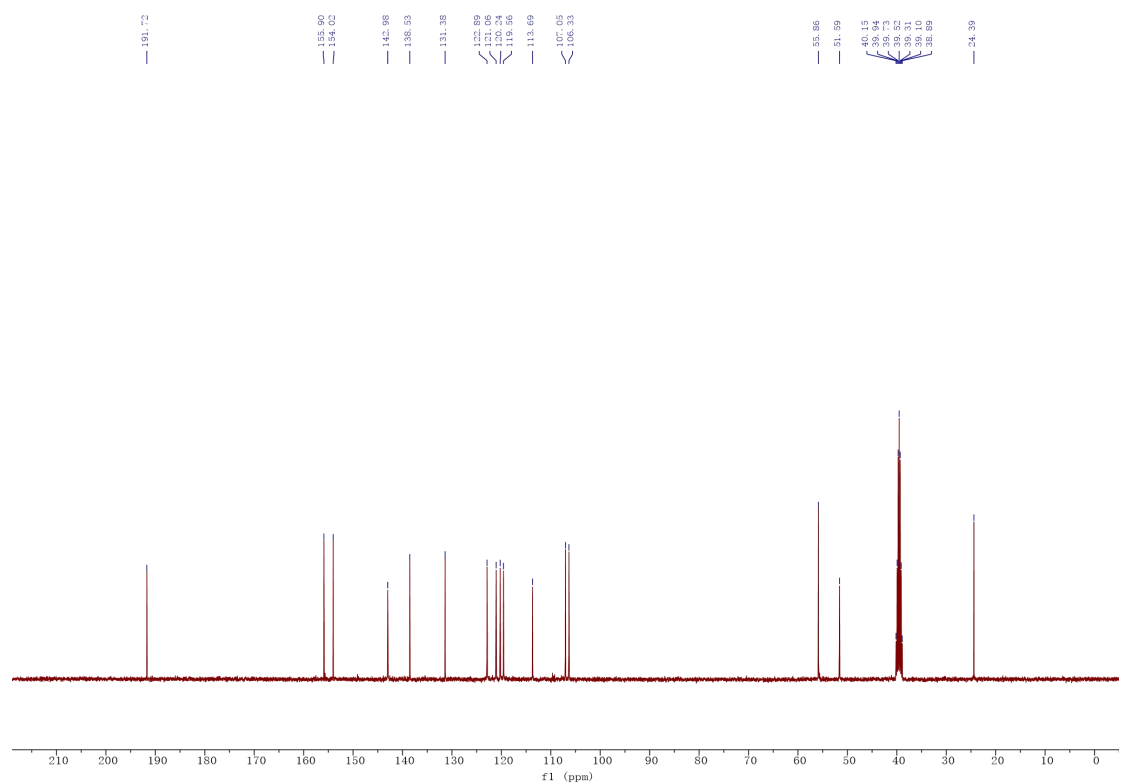
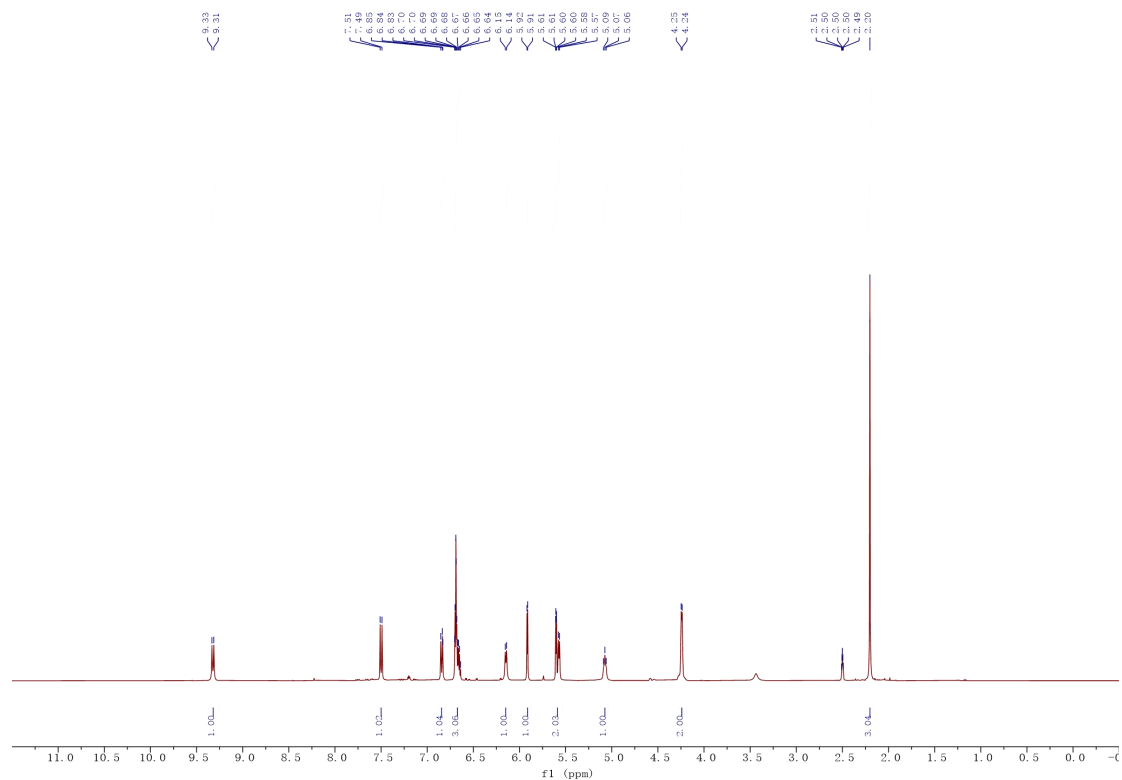
(DCM/MeOH=80:1 to 10:1)) to obtain the desired product. NMR yields were calculated by adding 1,3,5-trimethoxybenzene (56 mg, 1/3 equiv. compared to *o*-phenylenediamine) as internal standard. The internal standard was added to the crude mixture, dissolved with DMSO-*d*₆. NMR yields were obtained by comparing the integration of the methyl peak in 1,3,5-trimethoxybenzene (value 3 = 1/3 equiv. of a 9H peak) with the characteristic peaks in the product.

2.2 Characterization data of 1,5-benzodiazepines adducts

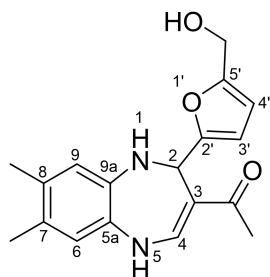
1-{2-[5-(Hydroxymethyl)furan-2-yl]-2,5-dihydro-1H-1,5-benzodiazepin-3-yl}ethan-1-one
(C₁₆H₁₆N₂O₃)



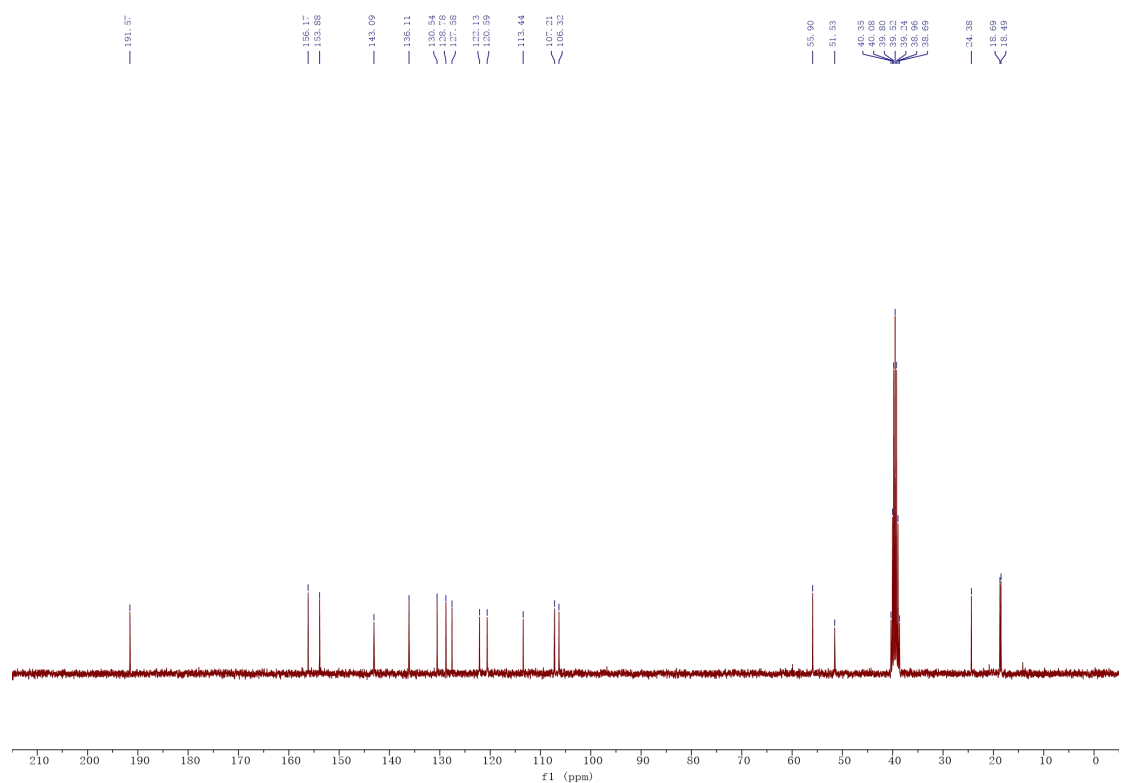
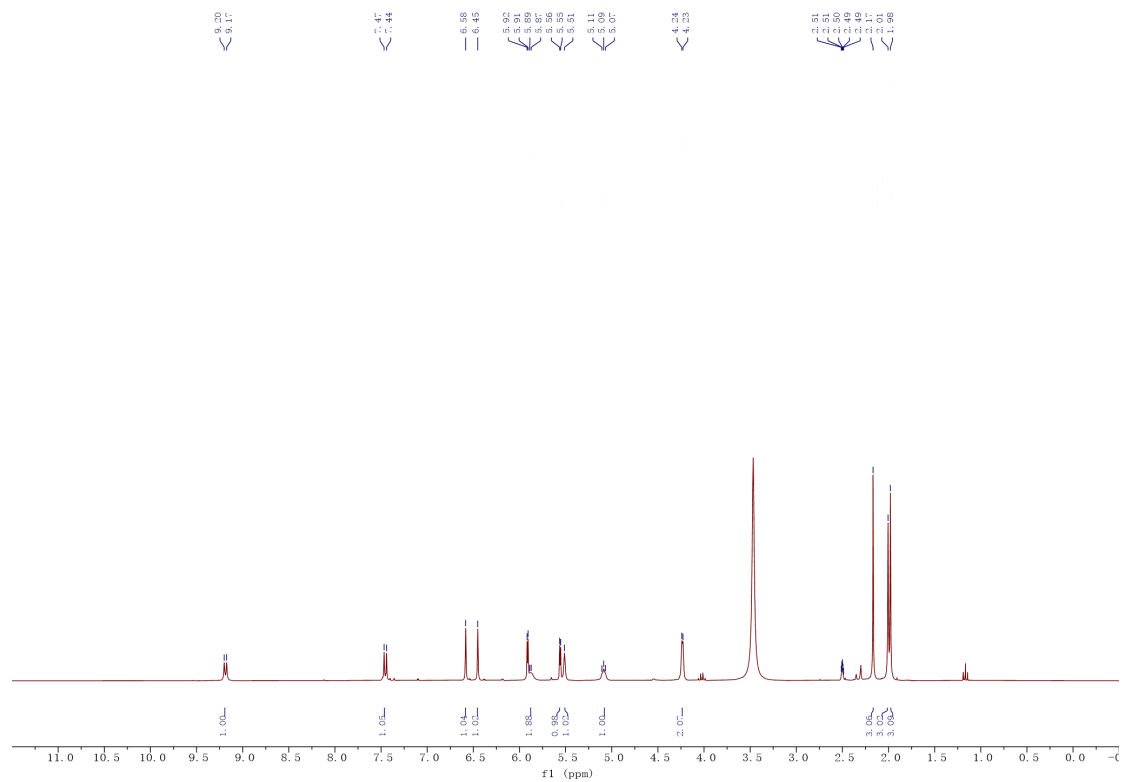
The reaction was carried out for 7 hours to give **4a** (199 mg, 70%) as a yellow solid. M.p. 139-140 °C. ¹H NMR (400 MHz, DMSO-*d*₆) δ 9.32 (d, *J* = 8.0 Hz, 1H, H₅), 7.50 (d, *J* = 8.0 Hz, 1H, H₄), 6.84 (d, *J* = 6.8 Hz, 1H, H₆ or 9), 6.72 – 6.62 (m, 3H, H_{Ar}), 6.15 (d, *J* = 5.6 Hz, 1H, H₁), 5.92 (d, *J* = 3.1 Hz, 1H, H_{4'}), 5.60 (d, *J* = 3.1 Hz, 1H, H_{3'}), 5.57 (d, *J* = 5.6 Hz, 1H, H₂), 5.07 (t, *J* = 5.0 Hz, 1H, OH), 4.24 (d, *J* = 5.0 Hz, 2H, CH₂OH), 2.20 (s, 3H, COCH₃). ¹³C NMR (100 MHz, DMSO-*d*₆) δ 191.7 (COCH₃), 155.9 (C_{2'}), 154.0 (C_{5'}), 143.0 (C₄), 138.5 (C_{9a}), 131.4 (C_{5a}), 122.9 (C₇ or 8), 121.1 (C₆ or 9), 120.2 (C₇ or 8), 119.6 (C₆ or 9), 113.7 (C₃), 107.0 (C_{4'}), 106.3 (C_{3'}), 55.9 (CH₂OH), 51.6 (C₂), 24.4 (COCH₃). HRMS (ESI) *m/z*: Calcd for [M+H]⁺ C₁₆H₁₇N₂O₃ = 285.1234; Found 285.1229. HRMS (ESI) *m/z*: Calcd for [M+Na]⁺ C₁₆H₁₆N₂NaO₃ = 307.1053; Found 307.1049.



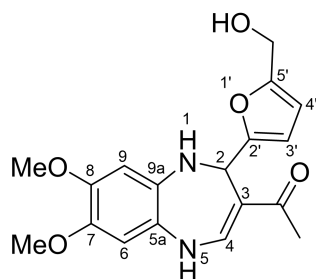
1-{2-[5-(Hydroxymethyl)furan-2-yl]-7,8-dimethyl-2,5-dihydro-1H-1,5-benzodiazepin-3-yl}ethan-1-one (C₁₈H₂₀N₂O₃)



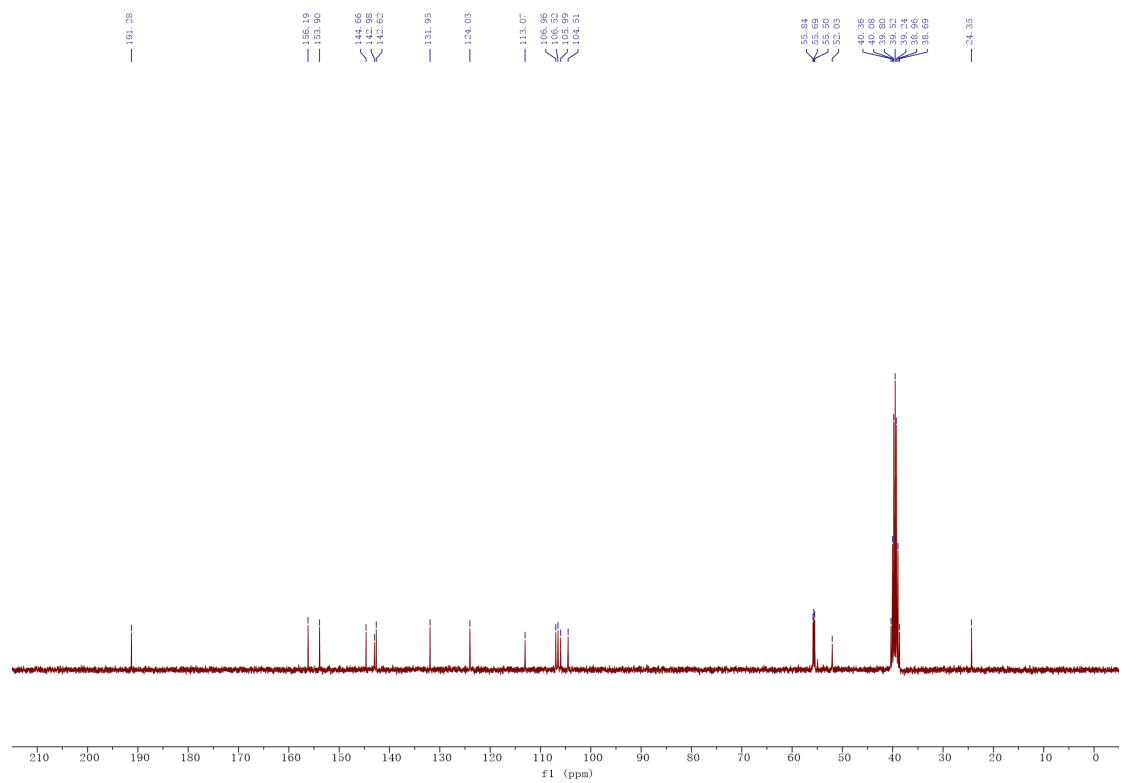
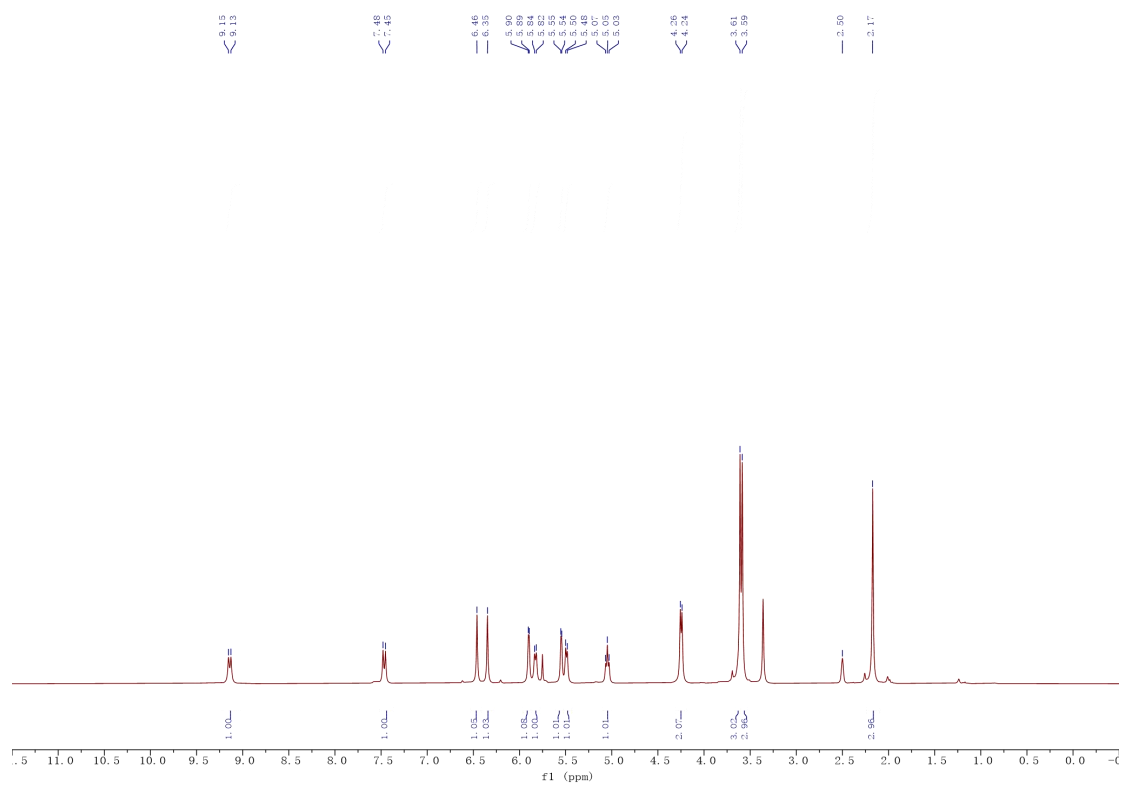
The reaction was carried out for 7 hours to give **4b** (187 mg, 60%) as a yellow solid. M.p. 174-175 °C. ¹H NMR (300 MHz, DMSO-*d*₆) δ 9.19 (d, *J* = 8.1 Hz, 1H, H₅), 7.45 (d, *J* = 8.1 Hz, 1H, H₄), 6.58 (s, 1H, H₆ or ₉), 6.45 (s, 1H, H₆ or ₉), 5.91 (d, *J* = 3.2 Hz, 1H, H_{4'}), 5.87 (bs, 1H, H₁), 5.56 (d, *J* = 3.2 Hz, 1H, H_{3'}), 5.51 (bs, 1H, H₂), 5.08 (t, *J* = 4.9 Hz, 1H, OH), 4.23 (d, *J* = 4.9 Hz, 2H, CH₂OH), 2.17 (s, 3H, COCH₃), 2.01 (s, 3H, CH₃), 1.98 (s, 3H, CH₃). ¹³C NMR (75 MHz, DMSO-*d*₆) δ 191.6 (COCH₃), 156.2 (C_{2'}), 153.9 (C_{5'}), 143.1 (C₄), 136.1 (C_{9a}), 130.5 (C₇ or ₈), 128.8 (C_{5a}), 127.6 (C₇ or ₈), 122.1 (C₆ or ₉), 120.6 (C₆ or ₉), 113.4 (C₃), 107.2 (C_{4'}), 106.3 (C_{3'}), 55.9 (CH₂OH), 51.5 (C₂), 24.4 (COCH₃), 18.7 (CH₃), 18.5 (CH₃). HRMS (ESI) *m/z*: Calcd for [M+H]⁺ C₁₈H₂₁N₂O₃ = 313.1547; Found 313.1548. HRMS (ESI) *m/z*: Calcd for [M+Na]⁺ C₁₈H₂₀N₂NaO₃ = 335.1366; Found 335.1362.



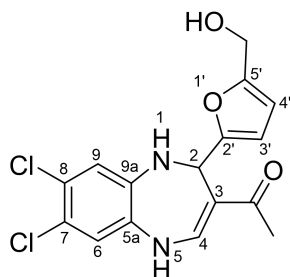
1-{2-[5-(Hydroxymethyl)furan-2-yl]-7,8-dimethoxy-2,5-dihydro-1H-1,5-benzodiazepin-3-yl}ethan-1-one (C₁₈H₂₀N₂O₅)



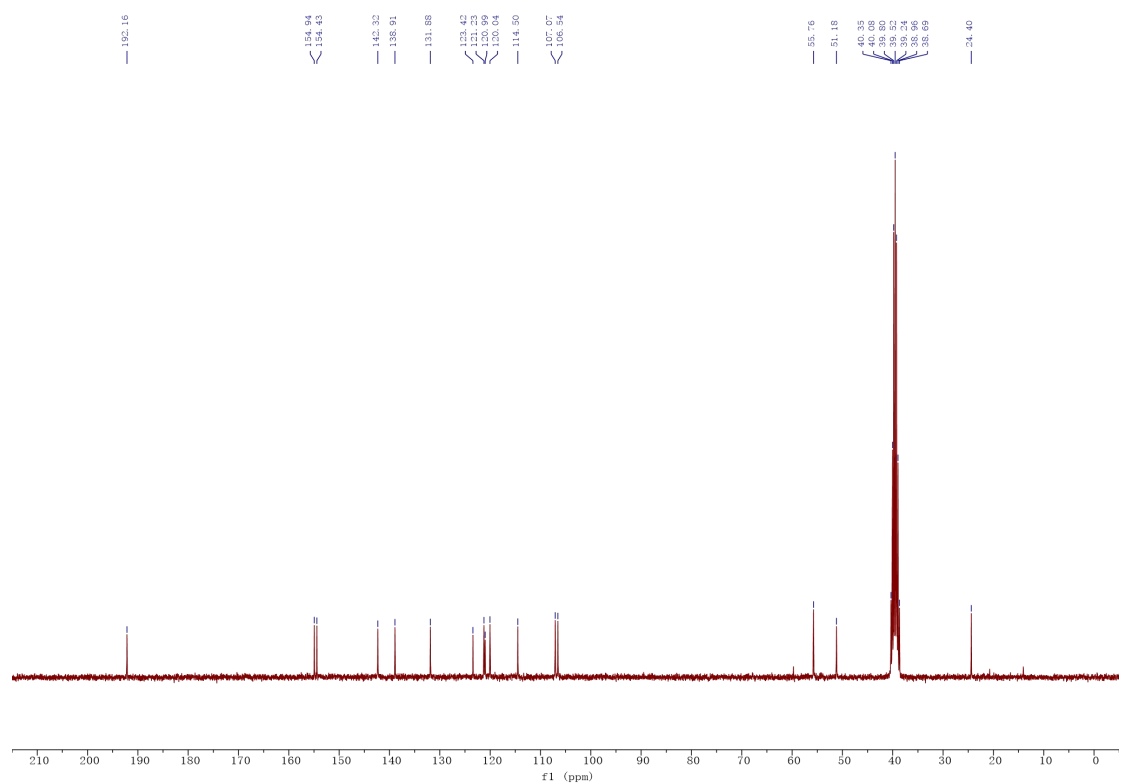
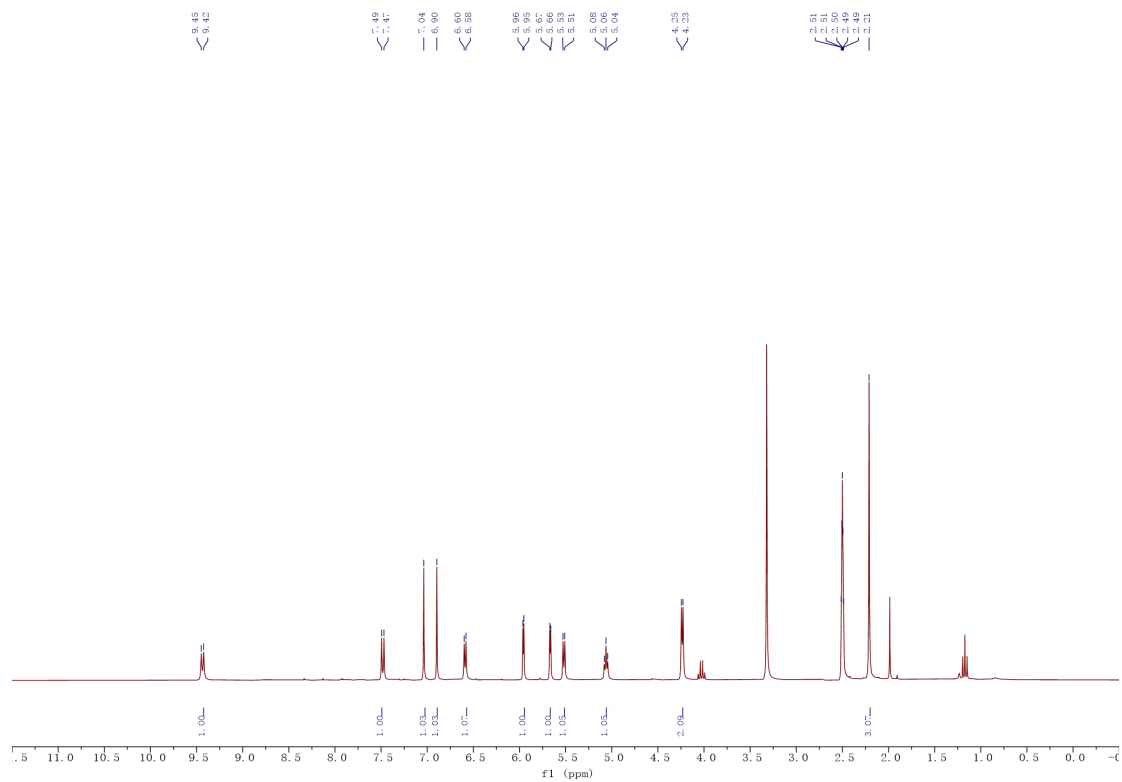
The reaction was carried out for 5 hours to give **4c** (138 mg, 40%) as a brown solid. M.p. 121-122 °C. ¹H NMR (300 MHz, DMSO-*d*₆) δ 9.14 (d, *J* = 8.0 Hz, 1H, H₅), 7.47 (d, *J* = 8.0 Hz, 1H, H₄), 6.46 (s, 1H, H_{Ar}), 6.35 (s, 1H, H_{Ar}), 5.90 (d, *J* = 3.0 Hz, 1H, H_{4'}), 5.83 (d, *J* = 5.7 Hz, 1H, H₁), 5.55 (d, *J* = 3.0 Hz, 1H, H_{3'}), 5.49 (d, *J* = 5.7 Hz, 1H, H₂), 5.05 (t, *J* = 5.6 Hz, 1H, OH), 4.25 (d, *J* = 5.6 Hz, 2H, CH₂OH), 3.61 (s, 3H, OCH₃), 3.59 (s, 3H, OCH₃), 2.17 (s, 3H, COCH₃). ¹³C NMR (75 MHz, DMSO) δ 191.3 (COCH₃), 156.2 (C_{2'}), 153.9 (C_{5'}), 144.7 (C_{Ar}), 143.0 (C₄), 142.6 (C_{Ar}), 131.9 (C_{Ar}), 124.0 (C_{Ar}), 113.1 (C₃), 107.0 (C_{4'}), 106.5 (C_{3'}), 106.0 (CH_{Ar}), 104.5 (CH_{Ar}), 55.8 (CH₂OH), 55.7 (OCH₃), 55.5 (OCH₃), 52.0 (C₂), 24.4 (COCH₃). HRMS (ESI) *m/z*: Calcd for [M+H]⁺ C₁₈H₂₁N₂O₅ = 345.1445; Found 345.1442. HRMS (ESI) *m/z*: Calcd for [M+Na]⁺ C₁₈H₂₀N₂NaO₅ = 367.1264; Found 367.1261.



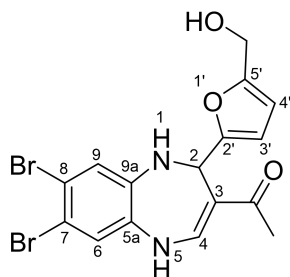
1-{7,8-Dichloro-2-[5-(hydroxymethyl)furan-2-yl]-2,5-dihydro-1H-1,5-benzodiazepin-3-yl}ethan-1-one (C₁₆H₁₄Cl₂N₂O₃)



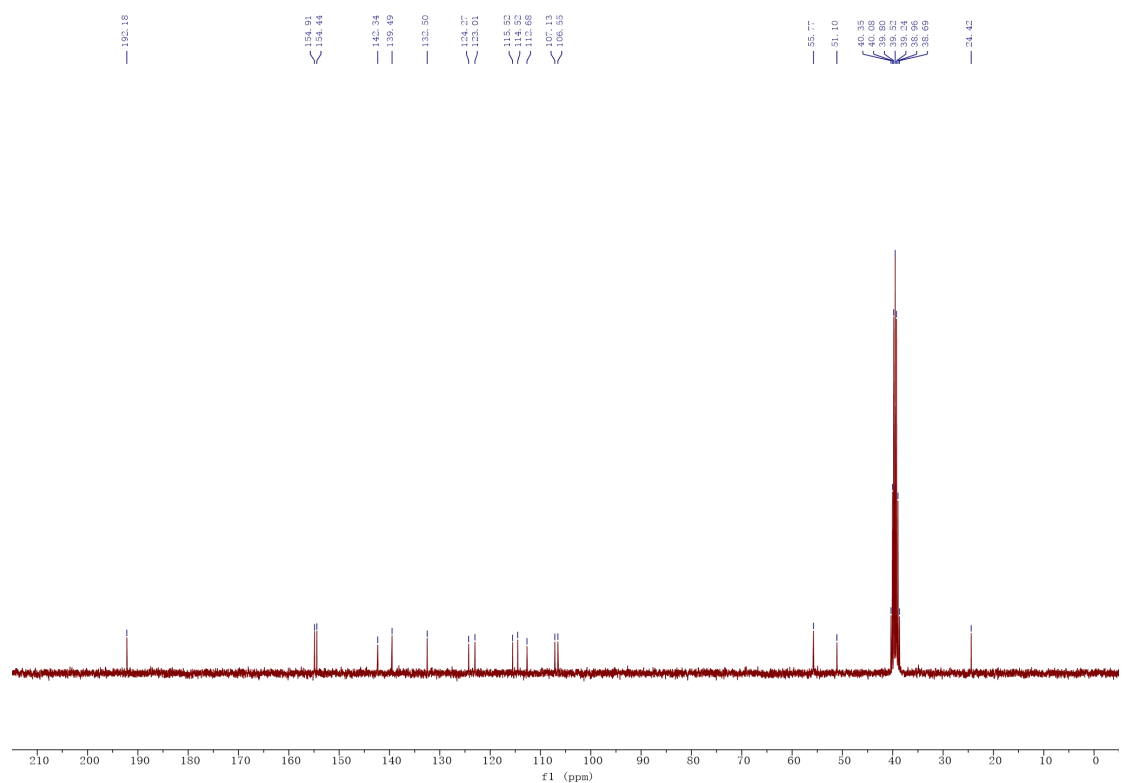
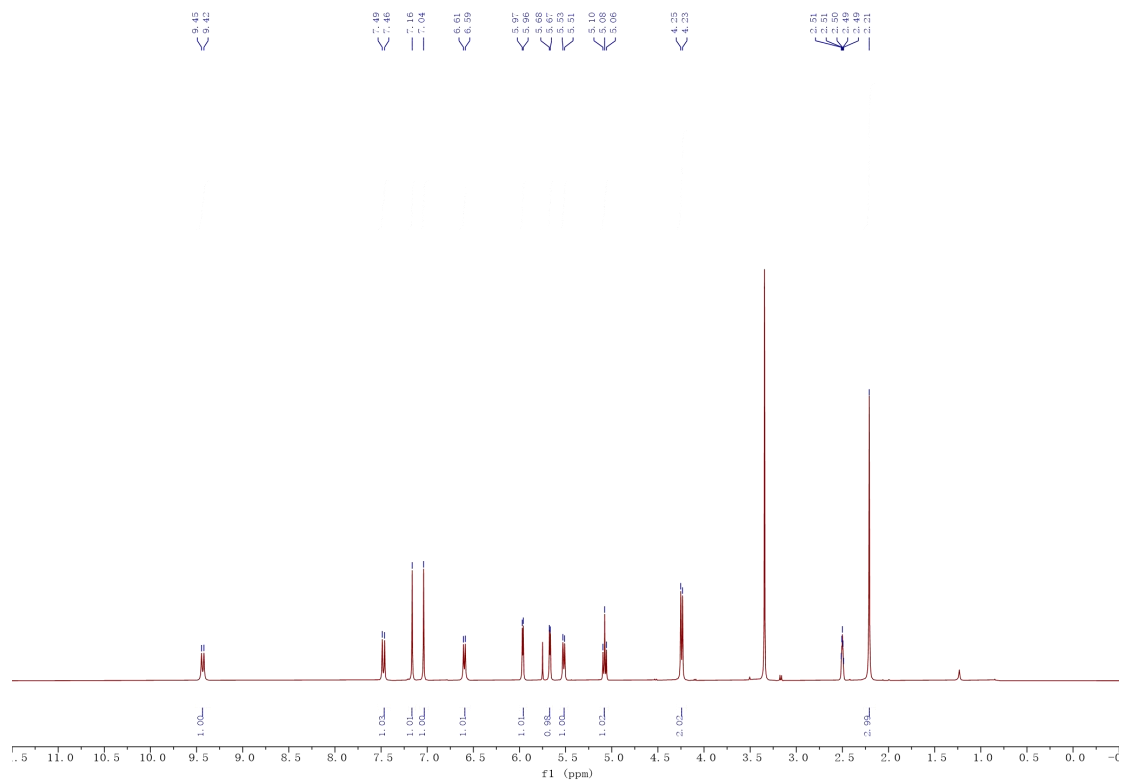
The reaction was carried out for 7 hours to give **4d** (149 mg, 42%) as a bronze solid. M.p. 180-181 °C. ¹H NMR (300 MHz, DMSO-*d*₆) δ 9.44 (d, *J* = 7.7 Hz, 1H, H₅), 7.48 (d, *J* = 7.7 Hz, 1H, H₄), 7.04 (s, 1H, H₆ or 9), 6.90 (s, 1H, H₆ or 9), 6.59 (d, *J* = 5.8 Hz, 1H, H₁), 5.96 (d, *J* = 3.1 Hz, 1H, H_{4'}), 5.67 (d, *J* = 3.1, 1H, H_{3'}), 5.52 (d, *J* = 5.8 Hz, 1H, H₂), 5.06 (t, *J* = 5.4 Hz, 1H, OH), 4.24 (d, *J* = 5.4 Hz, 2H, CH₂OH), 2.21 (s, 3H, COCH₃). ¹³C NMR (75 MHz, DMSO-*d*₆) δ 192.2 (COCH₃), 154.9 (C_{2'}), 154.4 (C_{5'}), 142.3 (C₄), 138.9 (C_{9a}), 131.9 (C_{5a}), 123.4 (C₇ or 8), 121.2 (C₆ or 9), 121.0 (C₇ or 8), 120.0 (C₆ or 9), 114.5 (C₃), 107.1 (C_{4'}), 106.5 (C_{3'}), 55.8 (CH₂OH), 51.2 (C₂), 24.4 (COCH₃). HRMS (ESI) *m/z*: Calcd for [M+H]⁺ C₁₆H₁₅Cl₂N₂O₃ = 353.0454; Found 353.0451. HRMS (ESI) *m/z*: Calcd for [M+Na]⁺ C₁₆H₁₄ Cl₂N₂NaO₃ = 375.0274; Found 375.0270.



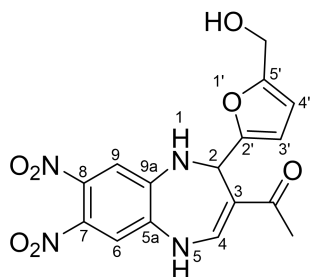
1-{7,8-Dibromo-2-[5-(hydroxymethyl)furan-2-yl]-2,5-dihydro-1H-1,5-benzodiazepine-3-yl}ethan-1-one (C₁₆H₁₄Br₂N₂O₃)



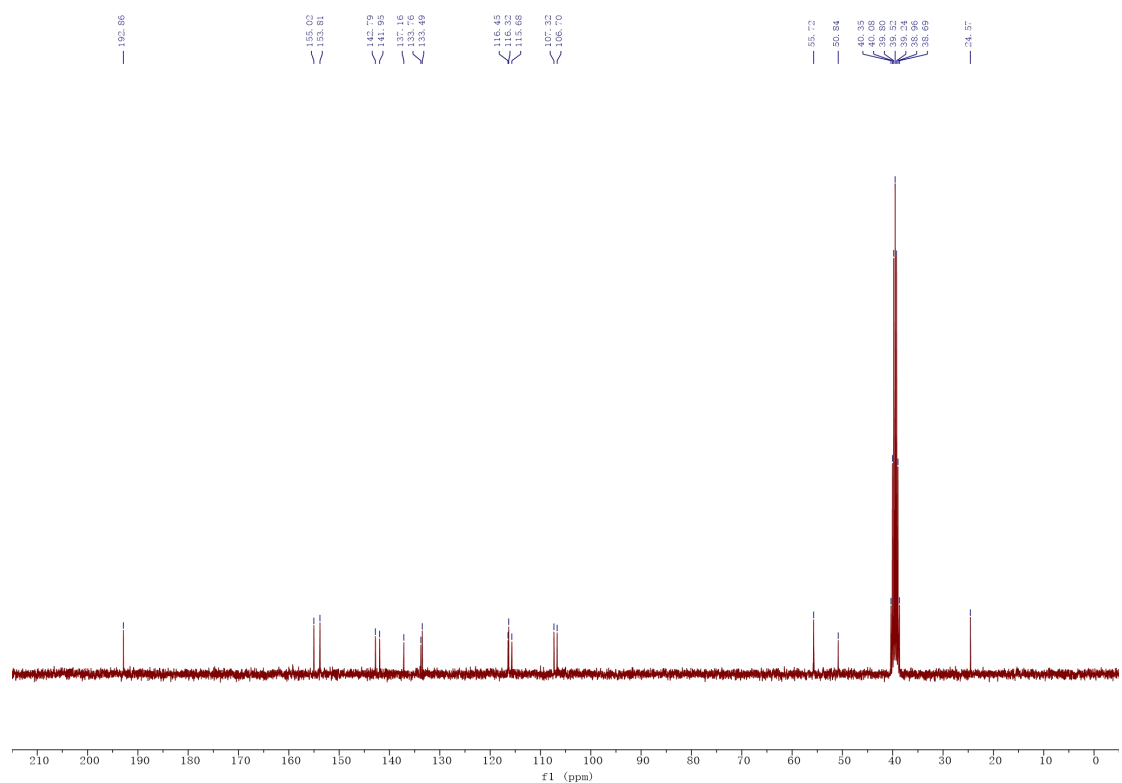
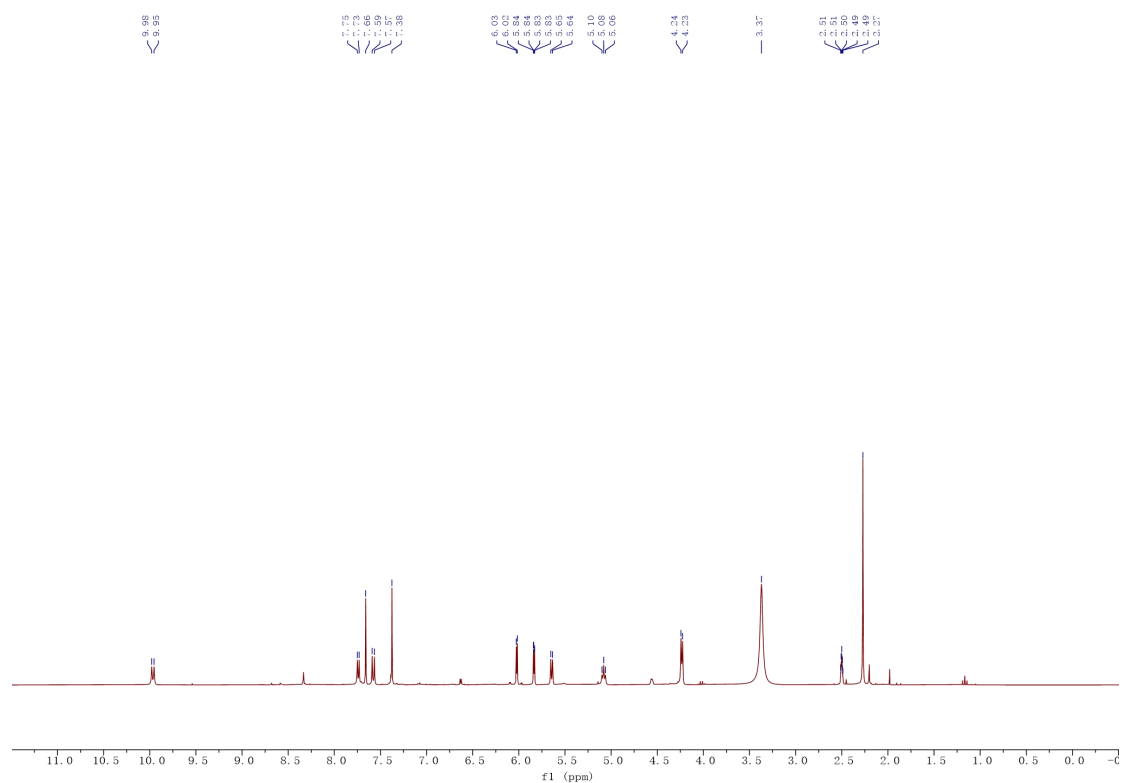
The reaction was carried out for 7 hours to give **4e** (230 mg, 52%) as a yellow solid. M.p. 197-198 °C. ¹H NMR (300 MHz, DMSO-*d*₆) δ 9.43 (d, *J* = 7.7 Hz, 1H, H₅), 7.47 (d, *J* = 7.7 Hz, 1H, H₄), 7.16 (s, 1H, H_{Ar}), 7.04 (s, 1H, H_{Ar}), 6.60 (d, *J* = 5.8 Hz, 1H, H₁), 5.96 (d, *J* = 3.1 Hz, 1H, H_{4'}), 5.67 (d, *J* = 3.1, 1H, H_{3'}), 5.52 (d, *J* = 5.8 Hz, 1H, H₂), 5.08 (t, *J* = 5.6 Hz, 1H, OH), 4.24 (d, *J* = 5.6 Hz, 2H, CH₂OH), 2.21 (s, 3H, COCH₃). ¹³C NMR (75 MHz, DMSO) δ 192.2 (C=OCH₃), 154.9 (C_{2'}), 154.4 (C_{5'}), 142.3 (C₄), 139.5 (C_{Ar}), 132.5 (C_{Ar}), 124.3 (CH_{Ar}), 123.0 (CH_{Ar}), 115.5 (C_{Ar}), 114.5 (C₃), 112.7 (C_{Ar}), 107.1 (C_{4'}), 106.5 (C_{3'}), 55.8 (CH₂OH), 51.1 (C₂), 24.4 (COCH₃). HRMS (ESI) *m/z*: Calcd for [M+H]⁺ C₁₆H₁₅Br₂N₂O₃ = 440.9444; Found 440.9446. HRMS (ESI) *m/z*: Calcd for [M+Na]⁺ C₁₆H₁₄Br₂N₂NaO₃ = 462.9263; Found 462.9266.



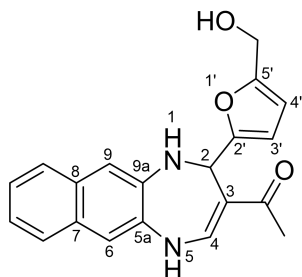
1-{2-[5-(Hydroxymethyl)furan-2-yl]-7,8-dinitro-2,5-dihydro-1H-1,5-benzodiazepin-3-yl}ethan-1-one (C₁₆H₁₄N₄O₇)



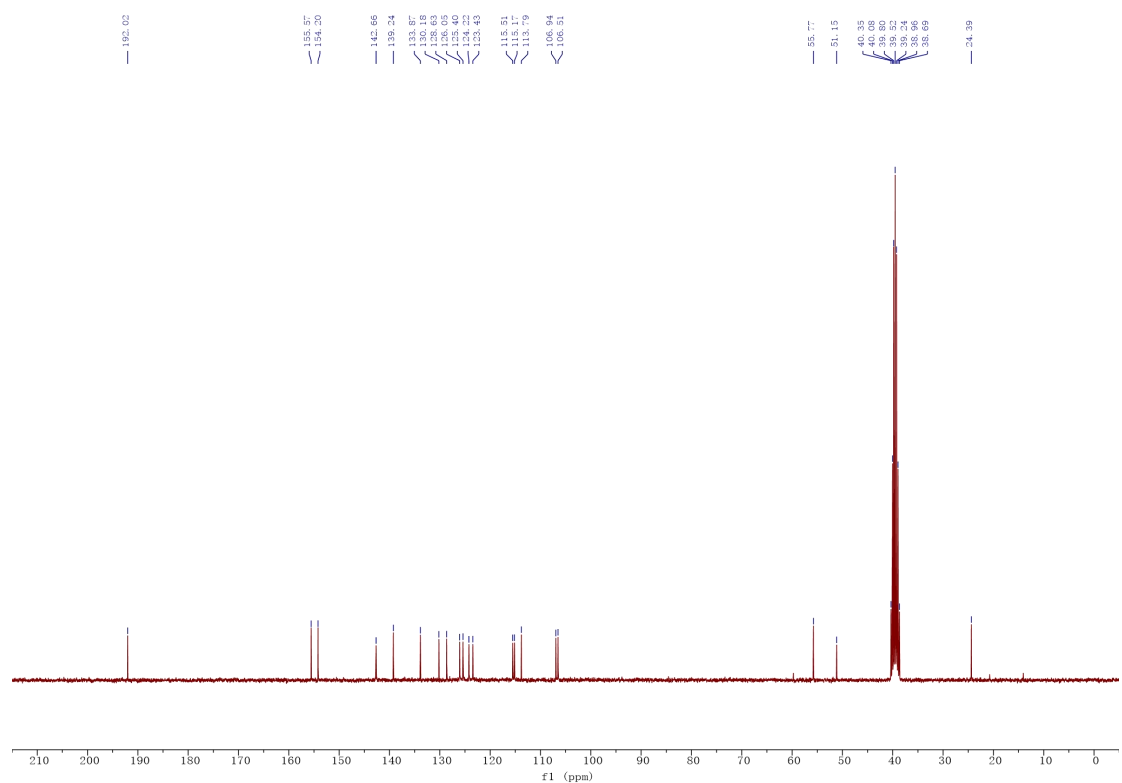
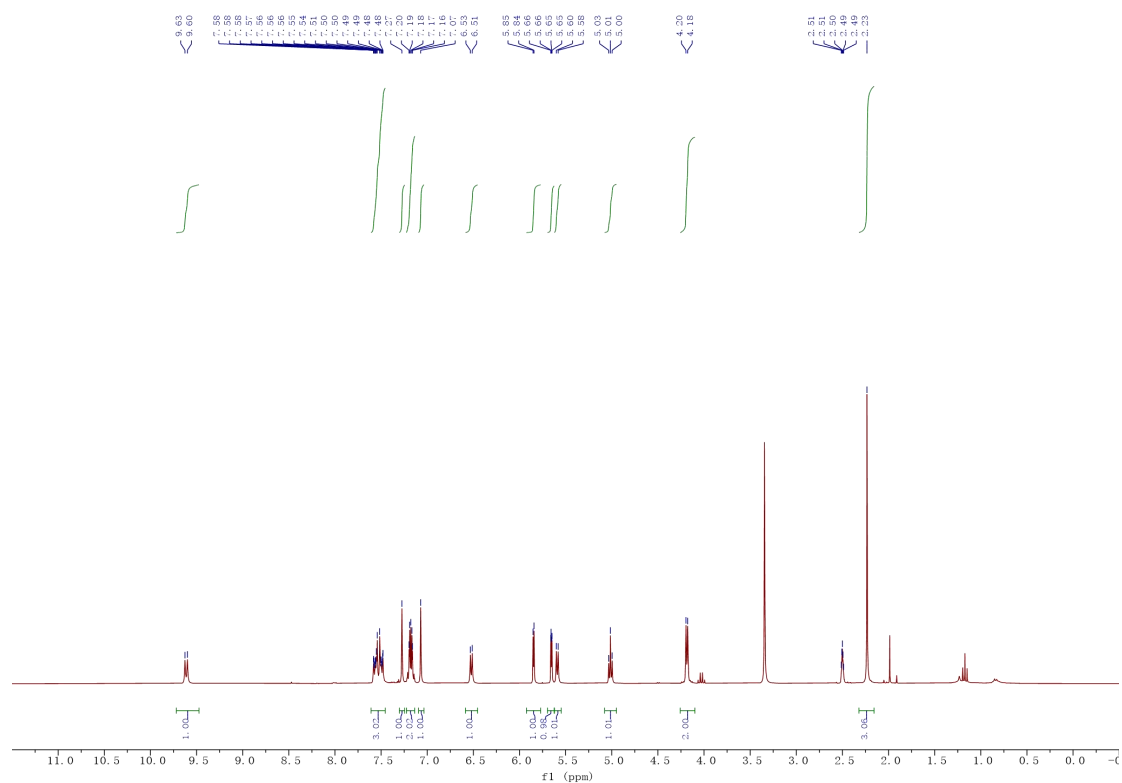
The reaction was carried out for 7 hours to give **4f** (90 mg, 24%) as a brown solid. M.p. 70-71 °C. ¹H NMR (300 MHz, DMSO-*d*₆) δ 9.97 (d, *J* = 7.4 Hz, 1H, H₅), 7.74 (d, *J* = 6.0 Hz, 1H, H₁), 7.66 (s, 1H, CH_{Ar}), 7.58 (d, *J* = 7.4 Hz, 1H, C₄), 7.38 (s, 1H, CH_{Ar}), 6.02 (d, *J* = 3.1 Hz, 1H, C_{4'}), 5.84 (dd, *J* = 3.1, 0.9 Hz, 1H, C_{3'}), 5.64 (d, *J* = 5.8 Hz, 1H, C₂), 5.08 (t, *J* = 5.6 Hz, 1H, OH), 4.23 (d, *J* = 5.1 Hz, 2H, CH₂OH), 2.27 (s, 3H, COCH₃). ¹³C NMR (75 MHz, DMSO) δ 192.9 (COCH₃), 155.0 (C_{5'}), 153.8 (C_{2'}), 142.8 (C_{Ar}), 142.0 (C₄), 137.2 (C_{Ar}), 133.8 (C_{Ar}), 133.5 (C_{Ar}), 116.4 (CH_{Ar}), 116.3 (C₃), 115.7 (CH_{Ar}), 107.3 (C_{4'}), 106.7 (C_{3'}), 55.7 (CH₂OH), 50.8 (C₂), 24.6 (COCH₃). HRMS (ESI) *m/z*: Calcd for [M+H]⁺ C₁₆H₁₅N₄O₇=375.0935; Found 375.0931. HRMS (ESI) *m/z*: Calcd for [M+Na]⁺ C₁₆H₁₄N₄NaO₇=397.0755; Found 397.0750.



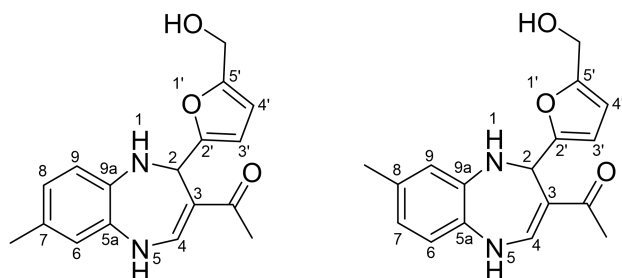
1-{2-[5-(Hydroxymethyl)furan-2-yl]-2,5-dihydro-1H-1,5-naphthodiazepin-3-yl}ethan-1-one
(C₂₀H₁₈N₂O₃)



The reaction was carried out for 7 hours to give **4g** (70 mg, 21%) as a brown solid. M.p. 125-126 °C. ¹H NMR (300 MHz, DMSO-*d*₆) δ 9.61 (d, *J* = 7.9 Hz, 1H, H₅), 7.61 – 7.45 (m, 3H, H₄, 2H_{Ar}), 7.27 (s, 1H, H₆ or 11), 7.23 – 7.14 (m, 2H, H_{Ar}), 7.07 (s, 1H, H₆ or 11), 6.52 (d, *J* = 6.0 Hz, 1H, H₁), 5.85 (d, *J* = 3.1 Hz, 1H, H_{4'}), 5.65 (dd, *J* = 3.1, 0.9 Hz, 1H, H_{3'}), 5.59 (d, *J* = 6.0 Hz, 1H, H₂), 5.01 (t, *J* = 5.6 Hz, 1H, OH), 4.19 (d, *J* = 5.6 Hz, 2H, CH₂OH), 2.23 (s, 3H, COCH₃). ¹³C NMR (75 MHz, DMSO-*d*₆) δ 192.0 (C=O), 155.6 (C_{2'}), 154.2 (C_{5'}), 142.7 (C₄), 139.2 (C_{11a}), 133.9 (C_{5a}), 130.2 (C_{6a} or 10a), 128.6 (C_{6a} or 10a), 126.0 (CH_{Ar}), 125.4 (CH_{Ar}), 124.2 (CH_{Ar}), 123.4 (CH_{Ar}), 115.5 (C₆ or 11), 115.2 (C₆ or 11), 113.8 (C₃), 106.9 (C_{4'}), 106.5 (C_{3'}), 55.8 (CH₂OH), 51.1 (C₂), 24.4 (COCH₃). HRMS (ESI) *m/z*: Calcd for [M+H]⁺ C₂₀H₁₉N₂O₃ = 335.1390; Found 335.1388. HRMS (ESI) *m/z*: Calcd for [M+Na]⁺ C₂₀H₁₈N₂NaO₃ = 357.1210; Found 357.1208.

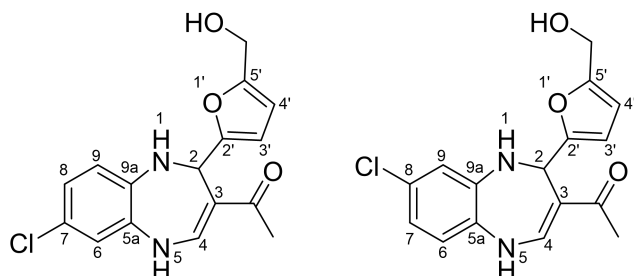


1-{2-[5-(Hydroxymethyl)furan-2-yl]-7-methyl-2,5-dihydro-1H-1,5-benzodiazepin-3-yl}ethan-1-one and 1-{2-[5-(Hydroxymethyl)furan-2-yl]-8-methyl-2,5-dihydro-1H-1,5-benzodiazepin-3-yl}ethan-1-one (C₁₇H₁₈N₂O₃)

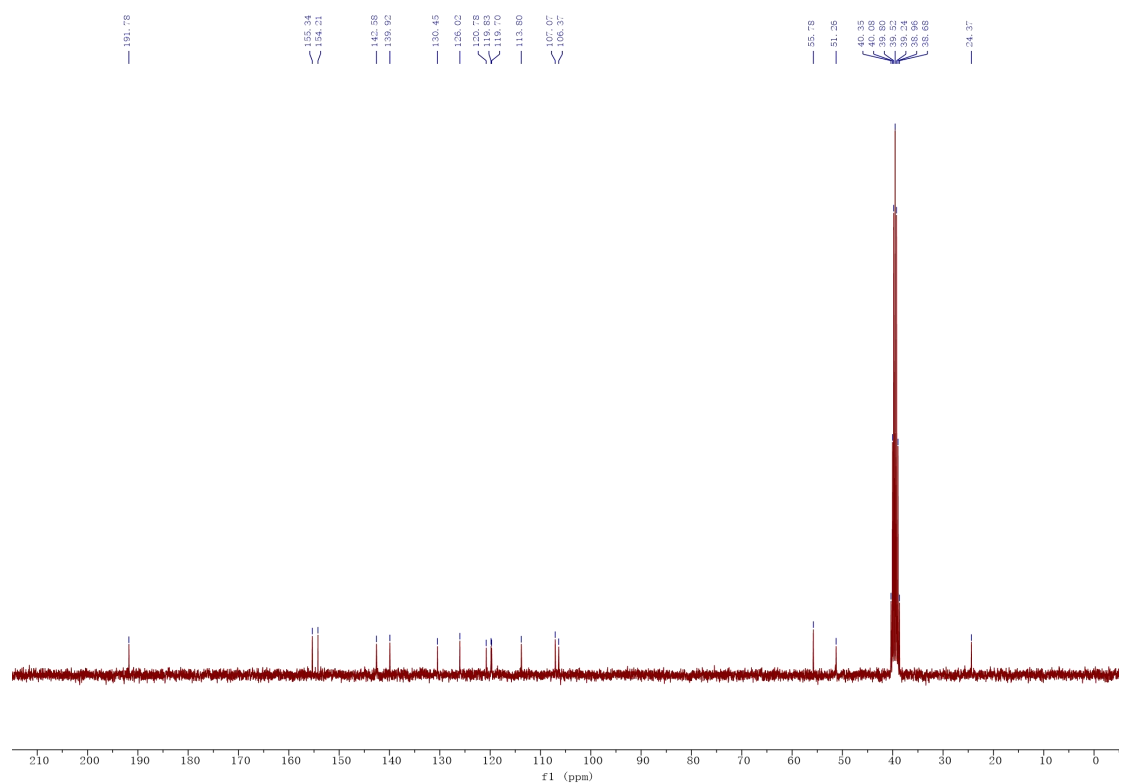
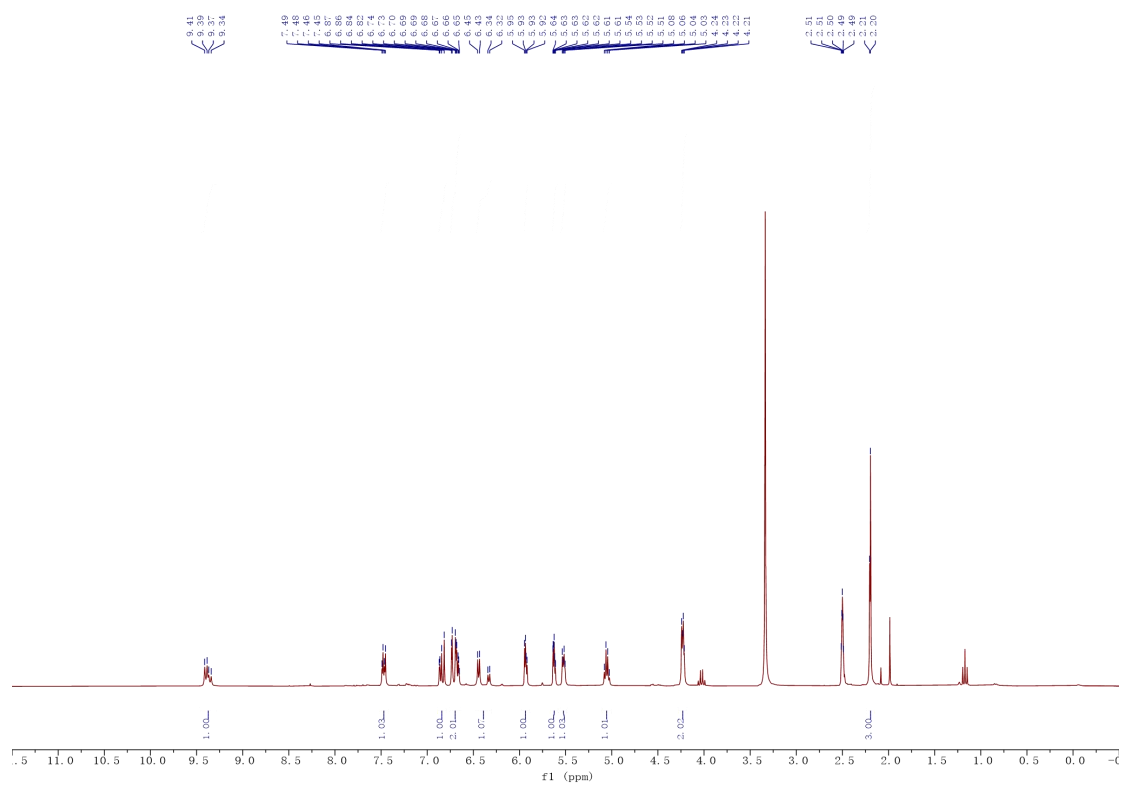


The reaction was carried out for 7 hours to give **4h'** and **4h'** (197 mg, 66%) as a mixed bronze solid. ¹H NMR (300 MHz, DMSO-*d*₆) δ 9.24 (m, 1H, H₅), 7.47 (2d, *J*₁ = 8.0 Hz, *J*₂ = 8.0 Hz, 1H, H₄), 6.75 – 6.61 (m, 1H, H_{Ar}), 6.59 – 6.44 (m, 2H, 2H_{Ar}), 6.00 (2d, *J*₁ = 5.9 Hz, *J*₂ = 5.9 Hz, 1H, H₁), 5.91 (2d, *J*₁ = 3.1 Hz, *J*₂ = 3.1 Hz, 1H, H_{4'}), 5.61 – 5.50 (m, 2H, H_{3'} and H₂), 5.06 (2t, *J*₁ = 5.6 Hz, *J*₂ = 5.6 Hz, 1H, OH), 4.24 (d, *J* = 5.4 Hz, 2H, CH₂OH), 2.18 (2s, 3H, COCH₃), 2.09 (2s, 3H, Ar-CH₃). ¹³C NMR (75 MHz, DMSO) δ 191.7 and 191.5 (C=O), 156.0(2) and 156.0 (C_{2'}), 154.0 and 153.9 (C_{5'}), 143.0 and 142.9 (C₄), 138.3 and 136.0 (C_{Ar}), 131.7 and 131.2 (C_{Ar}-CH₃), 128.9 and 128.8 (C_{Ar}), 123.7 and 121.3 and 121.1 and 120.9 (2CH_{Ar}) 119.8 and 119.5 (CH_{Ar}), 113.8 and 113.4 (C₃), 107.1 and 107.0 (C_{4'}), 106.4 and 106.2 (C_{3'}), 55.9 (CH₂OH), 51.7 and 51.4 (C₂), 24.4 and 24.3 (COCH₃), 20.3 and 20.1 (Ar-CH₃). HRMS (ESI) *m/z*: Calcd for [M+H]⁺ C₁₇H₁₉N₂O₃ = 299.1390; Found 299.1388. HRMS (ESI) *m/z*: Calcd for [M+Na]⁺ C₁₇H₁₈N₂NaO₃ = 321.1210; Found 321.1210.

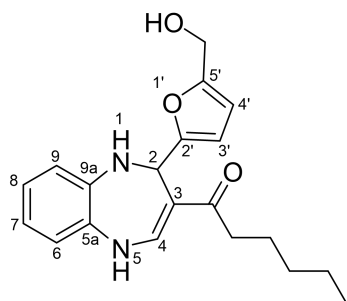
1-{2-[5-(Hydroxymethyl)furan-2-yl]-7-methyl-2,5-dihydro-1H-1,5-benzodiazepin-3-yl}ethan-1-one and 1-{2-[5-(Hydroxymethyl)furan-2-yl]-8-methyl-2,5-dihydro-1H-1,5-benzodiazepin-3-yl}ethan-1-one (C₁₆H₁₅ClN₂O₃)



The reaction was carried out for 7 hours to give **4i** and **4i'** (198 mg, 62%) as a mixed bronze solid. ¹H NMR (300 MHz, DMSO-*d*₆) δ 9.38 (2d, *J*₁ = 7.9 Hz, *J*₂ = 7.9 Hz, 1H, H₅), 7.47 (2d, *J*₁ = 7.9 Hz, *J*₂ = 7.9 Hz, 1H, H₄), 6.90 – 6.79 (m, 1H, H_{Ar}), 6.77 – 6.62 (m, 2H, 2H_{Ar}), 6.39 (2d, *J*₁ = 5.9 Hz, *J*₂ = 5.9 Hz, 1H, H₁), 5.93 (2d, *J*₁ = 3.1 Hz, *J*₂ = 3.1 Hz, 1H, H_{4'}), 5.62 (m, 1H, H_{3'}), 5.52 (m, 1H, H₂), 5.05 (m, 1H, OH), 4.23 (m, 2H, CH₂OH), 2.20 (2s, 3H, COCH₃). ¹³C NMR (75 MHz, DMSO) δ 191.8 (COCH₃), 155.3 (C_{2'}), 154.2 (C_{5'}), 142.6 (C₄), 139.9 (C_{5a/9a}), 130.5 (C_{5a/9a}), 126.0 (C_{Ar}), 120.8 (CH_{Ar}), 119.8 (CH_{Ar}), 119.7 (CH_{Ar}), 113.8 (C₃), 107.1 (C_{4'}), 106.4 (C_{3'}), 55.8 (CH₂OH), 51.3 (C₂), 24.4 (COCH₃). HRMS (ESI) *m/z*: Calcd for [M+H]⁺ C₁₆H₁₆ClN₂O₃ = 319.0844; Found 319.0841. HRMS (ESI) *m/z*: Calcd for [M+Na]⁺ C₁₆H₁₅ClN₂NaO₃ = 341.0663; Found 341.0663.

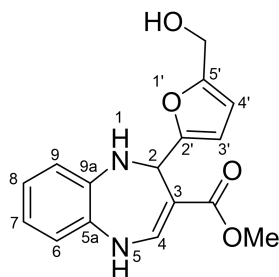


1-{2-[5-(Hydroxymethyl)furan-2-yl]-2,5-dihydro-1H-1,5-benzodiazepine-3-yl}hexan-1-one
(C₂₀H₂₄N₂O₃)



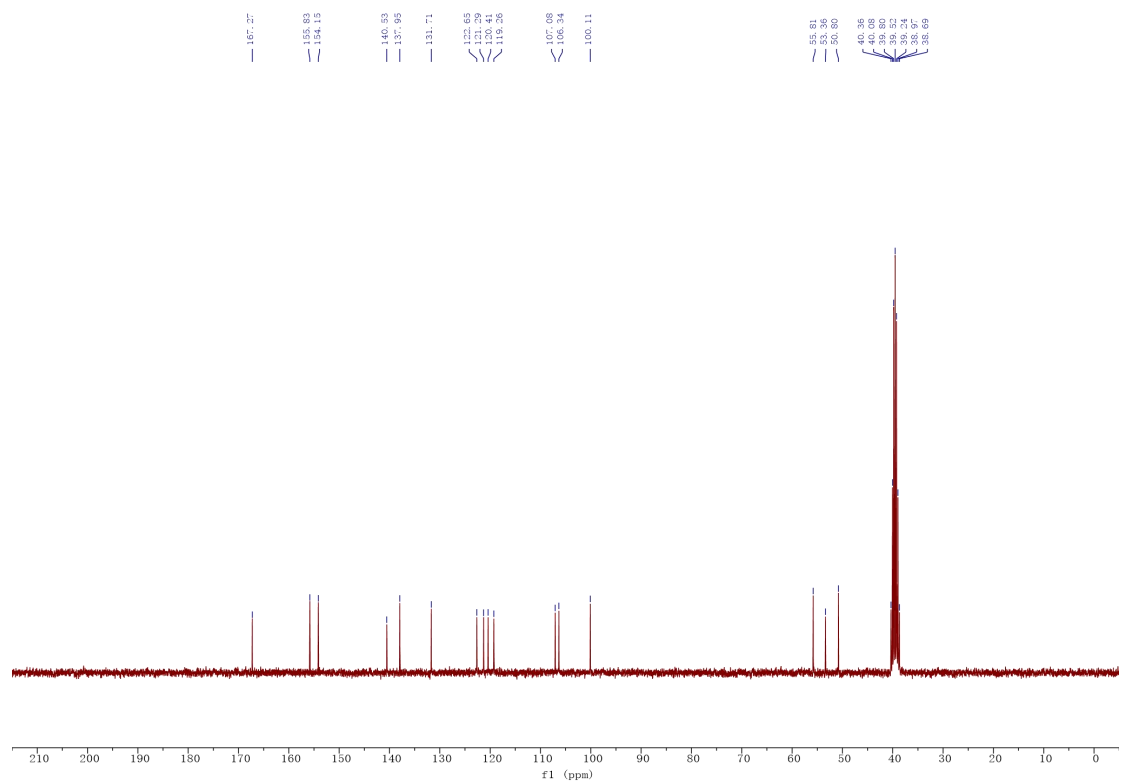
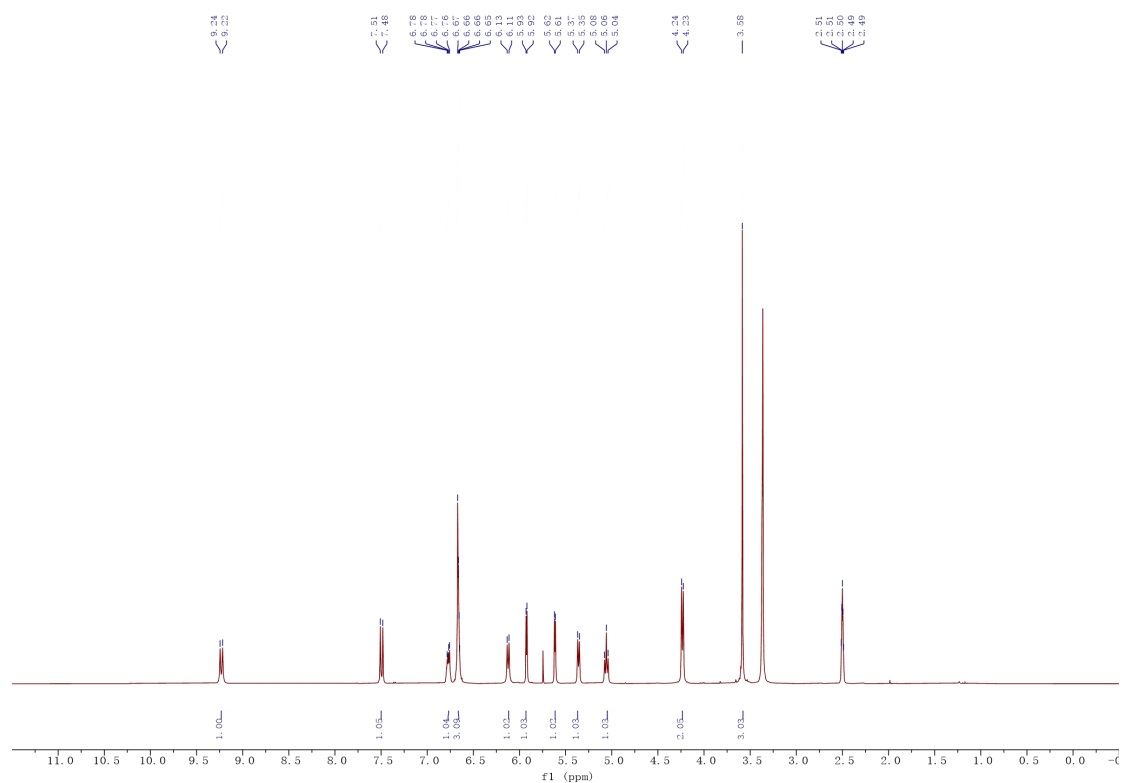
The reaction was carried out for 6 hours to give **4j** (250 mg, 74%) as a bronze solid. M.p. 135-136 °C. ¹H NMR (300 MHz, DMSO-*d*₆) δ 9.17 (d, *J* = 8.0 Hz, 1H, H₅), 7.44 (d, *J* = 8.0 Hz, 1H, H₄), 6.78 – 6.66 (m, 1H, H_{Ar}), 6.64 – 6.50 (m, 3H, H_{Ar}), 6.05 (d, *J* = 5.9 Hz, 1H, H₁), 5.82 (d, *J* = 3.2 Hz, 1H, H_{4'}), 5.54 – 5.45 (m, 2H, H_{3'}, H₂), 4.98 (t, *J* = 5.6 Hz, 1H, OH), 4.15 (d, *J* = 5.6 Hz, 2H, CH₂OH), 2.46 (m, 2H, CH₂), 1.50 – 1.39 (m, 2H, CH₂), 1.27 – 1.11 (m, 4H, 2CH₂), 0.78 (t, *J* = 6.8 Hz, 3H, CH₃). ¹³C NMR (75 MHz, DMSO) δ 194.3 (C=O), 155.9 (C_{2'}), 154.0 (C_{5'}), 142.2 (C₄), 138.5 (C_{Ar}), 131.4 (C_{Ar}), 122.8 (CH_{Ar}), 121.0 (CH_{Ar}), 120.2 (CH_{Ar}), 119.5 (CH_{Ar}), 113.2 (C₃), 107.0 (C_{4'}), 106.3 (C_{3'}), 55.9 (CH₂OH), 51.7 (C₂), 35.4 (CH₂), 31.2 (CH₂), 25.5 (CH₂), 22.1 (CH₂), 14.0 (CH₃). HRMS (ESI) *m/z*: Calcd for [M+H]⁺ C₂₀H₂₅N₂O₃ = 341.1860; Found 341.1861. HRMS (ESI) *m/z*: Calcd for [M+Na]⁺ C₂₀H₂₄N₂NaO₃ = 363.1679; Found 363.1680.

Methyl 2-[5-(hydroxymethyl)furan-2-yl]-2,5-dihydro-1H-1,5-benzodiazepine-3-carboxylate
(C₁₆H₁₆N₂O₄)

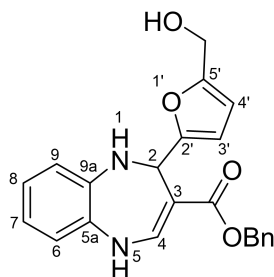


The reaction was carried out for 7 hours to give **4k** (138 mg, 46%) as a yellow oil.

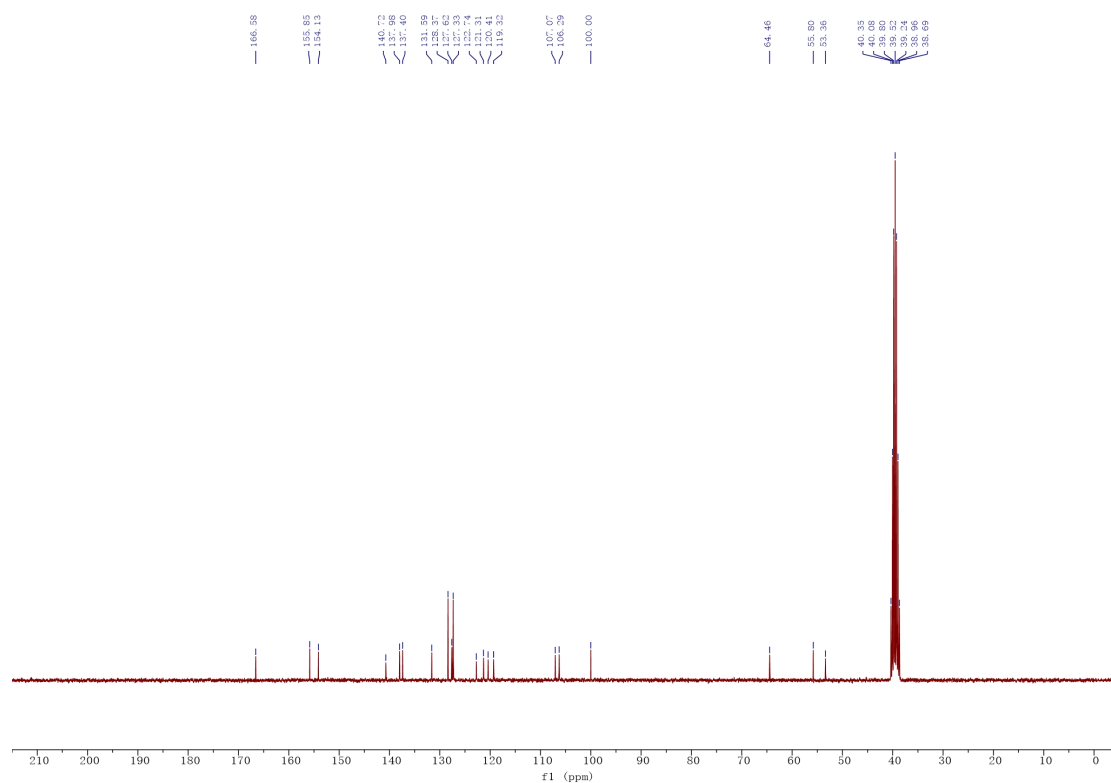
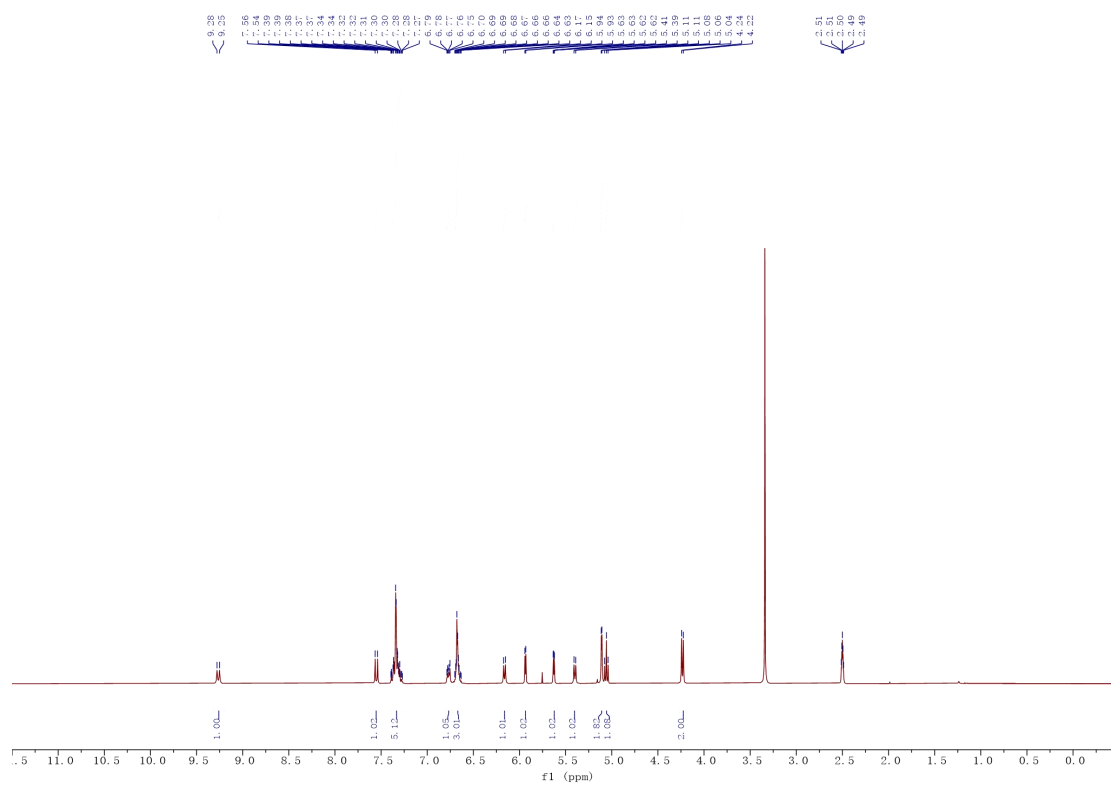
¹H NMR (300 MHz, DMSO-*d*₆) δ 9.23 (d, J = 8.0 Hz, 1H, H₅), 7.50 (d, J = 8.0 Hz, 1H, H₄), 6.78 (m, 1H, H₆ or 9), 6.73 – 6.60 (m, 3H, H_{Ar}), 6.12 (d, J = 5.7 Hz, 1H, H_I), 5.92 (d, J = 3.0 Hz, 1H, H_{4'}), 5.62 (d, J = 3.0 Hz, 1H, H_{3'}), 5.36 (d, J = 5.7 Hz, 1H, H₂), 5.06 (t, J = 5.5 Hz, 1H, OH), 4.23 (d, J = 5.5 Hz, 2H, CH₂OH), 3.58 (s, 3H, COOCH₃). ¹³C NMR (75 MHz, DMSO-*d*₆) δ 167.3 (COOCH₃), 155.8 (C_{2'}), 154.2 (C_{5'}), 140.5 (C₄), 138.0 (C_{9a}), 131.7 (C_{5a}), 122.7 (CH_{Ar}), 121.3 (CH_{Ar}), 120.4 (CH_{Ar}), 119.3 (CH_{Ar}), 107.1 (C_{4'}), 106.3 (C_{3'}), 100.1 (C₃), 55.8 (CH₂OH), 53.4 (C₂), 50.8 (COOCH₃). HRMS (ESI) m/z : Calcd for [M+H]⁺ C₁₆H₁₇N₂O₄ = 301.1183; Found 301.1181. HRMS (ESI) m/z : Calcd for [M+Na]⁺ C₁₆H₁₆N₂NaO₄ = 323.1002; Found 323.1000.



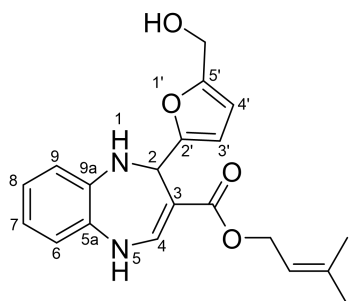
Benzyl 2-[5-(hydroxymethyl)furan-2-yl]-2,5-dihydro-1H-1,5-benzodiazepine-3-carboxylate
(C₂₂H₂₀N₂O₄)



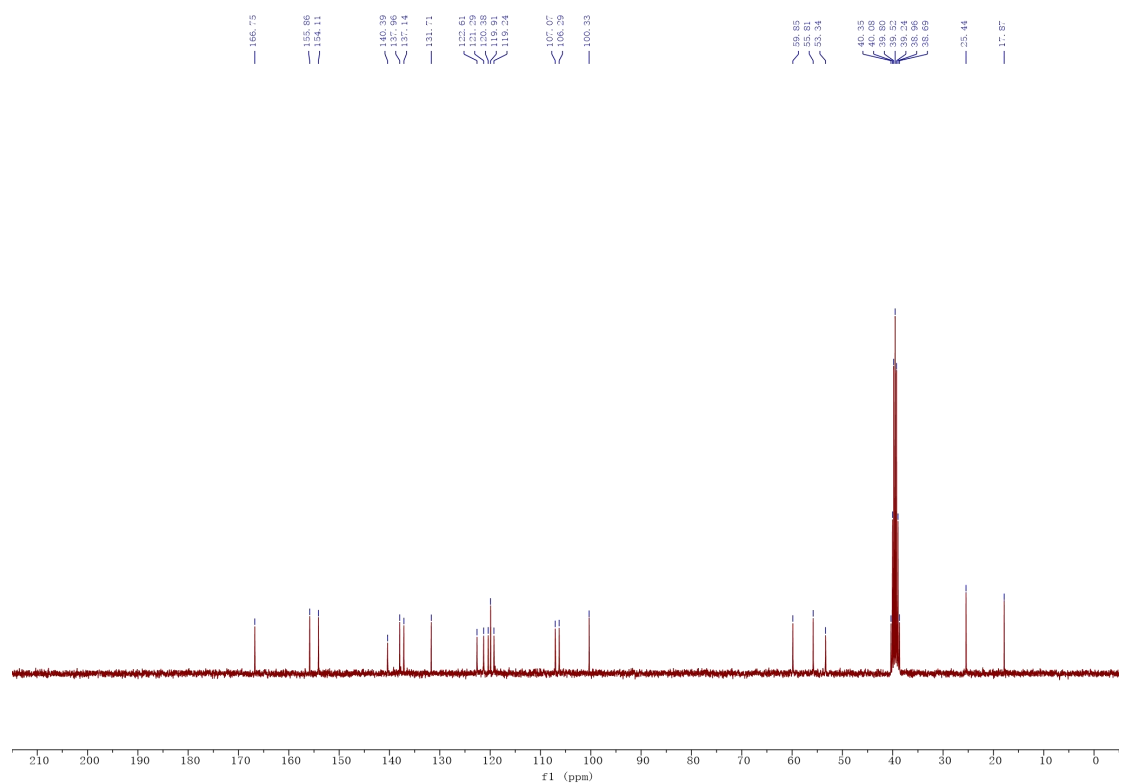
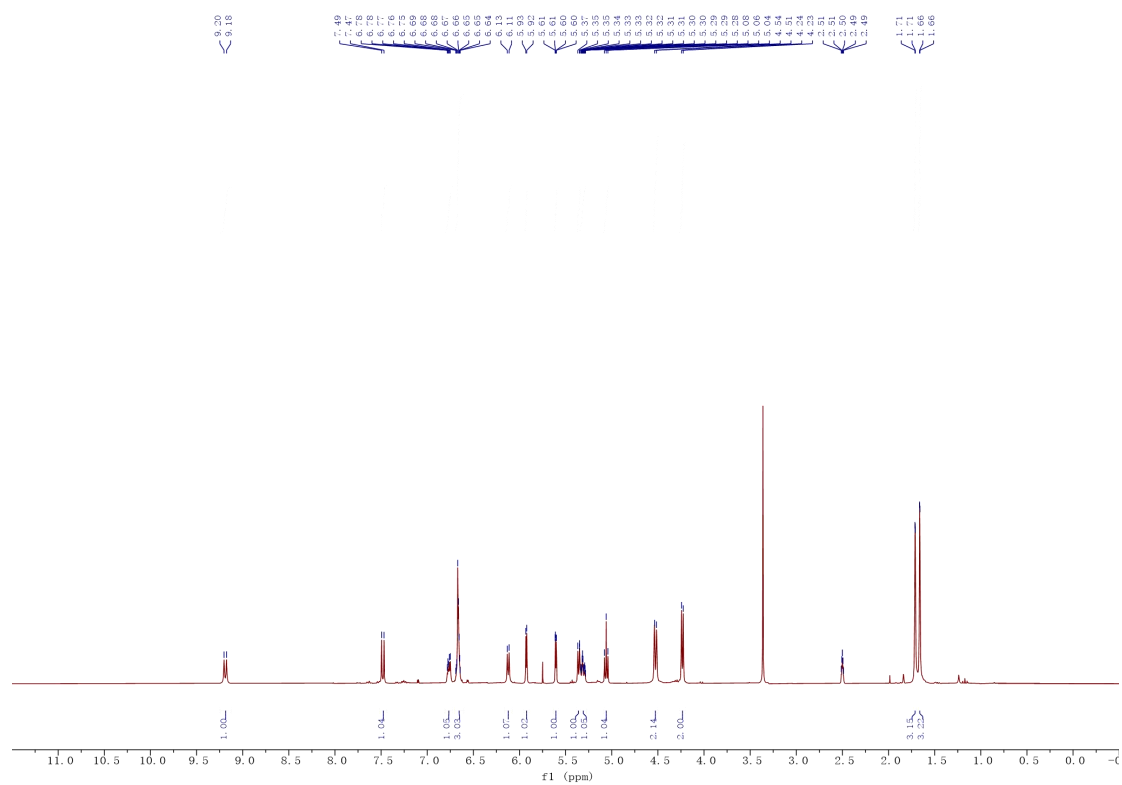
The reaction was carried out for 6 hours to give **4l** (192 mg, 51%) as a yellow solid. M.p. 81-82 °C. ¹H NMR (300 MHz, DMSO-*d*₆) δ 9.26 (d, *J* = 8.1 Hz, 1H, H₅), 7.55 (d, *J* = 8.1 Hz, 1H, H₄), 7.40 – 7.26 (m, 5H, H_{Ph}), 6.81 – 6.73 (m, 1H, H_{Ar}), 6.71 – 6.62 (m, 3H, H_{Ar}), 6.16 (d, *J* = 5.7 Hz, 1H, H₁), 5.94 (d, *J* = 3.1 Hz, 1H, H_{4'}), 5.63 (dd, *J* = 3.1, 0.9 Hz, 1H, H_{3'}), 5.40 (d, *J* = 5.7 Hz, 1H, H₂), 5.11 (d, *J* = 2.2 Hz, 2H, PhCH₂), 5.06 (t, *J* = 5.7 Hz, 1H, OH), 4.23 (d, *J* = 5.7 Hz, 2H, CH₂OH). ¹³C NMR (75 MHz, DMSO) δ 166.5 (C=O), 155.9 (C_{2'}), 154.1 (C_{5'}), 140.7 (C₄), 138.0 (C_{Ar}), 137.4 (C_{Ph}), 131.6 (C_{Ar}), 128.4 (CH_{Ph}), 127.6 (2CH_{Ph}), 127.3 (2CH_{Ph}), 122.7 (CH_{Ar}), 121.3 (CH_{Ar}), 120.4 (CH_{Ar}), 119.3 (CH_{Ar}), 107.1 (C_{4'}), 106.3 (C_{3'}), 100.0 (C₃), 64.5 (PhCH₂), 55.8 (CH₂OH), 53.4 (C₂). HRMS (ESI) *m/z*: Calcd for [M+H]⁺ C₂₂H₂₁N₂O₄ = 377.1496 ; Found 377.1484. HRMS (ESI) *m/z*: Calcd for [M+Na]⁺ C₂₂H₂₀N₂NaO₄ = 399.1315; Found 399.1302.



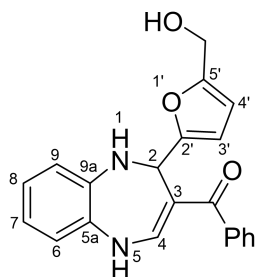
3-Methylbut-2-en-1-yl 2-[5-(hydroxymethyl)furan-2-yl]-2,5-dihydro-1H-1,5-benzodiazepine-3-carboxylate (C₂₀H₂₂N₂O₄)



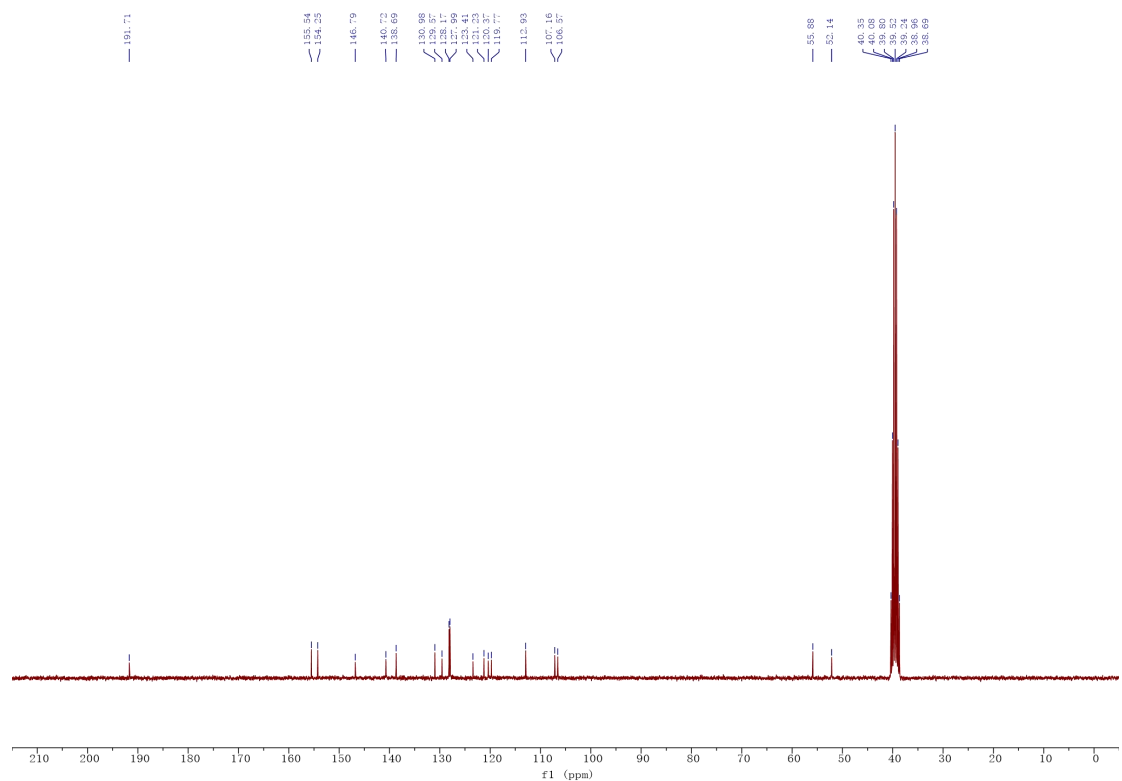
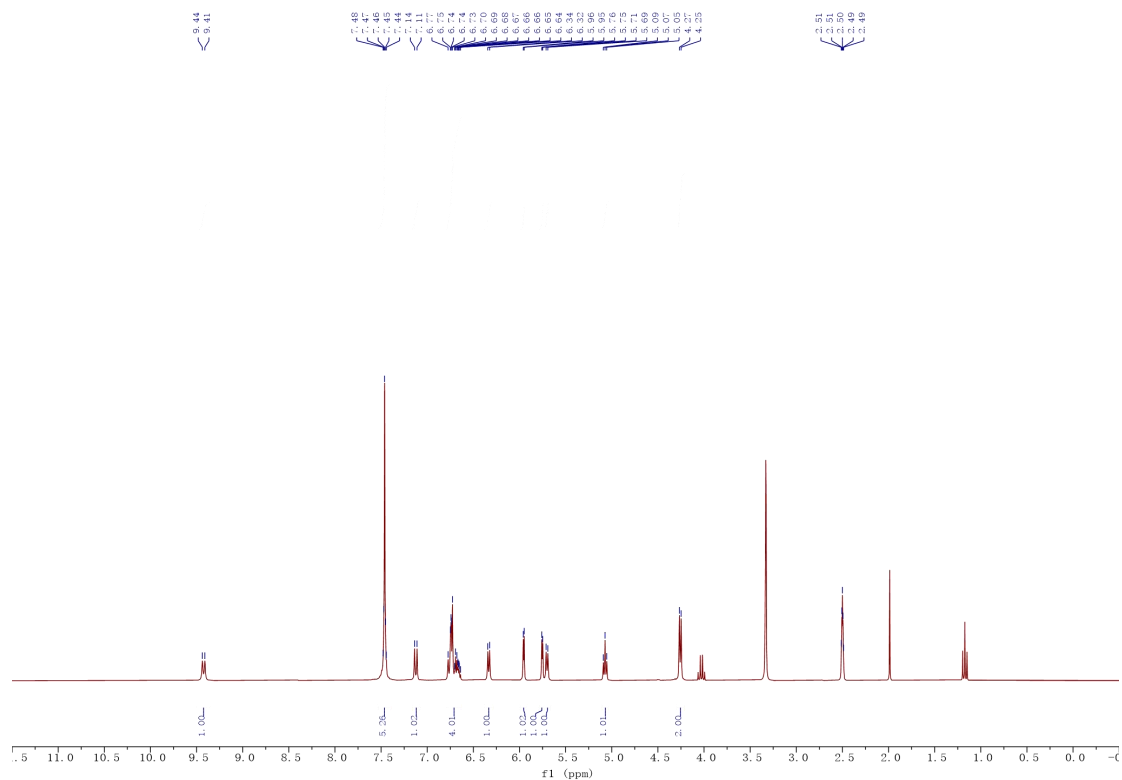
The reaction was carried out for 6 hours to give **4m** (174 mg, 49%) as a yellow solid. M.p. 55-56 °C. ¹H NMR (300 MHz, DMSO-*d*₆) δ 9.19 (d, *J* = 8.0 Hz, 1H, H₅), 7.48 (d, *J* = 8.0 Hz, 1H, H₄), 6.81 – 6.72 (m, 1H, H_{Ar}), 6.72 – 6.61 (m, 3H, H_{Ar}), 6.12 (d, *J* = 5.8 Hz, 1H, H₄), 5.93 (d, *J* = 3.1 Hz, 1H, H_{4'}), 5.61 (dd, *J* = 3.1, 0.9 Hz, 1H, H_{3'}), 5.36 (d, *J* = 5.5 Hz, 1H, H₂), 5.34 – 5.28 (m, 1H, CH), 5.06 (t, *J* = 5.6 Hz, 1H, OH), 4.53 (d, *J* = 6.4 Hz, 2H, COOCH₂), 4.23 (d, *J* = 5.6 Hz, 2H, CH₂OH), 1.71 (bs, 3H, CH₃), 1.66 (bs, 3H, CH₃). ¹³C NMR (75 MHz, DMSO) δ 166.7 (C=O), 155.9 (C_{2'}), 154.1 (C_{5'}), 140.4 (C₄), 138.0 (C_{Ar}), 137.1 (-C(CH₃)₂), 131.7 (C_{Ar}), 122.6 (CH_{Ar}), 121.3 (CH_{Ar}), 120.4 (CH_{Ar}), 119.9 (-CHC(CH₃)₂), 119.2 (CH_{Ar}), 107.1 (C_{4'}), 106.3 (C_{3'}), 100.3 (C₃), 59.8 (COOCH₂), 55.8 (CH₂OH), 53.3 (C₂), 25.4 (CH₃), 17.9 (CH₃). HRMS (ESI) *m/z*: Calcd for [M+H]⁺ C₂₀H₂₃N₂O₄=355.1652 ; Found 355.1661. HRMS (ESI) *m/z*: Calcd for [M+Na]⁺ C₂₀H₂₂N₂NaO₄= 377.1472; Found 377.1482.



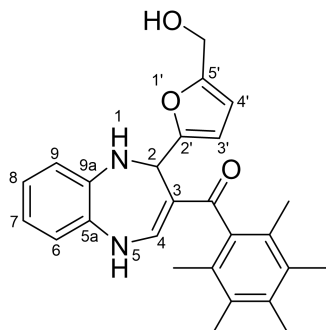
{2-[5-(Hydroxymethyl)furan-2-yl]-2,5-dihydro-1H-1,5-benzodiazepine-3-yl}(phenyl)methanone
(C₂₁H₁₈N₂O₃)



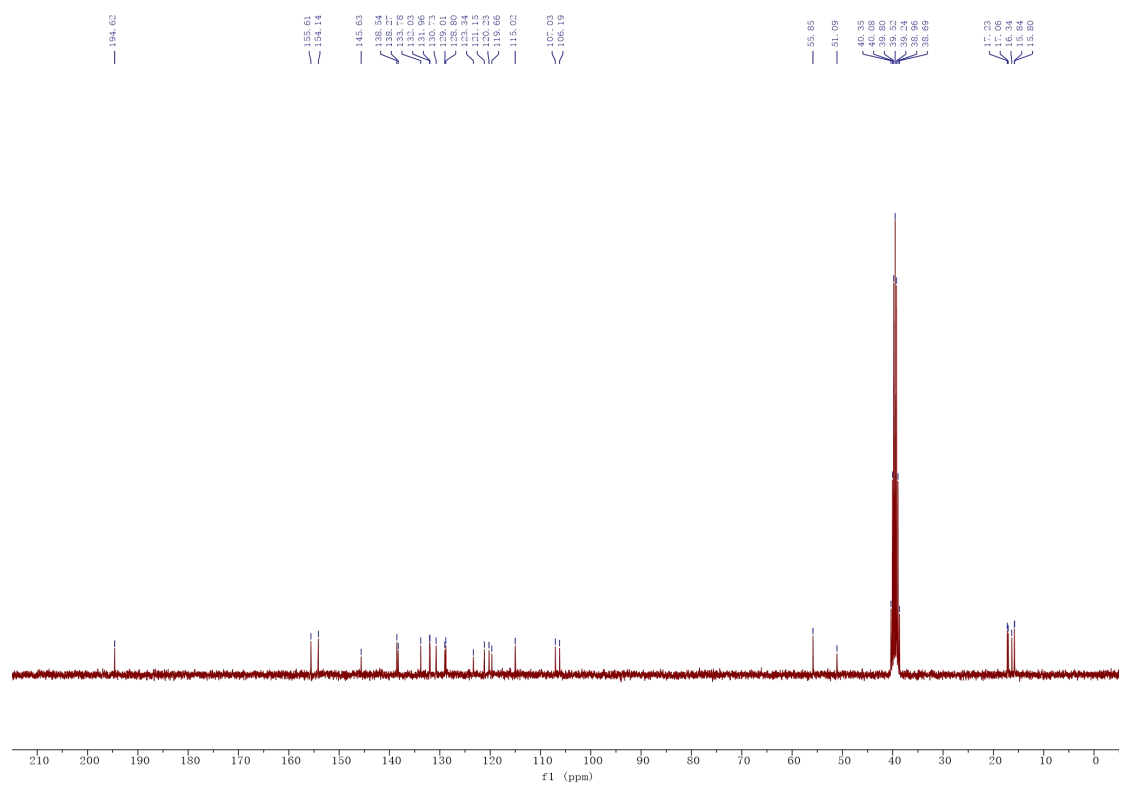
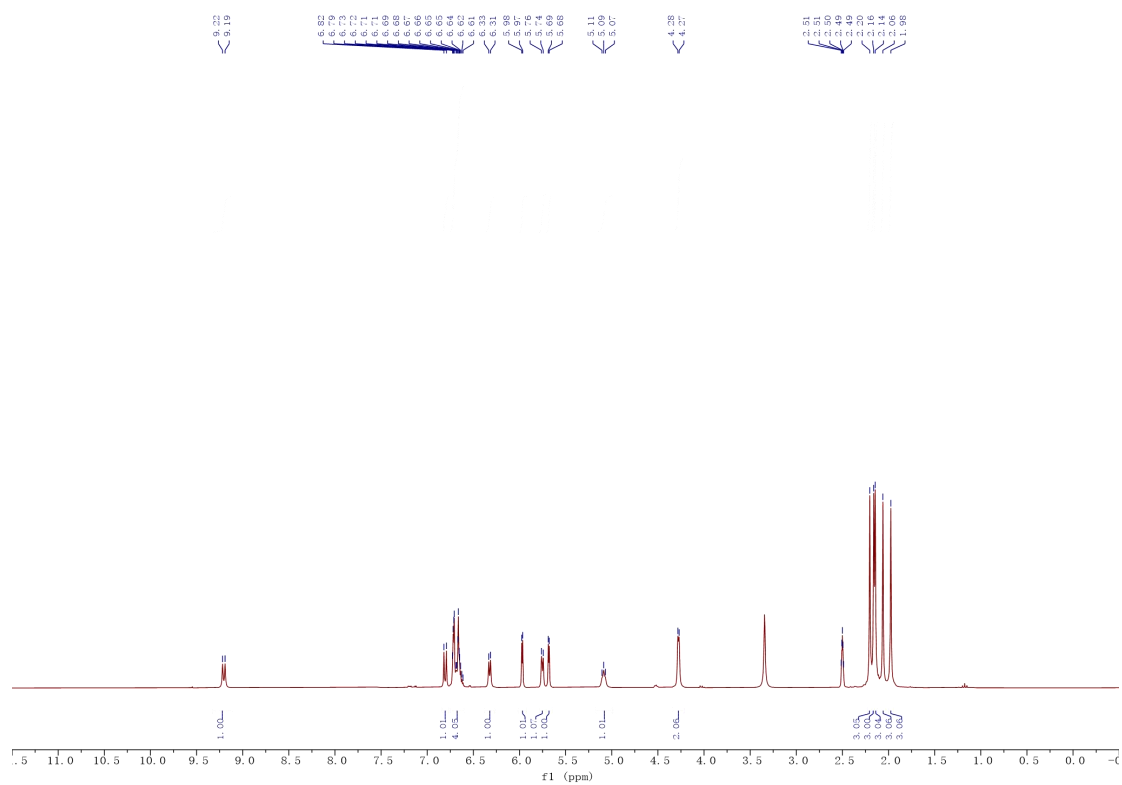
The reaction was carried out for 8 hours to give **4n** (232 mg, 67%) as a yellow solid. M.p. 164-165 °C. ¹H NMR (300 MHz, DMSO-*d*₆) δ 9.42 (d, *J* = 8.1 Hz, 1H, H₅), 7.53 – 7.39 (m, 5H, 5H_{Ph}), 7.12 (d, *J* = 8.1 Hz, 1H, H₄), 6.80 – 6.61 (m, 4H, 4H_{Ar}), 6.33 (d, *J* = 5.8 Hz, 1H, H₁), 5.95 (d, *J* = 3.0 Hz, 1H, H_{4'}), 5.75 (d, *J* = 3.0 Hz, 1H, H_{3'}), 5.70 (d, *J* = 5.8 Hz, 1H, H₂), 5.07 (t, *J* = 5.6 Hz, 1H, OH), 4.26 (d, *J* = 5.6 Hz, 2H, CH₂OH). ¹³C NMR (75 MHz, DMSO) δ 191.7 (C=O), 155.5 (C_{2'}), 154.3 (C_{5'}), 146.8 (C₄), 140.7 (C_{Ph}), 138.7 (C_{Ar}), 131.0 (C_{Ar}), 129.6 (CH_{Ph}), 128.2 (2CH_{Ph}), 128.0 (2CH_{Ph}), 123.4 (CH_{Ar}), 121.2 (CH_{Ar}), 120.4 (CH_{Ar}), 119.8 (CH_{Ar}), 112.9 (C₃), 107.2 (C_{4'}), 106.6 (C_{3'}), 55.9 (CH₂OH), 52.1 (C₂). HRMS (ESI) *m/z*: Calcd for [M+H]⁺ C₂₁H₁₉N₂O₃ = 347.1390; Found 347.1387. HRMS (ESI) *m/z*: Calcd for [M+Na]⁺ C₂₁H₁₈N₂NaO₃ = 369.1210; Found 369.1207.



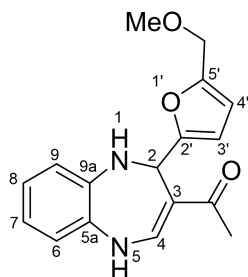
{2-[5-(Hydroxymethyl)furan-2-yl]-2,5-dihydro-1H-1,5-benzodiazepin-3-yl}(2,3,4,5,6-pentamethylphenyl)methanone (C₂₆H₂₈N₂O₃)



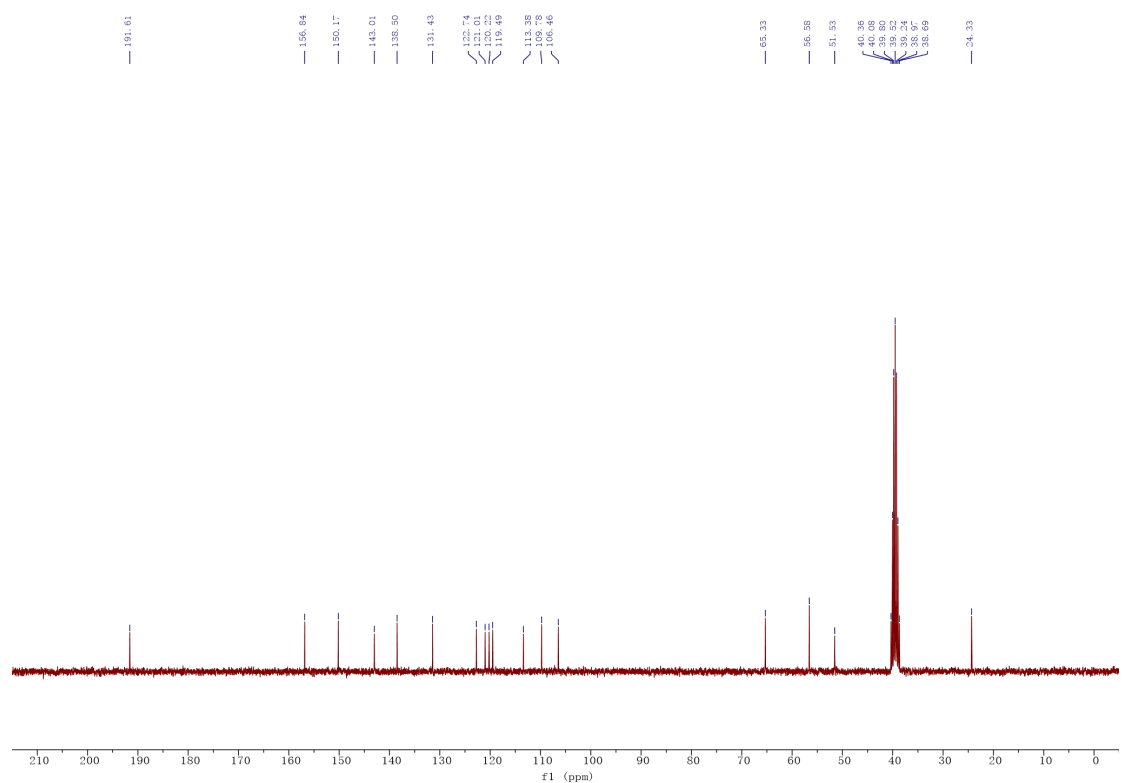
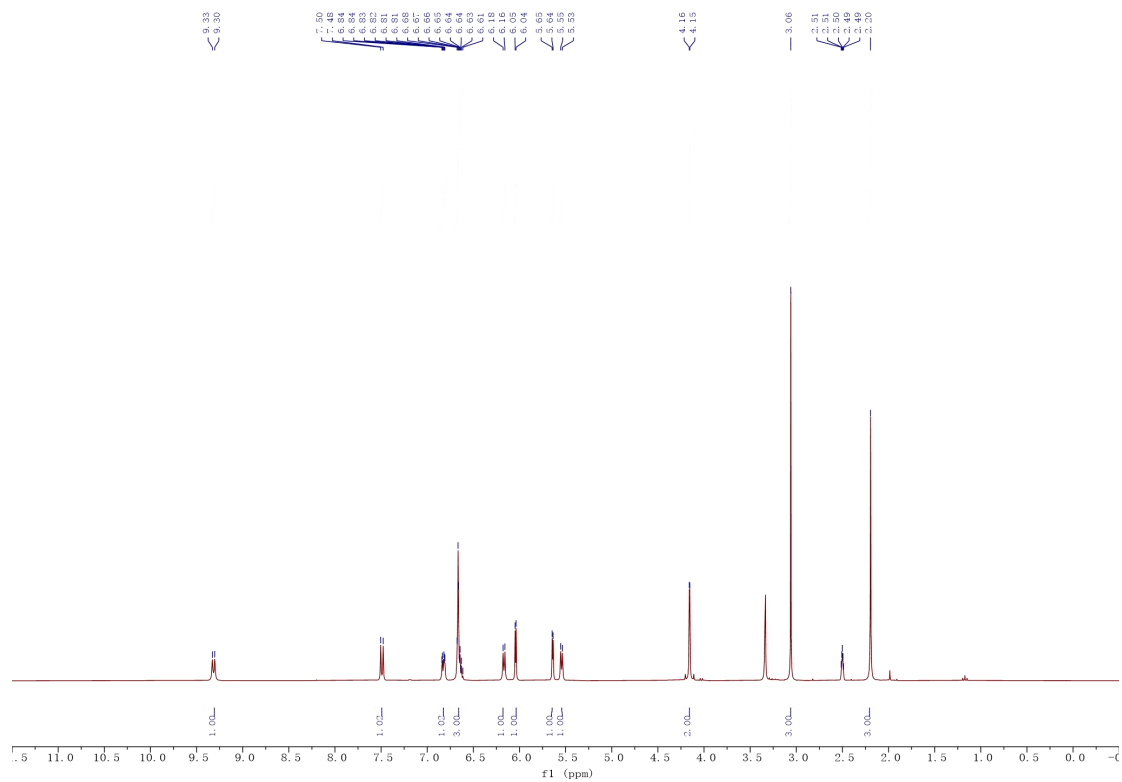
The reaction was carried out for 18 hours to give **4o** (283 mg, 68%) as a yellow solid. M.p. 179-180 °C. ¹H NMR (300 MHz, DMSO-*d*₆) δ 9.20 (d, *J* = 8.1 Hz, 1H, H₅), 6.81 (d, *J* = 8.1 Hz, 1H, H₄), 6.75 – 6.60 (m, 4H, 4H_{Ar}), 6.32 (d, *J* = 5.7 Hz, 1H, H₁), 5.97 (d, *J* = 3.1 Hz, 1H, H_{4'}), 5.75 (d, *J* = 5.7 Hz, 1H, H₂), 5.68 (d, *J* = 3.1 Hz, 1H, H_{3'}), 5.09 (t, *J* = 5.5 Hz, 1H, OH), 4.28 (d, *J* = 4.1 Hz, 2H, CH₂OH), 2.20 (s, 3H, CH₃), 2.16 (s, 3H, CH₃), 2.15 (s, 3H, CH₃), 2.06 (s, 3H, CH₃), 1.98 (s, 3H, CH₃). ¹³C NMR (75 MHz, DMSO) δ 194.6 (C=O), 155.6 (C_{2'}), 154.1 (C_{5'}), 145.6 (C₄), 138.5 (C_{Ar}), 138.3 (C_{Ph}), 133.8 (C_{Ph}), 132.0(3) (C_{Ph}), 131.9(6) (C_{Ph}), 130.7 (C_{Ar}), 129.0 (C_{Ph}), 128.8 (C_{Ph}), 123.3 (CH_{Ar}), 121.2 (CH_{Ar}), 120.2 (CH_{Ar}), 119.7 (CH_{Ar}), 115.0 (C₃), 107.0 (C_{4'}), 106.2 (C_{3'}), 55.9 (CH₂OH), 51.1 (C₂), 17.2 (CH₃), 17.1 (CH₃), 16.3 (CH₃), 15.8(4) (CH₃), 15.8(0) (CH₃). HRMS (ESI) *m/z*: Calcd for [M+H]⁺ C₂₆H₂₉N₂O₃ = 417.2173; Found 417.2169. HRMS (ESI) *m/z*: Calcd for [M+Na]⁺ C₂₆H₂₈N₂NaO₃ = 439.1992; Found 439.1988.



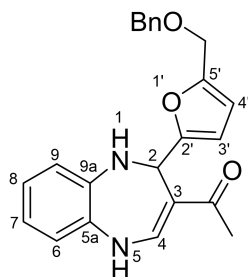
1-{2-[5-(Methoxymethyl)furan-2-yl]-2,5-dihydro-1H-1,5-benzodiazepin-3-yl}ethan-1-one
(C₁₇H₁₈N₂O₃)



The reaction was carried out for 5 hours to give **4p** (212 mg, 71%) as a yellow solid. M.p. 144-145 °C. ¹H NMR (300 MHz, DMSO-*d*₆) δ 9.32 (d, *J* = 7.9 Hz, 1H, H₅), 7.49 (d, *J* = 7.9 Hz, 1H, H₄), 6.88 – 6.76 (m, 1H, H₆ or 9), 6.72 – 6.60 (m, 3H, H_{Ar}), 6.17 (d, *J* = 5.8 Hz, 1H, H₁), 6.04 (d, *J* = 3.1 Hz, 1H, H_{4'}), 5.64 (d, *J* = 3.0 Hz, 1H, H_{3'}), 5.54 (d, *J* = 5.8 Hz, 1H, H₂), 4.16 (AB system, *J* = 12.9 Hz, 2H, CH₂), 3.06 (s, 3H, OCH₃), 2.20 (s, 3H, COCH₃). ¹³C NMR (75 MHz, DMSO-*d*₆) δ 191.6 (C=OCH₃), 156.8 (C_{2'}), 150.2 (C_{5'}), 143.0 (C₄), 138.5 (C_{9a}), 131.4 (C_{5a}), 122.7 (CH_{Ar}), 121.0 (CH_{Ar}), 120.2 (CH_{Ar}), 119.5 (CH_{Ar}), 113.4 (C₃), 109.8 (C_{4'}), 106.5 (C_{3'}), 65.3 (CH₂), 56.6 (OCH₃), 51.5 (C₂), 24.3 (COCH₃). HRMS (ESI) *m/z*: Calcd for [M+H]⁺ C₁₇H₁₉N₂O₃ =299.1390; Found 299.1389. HRMS (ESI) *m/z*: Calcd for [M+Na]⁺ C₁₇H₁₈N₂NaO₃ =321.1210; Found 321.1209.

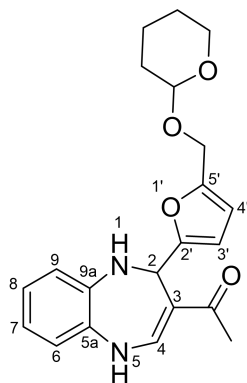


1-{2-[5-[(Benzyloxy)methyl]furan-2-yl]-2,5-dihydro-1H-1,5-benzodiazepin-3-yl}ethan-1-one
(C₂₃H₂₂N₂O₃)

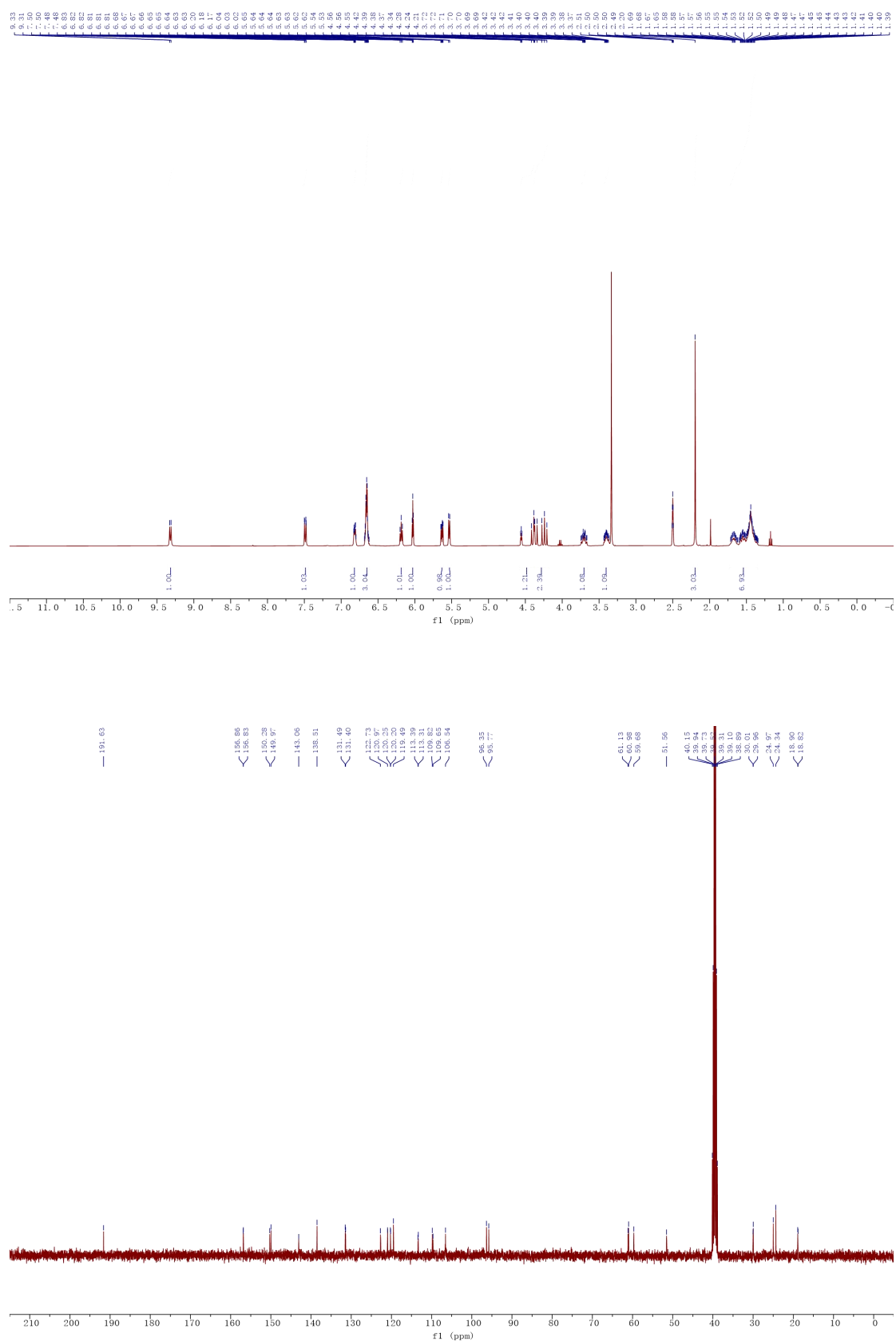


The reaction was carried out for 5 hours to give **4q** (225 mg, 60%) as a yellow solid. M.p. 166-167 °C. ¹H NMR (400 MHz, DMSO-*d*₆) δ 9.34 (d, *J* = 8.0 Hz, 1H, H₅), 7.50 (d, *J* = 8.0 Hz, 1H, H₄), 7.38 – 7.32 (m, 2H, H_{Ph}), 7.32 – 7.24 (m, 3H, H_{Ph}), 6.83 (dd, *J* = 7.6, 1.8 Hz, 1H, H₆ or 9), 6.70 – 6.56 (m, 3H, H_{Ar}), 6.21 (d, *J* = 5.8 Hz, 1H, H₁), 6.08 (d, *J* = 3.1 Hz, 1H, H_{4'}), 5.67 (dd, *J* = 3.1, 0.9 Hz, 1H, H_{3'}), 5.57 (d, *J* = 5.8 Hz, 1H, H₂), 4.35 – 4.23 (m, 4H, PhCH₂ and CH₂), 2.20 (s, 3H, COCH₃). ¹³C NMR (100 MHz, DMSO-*d*₆) δ 191.6 (COCH₃), 157.0 (C_{2'}), 150.3 (C_{5'}), 143.0 (C₄), 138.5 (C_{9a}), 138.2 (C_{Ph}), 131.5 (C_{5a}), 128.2 (2CH_{Ph}), 127.6 (2CH_{Ph}), 127.4 (CH_{Ph}), 122.7 (CH_{Ar}), 121.0 (CH_{Ar}), 120.2 (CH_{Ar}), 119.5 (CH_{Ar}), 113.4 (C₃), 109.9 (C_{4'}), 106.6 (C_{3'}), 70.5 (PhCH₂), 63.3 (CH₂), 51.6 (C₂), 24.4 (COCH₃). HRMS (ESI) *m/z*: Calcd for [M+H]⁺ C₂₃H₂₃N₂O₃ = 375.1703; Found 375.1699. HRMS (ESI) *m/z*: Calcd for [M+Na]⁺ C₂₃H₂₂N₂NaO₃ = 397.1523; Found 397.1519.

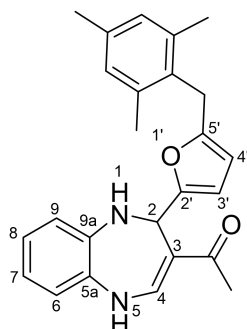
1-{2-[5-{[(Tetrahydro-2H-pyran-2-yl)oxy]methyl}furan-2-yl]-2,5-dihydro-1H-1,5-benzodiazepin-3-yl}ethan-1-one (C₂₁H₂₄N₂O₄)



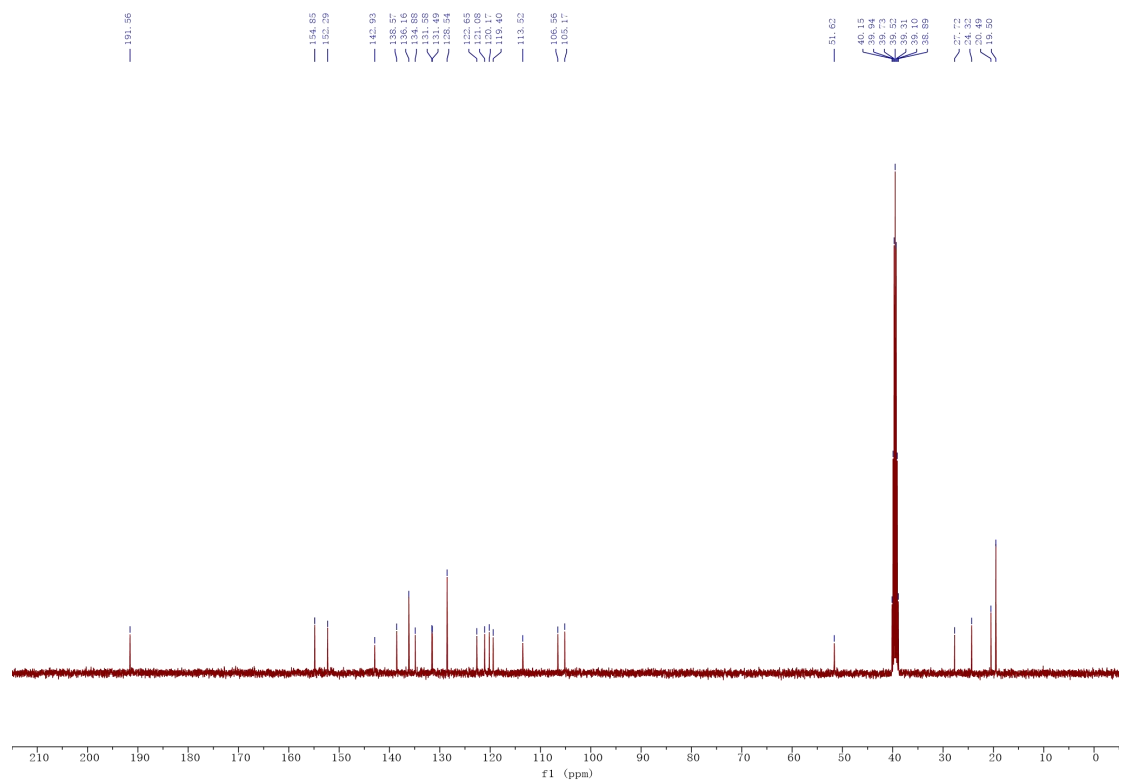
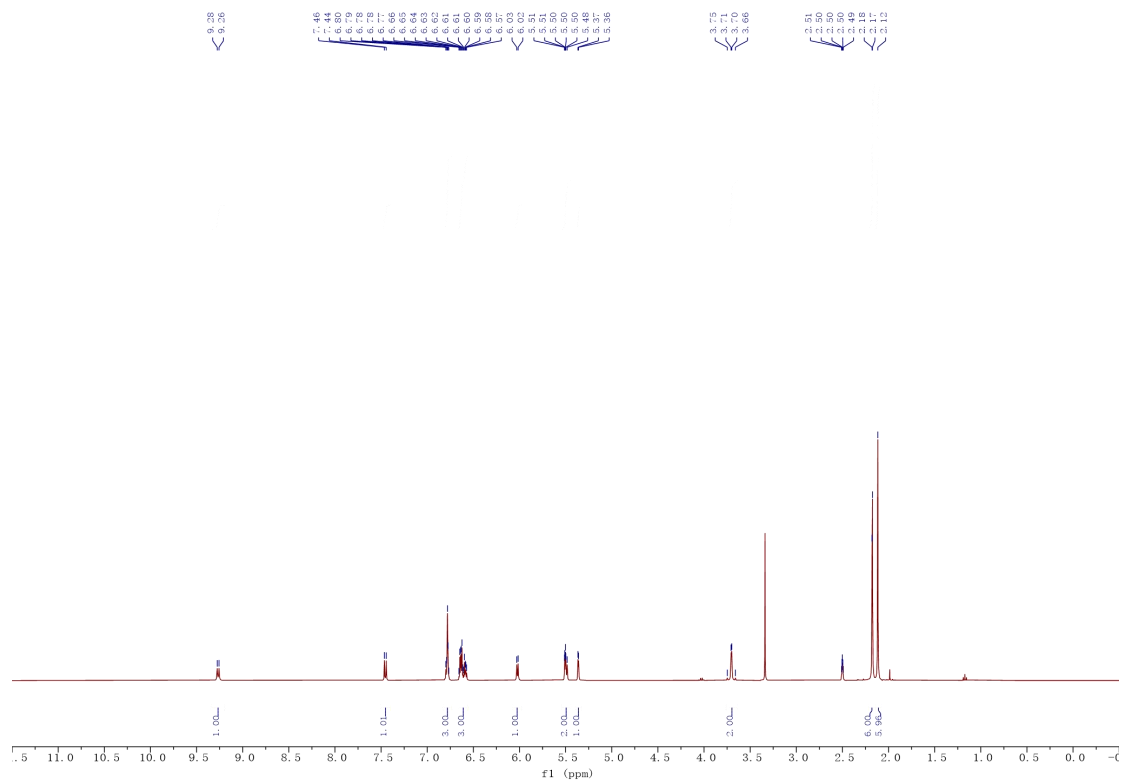
The reaction was carried out for 5 hours to give **4r** (240 mg, 65%) as a yellow solid. M.p. 172-173 °C. ¹H NMR (400 MHz, DMSO-*d*₆) δ 9.32 (d, *J* = 8.0 Hz, 1H, H₅), 7.49 (dd, *J* = 8.0, 1.5 Hz, 1H, H₄), 6.85 – 6.79 (m, 1H, H_{Ar}), 6.74 – 6.58 (m, 3H, H_{Ar}), 6.18 (m/2d-diastereoisomers 1:1, 1H, H₁), 6.03 (m/2d-diastereoisomers 1:1, 1H, H_{4'}), 5.69 – 5.56 (2dd-diastereoisomers 1:1, *J*₁ = 3.1 Hz, *J*₂ = 3.1 Hz, 1H, H_{3'}), 5.53 (d, *J* = 6.1 Hz, 1H, H₂), 4.58 – 4.39 (m, 1H, THP-CH), 4.44 – 4.19 (m, 2H, C_{5'}-CH₂), 3.77 – 3.34 (m, 2H, THP-CH₂), 2.20 (s, 3H, COCH₃), 1.73 – 1.35 (m, 6H, 3THP-CH₂). ¹³C NMR (100 MHz, DMSO-*d*₆) δ 191.6 (C=O), 156.9 and 156.8 (C_{2'}), 150.3 and 150.0 (C_{5'}), 143.1 (C₄), 138.5 (C_{9a}), 131.5 and 131.4 (C_{5a}), 122.7 (CH_{Ar}), 121.0 (CH_{Ar}), 120.3 and 120.2 (CH_{Ar}), 119.5 (CH_{Ar}), 113.4 and 113.3 (C₃), 109.8 and 109.7 (C_{4'}), 106.5 (C_{3'}), 96.4 and 95.8 (THP-CH), 61.1 and 61.0 (THP-CH₂), 59.7 (C_{5'}-CH₂), 51.6 (C₂), 30.0(1) and 29.9(7) (THP-CH₂), 25.0 (THP-CH₂), 24.3 (COCH₃), 18.9 and 18.8 (THP-CH₂). HRMS (ESI) *m/z*: Calcd for [M+H]⁺ C₂₁H₂₅N₂O₄ = 369.1809; Found 369.1805. HRMS (ESI) *m/z*: Calcd for [M+Na]⁺ C₂₁H₂₄N₂NaO₄ = 391.1628; Found 391.1624.



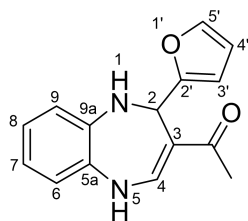
1-{2-[5-(2,4,6-Trimethylbenzyl)furan-2-yl]-2,5-dihydro-1H-1,5-benzodiazepin-3-yl}ethan-1-one (C₂₅H₂₆N₂O₂)



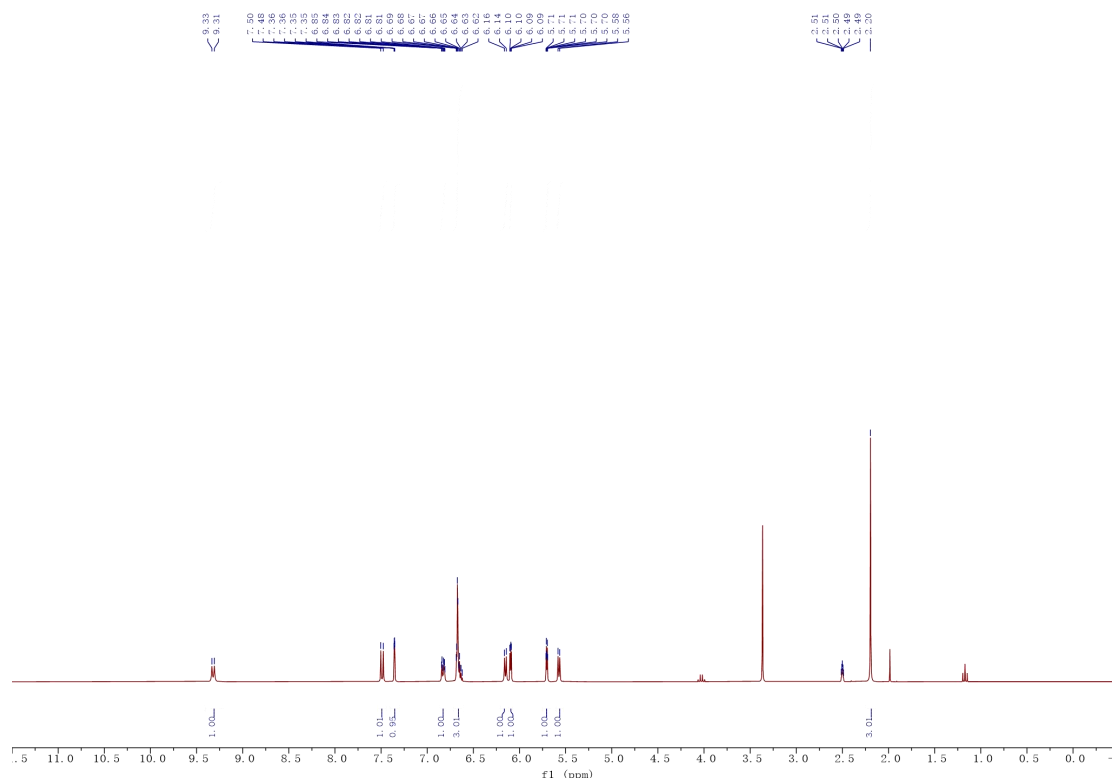
The reaction was carried out for 5 hours to give **4s** (275 mg, 71%) as a yellow solid. M.p. 184-185 °C. ¹H NMR (400 MHz, DMSO-*d*₆) δ 9.27 (d, *J* = 8.0 Hz, 1H, H₅), 7.45 (d, *J* = 8.0 Hz, 1H, H₄), 6.83 – 6.73 (m, 3H, 2H_{Ph} and H_{Ar}), 6.68 – 6.55 (m, 3H, H_{Ar}), 6.02 (d, *J* = 5.9 Hz, 1H, H₁), 5.54 – 5.44 (m, 2H, H_{3'}, H₂), 5.36 (d, *J* = 2.9 Hz, 1H, H_{4'}), 3.70 (AB system, *J* = 16.0 Hz, 2H, C_{5'}-CH₂), 2.18 (d, *J* = 1.5 Hz, 6H, COCH₃, Ph-CH₃), 2.12 (s, 6H, 2Ph-CH₃). ¹³C NMR (100 MHz, DMSO-*d*₆) δ 191.6 (C=O), 154.9 (C_{2'}), 152.3 (C_{5'}), 142.9 (C₄), 138.6 (C_{Ar}), 136.2 (2C_{Ph}), 134.9 (C_{Ph}), 131.6 (C_{Ar}), 131.5 (C_{Ph}), 128.5 (2CH_{Ph}), 122.6 (CH_{Ar}), 121.1 (CH_{Ar}), 120.2 (CH_{Ar}), 119.4 (CH_{Ar}), 113.5 (C₃), 106.6 (C_{3'}), 105.2 (C_{4'}), 51.6 (C₂), 27.7 (C_{5'}-CH₂), 24.3 (COCH₃), 20.5 (Ph-CH₃), 19.5 (2Ph-CH₃). HRMS (ESI) *m/z*: Calcd for [M+H]⁺ C₂₅H₂₇N₂O₂ = 387.2067; Found 387.2063. HRMS (ESI) *m/z*: Calcd for [M+Na]⁺ C₂₅H₂₆N₂NaO₂ = 409.1886; Found 409.1885.

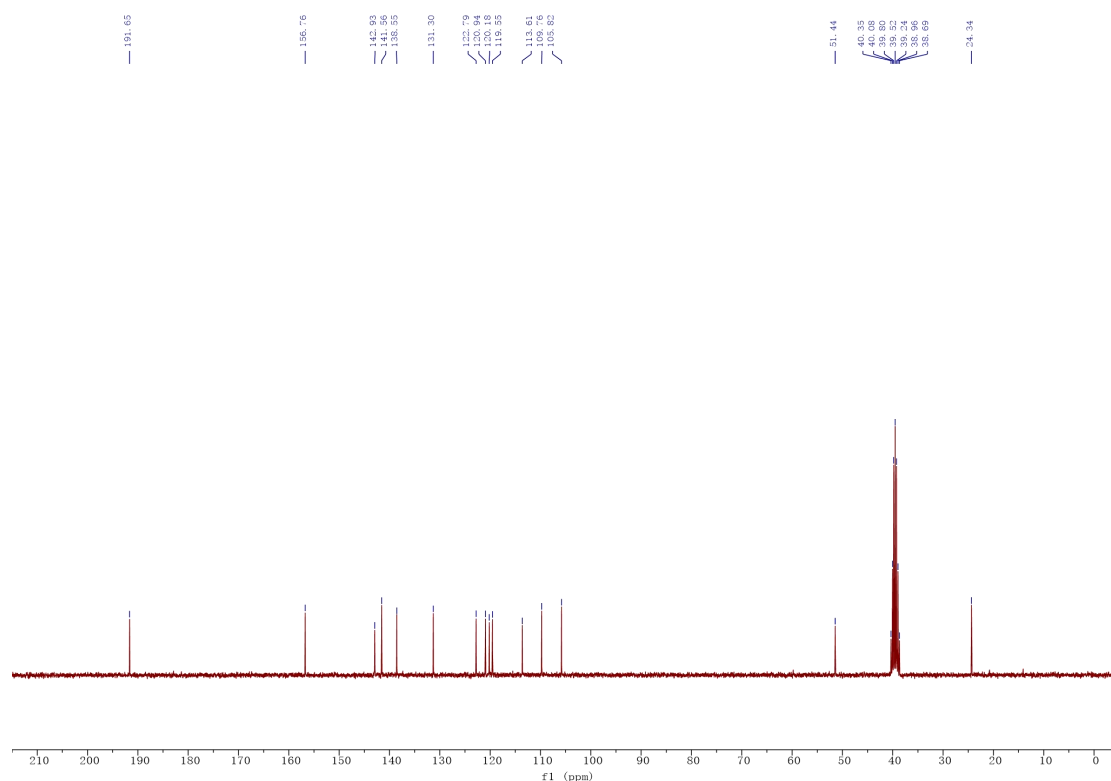


1-[2-(Furan-2-yl)-2,5-dihydro-1H-1,5-benzodiazepin-3-yl]ethan-1-one (C₁₅H₁₄N₂O₂)

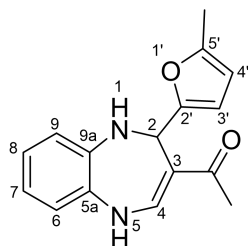


The reaction was carried out for 5 hours to give **4t** (164 mg, 64%) as a bronze solid. M.p. 177-178 °C. ¹H NMR (300 MHz, DMSO-*d*₆) δ 9.32 (d, *J* = 8.0 Hz, 1H, H₅), 7.49 (d, *J* = 8.0 Hz, 1H, H₄), 7.36 (dd, *J* = 1.8, 0.9 Hz, 1H, H_{5'}), 6.89 – 6.77 (m, 1H, H_{Ar}), 6.74 – 6.59 (m, 3H, H_{Ar}), 6.15 (d, *J* = 5.8 Hz, 1H, H₁), 6.10 (dd, *J* = 3.2, 1.8 Hz, 1H, H_{4'}), 5.70 (dt, *J* = 3.2, 0.9 Hz, 1H, H_{3'}), 5.57 (d, *J* = 5.8 Hz, 1H, H₂), 2.20 (s, 3H, COCH₃). ¹³C NMR (75 MHz, DMSO-*d*₆) δ 191.6 (C=OCH₃), 156.8 (C_{2'}), 142.9 (C₄), 141.6 (C_{5'}), 138.6 (C_{9a}), 131.3 (C_{5a}), 122.8 (CH_{Ar}), 120.9 (CH_{Ar}), 120.2 (CH_{Ar}), 119.6 (CH_{Ar}), 113.6 (C₃), 109.8 (C_{4'}), 105.8 (C_{3'}), 51.4 (C₂), 24.3 (COCH₃). HRMS (ESI) *m/z*: Calcd for [M+H]⁺ C₁₅H₁₅N₂O₂ = 255.1128; Found 255.1127. HRMS (ESI) *m/z*: Calcd for [M+Na]⁺ C₁₅H₁₄N₂NaO₂ = 277.0947; Found 277.0946.

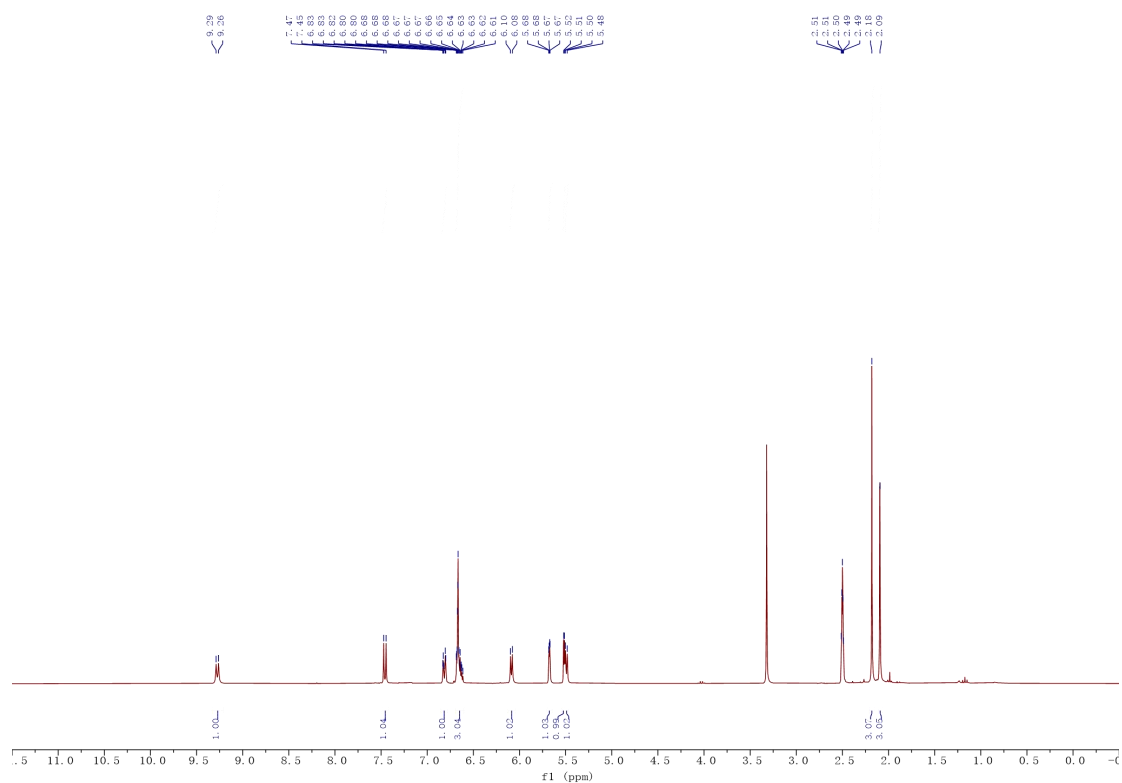




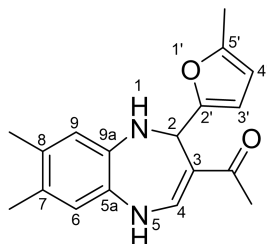
1-[2-(5-Methylfuran-2-yl)-2,5-dihydro-1H-1,5-benzodiazepin-3-yl]ethan-1-one (C₁₆H₁₆N₂O₂)



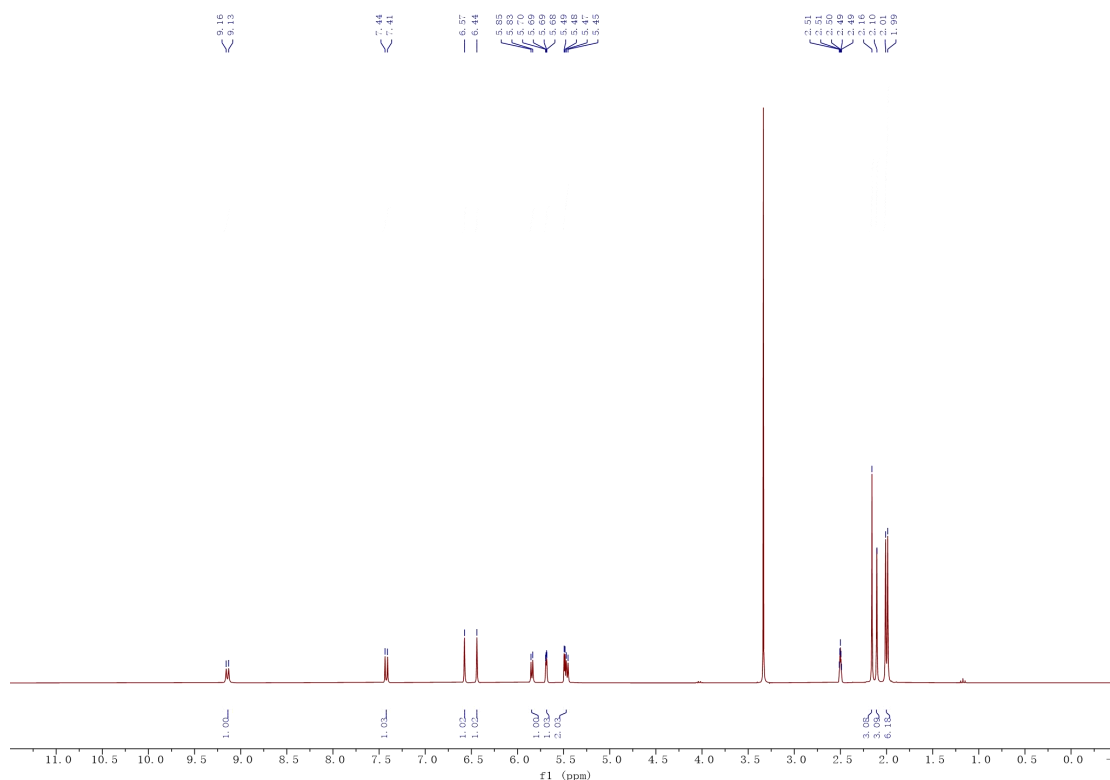
The reaction was carried out for 7 hours to give **4u** (187 mg, 70%) as a bronze solid. M.p. 155-156 °C. ¹H NMR (300 MHz, DMSO-*d*₆) δ 9.28 (d, *J* = 8.0 Hz, 1H, H₅), 7.46 (d, *J* = 8.0 Hz, 1H, H₄), 6.82 (m, 1H, H_{Ar}), 6.72 – 6.58 (m, 3H, H_{Ar}), 6.09 (d, *J* = 5.8 Hz, 1H, H₁), 5.68 (dd, *J* = 3.0, 1.2 Hz, 1H, H_{4'}), 5.52 (d, *J* = 3.0 Hz, 1H, H_{3'}), 5.49 (d, *J* = 5.8 Hz, 1H, H₂), 2.18 (s, 3H, COCH₃), 2.09 (s, 3H, CH₃). ¹³C NMR (75 MHz, DMSO-*d*₆) δ 191.6 (C=O), 154.8 (C_{2'}), 149.8 (C_{5'}), 142.8 (C₄), 138.6 (C_{9a}), 131.4 (C_{5a}), 122.7 (CH_{Ar}), 120.9 (CH_{Ar}), 120.1 (CH_{Ar}), 119.5 (CH_{Ar}), 113.7 (C₃), 106.4 (C_{3'}), 105.8 (C_{4'}), 51.4 (C₂), 24.3 (COCH₃), 13.4 (CH₃). HRMS (ESI) *m/z*: Calcd for [M+H]⁺ C₁₆H₁₇N₂O₂ = 269.1285; Found 269.1284. HRMS (ESI) *m/z*: Calcd for [M+Na]⁺ C₁₆H₁₆N₂NaO₂ = 291.1104; Found 291.1105.

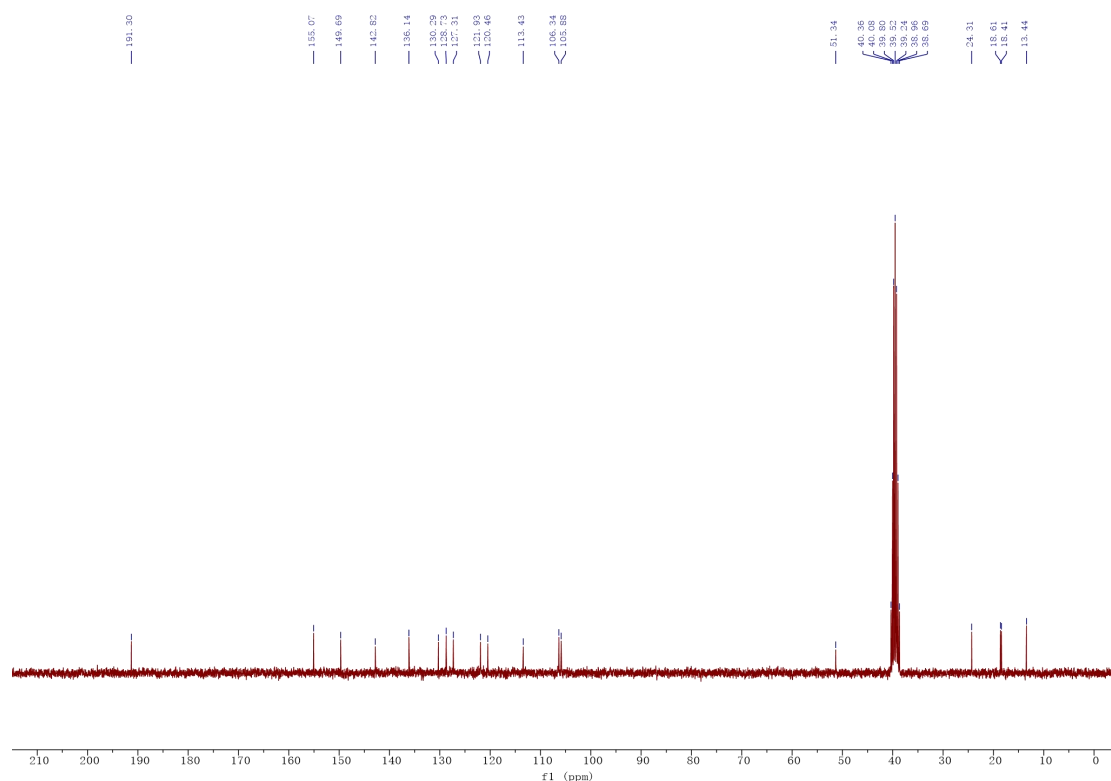


1-[7,8-Dimethyl-2-(5-methylfuran-2-yl)-2,5-dihydro-1H-1,5-benzodiazepin-3-yl]ethan-1-one
(C₁₈H₂₀N₂O₂)

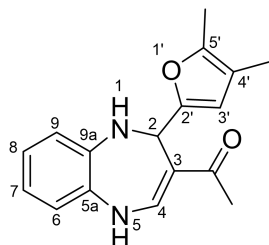


The reaction was carried out for 5 hours to give **4v** (190 mg, 64%) as a yellow solid. M.p. 179-180 °C. ¹H NMR (300 MHz, DMSO-*d*₆) δ 9.14 (d, *J* = 8.0 Hz, 1H, H₅), 7.42 (d, *J* = 8.0 Hz, 1H, H₄), 6.57 (s, 1H, H₆ or 9), 6.44 (s, 1H, H₆ or 9), 5.84 (d, *J* = 5.8 Hz, 1H, H₁), 5.69 (dd, *J* = 3.0, 1.2 Hz, 1H, H₄'), 5.49 (d, *J* = 3.0 Hz, 1H, H₃'), 5.46 (d, *J* = 5.8 Hz, 1H, H₂), 2.16 (s, 3H, COCH₃), 2.10 (s, 3H, C₅'-CH₃), 2.01 (s, 3H, C_{7/8}-CH₃), 1.99 (s, 3H, C_{7/8}-CH₃). ¹³C NMR (75 MHz, DMSO-*d*₆) δ 191.3 (C=O), 155.1 (C₂'), 149.7 (C₅'), 142.8 (C₄), 136.1 (C_{9a}), 130.3 (C₇ or 8), 128.7 (C_{5a}), 127.3 (C₇ or 8), 121.9 (C₉ or 6), 120.5 (C₉ or 6), 113.4 (C₃), 106.3 (C₃'), 105.9 (C₄'), 51.3 (C₂), 24.3 (COCH₃), 18.6 (C_{7/8}-CH₃), 18.4 (C_{7/8}-CH₃), 13.4 (C₅'-CH₃). HRMS (ESI) *m/z*: Calcd for [M+H]⁺ C₁₈H₂₁N₂O₂=297.1598; Found 297.1594. HRMS (ESI) *m/z*: Calcd for [M+Na]⁺ C₁₈H₂₀N₂NaO₂=319.1417; Found 319.1414.

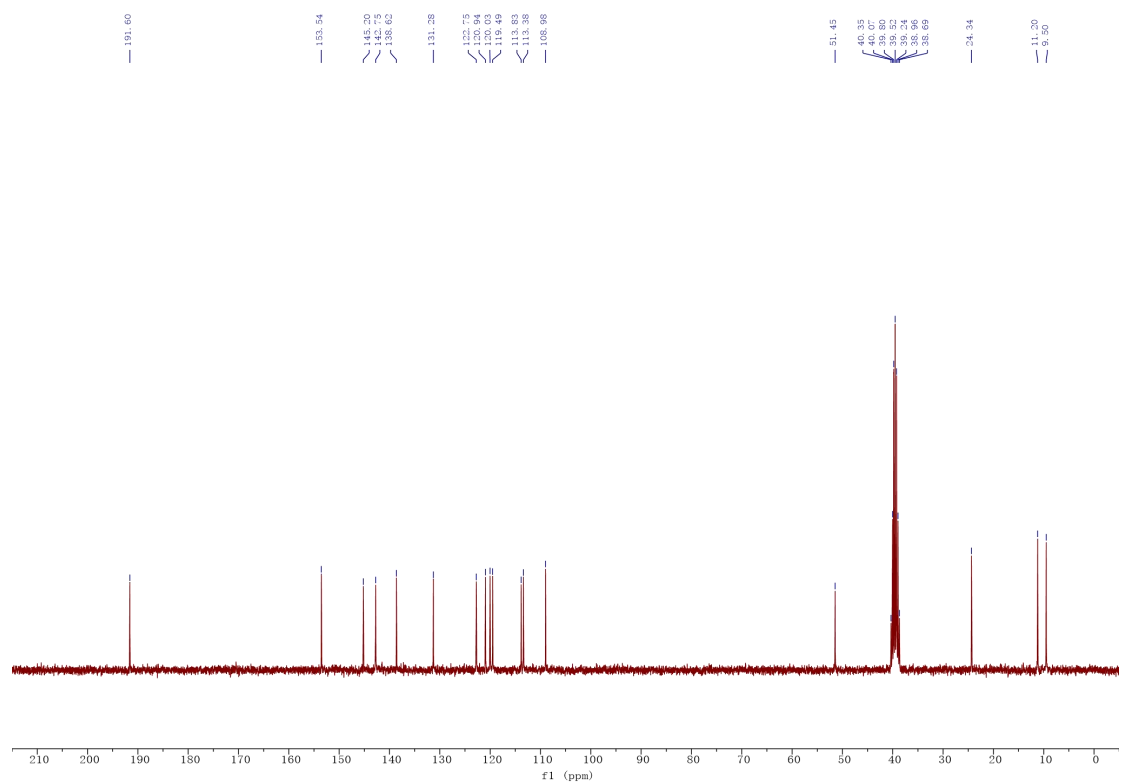
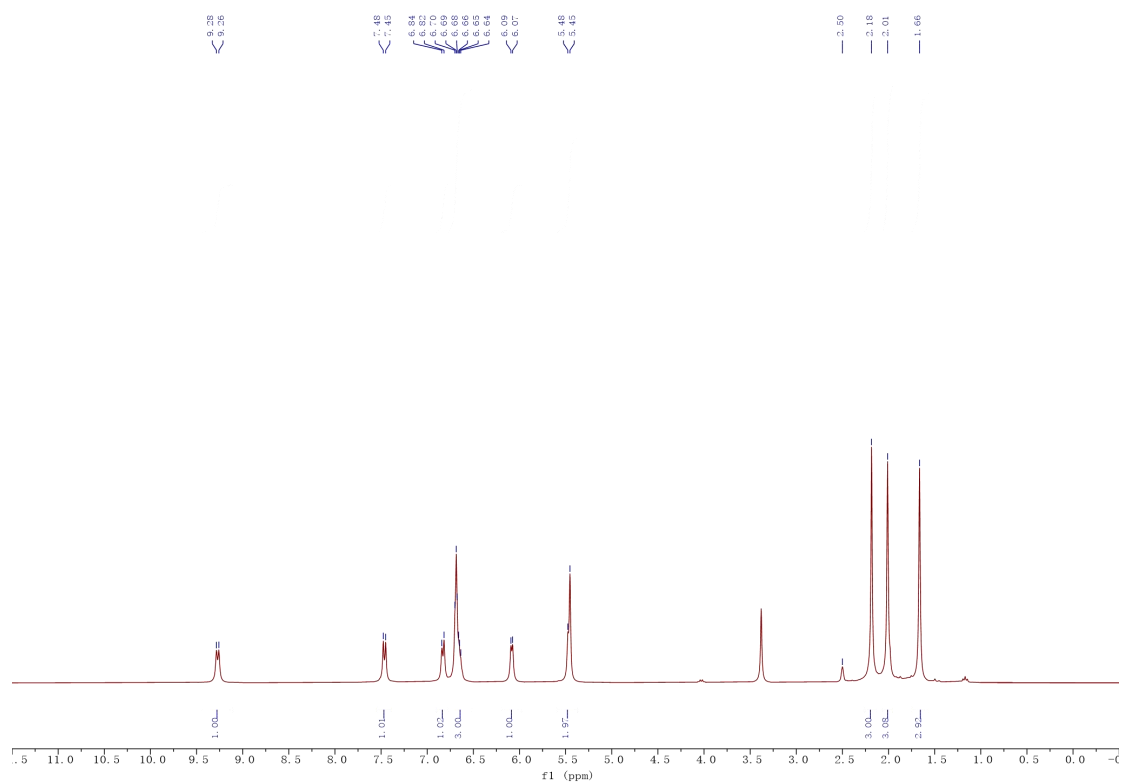




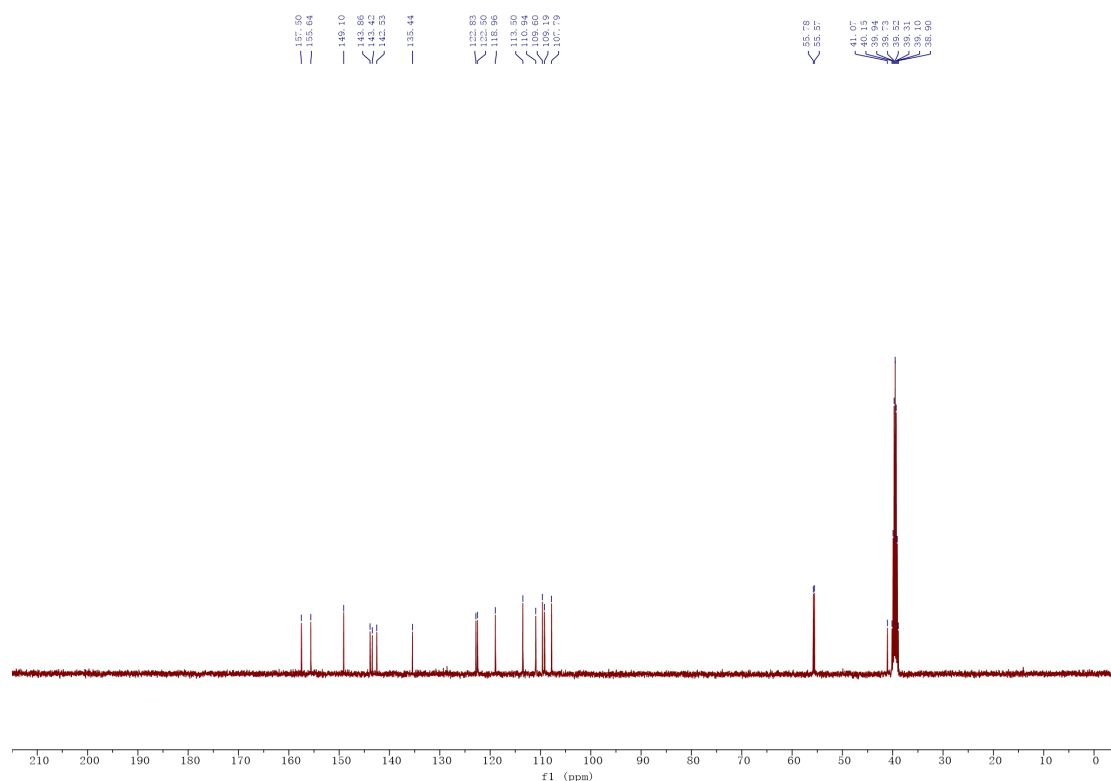
1-[2-(4,5-Dimethylfuran-2-yl)-2,5-dihydro-1H-1,5-benzodiazepin-3-yl]ethan-1-one
(C₁₇H₁₈N₂O₂)



The reaction was carried out for 5 hours to give **4w** (178 mg, 63%) as a yellow solid. M.p. 156-157 °C. ¹H NMR (300 MHz, DMSO-*d*₆) δ 9.27 (d, *J* = 7.9 Hz, 1H, H₅), 7.46 (d, *J* = 7.9 Hz, 1H, H₄), 6.83 (d, *J* = 7.2 Hz, 1H, H_{Ar}), 6.77 – 6.51 (m, 3H, H_{Ar}), 6.08 (d, *J* = 5.8 Hz, 1H, H₁), 5.59 – 5.37 (m, 2H, H_{3'}, H₂), 2.18 (s, 3H, COCH₃), 2.01 (s, 3H, C_{5'}-CH₃), 1.66 (s, 3H, C_{4'}-CH₃). ¹³C NMR (75 MHz, DMSO-*d*₆) δ 191.6 (C=O), 153.5 (C_{2'}), 145.2 (C_{5'}), 142.7 (C₄), 138.6 (C_{9a}), 131.3 (C_{5a}), 122.8 (CH_{Ar}), 120.9 (CH_{Ar}), 120.0 (CH_{Ar}), 119.5 (CH_{Ar}), 113.8 and 113.4 (C₃, C_{4'}), 109.0 (C_{3'}), 51.5 (C₂), 24.3 (COCH₃), 11.2 (C_{5'}-CH₃), 9.5 (C_{4'}-CH₃). HRMS (ESI) *m/z*: Calcd for [M+H]⁺ C₁₇H₁₉N₂O₂ = 283.1441; Found 283.1443. HRMS (ESI) *m/z*: Calcd for [M+Na]⁺ C₁₇H₁₈N₂NaO₂ = 305.1260; Found 305.1264.



¹H NMR spectrum of compound 10 in CDCl₃. The spectrum shows peaks from 0 to 10 ppm. Key features include a broad peak at ~7.2 ppm (2.11H), a multiplet at ~7.1 ppm (2.07H), a doublet at ~6.5 ppm (1.01H), a doublet at ~6.3 ppm (1.01H), a sharp singlet at ~5.7 ppm (2.04H), a multiplet at ~5.5 ppm (1.00H), a multiplet at ~5.1 ppm (1.00H), a doublet at ~4.5 ppm (2.05H), a doublet at ~4.3 ppm (2.10H), a small peak at ~3.5 ppm, a broad peak at ~2.5 ppm (2.05H), a small peak at ~2.1 ppm, and a small peak at ~1.2 ppm. Integration values are shown below the peaks.



3. Experimental section of the Hantzsch dihydropyridine reaction

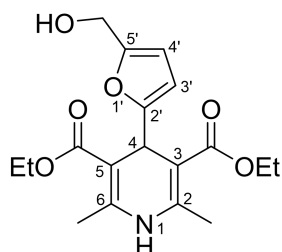
3.1 General procedure for the Hantzsch dihydropyridine reaction

General procedure A (compounds **11a to **11m**):** A mixture of aldehydes (**8**, 1.0 mmol, 1.0 equiv.), β -ketoesters (**9**, 2.0 mmol, 2.0 equiv.) and ammonium acetate (1.5 mmol, 1.5 equiv.) was stirred at 70-90 °C for indicated time. Procedure towards **11n**: A mixture of DFF (1.0 mmol, 1.0 equiv.), ethyl acetoacetate (4.0 mmol, 4.0 equiv.) and ammonium acetate (3.0 mmol, 3.0 equiv.) were stirred at 90 °C for 1 h. NMR yield: after cooling to room temperature, add 1/3 equivalent of 1,3,5-trimethoxybenzene (56 mg) as internal standard into the complete reaction mixture and dissolved with DMSO- d_6 , the NMR yield was calculated by comparing the ratio of the product with the internal standard. Isolated yield: after cooling down to room temperature, the reaction was diluted with EA or EA-MeOH (10-20 mL). The solution was concentrated and purified by flash column chromatography on silica gel to obtain the desired product. Products were purified by chromatography for full structural characterization purposes.

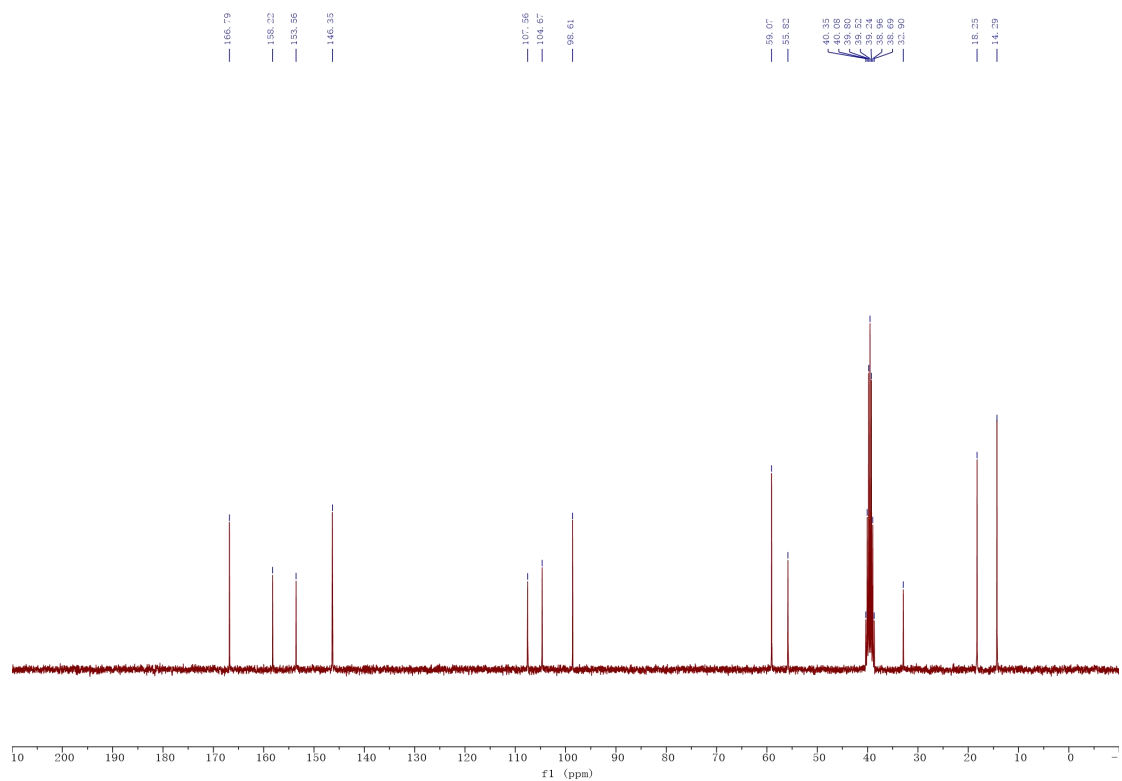
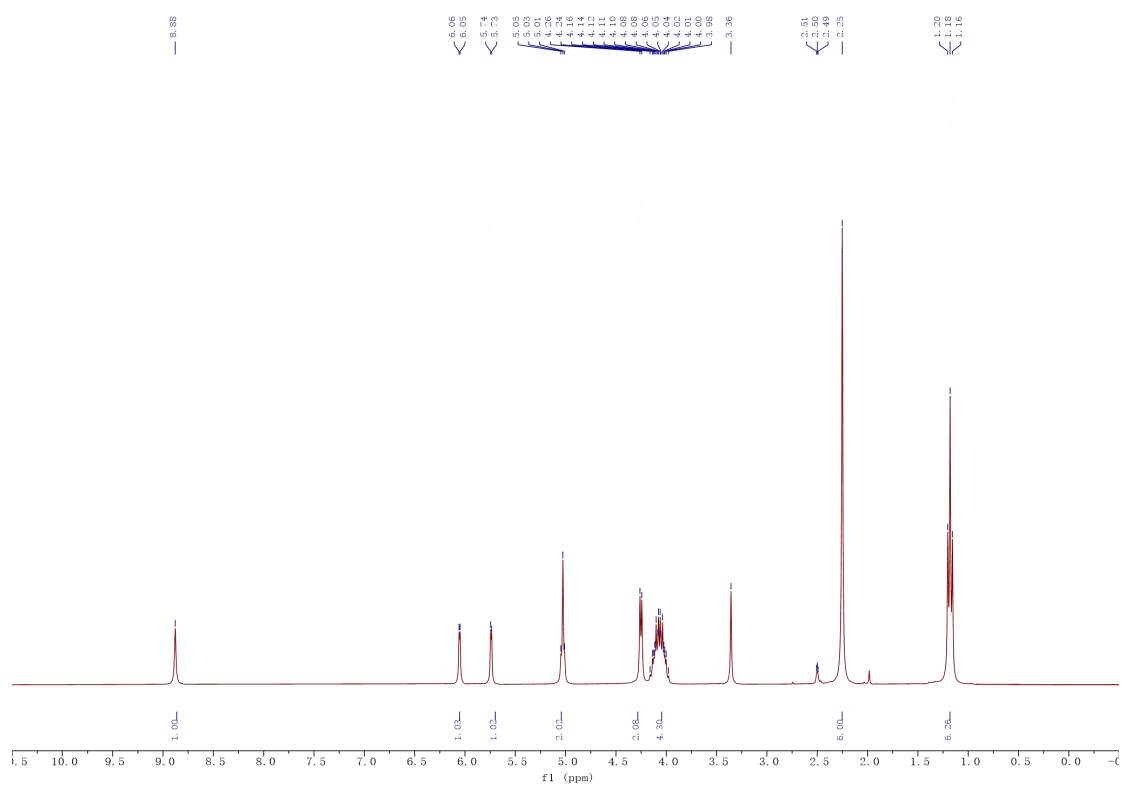
General procedure B (compounds 12a to 12h): A mixture of aldehydes (**8**, 1.0 mmol, 1.0 equiv.), β -ketoesters (**9**, 1.0 mmol, 1.0 equiv.), 5,5-dimethyl-1,3-cyclohexanedione (1.0 mmol, 1.0 equiv.) and ammonium acetate (1.5 mmol, 1.5 equiv.) was stirred in ethanol (0.5 mL) at 80 °C for indicated time. After cooling to room temperature, remove the solvent by a rotary evaporator, by adding 1/3 equivalent of 1,3,5-trimethoxybenzene (56 mg) as the internal standard to the complete reaction mixture, dissolving the crude mixture and internal standard with DMSO- d_6 , and performing proton nuclear magnetic resonance (^1H NMR) to obtain the NMR yield. Isolated yield: after cooling down to room temperature, the reaction was diluted or dissolved with EA/EA-MeOH (10-20 mL). The solution was concentrated and purified by flash column chromatography on silica gel (*n*-pentane/EA) to obtain the desired product. Products were purified by chromatography for full structural characterization purposes.

3.2 Characterization of 1,4-dihydropyridine products

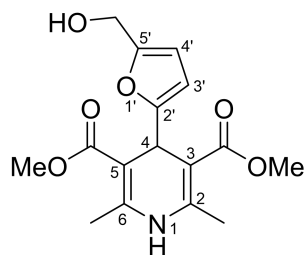
Diethyl 4-[5-(hydroxymethyl)furan-2-yl]-2,6-dimethyl-1,4-dihydropyridine-3,5-dicarboxylate
($\text{C}_{18}\text{H}_{23}\text{NO}_6$)



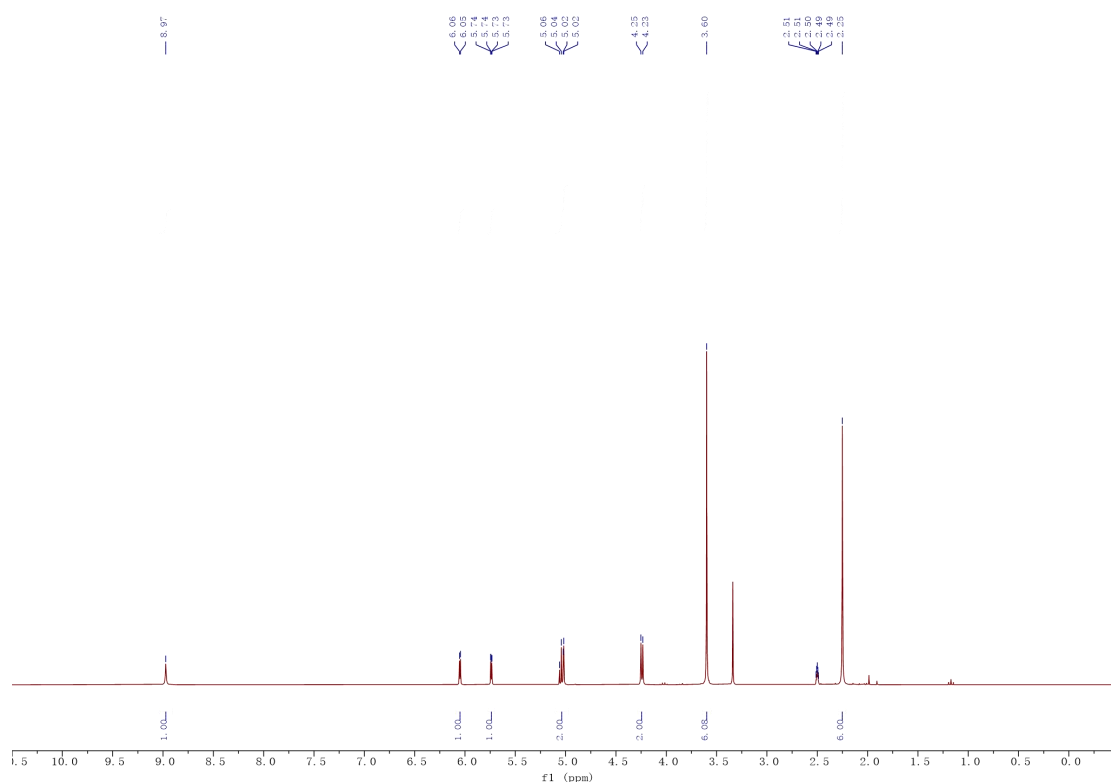
The reaction was carried out for at 70 °C 1 hour to give **11a** (325 mg, 93%) as a yellow solid. M.p. 136-138 °C. ^1H NMR (300 MHz, DMSO- d_6) δ 8.88 (s, 1H, NH), 6.05 (d, J = 3.1 Hz, 1H, $\text{H}_{4'}$), 5.74 (d, J = 3.1 Hz, 1H, $\text{H}_{3'}$), 5.17-4.91 (m, 2H, H_4 , OH), 4.25 (d, J = 5.6 Hz, 2H, CH_2OH), 4.21-3.88 (m, 4H, 2 CH_2CH_3), 2.25 (s, 6H, 2 CH_3), 1.18 (t, J = 7.1 Hz, 6H, 2 CH_2CH_3). ^{13}C NMR (75 MHz, DMSO) δ 166.8 (2 C=O), 158.2 ($\text{C}_{2'}$), 153.6 ($\text{C}_{5'}$), 146.3 (2 C_2), 107.6 ($\text{C}_{4'}$), 104.7 ($\text{C}_{3'}$), 98.6 (2 C_3), 59.1 (2 CH_2CH_3), 55.8 (CH_2OH), 32.9 (C_4), 18.2 (2 CH_3), 14.3 (2 CH_2CH_3). HRMS (ESI) m/z : Calcd for $[\text{M}+\text{H}]^+$ $\text{C}_{18}\text{H}_{24}\text{NO}_6$ = 350.1598; Found 350.1594. HRMS (ESI) m/z : Calcd for $[\text{M}+\text{Na}]^+$ $\text{C}_{18}\text{H}_{23}\text{NNaO}_6$ = 372.1418; Found 372.1420; Calcd for $[2\text{M}+\text{Na}]^+$ $\text{C}_{36}\text{H}_{46}\text{N}_2\text{NaO}_{12}$ = 721.2943; Found 721.2946.

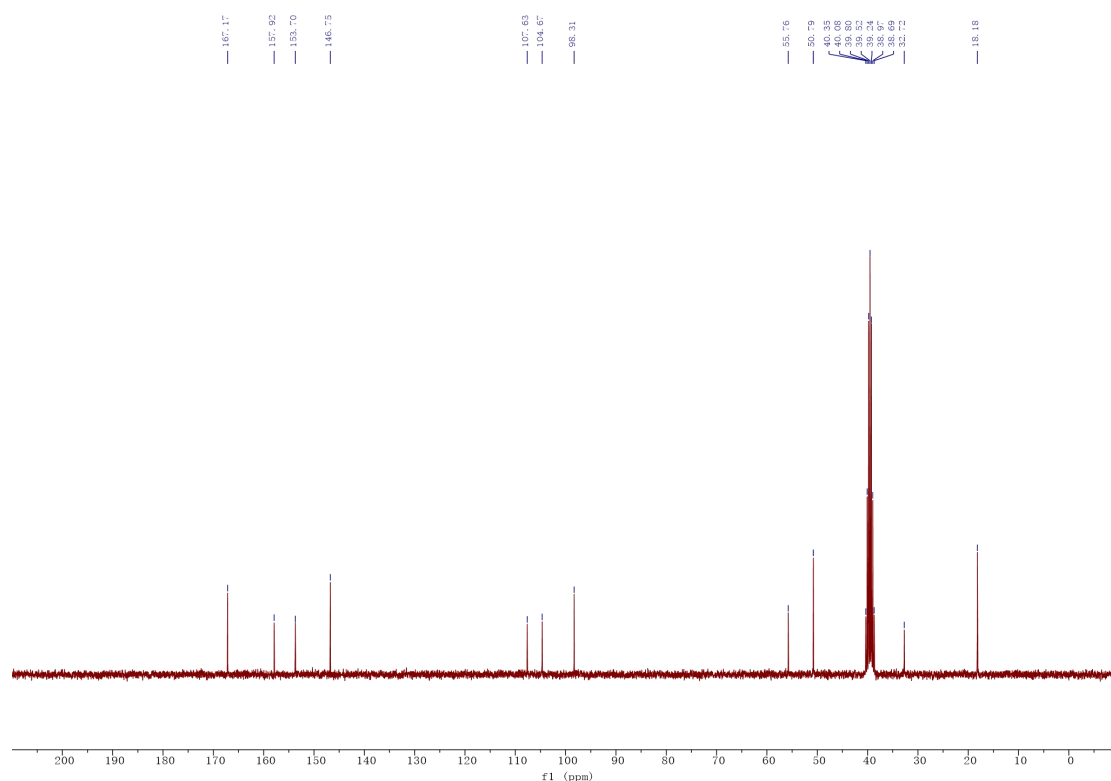


Dimethyl 4-[5-(hydroxymethyl)furan-2-yl]-2,6-dimethyl-1,4-dihydropyridine-3,5-dicarboxylate
(C₁₆H₁₉NO₆)

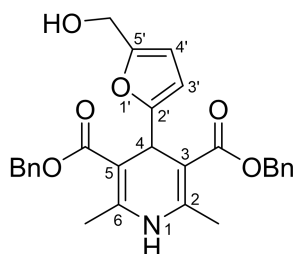


The reaction was carried out at 70 °C for 1 hour to give **11b** (296 mg, 92%) as a yellow solid. M.p. 137-139 °C. ¹H NMR (300 MHz, DMSO-*d*₆) δ 8.97 (s, 1H, NH), 6.05 (d, *J* = 3.0 Hz, 1H, H_{4'}), 5.74 (dd, *J* = 3.0, 0.8 Hz, 1H, H_{3'}), 5.10-4.97 (m, 2H, H₄, OH), 4.24 (d, *J* = 5.6 Hz, 2H, CH₂OH), 3.60 (s, 6H, 2 OCH₃), 2.25 (s, 6H, 2 CH₃). ¹³C NMR (75 MHz, DMSO) δ 167.2 (2 C=O), 157.9 (C_{2'}), 153.7 (C_{5'}), 146.8 (2 C₂), 107.6 (C_{4'}), 104.7 (C_{3'}), 98.3 (2 C₃), 55.8 (CH₂OH), 50.8 (2 OCH₃), 32.7 (C₄), 18.2 (2 CH₃). HRMS (ESI) *m/z*: Calcd for [M+Na]⁺ C₁₆H₁₉NNaO₆ = 344.1105; Found 344.1107.

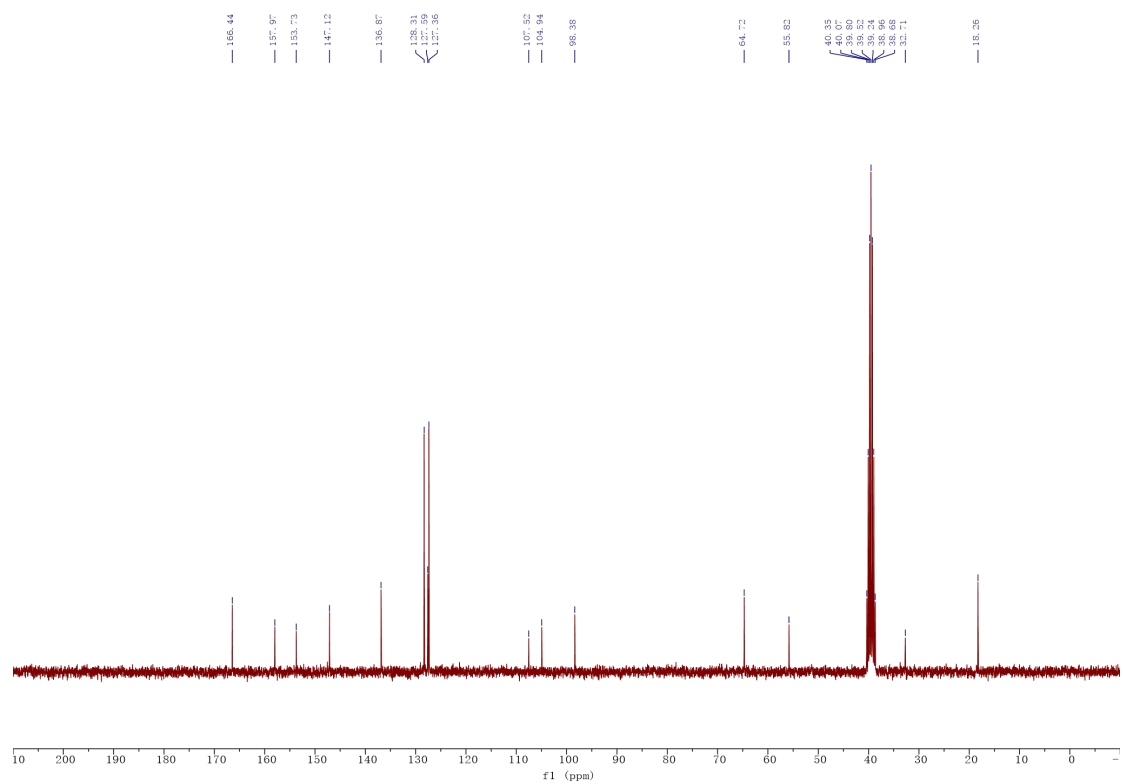
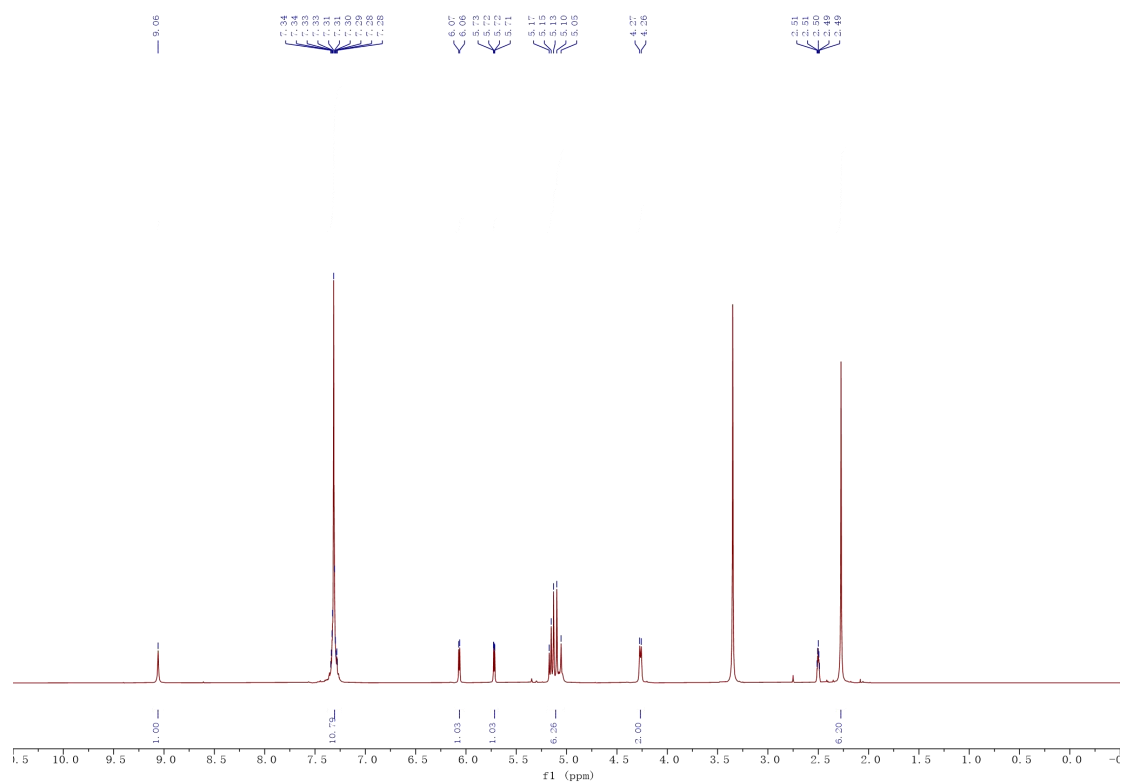




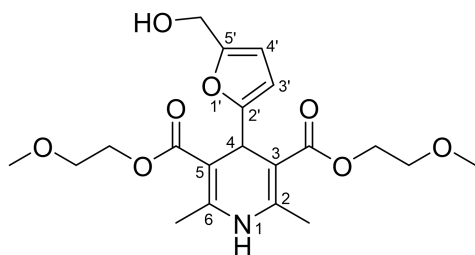
Dibenzy 4-[5-(hydroxymethyl)furan-2-yl]-2,6-dimethyl-1,4-dihydropyridine-3,5-dicarboxylate
(C₂₈H₂₇NO₆)¹³⁵



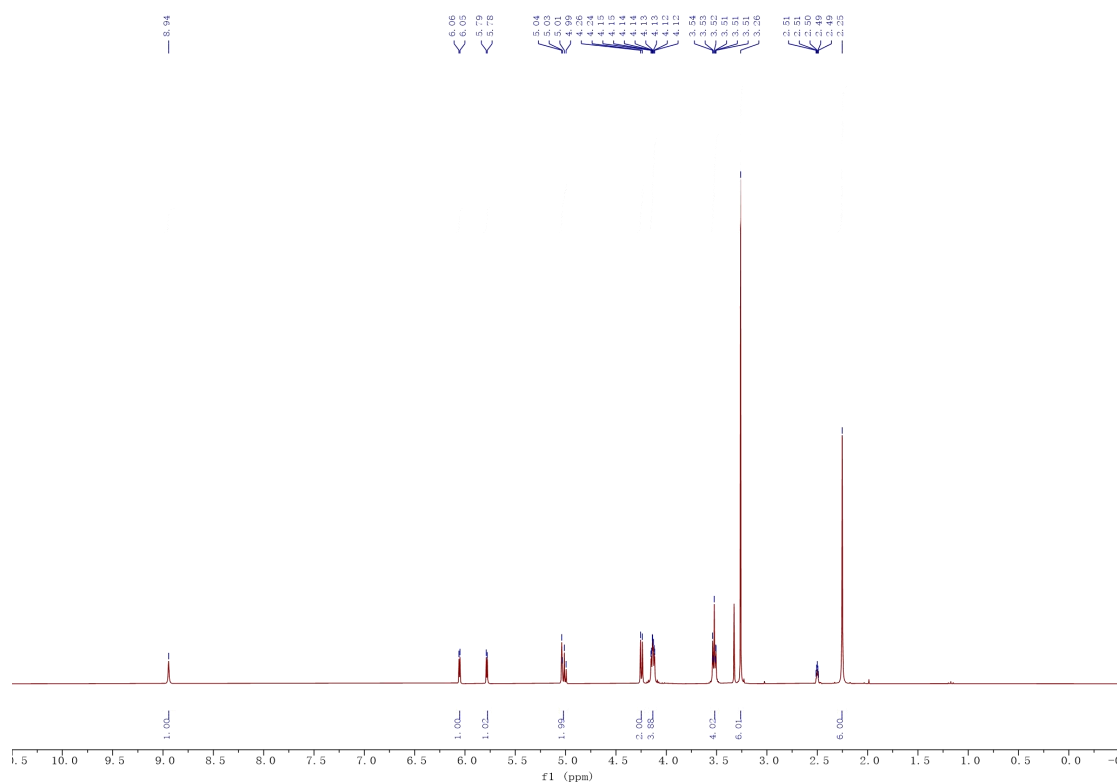
The reaction was carried out at 70 °C for 80 min to give **11c** (436 mg, 92%) as a gummy yellow product. ¹H NMR (300 MHz, DMSO-*d*₆) δ 9.06 (s, 1H, NH), 7.38-7.24 (m, 10H, 10 H_{Ar}), 6.07 (d, *J* = 3.1 Hz, 1H, H_{4'}), 5.72 (dd, *J* = 3.1, 0.7 Hz, 1H, H_{3'}), 5.20-5.02 (m, 6H, 2 Ph-CH₂, OH, H₄), 4.27 (d, *J* = 4.7 Hz, 2H, CH₂OH), 2.27 (s, 6H, 2 CH₃). ¹³C NMR (75 MHz, DMSO) δ 166.4 (2 CO₂), 158.0 (C_{2'}), 153.7 (C_{5'}), 147.1 (2 C₂), 136.9 (2 C_{qAr}), 128.3 (4 CH_{Ar}), 127.6 (2 CH_{Ar}), 127.4 (4 CH_{Ar}), 107.5 (C_{4'}), 104.9 (C_{3'}), 98.4 (2 C₃), 64.7 (2 Ph-CH₂), 55.8 (CH₂OH), 32.7 (C₄), 18.3 (2 CH₃). HRMS (ESI) *m/z*: Calcd for [M+Na]⁺ C₂₈H₂₇NNaO₆ = 496.1731; Found 496.1725; Calcd for [2M+Na]⁺ C₅₆H₅₄N₂NaO₁₂ = 969.3569; Found 969.3560.

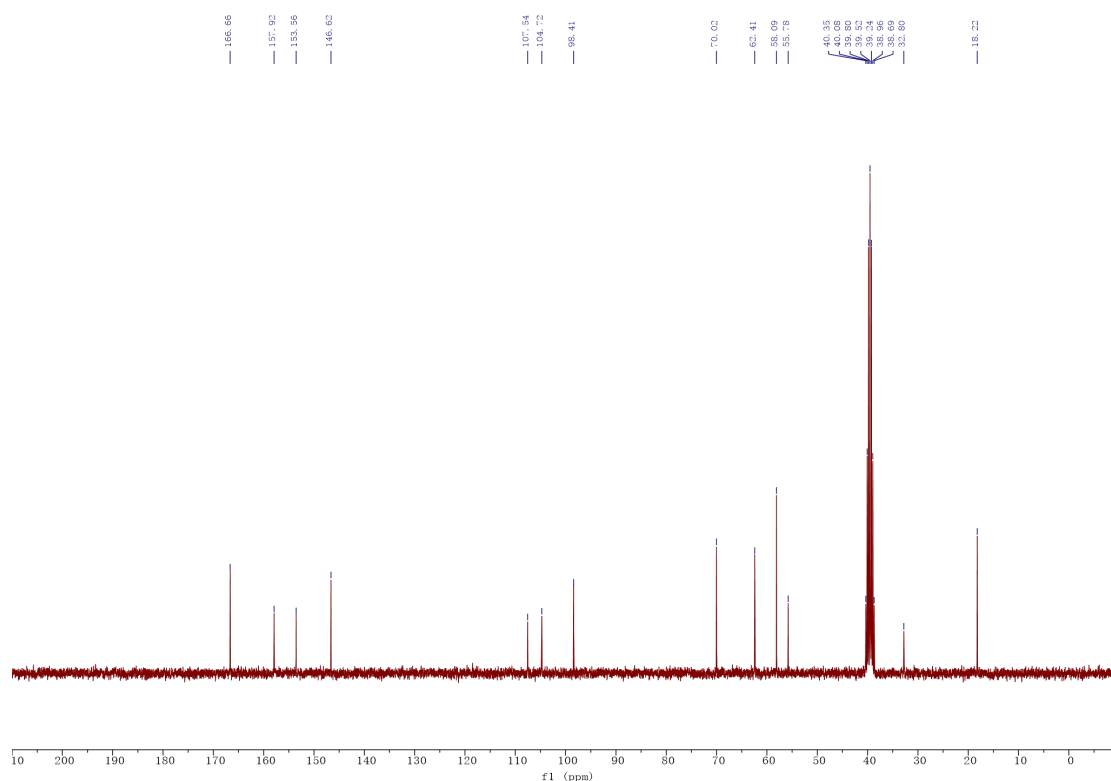


Bis(2-methoxyethyl) 4-[5-(hydroxymethyl)furan-2-yl]-2,6-dimethyl-1,4-dihydropyridine-3,5-dicarboxylate (C₂₀H₂₇NO₈)

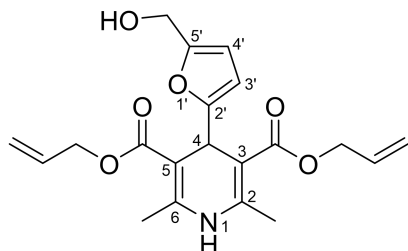


The reaction was carried out at 70 °C for 1 hour to give **11d** (381 mg, 93%) as a yellow solid. M.p. 99-100 °C. ¹H NMR (300 MHz, DMSO-*d*₆) δ 8.94 (s, 1H, NH), 6.05 (d, *J* = 3.1 Hz, 1H, H_{4'}), 5.78 (d, *J* = 3.0 Hz, 1H, H_{3'}), 5.06-4.98 (m, 2H, H₄, OH), 4.25 (d, *J* = 5.6 Hz, 2H, CH₂OH), 4.17-4.09 (m, 4H, 2 CH₂OCO), 3.56-3.48 (m, 4H, 2 CH₂OMe), 3.26 (s, 6H, 2 OCH₃), 2.25 (s, 6H, 2 CH₃). ¹³C NMR (75 MHz, DMSO) δ 166.7 (2 CO₂), 157.9 (C_{2'}), 153.6 (C_{5'}), 146.6 (2 C₂), 107.5 (C_{4'}), 104.7 (C_{3'}), 98.4 (2 C₃), 70.0 (2 CH₂OMe), 62.4 (2 CH₂OCO), 58.1 (2 OCH₃), 55.8 (CH₂OH), 32.8 (C₄), 18.2 (2 CH₃). HRMS (ESI) *m/z*: Calcd for [M+H]⁺ C₂₀H₂₈NO₈ = 410.1809; Found 410.1797; HRMS (ESI) *m/z*: Calcd for [M+Na]⁺ C₂₀H₂₇NNaO₈ = 432.1629; Found 432.1629.



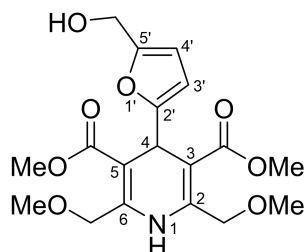


Diallyl 4-[5-(hydroxymethyl)furan-2-yl]-2,6-dimethyl-1,4-dihydropyridine-3,5-dicarboxylate
(C₂₀H₂₃NO₆)

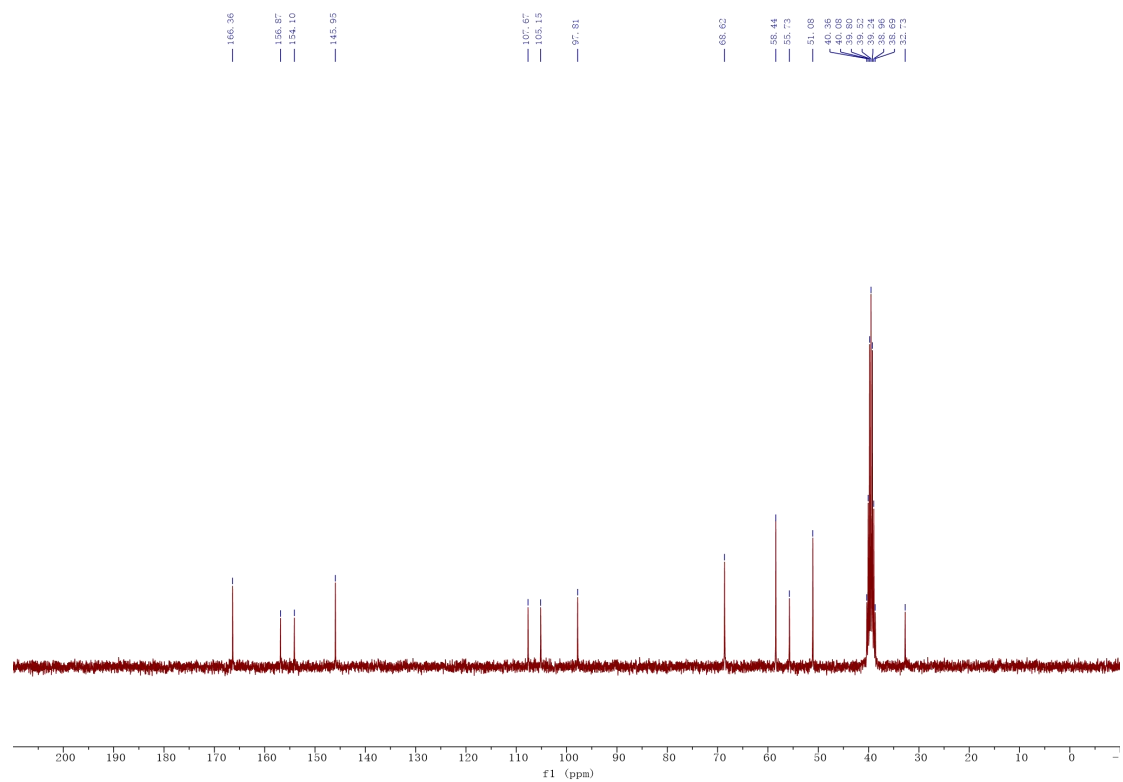
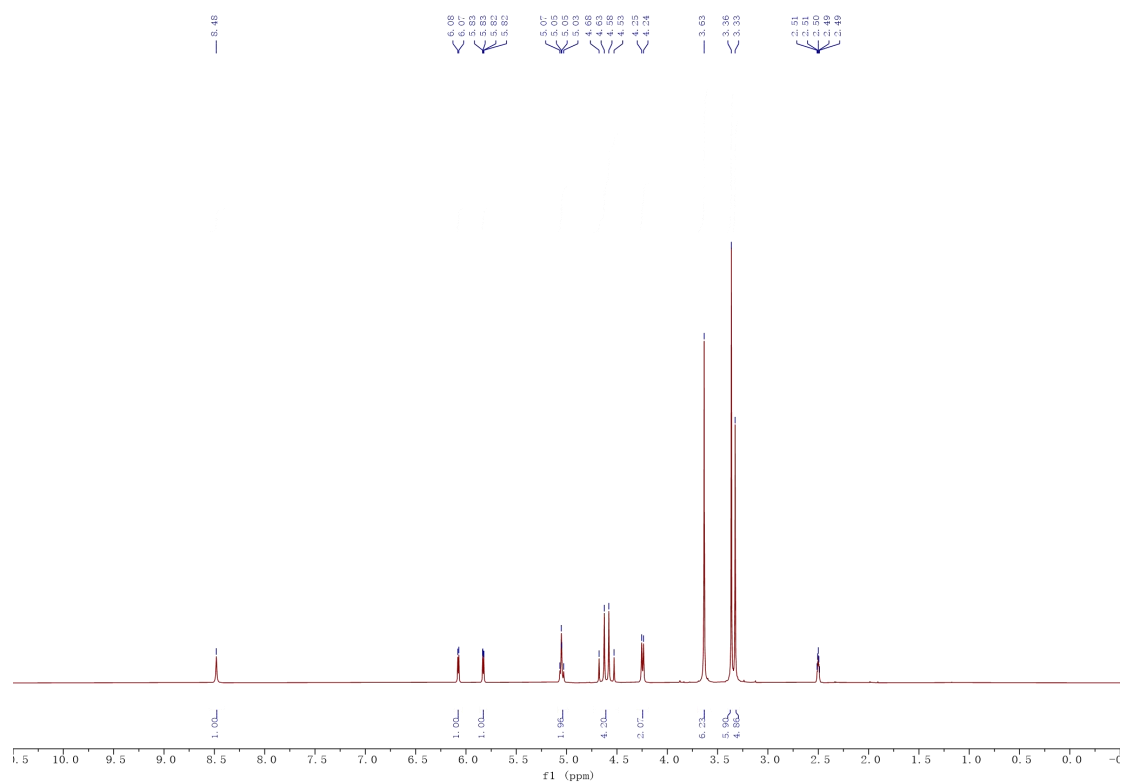


The reaction was carried out at 70 °C for 1 hour to give **11e** (314 mg, 84%) as a yellow solid. M.p. 109-110 °C. ¹H NMR (300 MHz, DMSO-*d*₆) δ 9.02 (s, 1H, NH), 6.06 (d, *J* = 3.1 Hz, 1H, H_{4'}), 6.00-5.84 (m, 2H, 2 CH_{allyl}), 5.75 (d, *J* = 3.1 Hz, 1H, H_{3'}), 5.31-5.13 (m, 4H, 2 CH=CH_{2allyl}), 5.10 (s, 1H, H₄), 5.02 (t, *J* = 5.6 Hz, 1H, OH), 4.67-4.48 (m, 4H, 2 CH₂), 4.25 (d, *J* = 5.6 Hz, 2H, CH₂OH), 2.27 (s, 6H, 2 CH₃). ¹³C NMR (75 MHz, DMSO) δ 166.2 (2 C=O), 157.9 (C_{2'}), 153.7 (C_{5'}), 146.9 (2 C₂), 133.3 (2 CHCH_{2allyl}), 116.7 (2 CHCH_{2allyl}), 107.5 (C_{4'}), 104.7 (C_{3'}), 98.3 (2 C₃), 63.6 (2 CH₂), 55.8 (CH₂OH), 32.7 (C₄), 18.2 (2 CH₃). HRMS (ESI) *m/z*: Calcd for [M+Na]⁺ C₂₀H₂₃NNaO₆ = 396.1418; Found 396.1415.

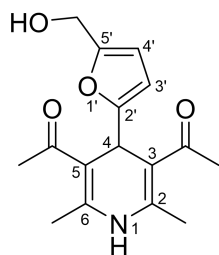
Dimethyl 4-[5-(hydroxymethyl)furan-2-yl]-2,6-bis(methoxymethyl)-1,4-dihydropyridine-3,5-dicarboxylate (C₁₈H₂₃NO₈)



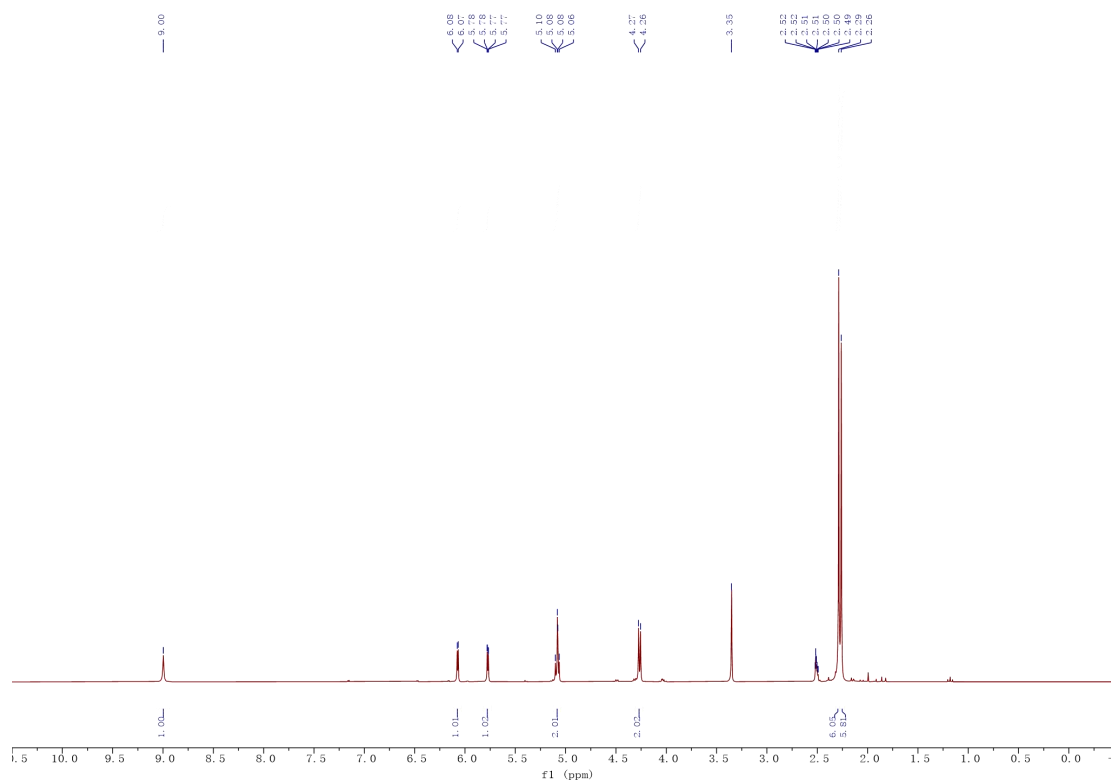
The reaction was carried out at 70 °C for 1 hour to give **11f** (206 mg, 54%) as a yellow solid. M.p. 91-93 °C. ¹H NMR (300 MHz, DMSO-*d*₆) δ 8.48 (s, 1H, NH), 6.08 (d, *J* = 3.1 Hz, 1H, H_{4'}), 5.83 (dd, *J* = 3.1, 0.7 Hz, 1H, H_{3'}), 5.09-4.99 (m, 2H, H₄, OH), 4.73-4.49 (AB system, 4H, 2 CH₂), 4.25 (d, *J* = 5.5 Hz, 2H, CH₂OH), 3.63 (s, 6H, 2 CO₂CH₃), 3.36 (s, 6H, 2 CH₃). ¹³C NMR (75 MHz, DMSO) δ 166.4 (2 C=O), 156.9 (C_{2'}), 154.1 (C_{5'}), 146.0 (2 C₂), 107.7 (C_{4'}), 105.2 (C_{3'}), 97.8 (2 C₃), 68.6 (2 CH₂), 58.4 (2 OCH₃), 55.7 (CH₂OH), 51.1 (2 CO₂CH₃), 32.7 (C₄). HRMS (ESI) *m/z*: Calcd for [M+H]⁺ C₁₈H₂₄NO₈ = 382.1496; Found 382.1495. HRMS (ESI) *m/z*: Calcd for [M+Na]⁺ C₁₈H₂₃NNaO₈ = 404.1316; Found 404.1314; Calcd for [2M+Na]⁺ C₃₆H₄₆N₂NaO₁₆ = 785.2740; Found 785.2734.

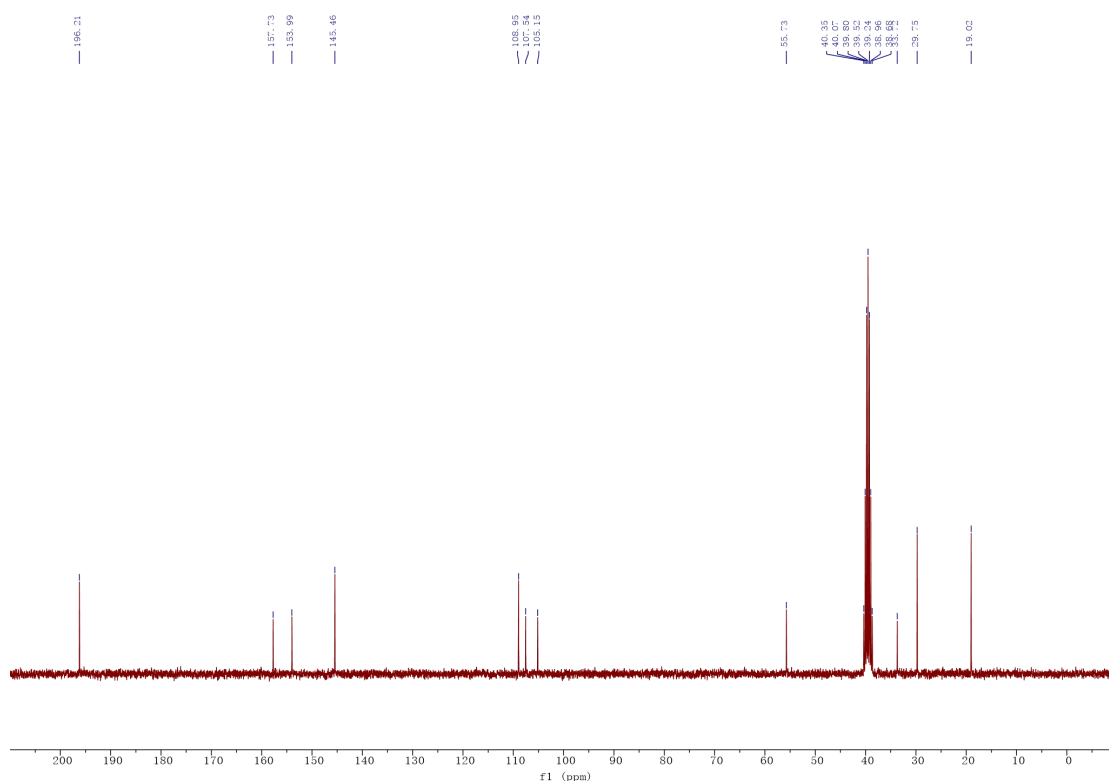


1,1'-{4-(5-[Hydroxymethyl]furan-2-yl)-2,6-dimethyl-1,4-dihydropyridine-3,5-diyl}bis(ethan-1-one) (C₁₆H₁₉NO₄)

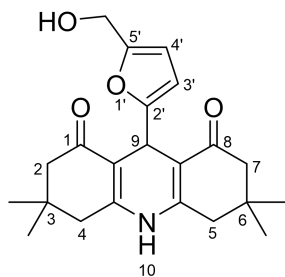


The reaction was carried out at 90 °C for 1 hour to give **11g** (209 mg, 72%) as a yellow solid. M.p. 146-148 °C. ¹H NMR (300 MHz, DMSO-*d*₆) δ 9.00 (s, 1H, NH), 6.07 (d, *J* = 3.1 Hz, 1H, H_{4'}), 5.77 (dd, *J* = 3.0, 0.8 Hz, 1H, H_{3'}), 5.12-5.05 (m, 2H, H₄, OH), 4.27 (d, *J* = 5.6 Hz, 2H, CH₂OH), 2.29 (s, 6H, 2 COCH₃), 2.26 (s, 6H, 2 CH₃). ¹³C NMR (75 MHz, DMSO) δ 196.2 (2 C=O), 157.7 (C_{2'}), 154.0 (C_{5'}), 145.5 (2 C₂), 108.9 (2 C₃), 107.5 (C_{4'}), 105.1 (C_{3'}), 55.7 (CH₂OH), 33.7 (C₄), 29.8 (2 COCH₃), 19.0 (2 CH₃). HRMS (ESI) *m/z*: Calcd for [M+Na]⁺ C₁₆H₁₉NNaO₄ = 312.1206; Found 312.1205; Calcd for [2M+Na]⁺ C₃₂H₃₈N₂NaO₈ = 601.2520; Found 601.2519.



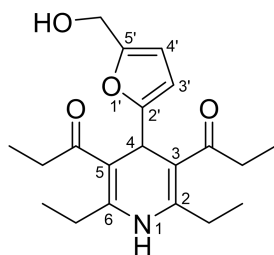


9-[5-(Hydroxymethyl)furan-2-yl]-3,3,6,6-tetramethyl-3,4,6,7,9,10-hexahydroacridine-1,8(2H, 5H)-dione (C₂₂H₂₇NO₄)



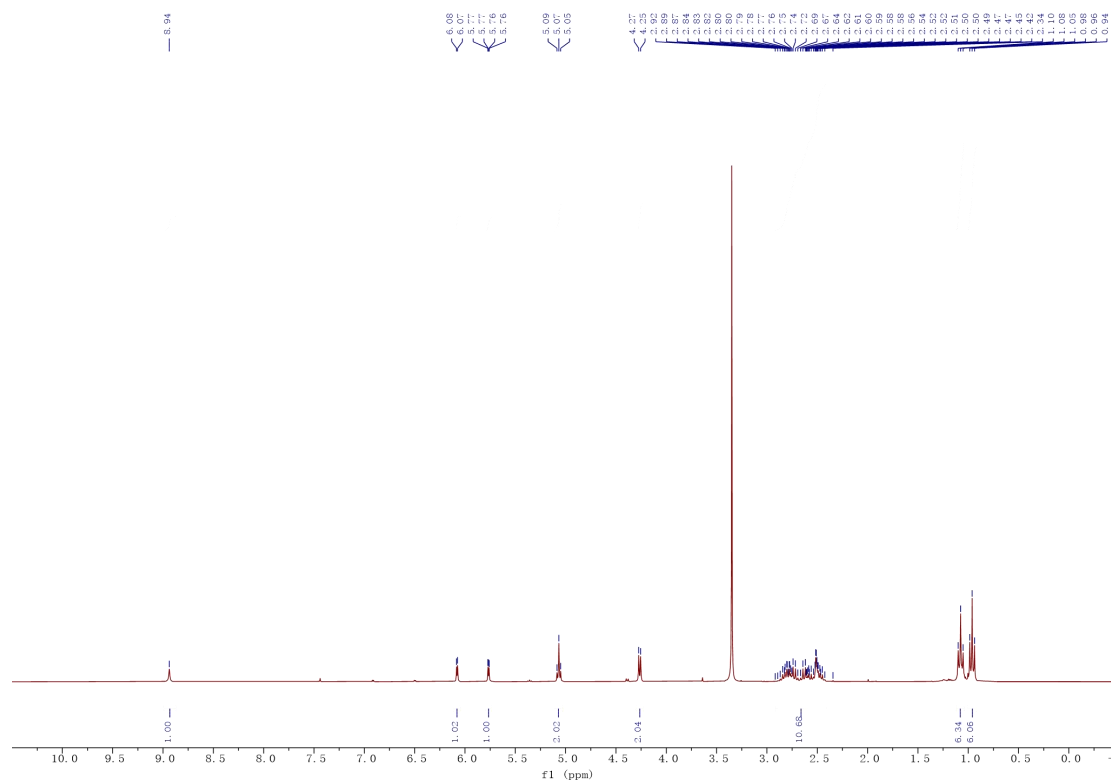
The reaction was carried out at 90 °C for 2 hours to give **11h** (210 mg, 57%) as a yellow solid. M.p. 189-191 °C. ¹H NMR (300 MHz, DMSO-*d*₆) δ 9.33 (s, 1H, NH), 6.01 (d, *J* = 3.1 Hz, 1H, H_{4'}), 5.73 (d, *J* = 3.1 Hz, 1H, H_{3'}), 5.09-4.84 (m, 2H, H₄, OH), 4.19 (d, *J* = 5.0 Hz, 2H, CH₂OH), 2.472.01 (m, 8H, 4 CH₂), 1.02 (s, 6H, 2 CH₃), 0.94 (s, 6H, 2 CH₃). ¹³C NMR (75 MHz, DMSO) δ 194.3 (2 C=O), 157.5 (C_{2'}), 152.8 (C_{5'}), 150.0 (2 C_q-NH), 108.6 (2 C_q-CO), 107.5 (C_{4'}), 104.7 (C_{3'}), 55.7 (CH₂OH), 50.3 (2 CH₂), 39.7 (2 CH₂), 32.1 (2 C_q), 29.2 (2 CH₃), 26.3 (2 CH₃), 26.2 (C₄). HRMS (ESI) *m/z*: Calcd for [M+Na]⁺ C₂₂H₂₇NNaO₄ = 392.1832; Found 392.1832. Calcd for [2M+Na]⁺ C₄₄H₅₄N₂NaO₈ = 761.3772; Found 761.3763.

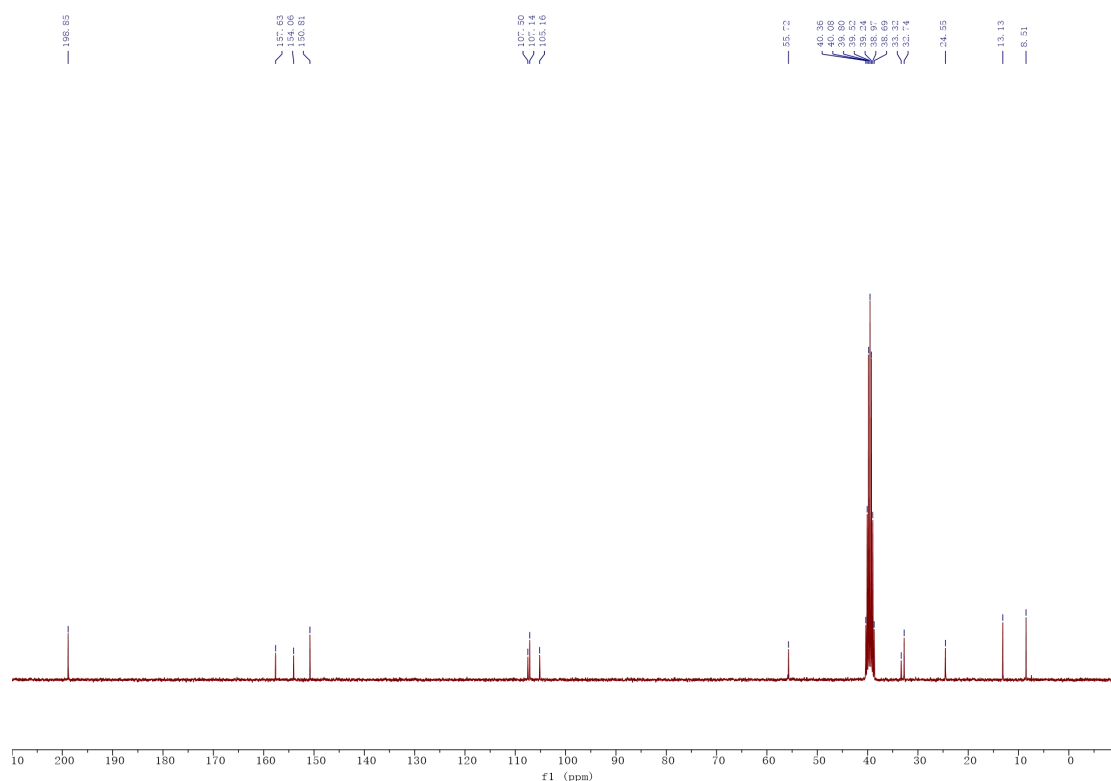
1,1'-{2,6-Diethyl-4-[5-(hydroxymethyl)furan-2-yl]-1,4-dihydropyridine-3,5-diyl}bis(propan-1-one) (C₂₀H₂₇NO₄)



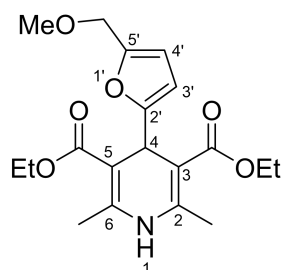
The reaction was carried out at 90 °C for 1 hour to give **11i** (42 mg, 12%) as a yellow solid.

¹H NMR (300 MHz, DMSO-*d*₆) δ 8.94 (s, 1H, NH), 6.08 (d, *J* = 3.1 Hz, 1H, H_{4'}), 5.77 (dd, *J* = 3.1, 0.6 Hz, 1H, H_{3'}), 5.11-5.03 (m, 2H, H₄, OH), 4.26 (d, *J* = 5.7 Hz, 2H, CH₂OH), 2.92-2.41 (m, 8H, 4 CH₂), 1.08 (t, *J* = 7.3 Hz, 6H, 2 CH₃), 0.96 (t, *J* = 7.1 Hz, 6H, 2 CH₃). ¹³C NMR (75 MHz, DMSO) δ 198.9 (2 CO), 157.6 (C_{2'}), 154.1 (C_{5'}), 150.8 (2 C₂), 107.5 (C_{4'}), 107.1 (2 C₃), 105.2 (C_{3'}), 55.7 (CH₂OH), 33.3 (C₄), 32.7 (2 CH₂), 24.5 (2 CH₂), 13.1 (2 CH₃), 8.5 (2 CH₃). HRMS (ESI) *m/z*: Calcd for [M+H]⁺ C₂₀H₂₈NO₄ = 346.2013; Found 346.2007. HRMS (ESI) *m/z*: Calcd for [M+Na]⁺ C₂₀H₂₇NNaO₄ = 368.1832; Found 368.1827; Calcd for [2M+Na]⁺ C₄₀H₅₄N₂NaO₈ = 713.3772; Found 713.3753.

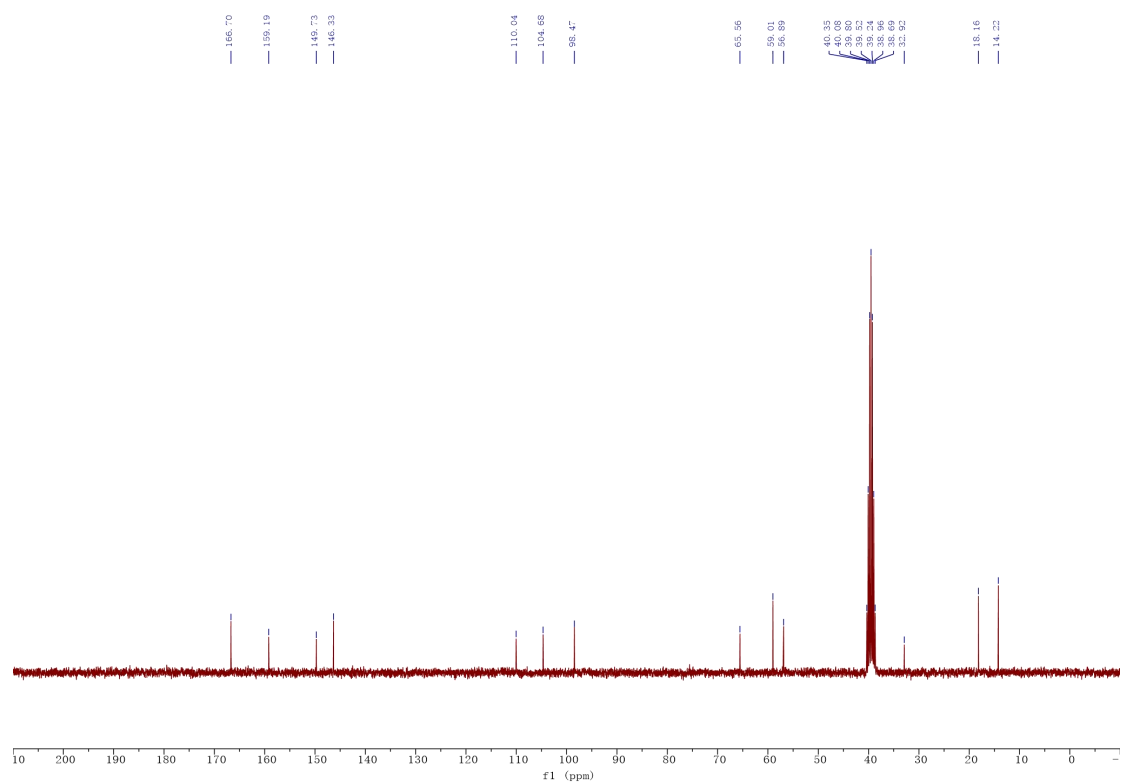
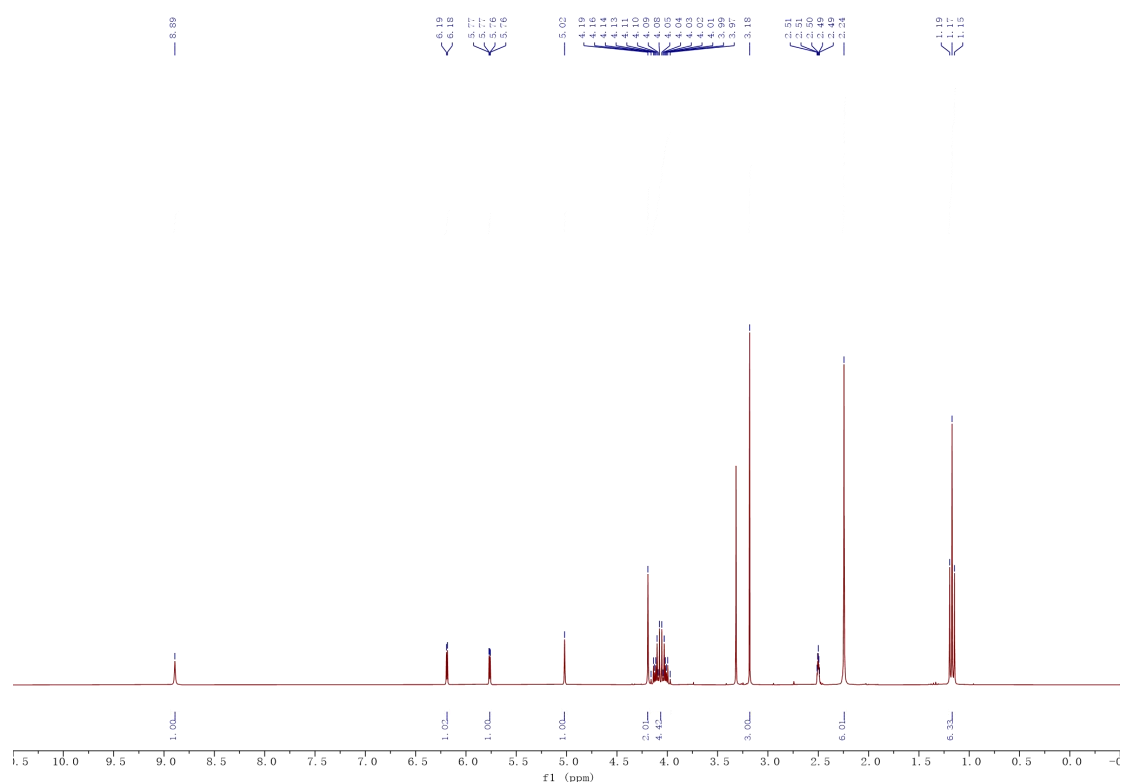




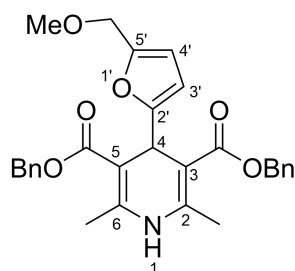
Diethyl 4-[5-(methoxymethyl)furan-2-yl]-2,6-dimethyl-1,4-dihydropyridine-3,5-dicarboxylate
(C₁₉H₂₅NO₆)



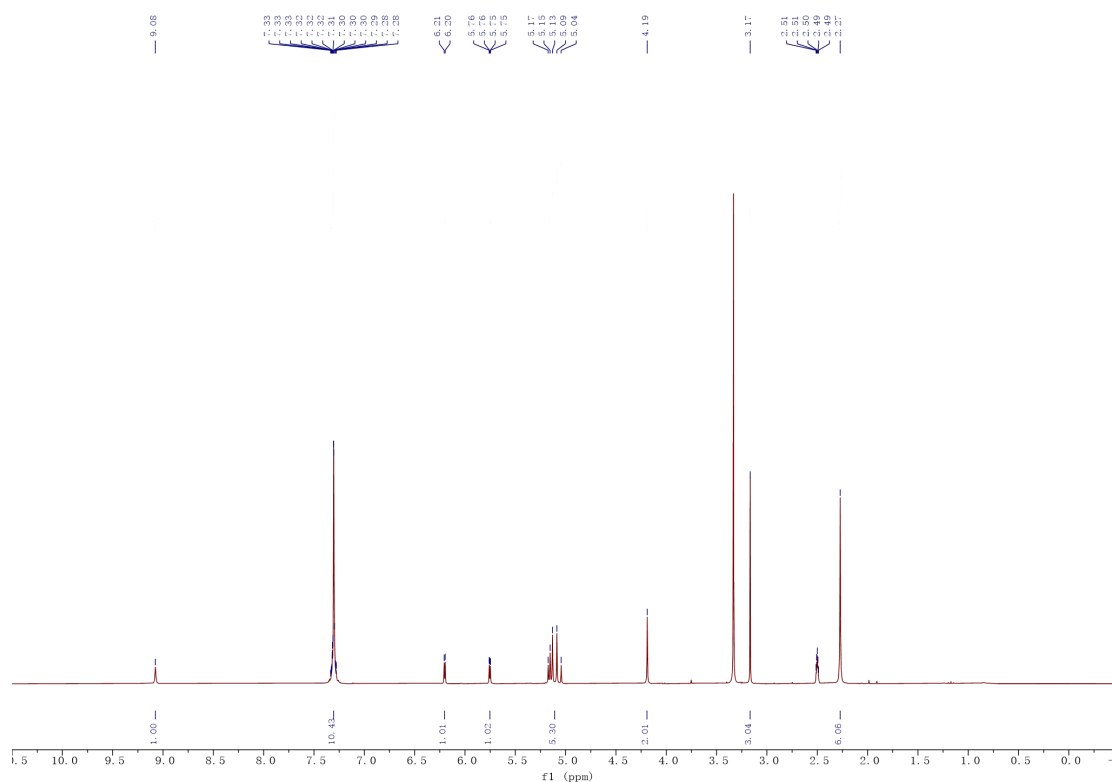
The reaction was carried out at 70 °C for 1 hour to give **11j** (334 mg, 92%) as a yellow solid. M.p. 64-65 °C. ¹H NMR (300 MHz, DMSO-*d*₆) δ 8.89 (s, 1H, NH), 6.19 (d, *J* = 3.1 Hz, 1H, H_{4'}), 5.76 (dd, *J* = 3.1, 0.7 Hz, 1H, H_{3'}), 5.02 (s, 1H, H₄), 4.19 (s, 2H, CH₂OCH₃), 4.17-3.96 (m, 4H, 2 CH₂), 3.18 (s, 3H, OCH₃), 2.24 (s, 6H, 2 CH₃), 1.17 (t, *J* = 7.1 Hz, 6H, 2 CH₂CH₃). ¹³C NMR (75 MHz, DMSO) δ 166.7 (2 C=O), 159.2 (C_{2'}), 149.7 (C_{5'}), 146.3 (2 C₂), 110.0 (C_{4'}), 104.7 (C_{3'}), 98.5 (2 C₃), 65.6 (CH₂OCH₃), 59.0 (2 CH₂), 56.9 (OCH₃), 32.9 (C₄), 18.2 (2 CH₃), 14.2 (2 CH₂CH₃). HRMS (ESI) *m/z*: Calcd for [M+H]⁺ C₁₉H₂₆NO₆ = 364.1755; Found 364.1748. HRMS (ESI) *m/z*: Calcd for [M+Na]⁺ C₁₉H₂₅NNaO₆ = 386.1574; Found 386.1572; Calcd for [2M+Na]⁺ C₃₈H₅₀N₂NaO₁₂ = 749.3256; Found 749.3247.

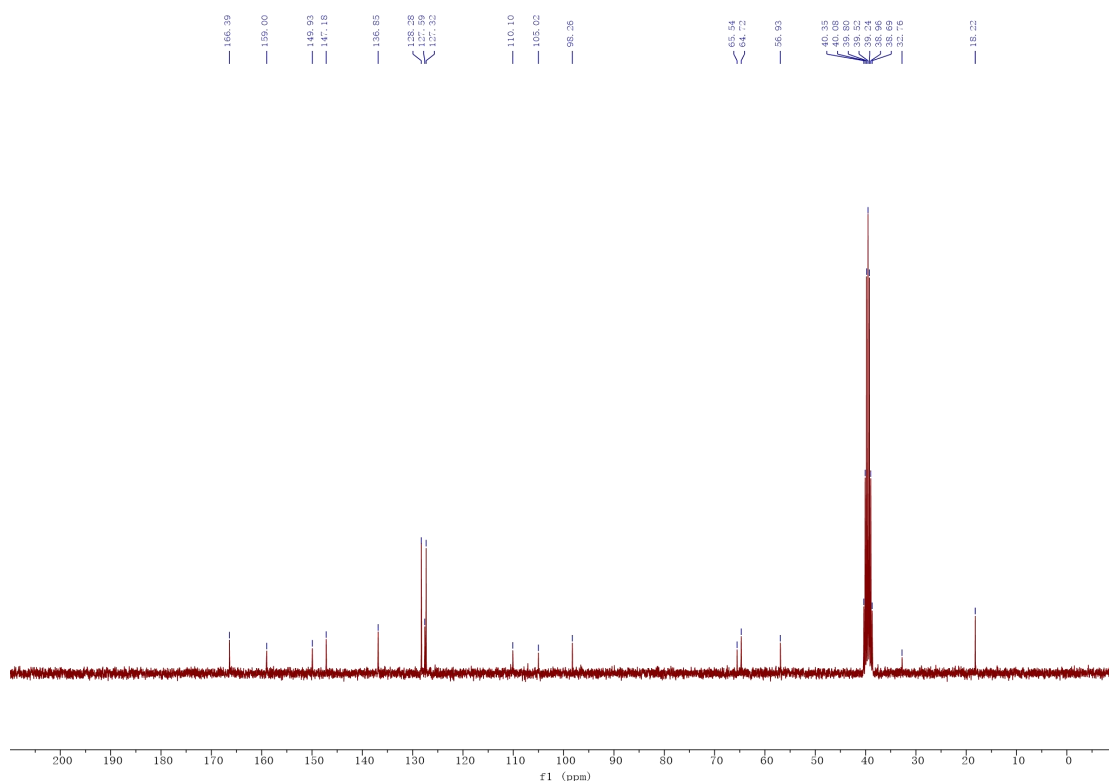


Dibenzyl 4-[5-(methoxymethyl)furan-2-yl]-2,6-dimethyl-1,4-dihydropyridine-3,5-dicarboxylate
(C₂₉H₂₉NO₆)

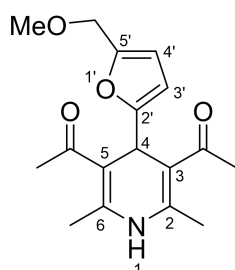


The reaction was carried out at 70 °C for 80 min to give **11k** (405 mg, 83%) as a gummy yellow product. ¹H NMR (300 MHz, DMSO-*d*₆) δ 9.08 (s, 1H, NH), 7.35-7.26 (m, 10H, 10 H_{Ar}), 6.20 (d, *J* = 3.1 Hz, 1H, H_{4'}), 5.75 (dd, *J* = 3.1, 0.7 Hz, 1H, H_{3'}), 5.19-5.03 (m, 5H, H₄, 2 CH₂), 4.19 (s, 2H, CH₂OCH₃), 3.17 (s, 3H, OCH₃), 2.27 (s, 6H, 2 CH₃). ¹³C NMR (75 MHz, DMSO) δ 166.4 (2 CO₂), 159.0 (C_{2'}), 149.9 (C_{5'}), 147.2 (2 C₂), 136.8 (2 C_{qAr}), 128.3 (4 CH_{Ar}), 127.6 (2 CH_{Ar}), 127.3 (4 CH_{Ar}), 110.1 (C_{4'}), 105.0 (C_{3'}), 98.3 (2 C₃), 65.5 (CH₂OCH₃), 64.7 (2 CH₂Ar), 56.9 (OCH₃), 32.8 (C₄), 18.2 (2 CH₃). HRMS (ESI) *m/z*: Calcd for [M+Na]⁺ C₂₉H₂₉NNaO₆ = 510.1887; Found 510.1883; Calcd for [2M+Na]⁺ C₅₈H₅₈N₂NaO₁₂ = 997.3882; Found 997.3869.

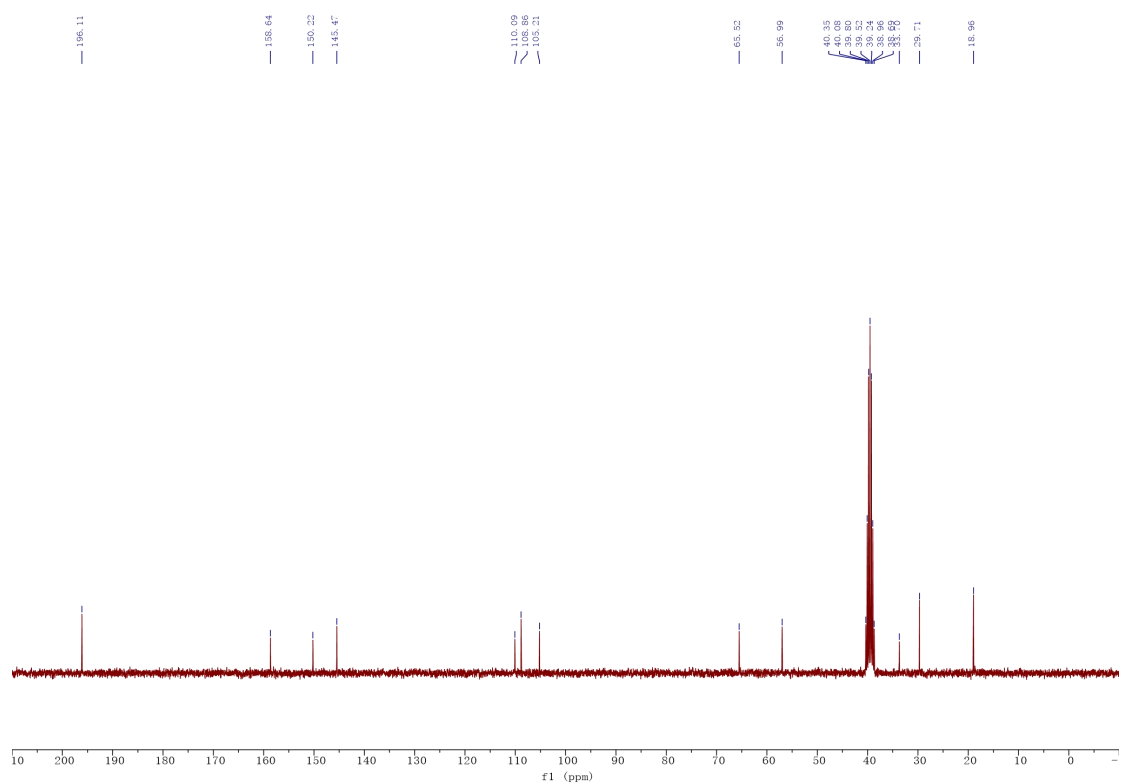
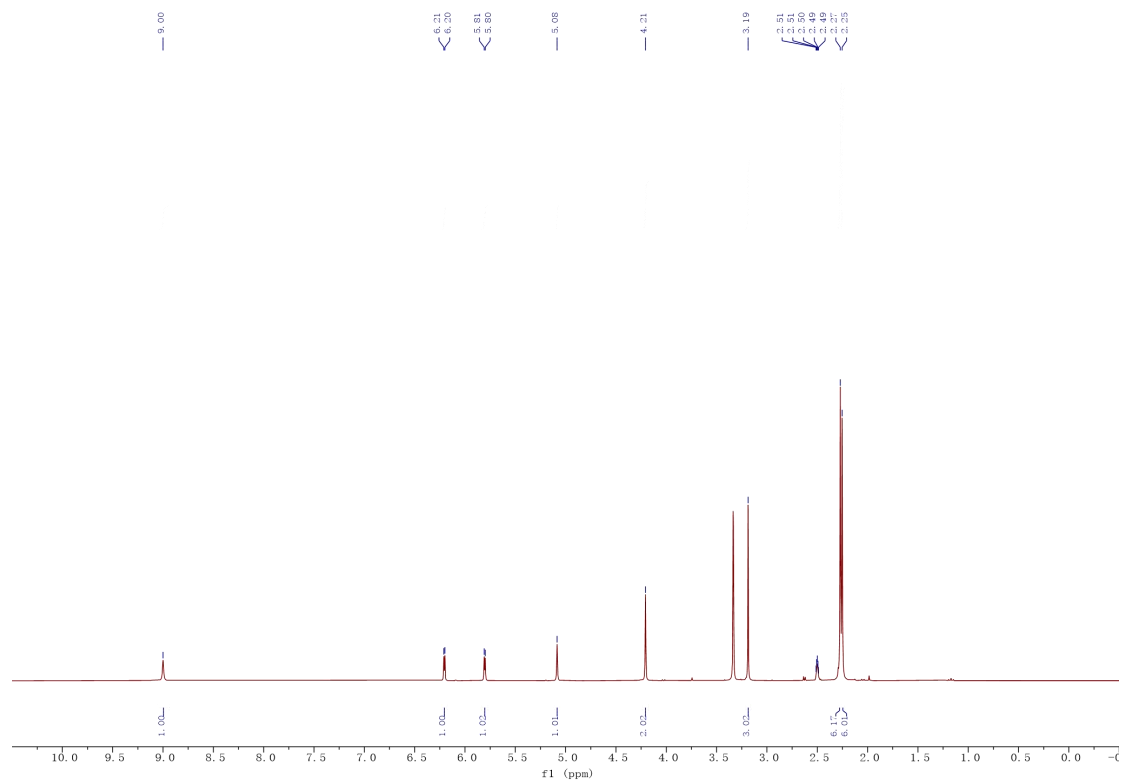




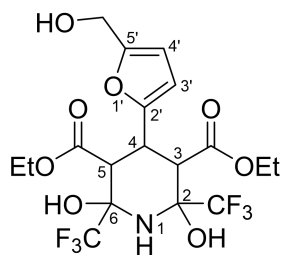
1,1'-{4-[5-(Methoxymethyl)furan-2-yl]-2,6-dimethyl-1,4-dihydropyridine-3,5-diyl}bis(ethan-1-one) (C₁₇H₂₁NO₄)



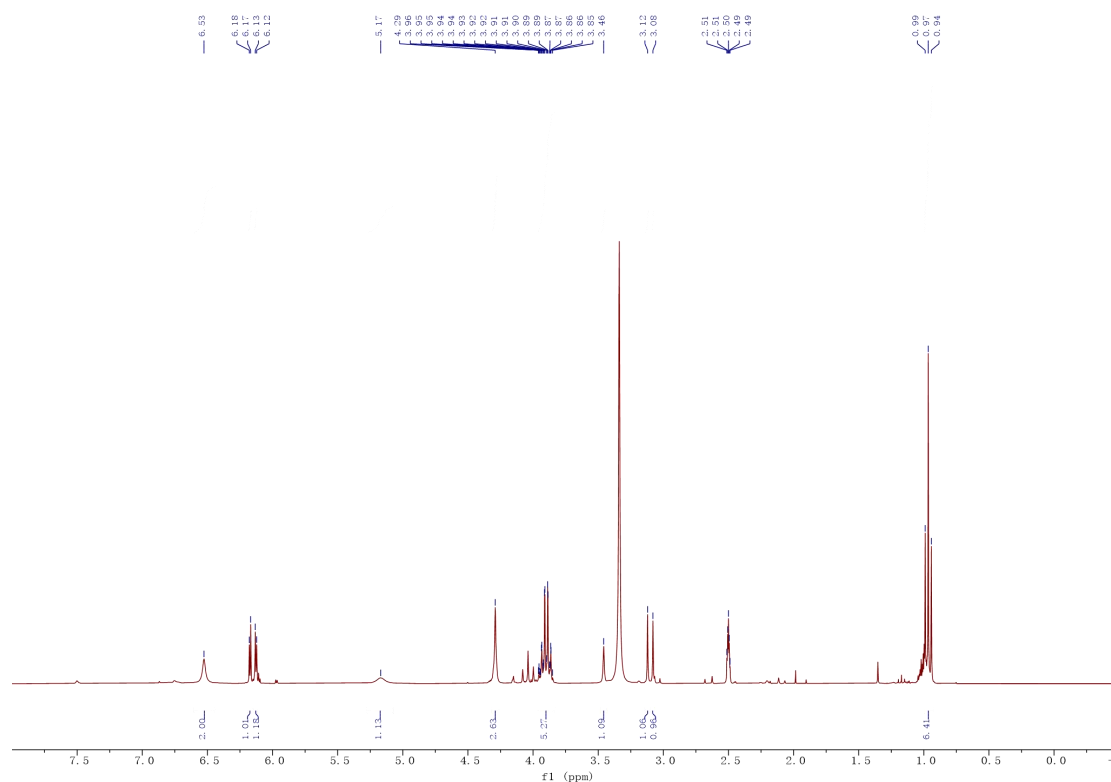
The reaction was carried out at 90 °C for 1 hour to give **11I** (182 mg, 60%) as a yellow solid. M.p. 147-149 °C. ¹H NMR (300 MHz, DMSO-*d*₆) δ 9.00 (s, 1H, NH), 6.20 (d, *J* = 3.1 Hz, 1H, H_{4'}), 5.80 (d, *J* = 3.1 Hz, 1H, H_{3'}), 5.08 (s, 1H, H₄), 4.21 (s, 2H, CH₂OCH₃), 3.19 (s, 3H, OCH₃), 2.27 (s, 6H, 2 COCH₃), 2.25 (s, 6H, 2 CH₃). ¹³C NMR (75 MHz, DMSO) δ 196.1 (2 C=O), 158.6 (C_{2'}), 150.2 (C_{5'}), 145.5 (2 C₂), 110.1 (C_{4'}), 108.9 (2 C₃), 105.2 (C_{3'}), 65.5 (CH₂OCH₃), 57.0 (OCH₃), 33.7 (C₄), 29.7 (2 COCH₃), 19.0 (2 CH₃). HRMS (ESI) *m/z*: Calcd for [M+H]⁺ C₁₇H₂₂NO₄ = 304.1543; Found 304.1538. HRMS (ESI) *m/z*: Calcd for [M+Na]⁺ C₁₇H₂₁NNaO₄ = 326.1363; Found 326.1359; Calcd for [2M+Na]⁺ C₃₄H₄₂N₂NaO₈ = 629.2833; Found 629.2823.

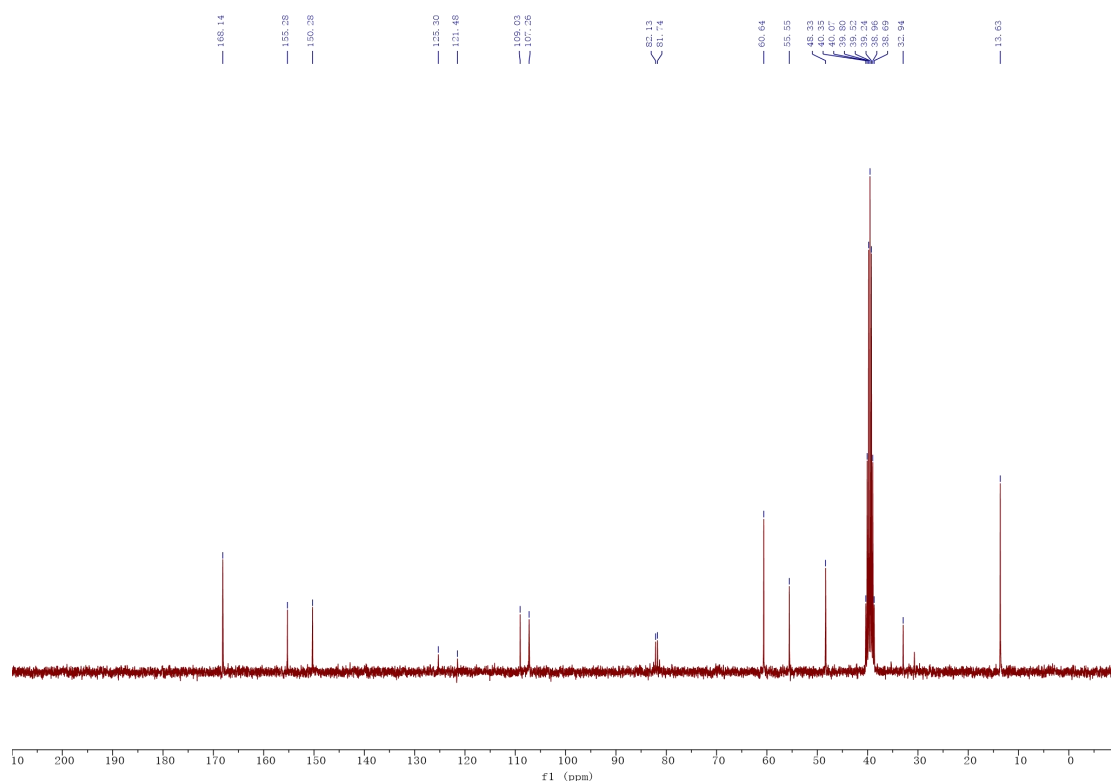


Diethyl 2,6-dihydroxy-4-[5-(hydroxymethyl)furan-2-yl]-2,6-bis(trifluoromethyl)piperidine-3,5-dicarboxylate (C₁₈H₂₁F₆NO₈)

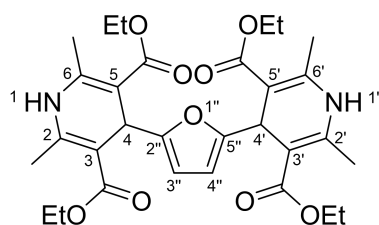


The reaction was carried out at 90 °C for 1 hour to give **11m** (350 mg, contains few difficult-to-separate impurities, NMR yield of **11m**: 67%) as a gummy yellow product. ¹H NMR (300 MHz, DMSO-*d*₆) δ 6.53 (s, 2H, 2 OH), 6.17 (d, *J* = 3.1 Hz, 1H, H_{3'}), 6.13 (d, *J* = 3.1 Hz, 1H, H_{4'}), 5.17 (s, 1H, CH₂OH), 4.29 (m, 2H, CH₂OH), 4.04 (t, *J* = 12.3 Hz, 1H, H₄), 3.97-3.83 (m, 4H, 2 CH₂), 3.46 (s, 1H, NH), 3.12 (s, 1H, H_{3/5}), 3.08 (s, 1H, H_{3/5}), 0.97 (t, *J* = 7.1 Hz, 6H, 2 CH₃). ¹³C NMR (75 MHz, DMSO) δ 168.1 (2 CO), 155.3 (C_{5'}), 150.3 (C_{2'}), 123.4 (q, 2 CF₃), 109.0 (CH_{3'}), 107.3 (CH_{4'}), 81.9 (q, 2 C₂), 60.6 (2 CH₂), 55.6 (CH₂OH), 48.3 (2 CHCO), 32.9 (C₄), 13.6 (2 CH₃). HRMS (ESI) *m/z*: Calcd for [M+Na]⁺ C₁₈H₂₁F₆NNaO₈ = 516.1064; Found 516.1060.

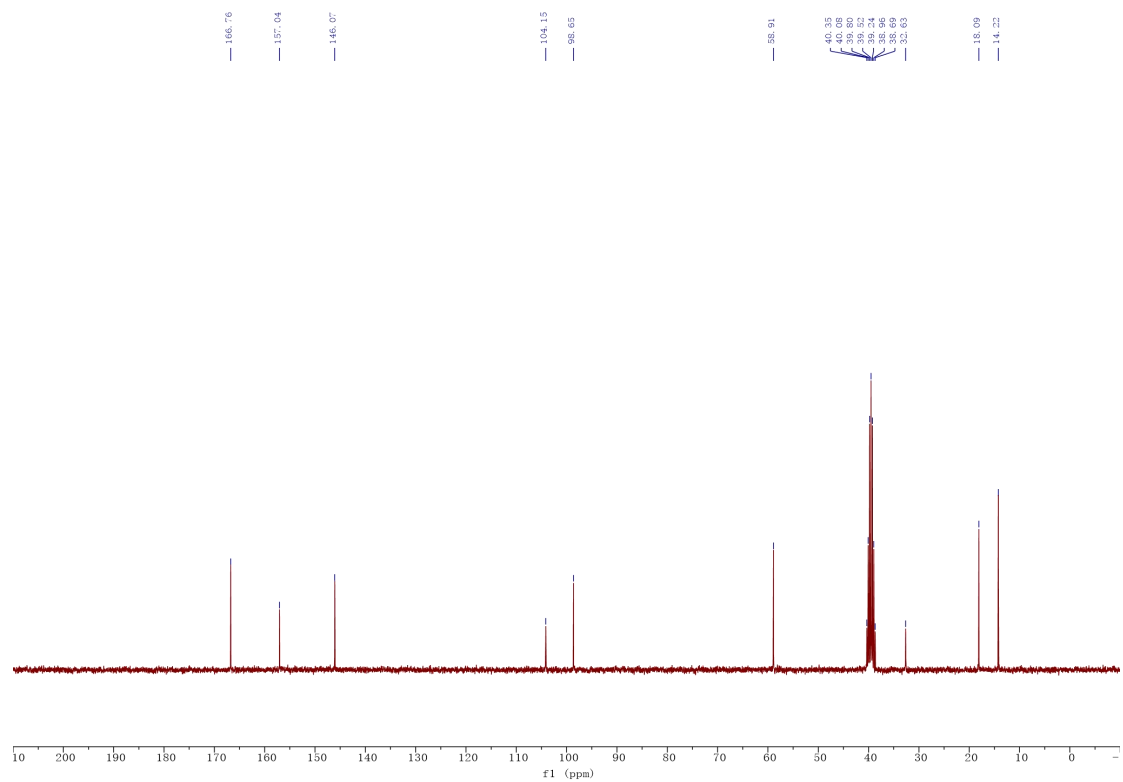
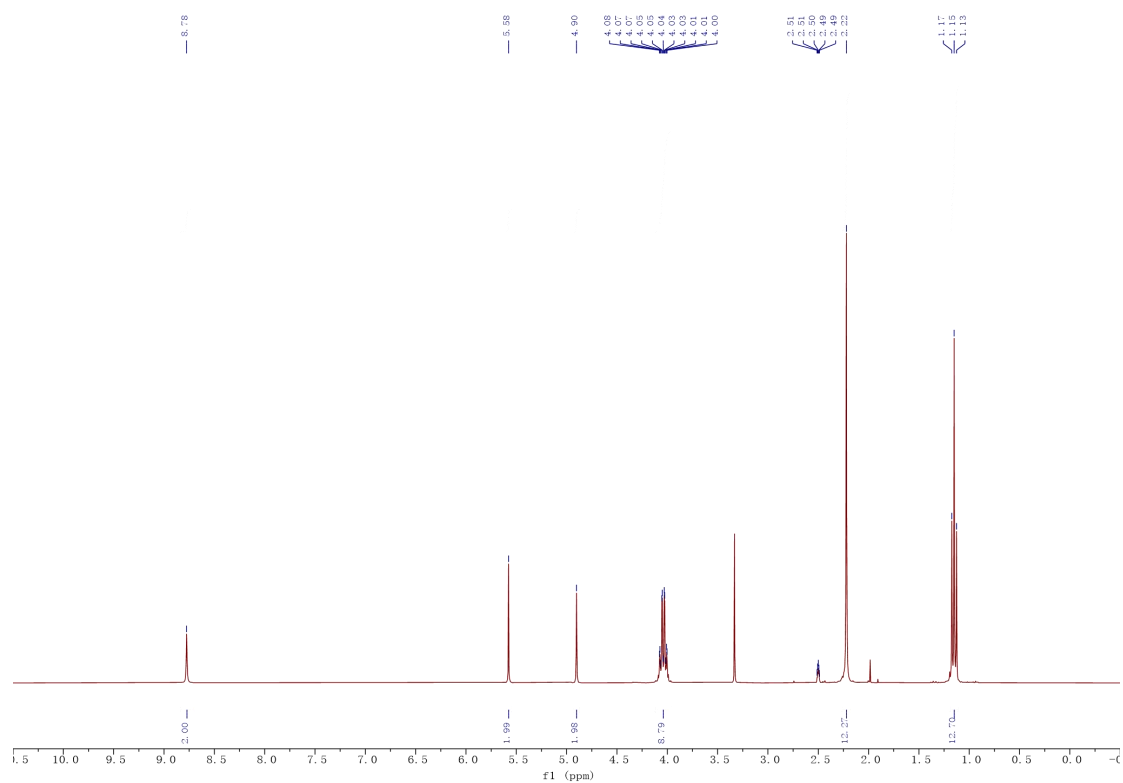




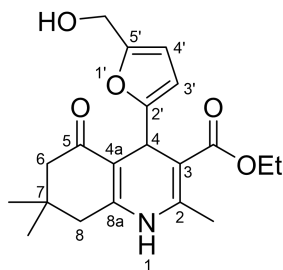
Tetraethyl 4,4'-(furan-2,5-diyl)bis(2,6-dimethyl-1,4-dihydropyridine-3,5-dicarboxylate)
(C₃₀H₃₈N₂O₉)



The reaction was carried out at 90 °C for 1 hour to give **11n** (518 mg, 91%) as a yellow solid. M.p. 156-158 °C. ¹H NMR (300 MHz, DMSO-*d*₆) δ 8.78 (s, 2H, 2 NH), 5.58 (s, 2H, H_{3''}), 4.90 (s, 2H, H_{4'}), 4.12-3.96 (m, 8H, 4 CH₂), 2.22 (s, 12H, 4 CH₃), 1.15 (t, *J* = 7.1 Hz, 12H, 4 CH₂CH₃). ¹³C NMR (75 MHz, DMSO) δ 166.8 (4 CO₂), 157.0 (2 C₂), 146.1 (4 C_{2'}), 104.1 (2 C_{3''}), 98.7 (4 C_{3'}), 58.9 (4 CH₂), 32.6 (2 C₄, C_{4'}), 18.1 (4 CH₃), 14.2 (4 CH₂CH₃). HRMS (ESI) *m/z*: Calcd for [M+H]⁺ C₃₀H₃₉N₂O₉ = 571.2650; Found 571.2646. HRMS (ESI) *m/z*: Calcd for [M+Na]⁺ C₃₀H₃₈N₂NaO₉ = 593.2470; Found 593.2468.



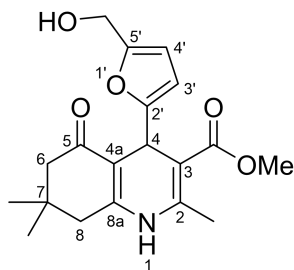
Ethyl 4-[5-(hydroxymethyl)furan-2-yl]-2,7,7-trimethyl-5-oxo-1,4,5,6,7,8-hexahydroquinoline-3-carboxylate (C₂₀H₂₅NO₅)²¹⁷



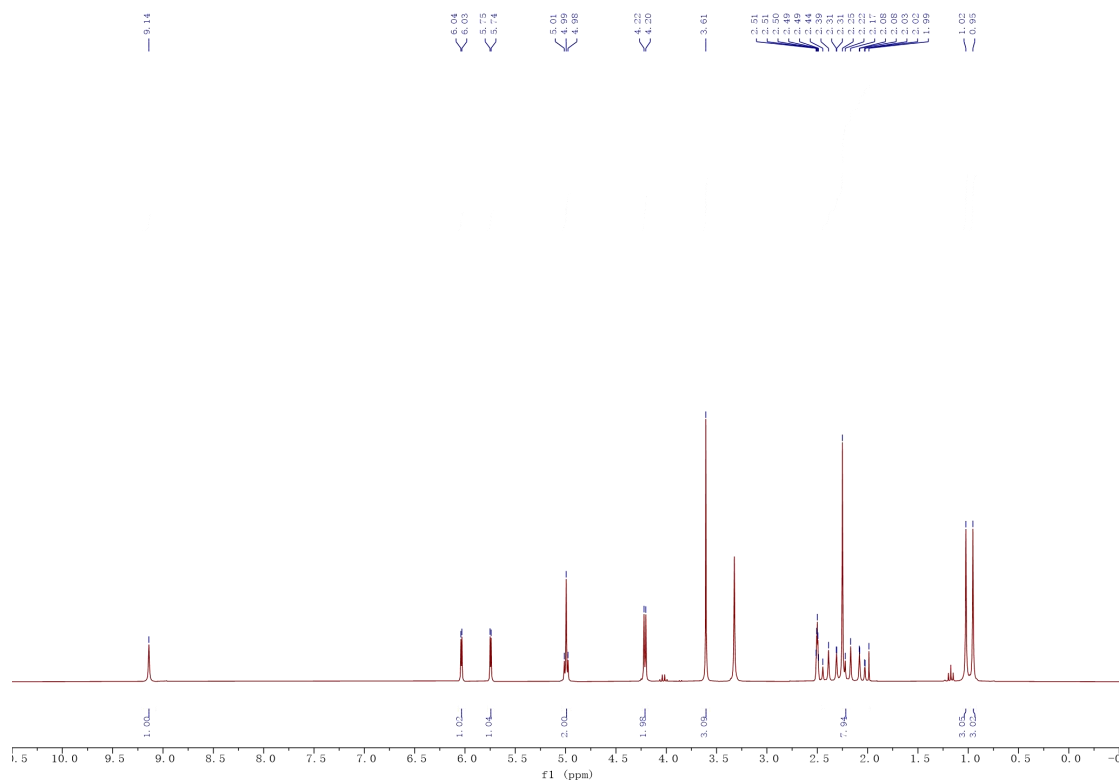
The reaction was carried out at 80 °C for 80 min to give **12a** (316 mg, 88%) as a yellow solid.

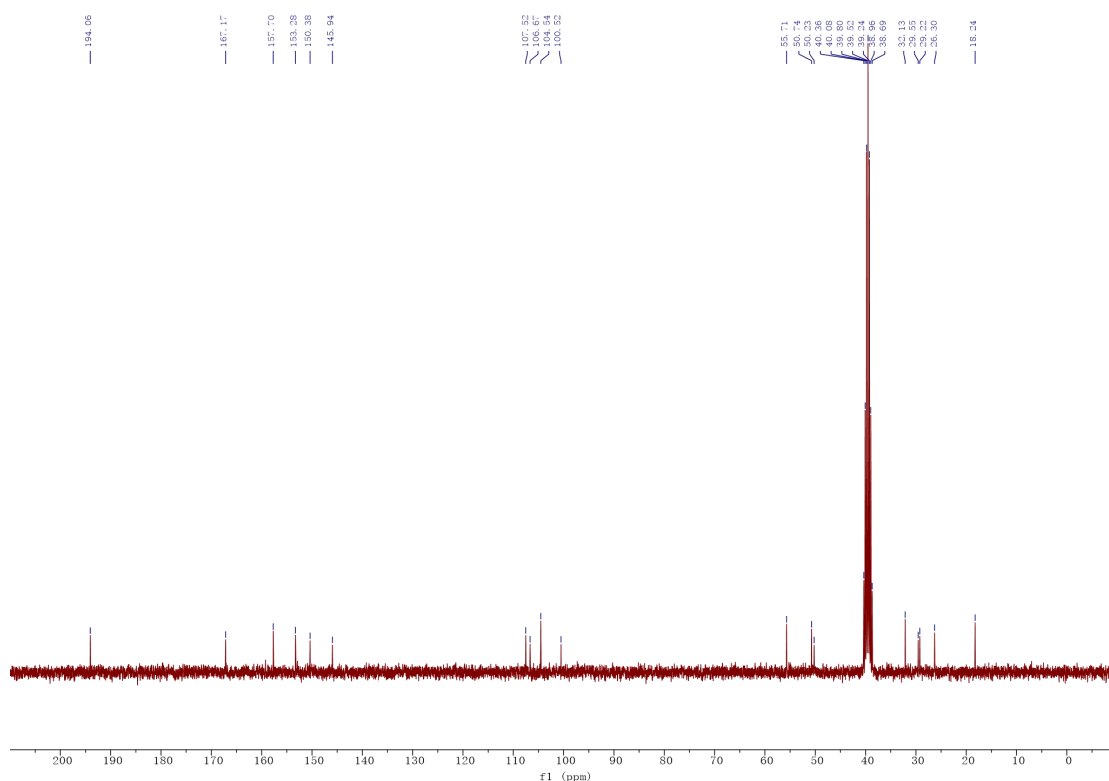
¹H NMR (300 MHz, DMSO-*d*₆) δ 9.11 (s, 1H, NH), 6.04 (d, *J* = 3.0 Hz, 1H, H_{4'}), 5.75 (d, *J* = 3.1 Hz, 1H, H_{3'}), 5.04-4.94 (m, 2H, H₄, OH), 4.22 (d, *J* = 5.6 Hz, 2H, CH₂OH), 4.16-3.97 (m, 2H, CH₂CH₃), 2.47-1.97 (m, 7H, 2 CH₂, CH₃), 1.20 (t, *J* = 7.1 Hz, 3H, CH₂CH₃), 1.03 (s, 3H, CH₃), 0.96 (s, 3H, CH₃). ¹³C NMR (75 MHz, DMSO) δ 194.1 (C=O), 166.7 (COO), 157.8 (C_{2'}), 153.2 (C_{5'}), 150.5 (C_{8a}), 145.6 (C₂), 107.5 (C_{4'}), 106.6 (C_{4a}), 104.6 (C_{3'}), 100.9 (C₃), 59.1 (CH₂CH₃), 55.7 (CH₂OH), 50.3 (CH₂), 39.5 (CH₂), 32.1 (C₇), 29.6 (C₄), 29.2 (CH₃), 26.3 (CH₃), 18.24 (CH₃), 14.3 (CH₂CH₃). HRMS (ESI) *m/z*: Calcd for [M+H]⁺ C₂₀H₂₆NO₅ = 360.1805; Found 360.1805. HRMS (ESI) *m/z*: Calcd for [M+Na]⁺ C₂₀H₂₅NNaO₅ = 382.1625; Found 382.1622.

Methyl 4-[5-(hydroxymethyl)furan-2-yl]-2,7,7-trimethyl-5-oxo-1,4,5,6,7,8-hexahydroquinoline-3-carboxylate (C₁₉H₂₃NO₅)

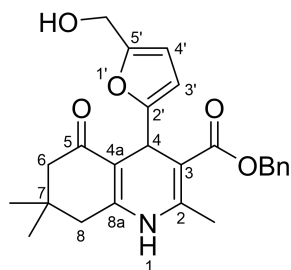


The reaction was carried out at 80 °C for 80 min to give **12b** (290 mg, 84%) as a yellow solid. M.p. 183-185 °C. ¹H NMR (300 MHz, DMSO-*d*₆) δ 9.14 (s, 1H, NH), 6.04 (d, *J* = 3.1 Hz, 1H, H_{4'}), 5.75 (d, *J* = 3.1 Hz, 1H, H_{3'}), 5.04-4.95 (s, t, 2H, H₄, OH), 4.21 (d, *J* = 5.6 Hz, 2H, CH₂OH), 3.61 (s, 3H, OCH₃), 2.46-1.98 (m, 7H, 2 CH₂, CH₃), 1.02 (s, 3H, CH₃), 0.95 (s, 3H, CH₃). ¹³C NMR (75 MHz, DMSO) δ 194.1 (C=O), 167.2 (C=O₂), 157.7 (C_{2'}), 153.3 (C_{5'}), 150.4 (C_{8a}), 145.9 (C₂), 107.5 (C_{4'}), 106.7 (C_{4a}), 104.5 (C_{3'}), 100.5 (C₃), 55.7 (CH₂OH), 50.7 (OCH₃), 50.2 (CH₂), 39.5 (CH₂), 32.1 (C₇), 29.5 (C₄), 29.2 (CH₃), 26.3 (CH₃), 18.2 (CH₃). HRMS (ESI) *m/z*: Calcd for [M+H]⁺ C₁₉H₂₄NO₅ = 346.1649; Found 346.1647. HRMS (ESI) *m/z*: Calcd for [M+Na]⁺ C₁₉H₂₃NNaO₅ = 368.1468; Found 368.1467.

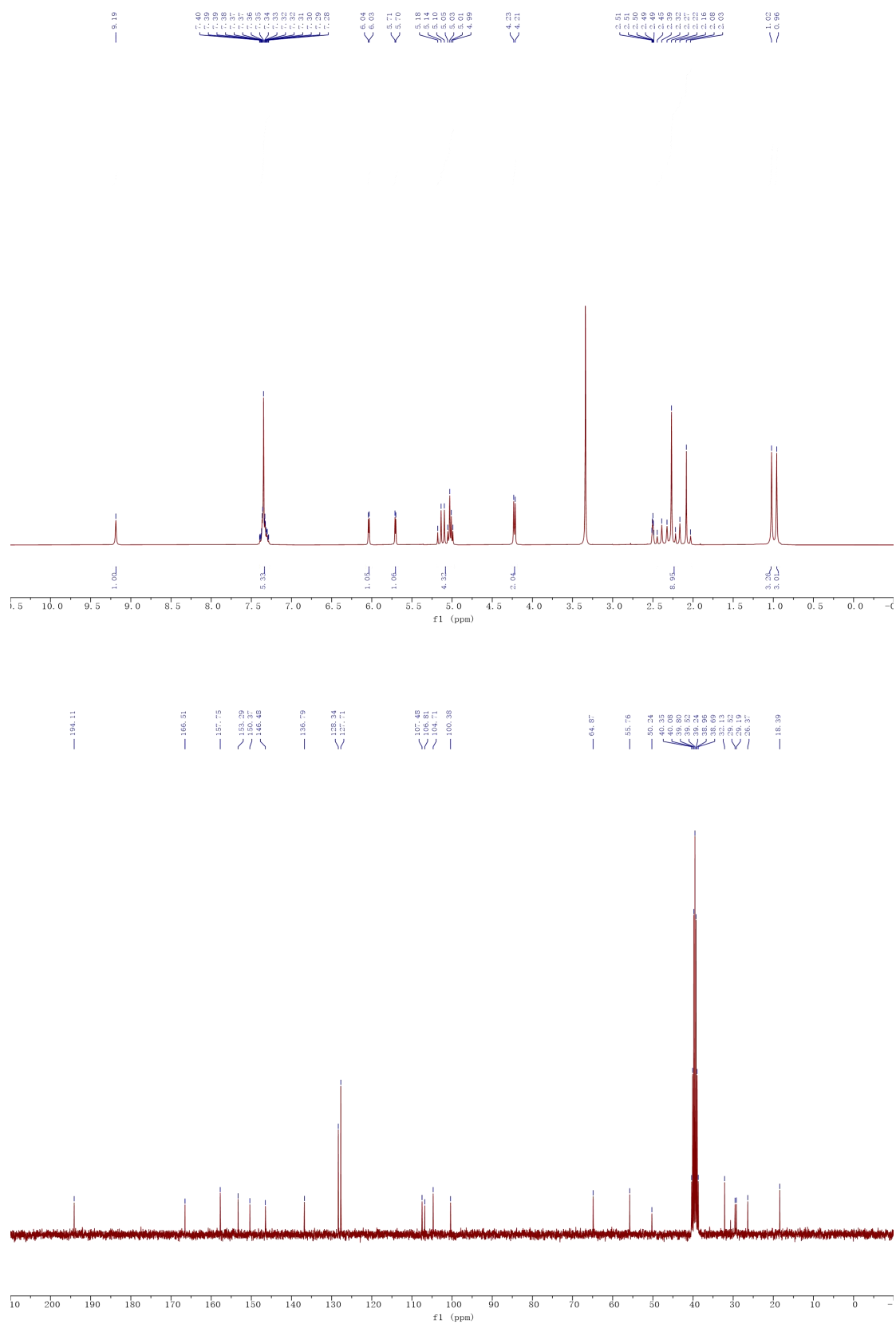




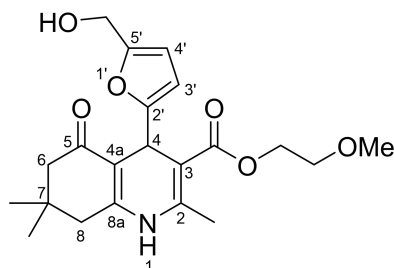
Benzyl 4-[5-(hydroxymethyl)furan-2-yl]-2,7,7-trimethyl-5-oxo-1,4,5,6,7,8-hexahydroquinoline-3-carboxylate (C₂₅H₂₇NO₅)



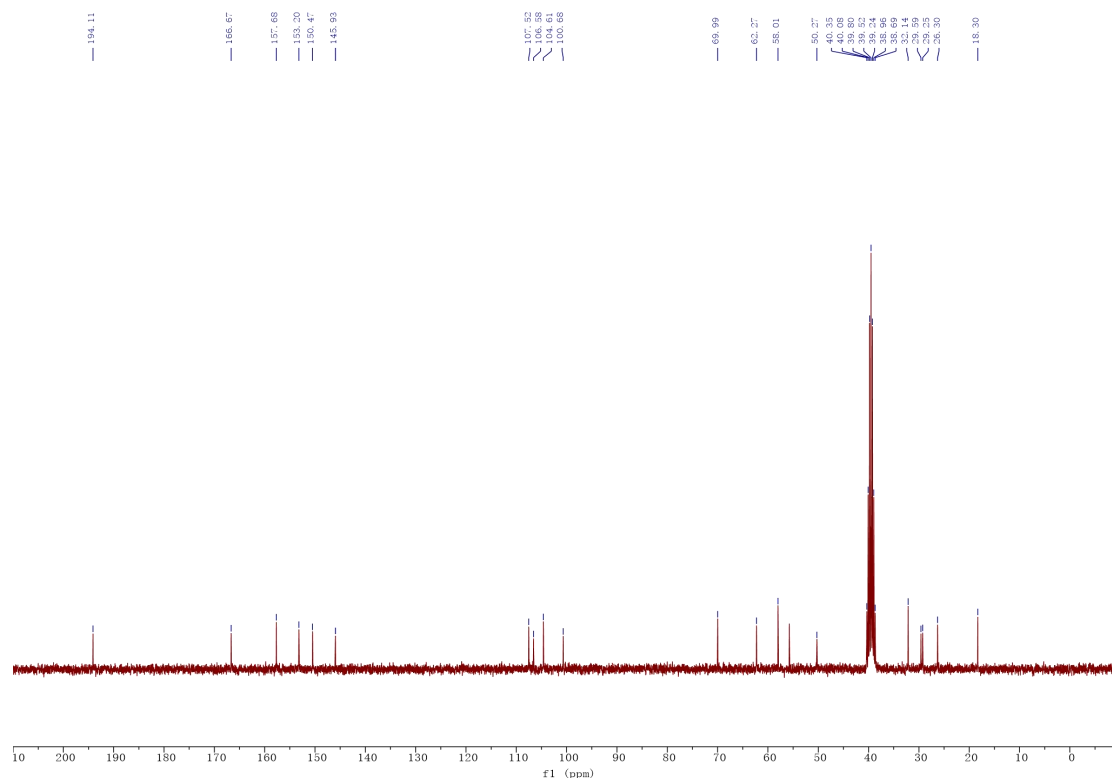
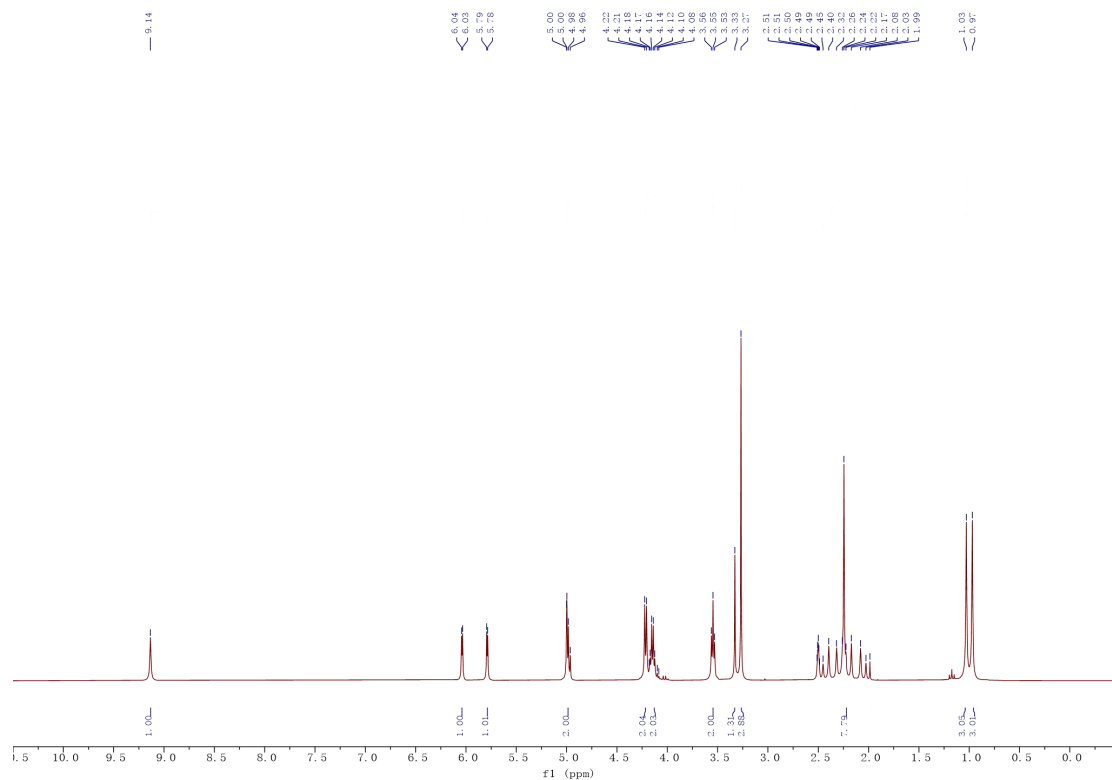
The reaction was carried out at 80 °C for 80 min to give **12c** (371 mg, 88%) as a yellow sugar-like solid. M.p. 126-127 °C. ¹H NMR (300 MHz, DMSO-*d*₆) δ 9.19 (s, 1H, NH), 7.40-7.27 (m, 5H, 5 H_{Ar}), 6.04 (d, *J* = 3.1 Hz, 1H, H_{4'}), 5.71 (d, *J* = 3.1 Hz, 1H, H_{3'}), 5.19-4.97 (m, 4H, H₄, OH, ArCH₂), 4.22 (d, *J* = 5.6 Hz, 2H, CH₂OH), 2.46-2.02 (m, 7H, 2 CH₂, CH₃), 1.02 (s, 3H, CH₃), 0.96 (s, 3H, CH₃). ¹³C NMR (75 MHz, DMSO) δ 194.1 (C=O), 166.5 (C=O₂), 157.7 (C_{2'}), 153.3 (C_{5'}), 150.4 (C_{8a}), 146.5 (C₂), 136.8 (C_{qAr}), 128.3 (2 CH_{Ar}), 127.7 (3 CH_{Ar}), 107.5 (C_{4'}), 106.8 (C_{4a}), 104.7 (C_{3'}), 100.4 (C₃), 64.9 (Ar-CH₂), 55.8 (CH₂OH), 50.2 (CH₂), 39.9 (CH₂), 32.1 (C₇), 29.5 (C₄), 29.2 (CH₃), 26.4 (CH₃), 18.4 (CH₃). HRMS (ESI) *m/z*: Calcd for [M+Na]⁺ C₂₅H₂₇NNaO₅ = 444.1781; Found 444.1771.



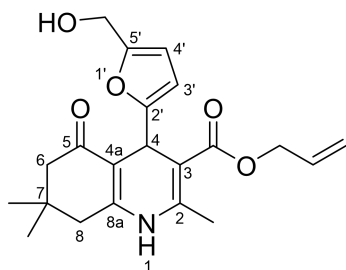
2-Methoxyethyl 4-[5-(hydroxymethyl)furan-2-yl]-2,7,7-trimethyl-5-oxo-1,4,5,6,7,8-hexahydroquinoline-3-carboxylate (C₂₁H₂₇NO₆)



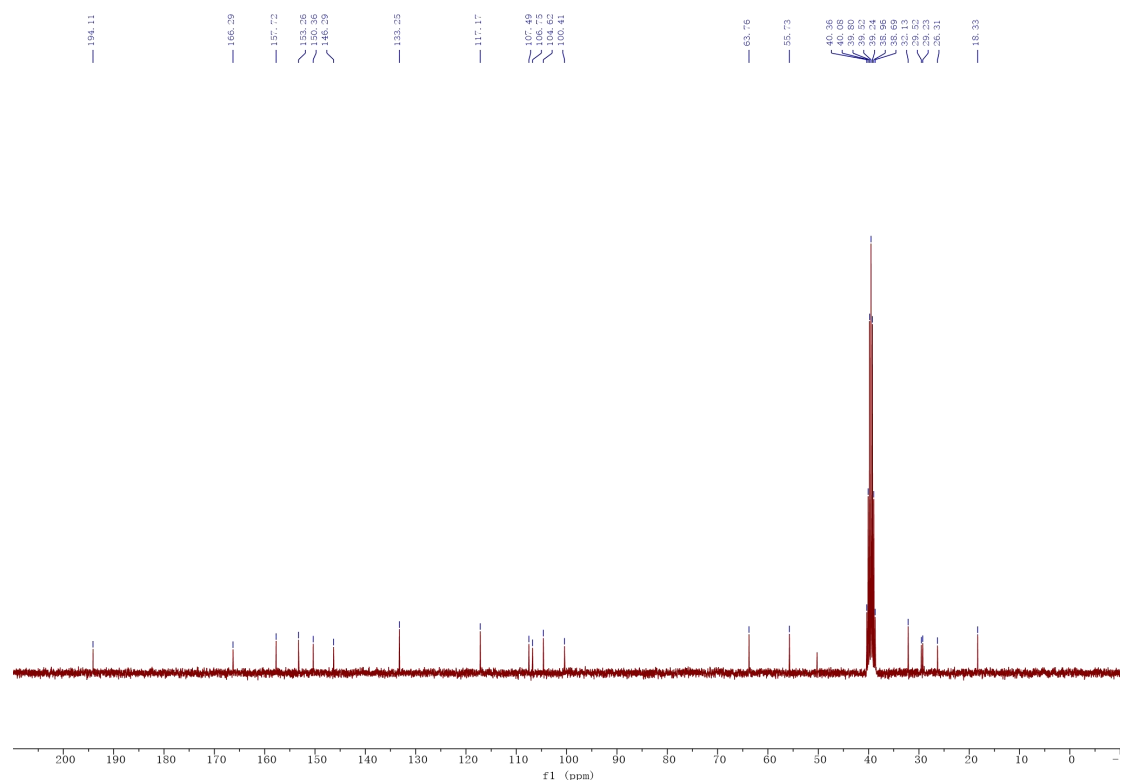
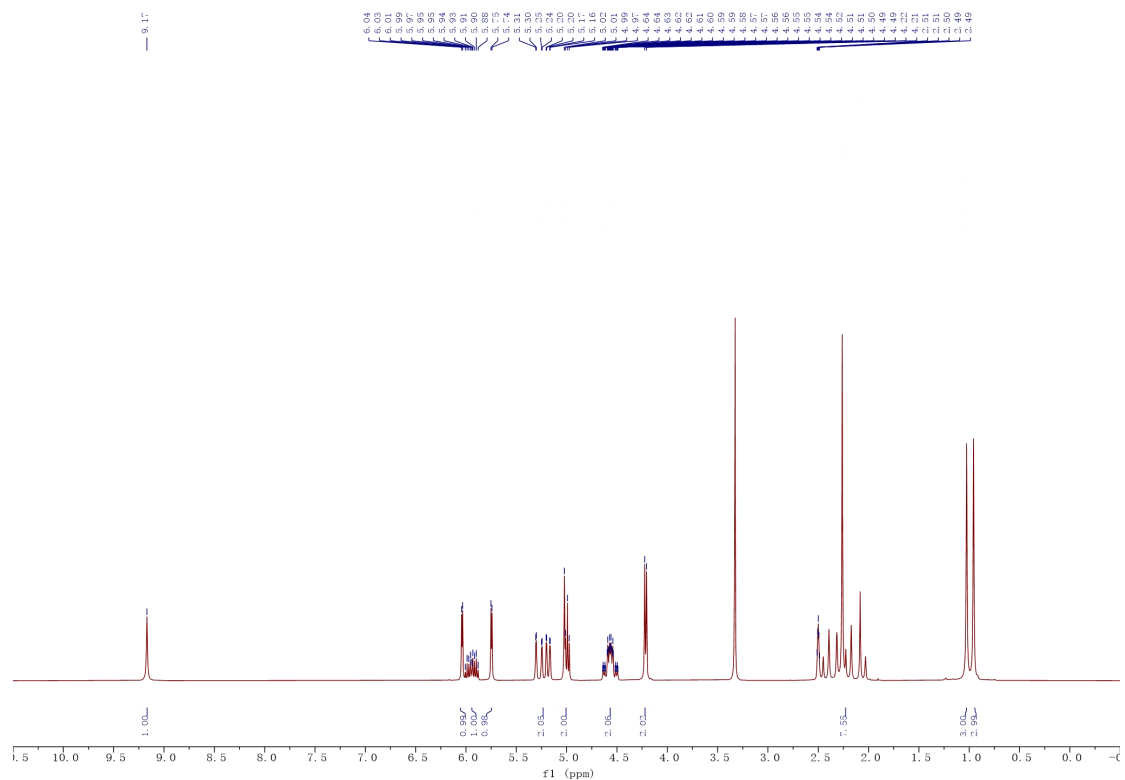
The reaction was carried out at 80 °C for 80 min to give **12d** (315 mg, 81%) as a yellow solid. M.p. 140-142 °C. ¹H NMR (300 MHz, DMSO-*d*₆) δ 9.14 (s, 1H, NH), 6.04 (d, *J* = 3.1 Hz, 1H, H_{4'}), 5.79 (d, *J* = 3.1 Hz, 1H, H_{3'}), 5.05-4.92 (m, 2H, H₄, OH), 4.22 (d, *J* = 5.6 Hz, 2H, CH₂OH), 4.19-4.07 (m, 2H, CO₂CH₂), 3.55 (t, *J* = 4.8 Hz, 2H, CH₂OCH₃), 3.27 (s, 3H, OCH₃), 2.47-1.97 (m, 7H, 2 CH₂, CH₃), 1.03 (s, 3H, CH₃), 0.97 (s, 3H, CH₃). ¹³C NMR (75 MHz, DMSO) δ 194.1 (C=O), 166.7 (C=O₂), 157.7 (C_{2'}), 153.2 (C_{5'}), 150.5 (C_{8a}), 145.9 (C₂), 107.5 (C_{4'}), 106.6 (C_{4a}), 104.6 (C_{3'}), 100.7 (C₃), 70.0 (CH₂OCH₃), 62.3 (COOCH₂), 58.0 (OCH₃), 55.7 (CH₂OH), 50.3 (CH₂), 39.5 (CH₂), 32.1 (C₇), 29.6 (C₄), 29.2 (CH₃), 26.3 (CH₃), 18.3 (CH₃). HRMS (ESI) *m/z*: Calcd for [M+H]⁺ C₂₁H₂₈NO₆ = 390.1911; Found 390.1909. HRMS (ESI) *m/z*: Calcd for [M+Na]⁺ C₂₁H₂₇NNaO₆ = 412.1731; Found 412.1730.



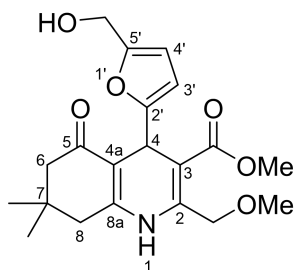
Allyl 4-[5-(hydroxymethyl)furan-2-yl]-2,7,7-trimethyl-5-oxo-1,4,5,6,7,8-hexahydroquinoline-3-carboxylate (C₂₁H₂₅NO₅)



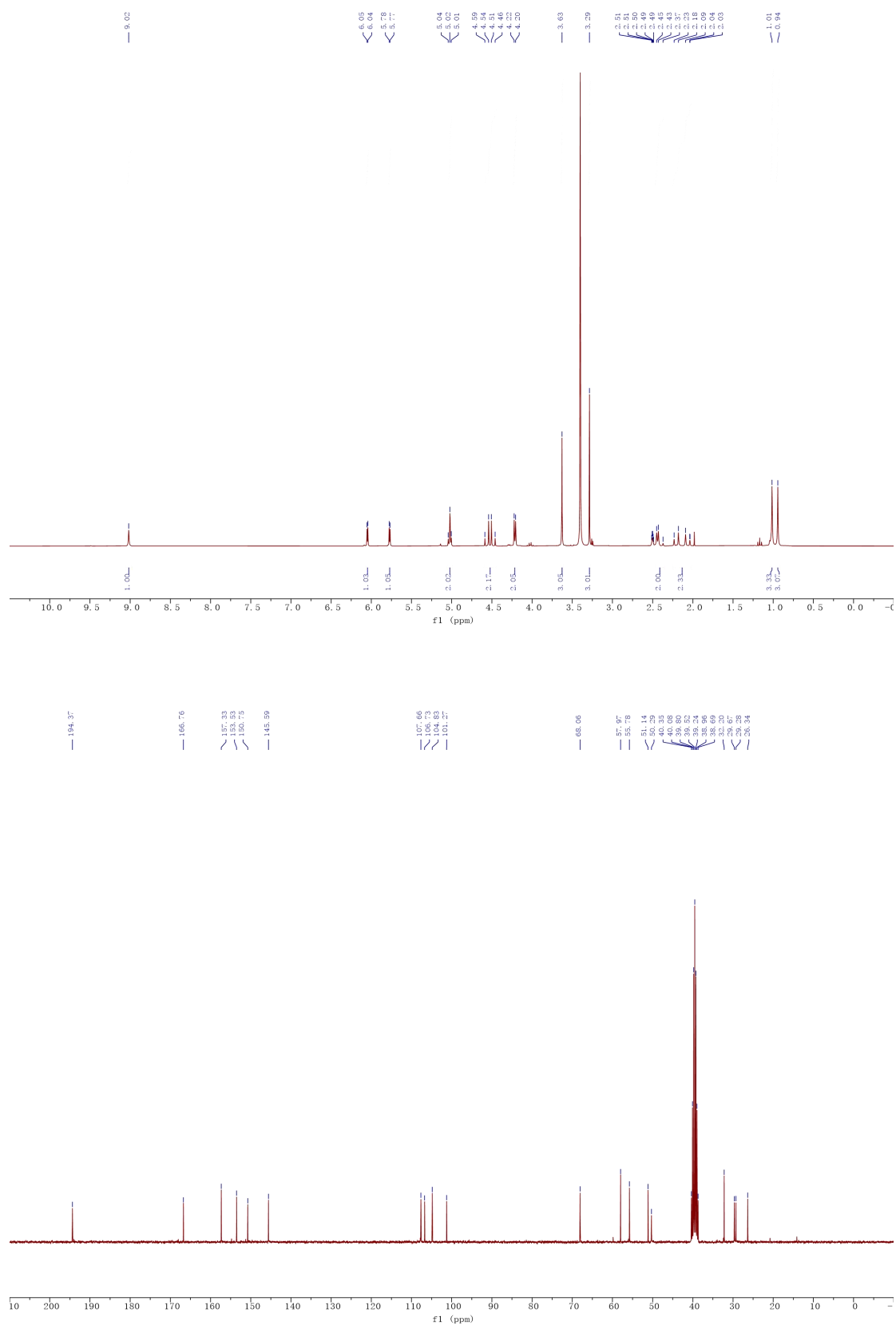
The reaction was carried out at 80 °C for 80 min to give **12e** (296 mg, 80%) as a sugar-like yellow solid. M.p. 120-121 °C. ¹H NMR (300 MHz, DMSO-*d*₆) δ 9.17 (s, 1H, NH), 6.04 (d, *J* = 3.1 Hz, 1H, H_{4'}), 6.02-5.87 (m, 1H, CHCH₂), 5.75 (d, *J* = 3.1 Hz, 1H, H_{3'}), 5.33-5.13 (m, 2H, CHCH₂), 5.06-4.95 (m, 2H, H₄, OH), 4.66-4.47 (m, 2H, OCH₂), 4.22 (d, *J* = 5.6 Hz, 2H, CH₂OH), 2.47-1.99 (m, 7H, 2 CH₂, CH₃), 1.03 (s, 3H, CH₃), 0.96 (s, 3H, CH₃). ¹³C NMR (75 MHz, DMSO) δ 194.1 (C=O), 166.3 (C=O₂), 157.7 (C_{2'}), 153.3 (C_{5'}), 150.4 (C_{8a}), 146.3 (C₂), 133.2 (CHCH₂), 117.2 (CHCH₂), 107.5 (C_{4'}), 106.8 (C_{4a}), 104.6 (C_{3'}), 100.4 (C₃), 63.8 (OCH₂), 55.7 (CH₂OH), 50.2 (CH₂), 39.5 (CH₂), 32.1 (C₇), 29.5 (C₄), 29.2 (CH₃), 26.3 (CH₃), 18.3 (C₂-CH₃). HRMS (ESI) *m/z*: Calcd for [M+Na]⁺ C₂₁H₂₅NNaO₅ = 394.1625; Found 394.1615.



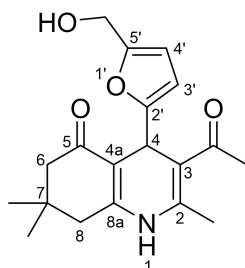
Methyl 4-[5-(hydroxymethyl)furan-2-yl]-2-(methoxymethyl)-7,7-dimethyl-5-oxo-1,4,5,6,7,8-hexahydroquinoline-3-carboxylate (C₂₀H₂₅NO₆)



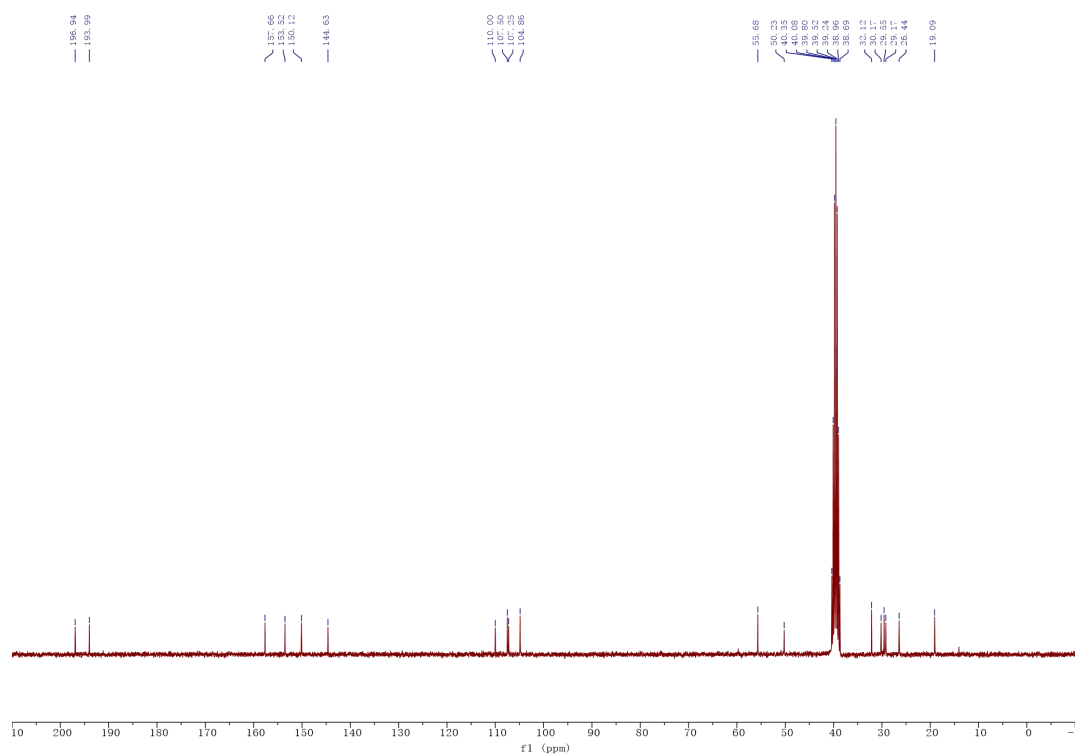
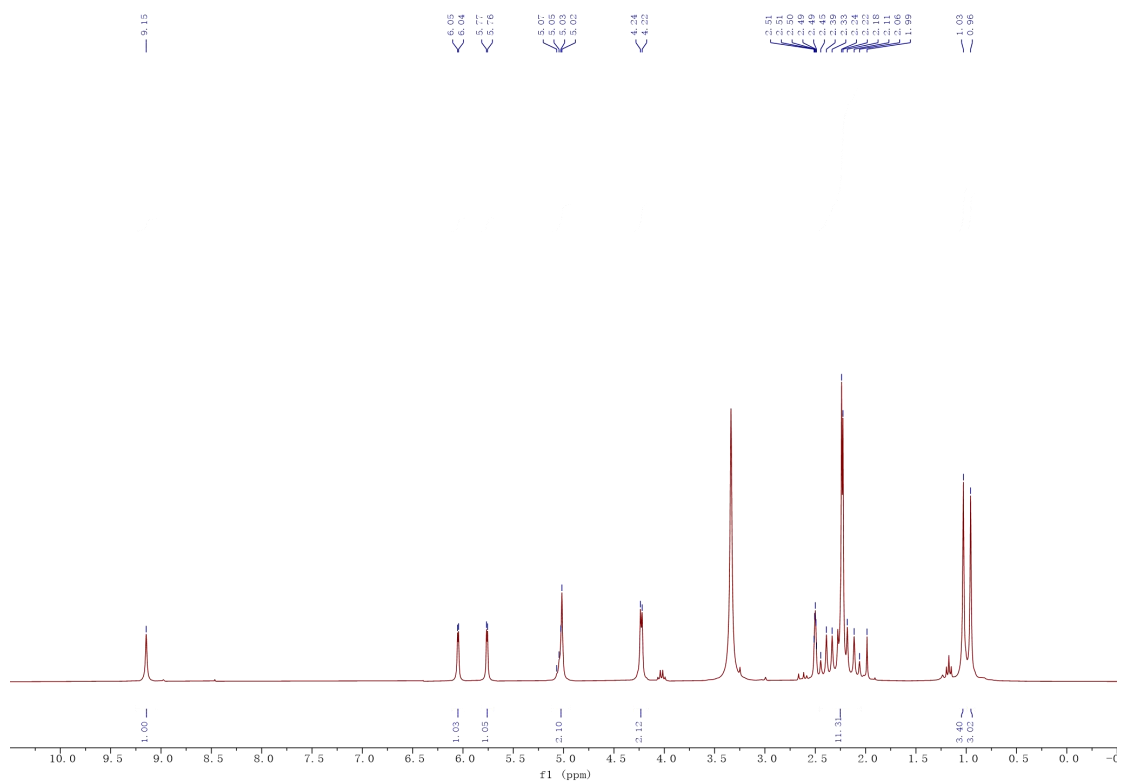
The reaction was carried out at 80 °C for 80 min to give **12f** (170 mg, 45%) as a gummy yellow product. ¹H NMR (300 MHz, DMSO-*d*₆) δ 9.02 (s, 1H, NH), 6.05 (d, *J* = 3.1 Hz, 1H, H_{4'}), 5.77 (d, *J* = 3.1 Hz, 1H, H_{3'}), 5.06-4.99 (m, 2H, H₄, OH), 4.60-4.44 (m, 2H, CH₂OCH₃), 4.21 (d, *J* = 5.6 Hz, 2H, CH₂OH), 3.63 (s, 3H, CO₂CH₃), 3.29 (s, 3H, CH₂OCH₃), 2.47-2.35 (m, 2H, CH₂), 2.25-2.02 (m, 2H, CH₂), 1.01 (s, 3H, CH₃), 0.94 (s, 3H, CH₃). ¹³C NMR (75 MHz, DMSO) δ 194.4 (C=O), 166.8 (C=O₂), 157.3 (C_{2'}), 153.5 (C_{5'}), 150.7 (C_{8a}), 145.6 (C₂), 107.7 (C_{4'}), 106.7 (C_{4a}), 104.8 (C_{3'}), 101.3 (C₃), 68.1 (CH₂OCH₃), 58.0 (CH₂OCH₃), 55.8 (CH₂OH), 51.1 (CO₂CH₃), 50.3 (CH₂), 39.5 (CH₂), 32.2 (C₇), 29.7 (C₄), 29.3 (CH₃), 26.3 (CH₃). HRMS (ESI) *m/z*: Calcd for [M+Na]⁺ C₂₀H₂₅NNaO₆ = 398.1574; Found 398.1573; Calcd for [2M+Na]⁺ C₄₀H₅₀N₂NaO₁₂ = 773.3256; Found 773.3249.



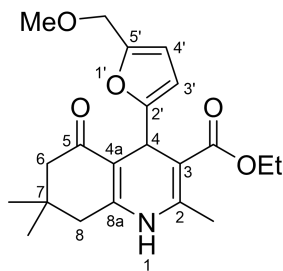
3-Acetyl-4-[5-(hydroxymethyl)furan-2-yl]-2,7,7-trimethyl-4,6,7,8-tetrahydroquinolin-5(1H)-one (C₁₉H₂₃NO₄)



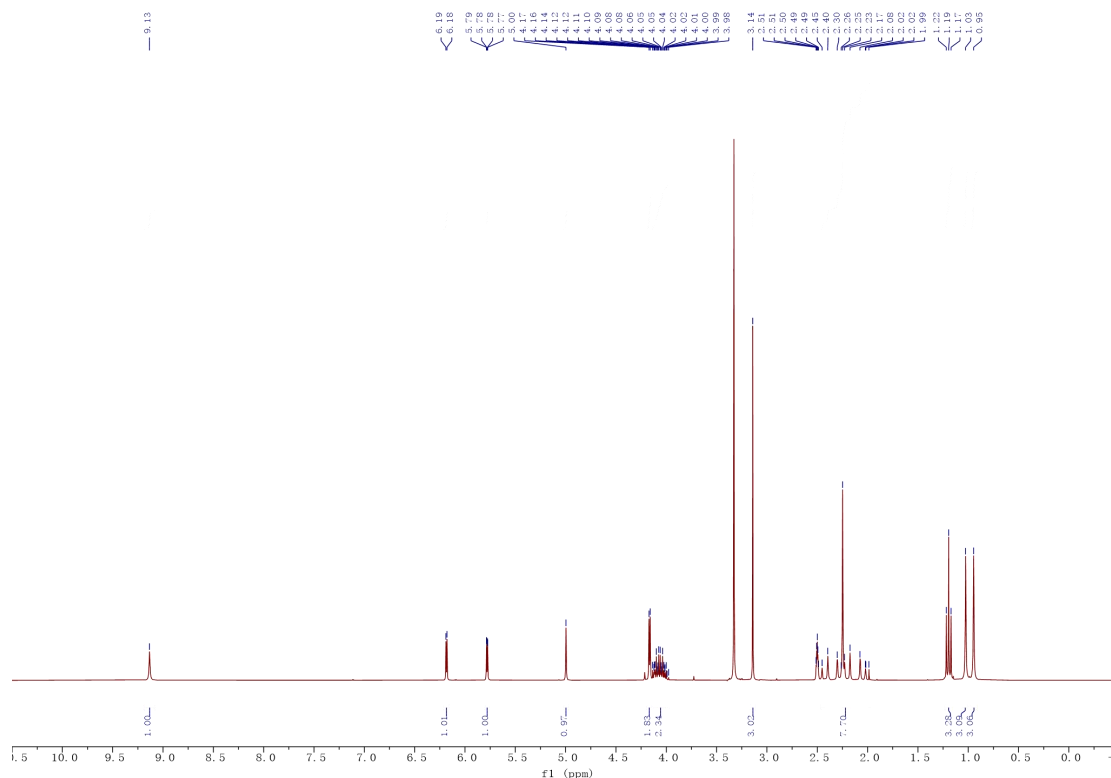
The reaction was carried out at 80 °C for 80 min to give **12g** (200 mg, 61%) as a yellow solid. M.p. 47-49 °C. ¹H NMR (300 MHz, DMSO-*d*₆) δ 9.15 (s, 1H, NH), 6.05 (d, *J* = 3.1 Hz, 1H, H_{4'}), 5.76 (d, *J* = 3.1 Hz, 1H, H_{3'}), 5.12-4.93 (m, 2H, H₄, OH), 4.23 (d, *J* = 5.1 Hz, 2H, CH₂OH), 2.46-2.04 (m, 10H, 2 CH₂, CH₃, COCH₃), 1.03 (s, 3H, CH₃), 0.96 (s, 3H, CH₃). ¹³C NMR (75 MHz, DMSO) δ 196.9 (COCH₃), 194.0 (CO), 157.7 (C_{2'}), 153.5 (C_{5'}), 150.1 (C_{8a}), 144.6 (C₂), 110.0 (C₃), 107.5 (C_{4'}), 107.3 (C_{4a}), 104.9 (C_{3'}), 55.7 (CH₂OH), 50.2 (CH₂), 39.5 (CH₂), 32.1 (C₇), 30.2 (C₄), 29.5 (COCH₃), 29.2 (CH₃), 26.4 (CH₃), 19.1 (CH₃). HRMS (ESI) *m/z*: Calcd for [M+Na]⁺ C₁₉H₂₃NNaO₄ = 352.1519; Found 352.1516; Calcd for [2M+Na]⁺ C₃₈H₄₆N₂NaO₈ = 681.3146; Found 681.3135.

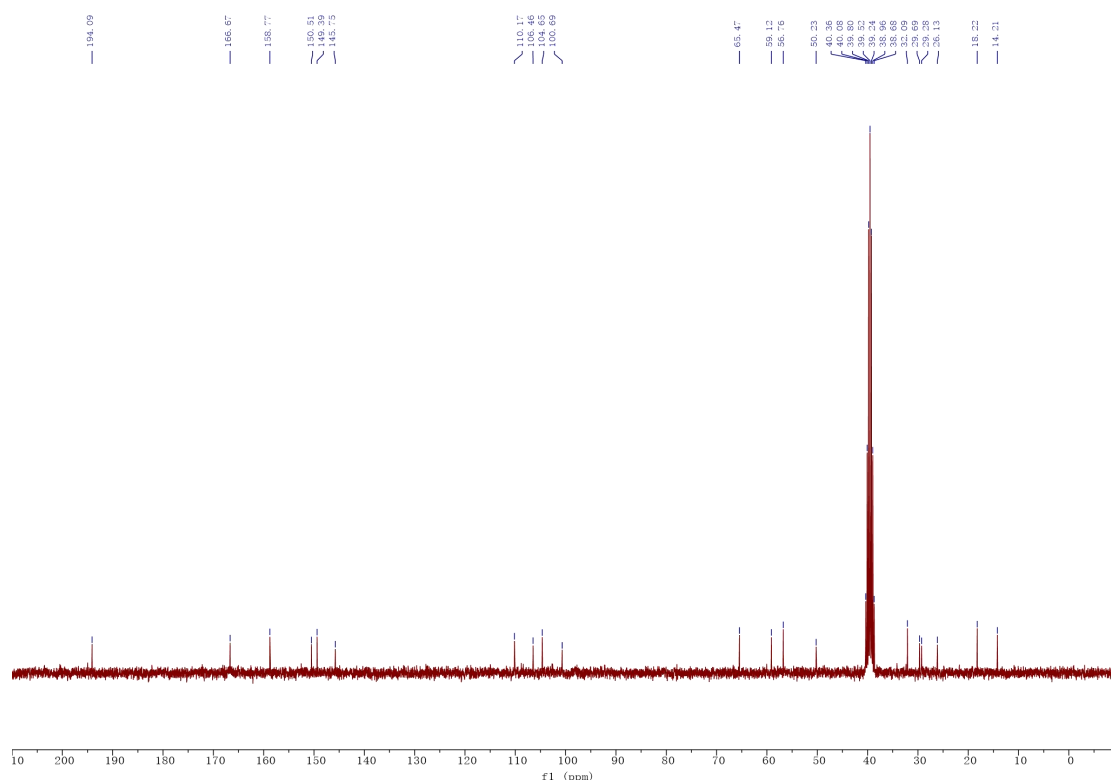


Ethyl 4-[5-(methoxymethyl)furan-2-yl]-2,7,7-trimethyl-5-oxo-1,4,5,6,7,8-hexahydroquinoline-3-carboxylate (C₂₁H₂₇NO₅)

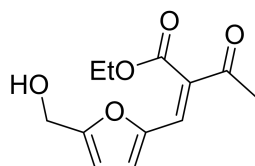


The reaction was carried out at 80 °C for 80 min to give **12h** (270 mg, 72%) as a yellow solid. M.p. 135-136 °C. ¹H NMR (300 MHz, DMSO-*d*₆) δ 9.13 (s, 1H NH), 6.18 (d, *J* = 3.1 Hz, 1H, H_{4'}), 5.78 (dd, *J* = 3.1, 0.7 Hz, 1H, H_{3'}), 5.00 (s, 1H, H₄), 4.17 (d, *J* = 3.4 Hz, 2H, CH₂OCH₃), 4.14-3.97 (m, 2H, CH₂CH₃), 3.14 (s, 3H, OCH₃), 2.46-1.98 (m, 7H, 2 CH₂, CH₃), 1.19 (t, *J* = 7.1 Hz, 3H, OCH₂CH₃), 1.03 (s, 3H, CH₃), 0.95 (s, 3H, CH₃). ¹³C NMR (75 MHz, DMSO) δ 194.1 (C=O), 166.7 (CO₂), 158.8 (C_{2'}), 150.5 (C_{8a}), 149.4 (C_{5'}), 145.8 (C₂), 110.2 (C_{4'}), 106.5 (C_{4a}), 104.6 (C_{3'}), 100.7 (C₃), 65.5 (CH₂OCH₃), 59.1 (OCH₂CH₃), 56.8 (OCH₃), 50.2 (CH₂), 39.5 (CH₂), 32.1 (C₇), 29.7 (C₄), 29.3 (CH₃), 26.1 (CH₃), 18.2 (CH₃), 14.2 (OCH₂CH₃). HRMS (ESI) *m/z*: Calcd for [M+Na]⁺ C₂₁H₂₇NNaO₅ = 396.1781; Found 396.1780; Calcd for [2M+Na]⁺ C₄₂H₅₄N₂NaO₁₀ = 769.3671; Found 769.3663.



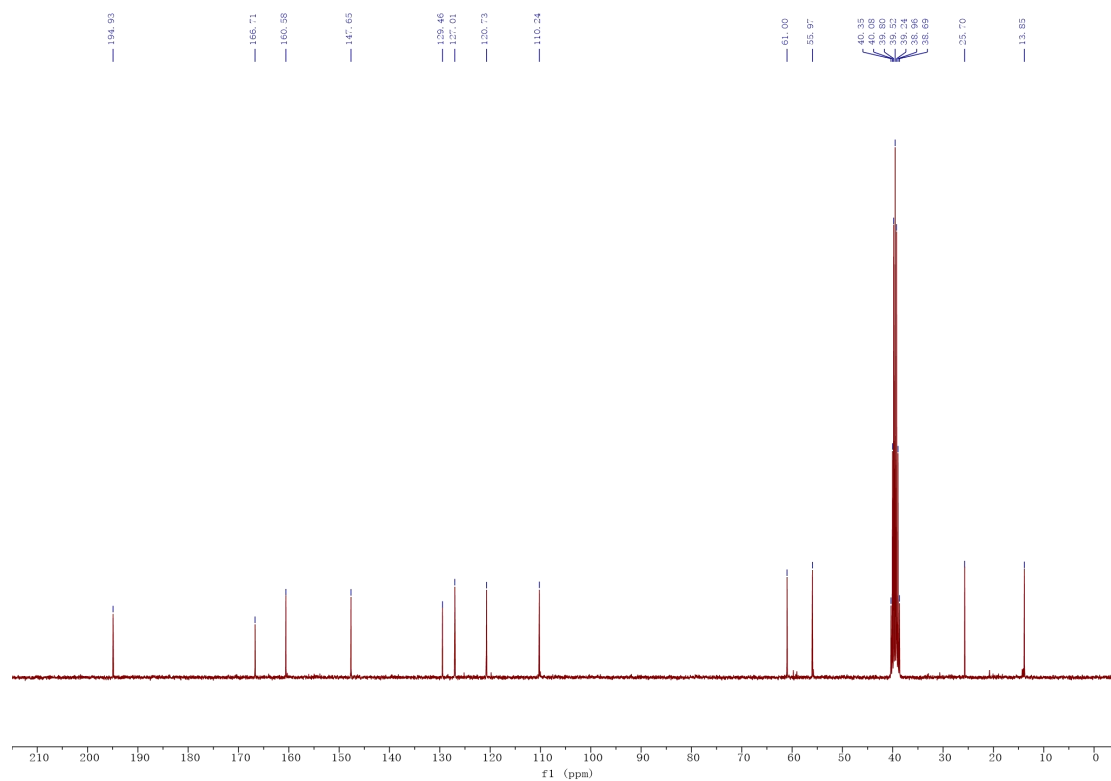
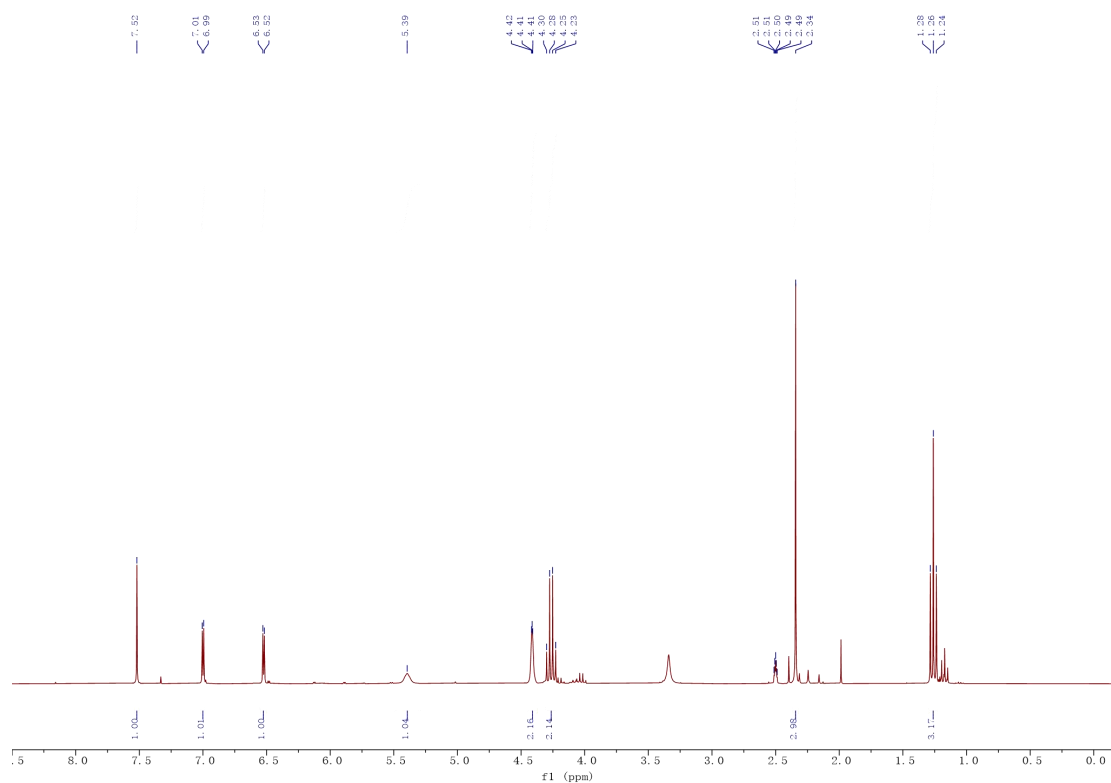


Ethyl (Z)-2-((5-(hydroxymethyl)furan-2-yl)methylene)-3-oxobutanoate (major Intermediate N, $C_{12}H_{14}O_5$)



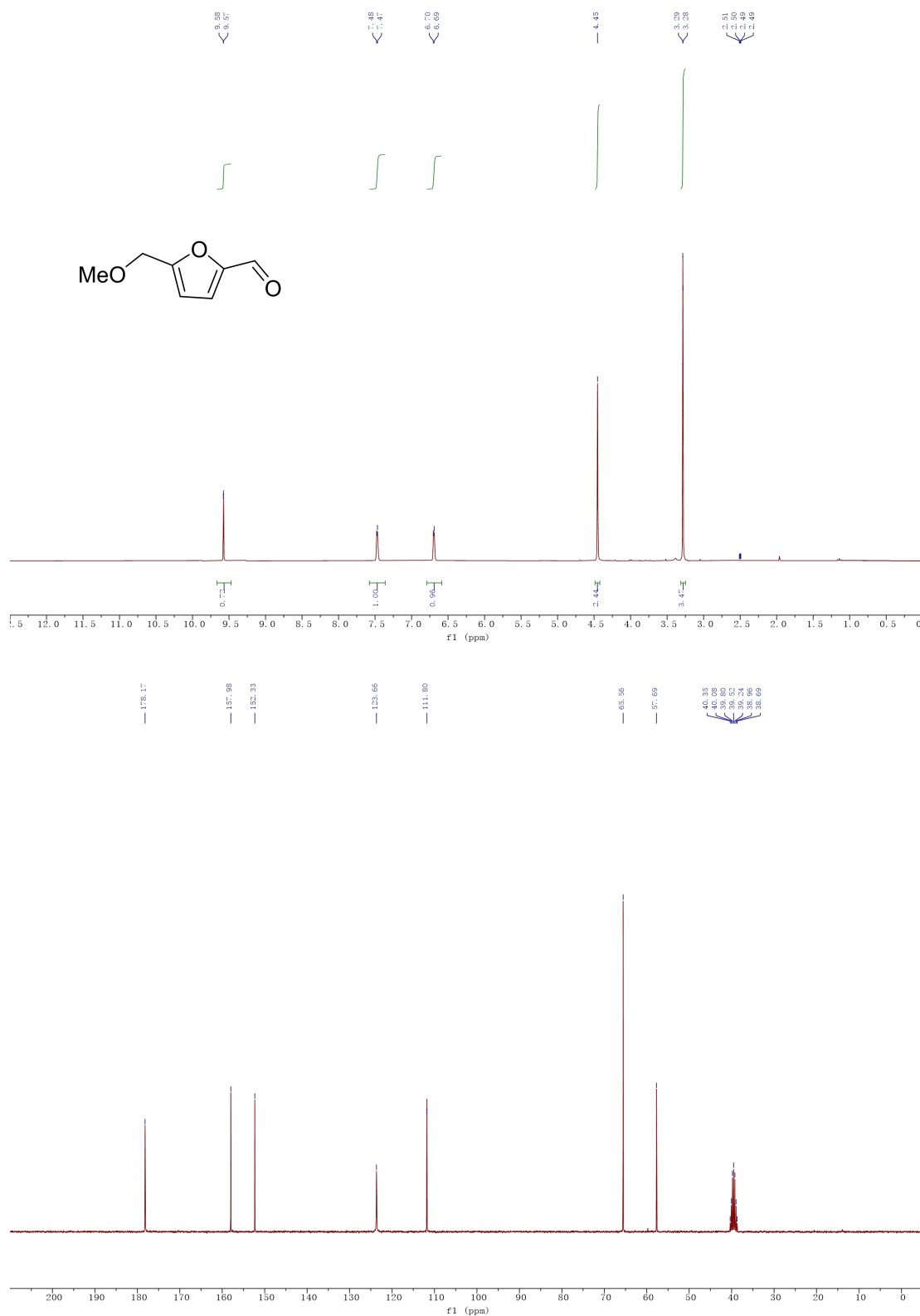
Intermediate N (the major one) was isolated as pale-yellow liquid.

1H NMR (300 MHz, $DMSO-d_6$) δ 7.52 (s, 1H, CH), 7.00 (d, $J = 3.4$ Hz, 1H, CH_{fur}), 6.52 (d, $J = 3.4$ Hz, 1H, CH_{fur}), 5.39 (s, 1H, OH), 4.45-4.37 (m, 2H, CH_2OH), 4.26 (q, $J = 7.1$ Hz, 2H, CH_2CH_3), 2.34 (s, 3H, $COCH_3$), 1.26 (t, $J = 7.1$ Hz, 3H, CH_2CH_3). ^{13}C NMR (75 MHz, DMSO) δ 194.9 ($COCH_3$), 166.7 (CO_2Et), 160.6 (C_{fur}), 147.6 (C_{fur}), 129.5 ($C=CH$), 127.0 (CH), 120.7 (CH_{fur}), 110.2 (CH_{fur}), 61.0 (CH_2CH_3), 56.0 (CH_2OH), 25.7 ($COCH_3$), 13.9 (CH_2CH_3). MS (ESI) m/z : found $[M+H]^+$ $C_{12}H_{15}O_5 = 239.1$, $[M+Na]^+$ $C_{12}H_{14}O_5Na = 261.1$, $[2M+Na]^+$ $C_{24}H_{28}O_{10}Na = 499.1$.

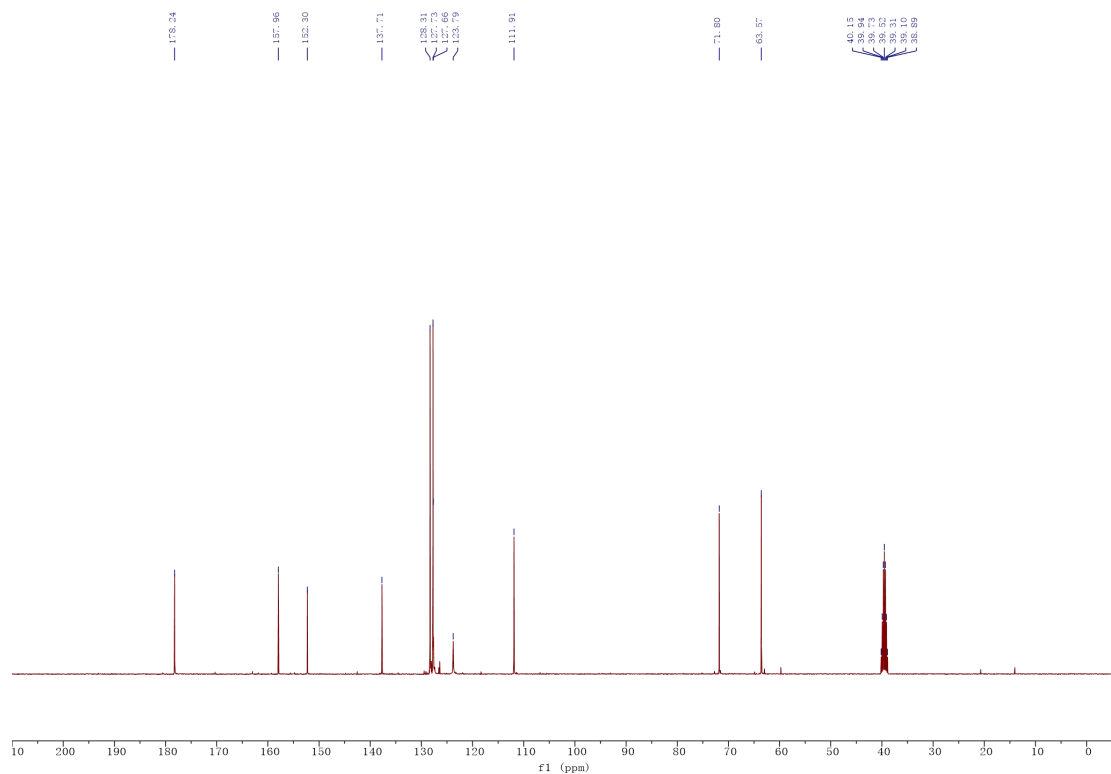
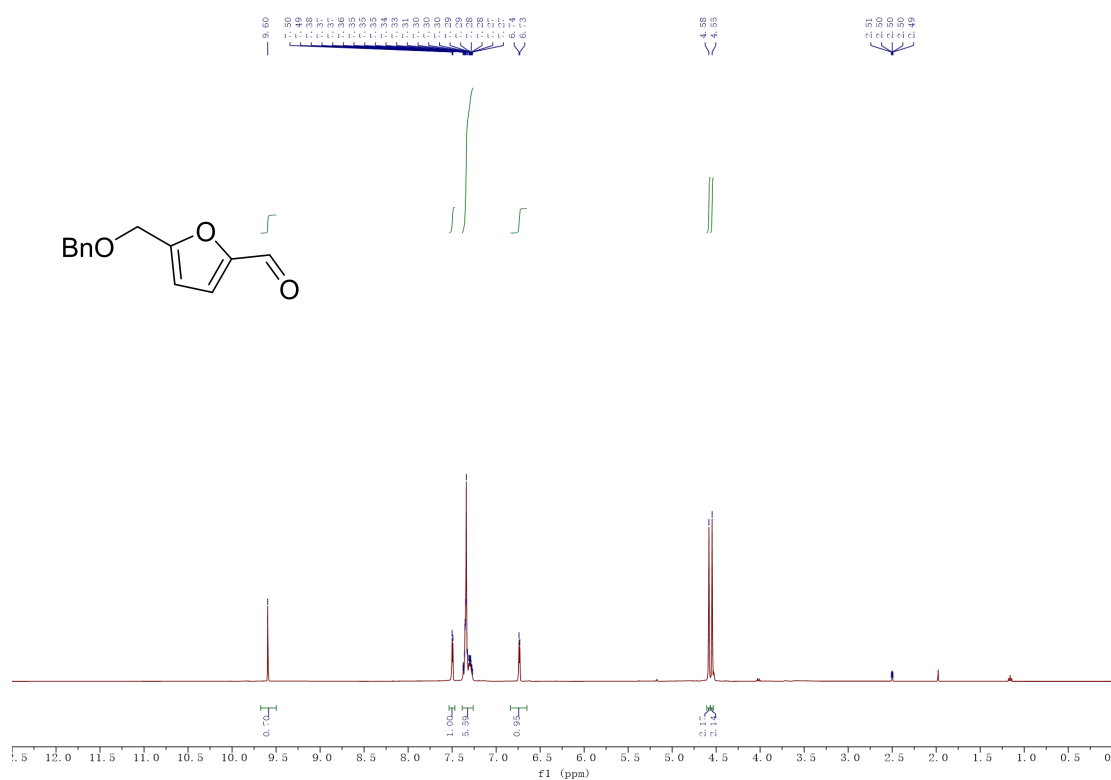


4. Spectrum of prepared substrates

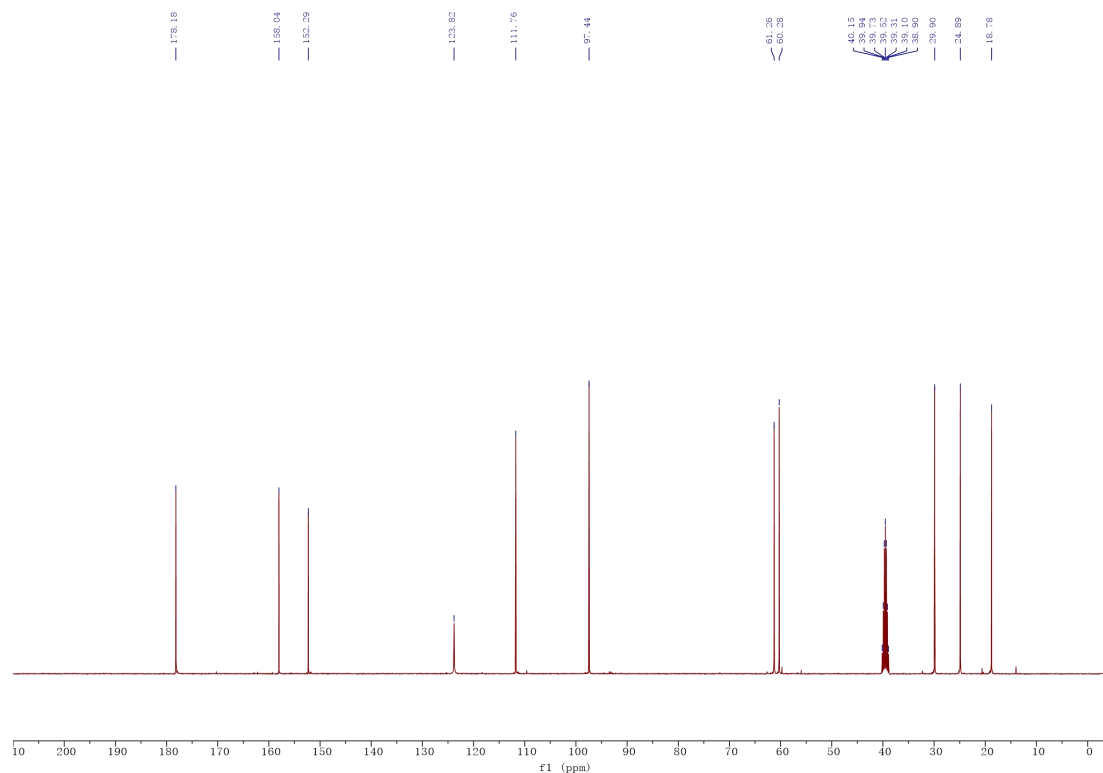
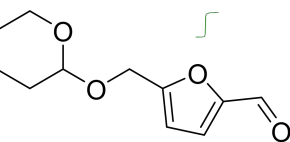
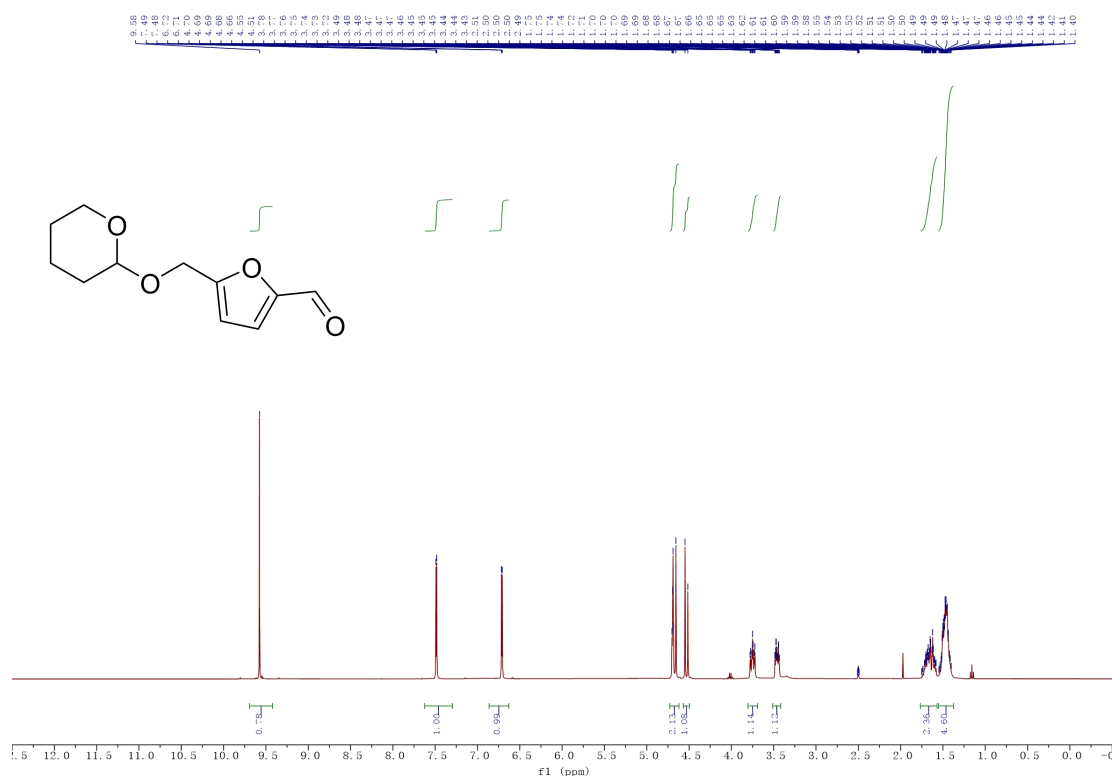
5-Methoxymethylfuran-2-carbaldehyde (C₇H₈O₃)



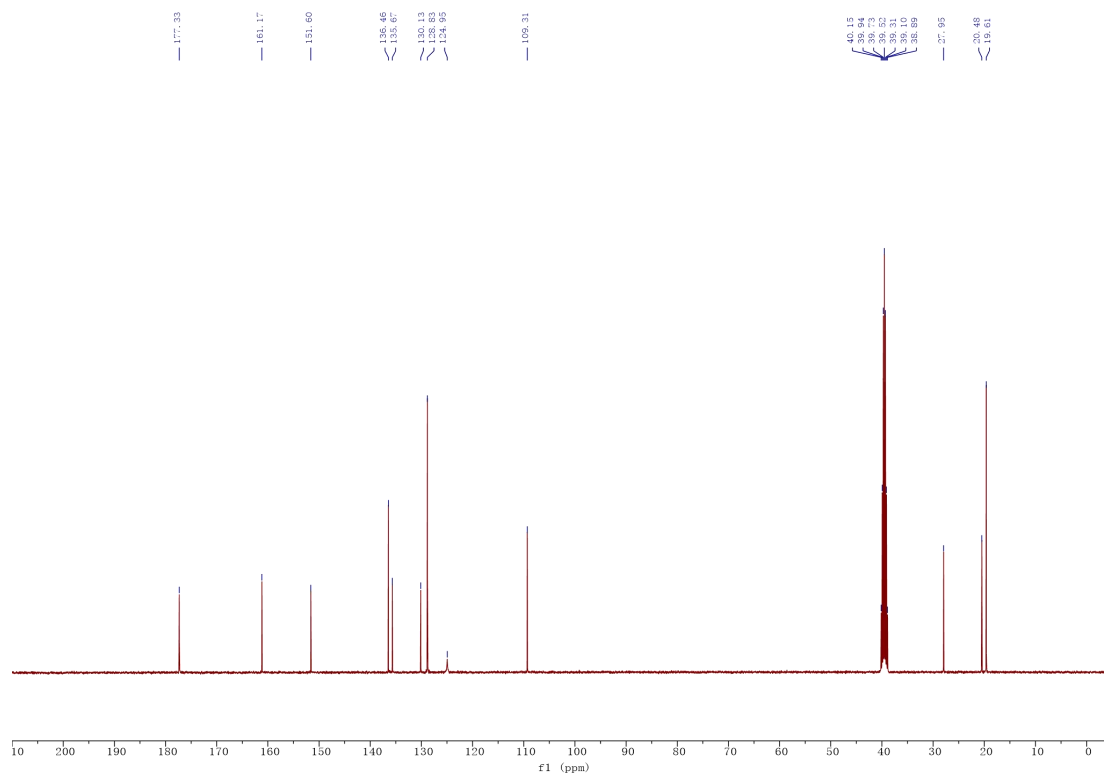
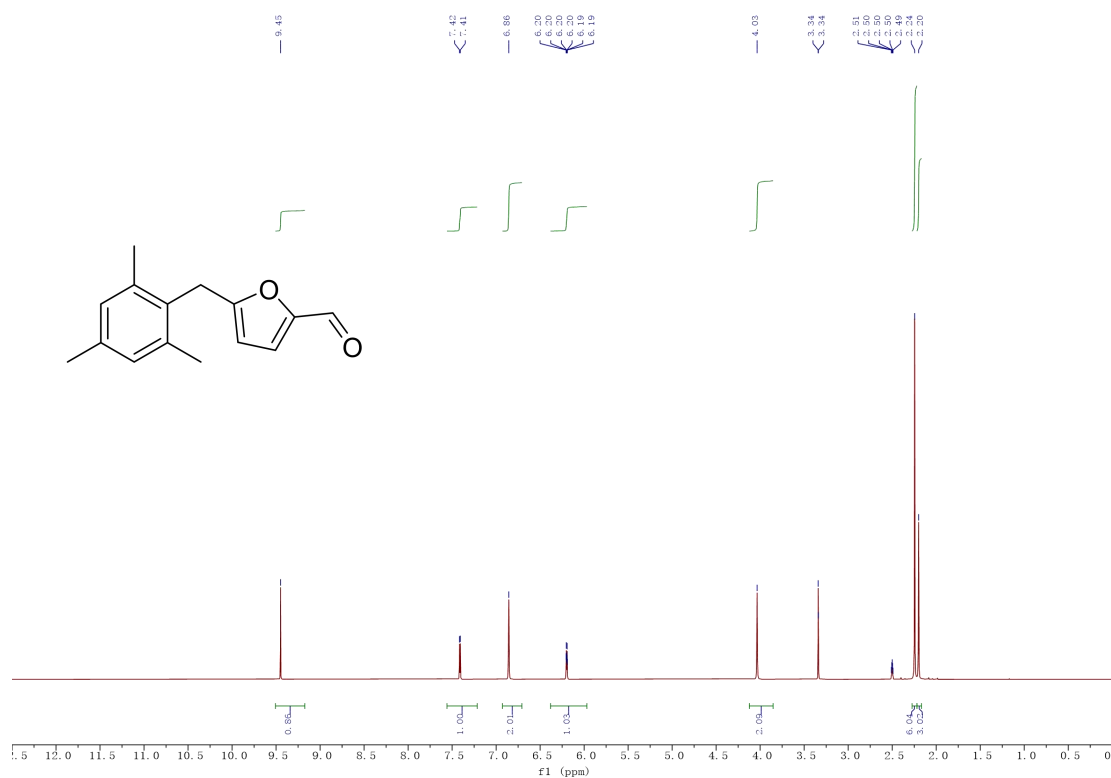
5-((Benzyloxy)methyl)furan-2-carbaldehyde (C₁₃H₁₂O₃)



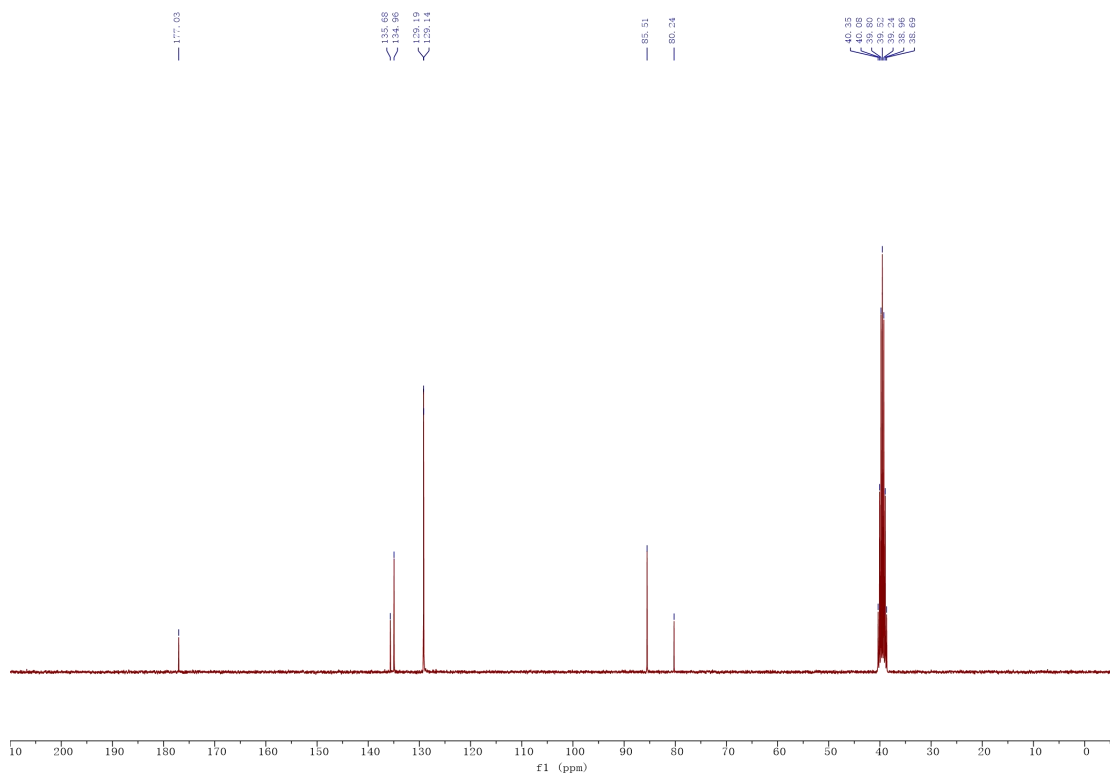
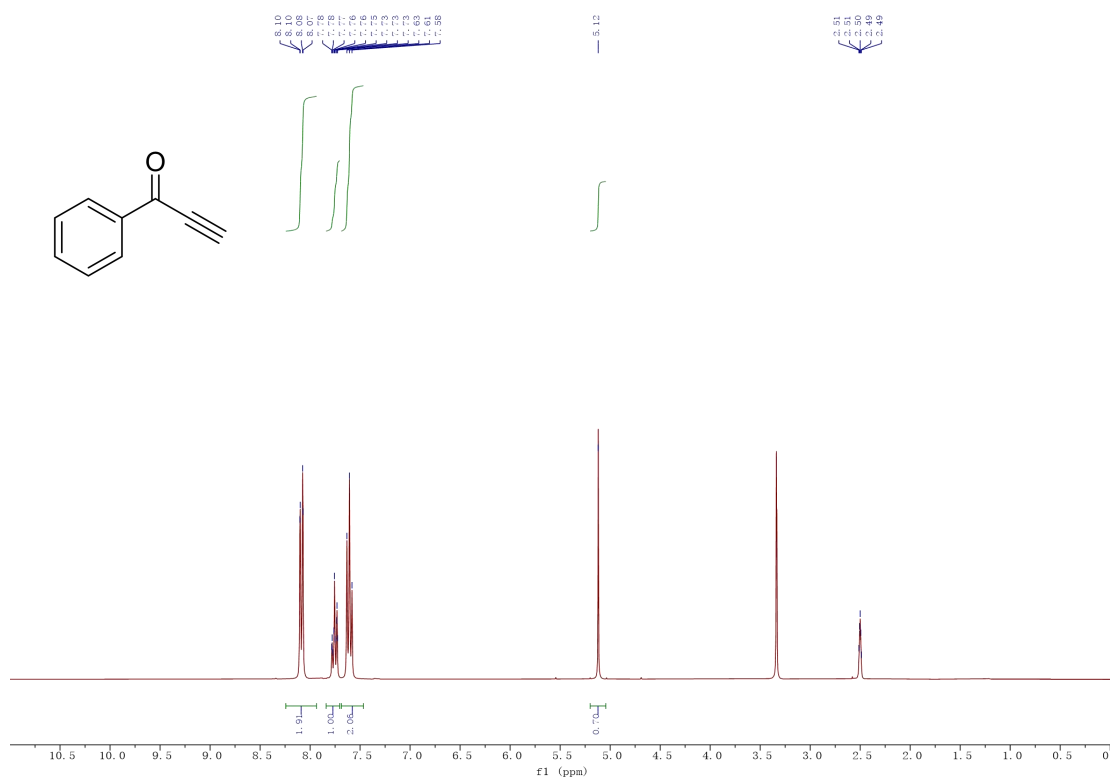
5-(((Tetrahydro-2H-pyran-2-yl)oxy)methyl)furan-2-carbaldehyde (C₁₁H₁₄O₄)



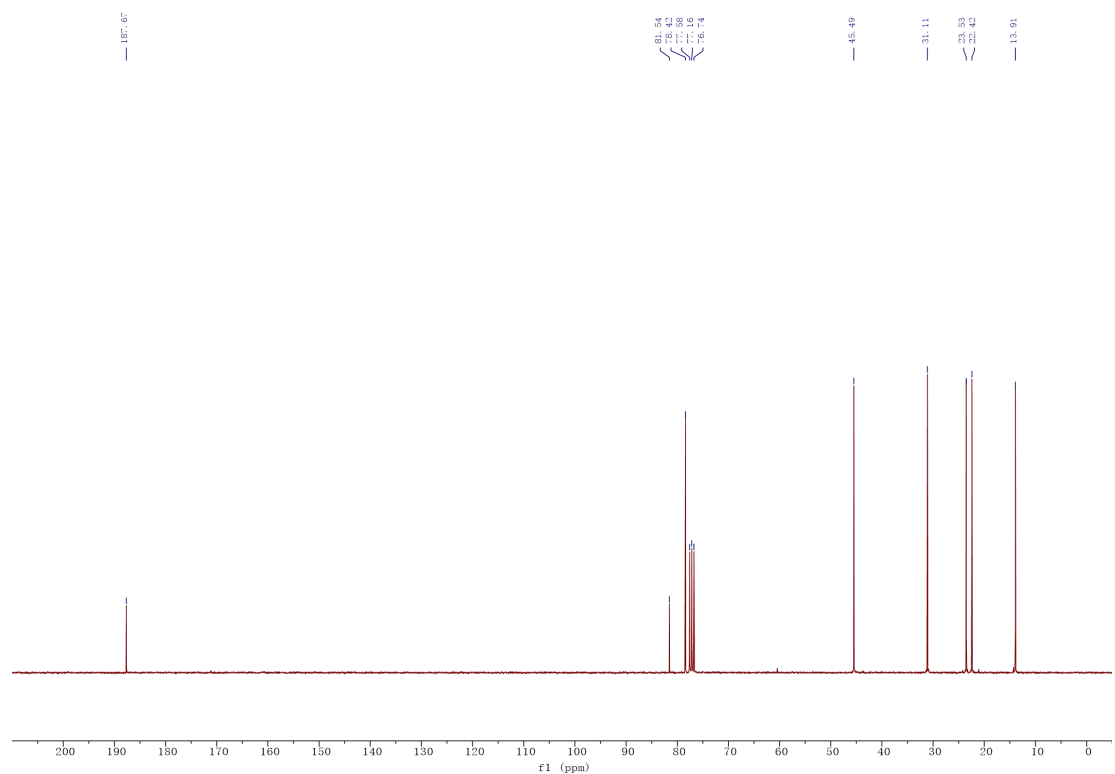
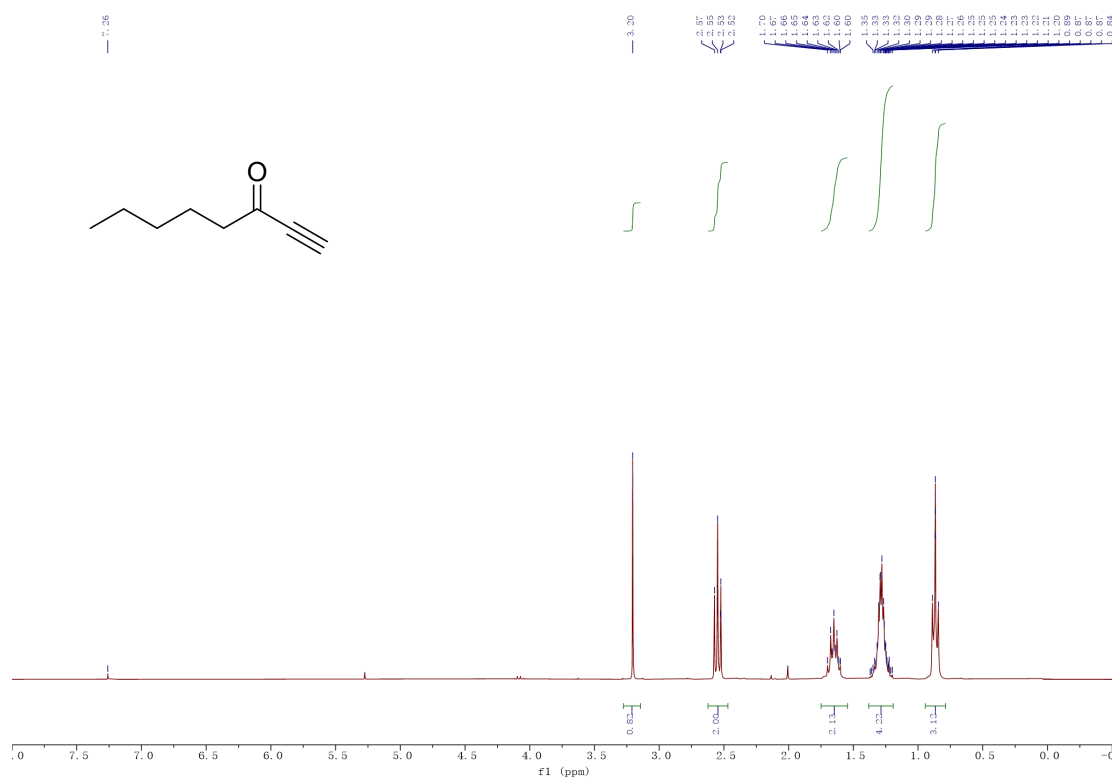
5-(2,4,6-Trimethylbenzyl)furan-2-carbaldehyde (C₁₅H₁₆O₂)



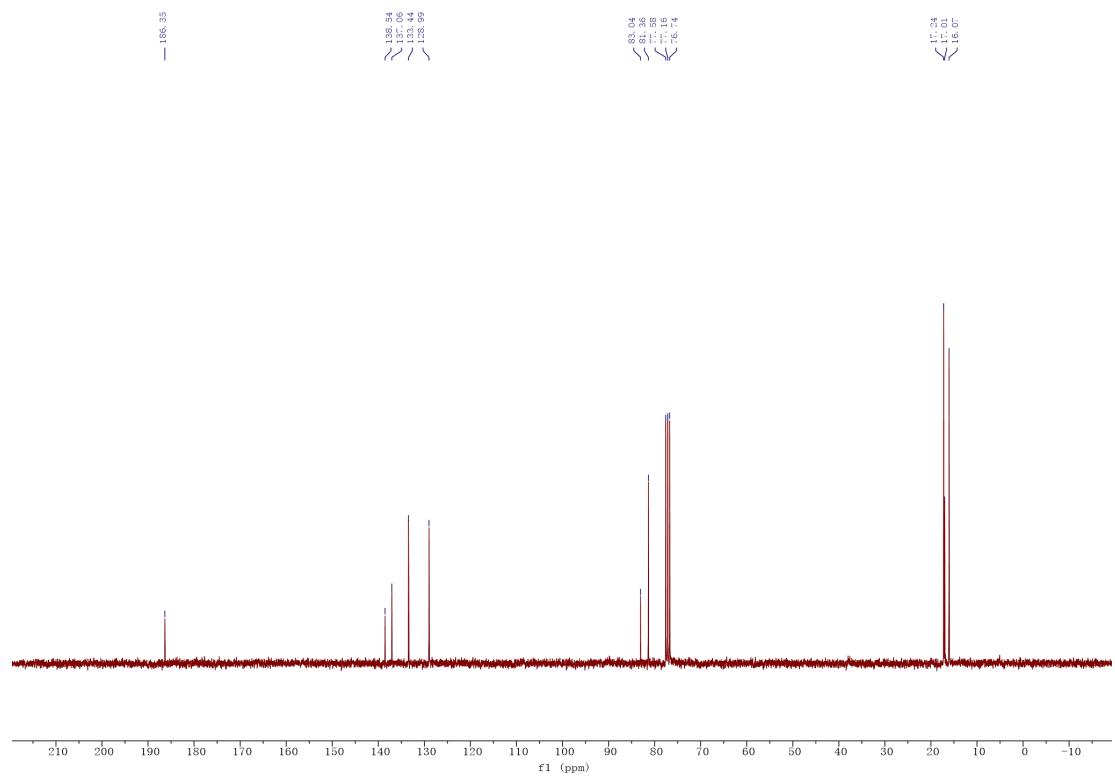
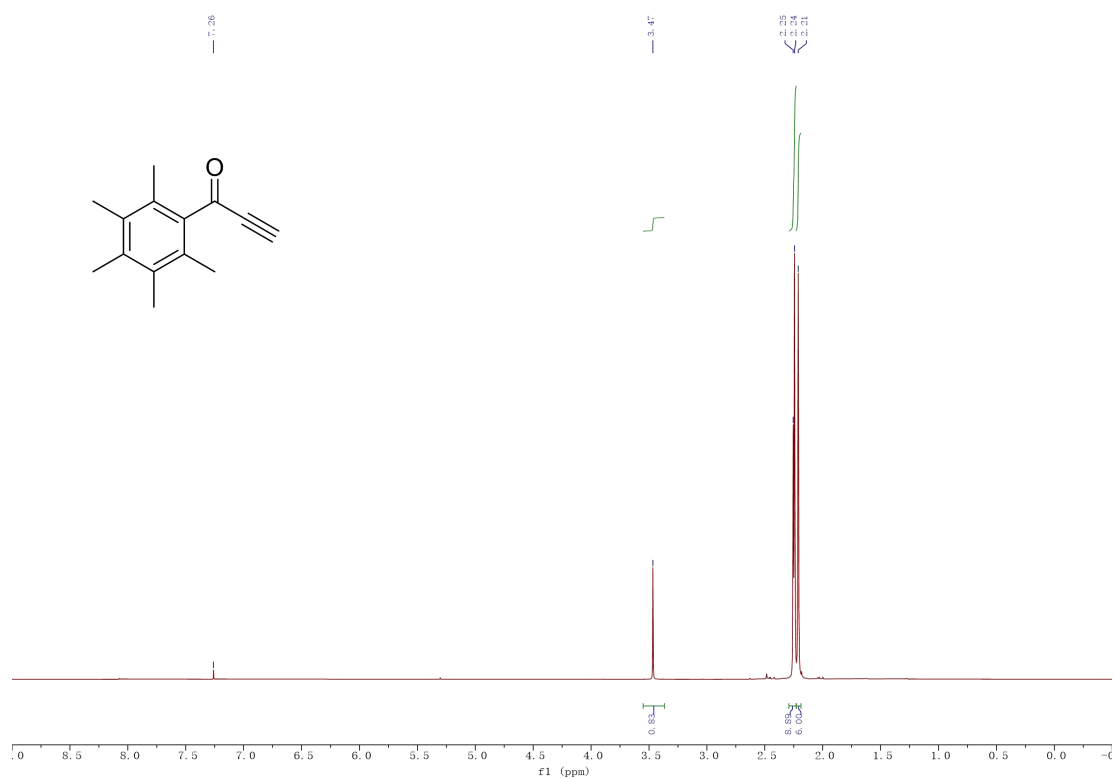
1-Phenylprop-2-yn-1-one (C₉H₆O)



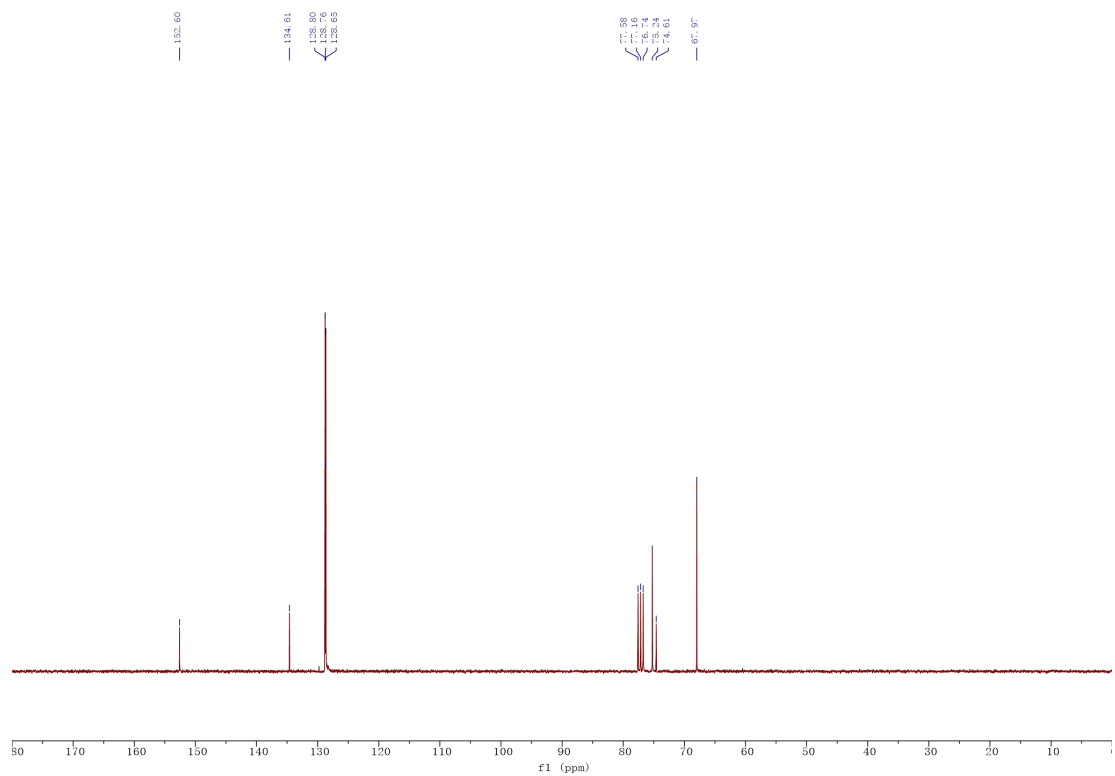
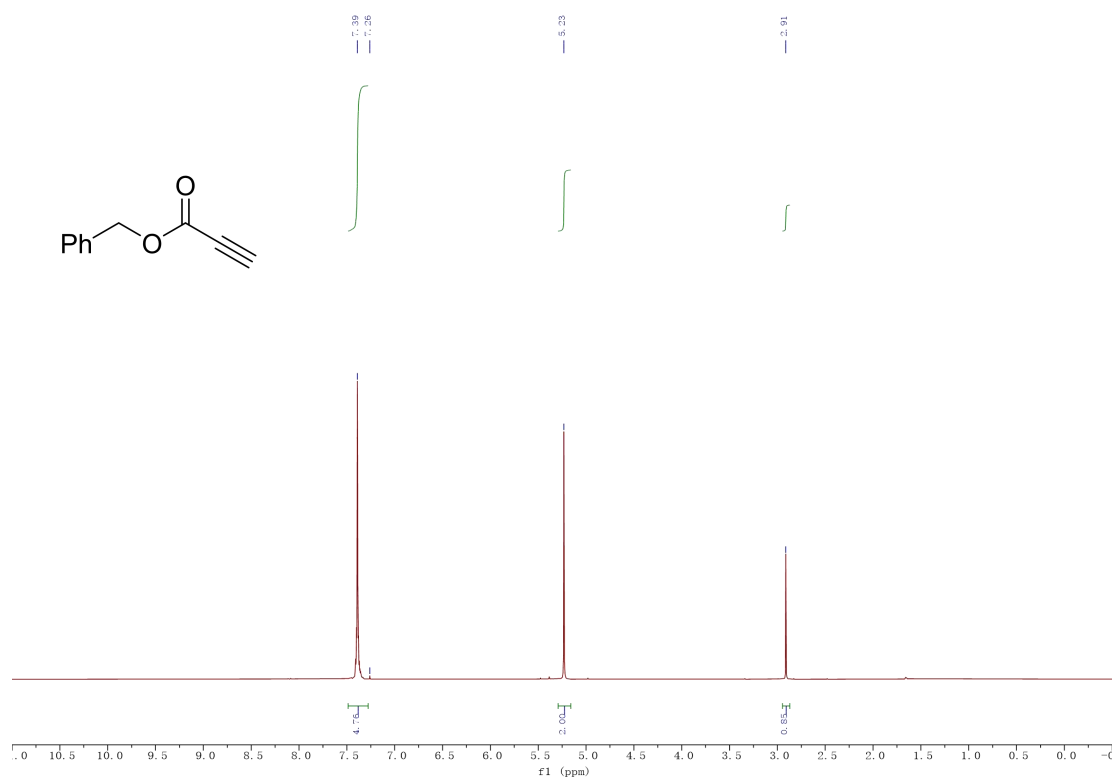
Oct-1-yn-3-one (C₈H₁₂O)



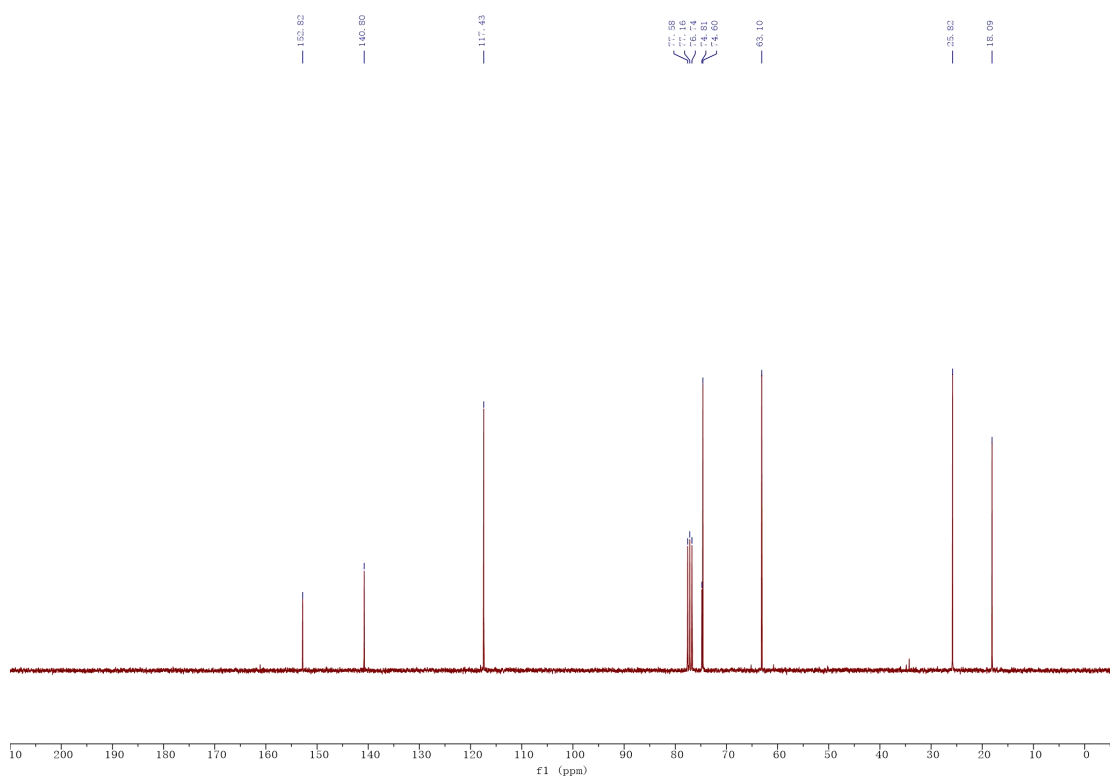
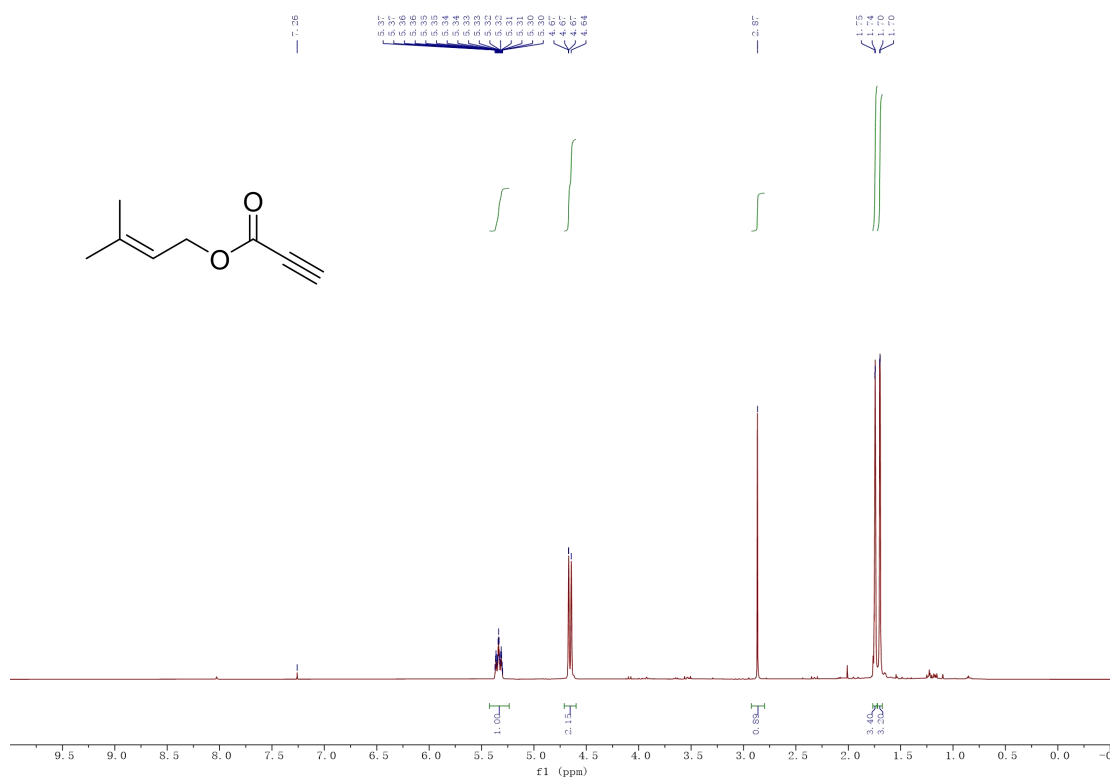
1-(2,3,4,5,6-Pentamethylphenyl)prop-2-yn-1-one (C₁₄H₁₆O)



Benzyl propiolate (C₁₀H₈O₂)



3-Methylbut-2-en-1-yl propiolate (C₈H₁₀O₂)



References

References

- [1] Albini, A.; Fagnoni, M., 1908: Giacomo Ciamician and the concept of green chemistry. *ChemSusChem: Chemistry & Sustainability Energy & Materials* **2008**, *1*, 63-66.
- [2] Anastas, P. T.; Warner, J. C., *Green chemistry: theory and practice*. Oxford university press: **2000**.
- [3] Sheldon, R. A., Green and sustainable manufacture of chemicals from biomass: state of the art. *Green Chem.* **2014**, *16*, 950-963.
- [4] Serrano-Ruiz, J. C.; Luque, R.; Sepúlveda-Escribano, A., Transformations of biomass-derived platform molecules: from high added-value chemicals to fuels *via* aqueous-phase processing. *Chem. Soc. Rev.* **2011**, *40*, 5266-5281.
- [5] Ryu, H. W.; Kim, D. H.; Jae, J.; Lam, S. S.; Park, E. D.; Park, Y.-K., Recent advances in catalytic co-pyrolysis of biomass and plastic waste for the production of petroleum-like hydrocarbons. *Bioresour. technol.* **2020**, *310*, 123473.
- [6] Lynd, L. R.; Larson, E.; Greene, N.; Laser, M.; Sheehan, J.; Dale, B. E.; McLaughlin, S.; Wang, M., The role of biomass in America's energy future: framing the analysis. *Biofuels, Bioprod. Biorefin.* **2009**, *3*, 113-123.
- [7] Queneau, Y.; Han, B., Biomass: Renewable carbon resource for chemical and energy industry. *The innovation* **2022**, *3*.
- [8] Werpy, T.; Petersen, G., Top value added chemicals from biomass. US Department of Energy, Office of Scientific and Technical Information, No.: DOE/GO-102004-1992, www.osti.gov/bridge **2004**.
- [9] Bozell, J. J.; Petersen, G. R., Technology development for the production of biobased products from biorefinery carbohydrates-the US Department of Energy's "Top 10" revisited. *Green Chem.* **2010**, *12*, 539-554.
- [10] Isikgor, F. H.; Becer, C. R., Lignocellulosic biomass: a sustainable platform for the production of bio-based chemicals and polymers. *Polym. Chem.* **2015**, *6*, 4497-4559.
- [11] Zhang, Z.; Song, J.; Han, B., Catalytic transformation of lignocellulose into chemicals and fuel products in ionic liquids. *Chem. Rev.* **2017**, *117*, 6834-6880.

- [12] Brodeur, G.; Yau, E.; Badal, K.; Collier, J.; Ramachandran, K.; Ramakrishnan, S., Chemical and physicochemical pretreatment of lignocellulosic biomass: a review. *Enzyme Res.* **2011**, *2011*.
- [13] Agbor, V. B.; Cicek, N.; Sparling, R.; Berlin, A.; Levin, D. B., Biomass pretreatment: fundamentals toward application. *Biotechnol. Adv.* **2011**, *29*, 675-685.
- [14] Mankar, A. R.; Pandey, A.; Modak, A.; Pant, K., Pretreatment of lignocellulosic biomass: A review on recent advances. *Bioresour. Technol.* **2021**, *334*, 125235.
- [15] Mika, L. T.; Cséfalvay, E.; Németh, Á., Catalytic conversion of carbohydrates to initial platform chemicals: chemistry and sustainability. *Chem. Rev.* **2018**, *118*, 505-613.
- [16] Gallezot, P., Conversion of biomass to selected chemical products. *Chem. Soc. Rev.* **2012**, *41*, 1538-1558.
- [17] Jang, Y. S.; Kim, B.; Shin, J. H.; Choi, Y. J.; Choi, S.; Song, C. W.; Lee, J.; Park, H. G.; Lee, S. Y., Bio-based production of C₂-C₆ platform chemicals. *Biotechnol. Bioeng.* **2012**, *109*, 2437-2459.
- [18] Gerardy, R.; Debecker, D. P.; Estager, J.; Luis, P.; Monbaliu, J.-C. M., Continuous flow upgrading of selected C₂-C₆ platform chemicals derived from biomass. *Chem. Rev.* **2020**, *120*, 7219-7347.
- [19] Balat, M.; Balat, H.; Öz, C., Progress in bioethanol processing. *Prog. Energy Combust. Sci.* **2008**, *34*, 551-573.
- [20] Sun, J.; Wang, Y., Recent advances in catalytic conversion of ethanol to chemicals. *ACS Catal.* **2014**, *4*, 1078-1090.
- [21] Morschbacker, A., Bio-ethanol based ethylene. *Journal of Macromolecular Science®*, *Part C: Polym. Rev.* **2009**, *49*, 79-84.
- [22] Aditiya, H.; Mahlia, T.; Chong, W.; Nur, H.; Sebayang, A., Second generation bioethanol production: A critical review. *Renew. Sust. Energ.* **2016**, *66*, 631-653.
- [23] John, R. P.; Anisha, G.; Nampoothiri, K. M.; Pandey, A., Direct lactic acid fermentation: Focus on simultaneous saccharification and lactic acid production. *Biotechnol. Adv.* **2009**, *27*, 145-152.

- [24] Juturu, V.; Wu, J. C., Microbial production of lactic acid: the latest development. *Crit. Rev. Biotechnol.* **2016**, *36*, 967-977.
- [25] Zabed, H. M.; Akter, S.; Rupani, P. F.; Akor, J.; Zhang, Y.; Zhao, M.; Zhang, C.; Ragauskas, A. J.; Qi, X., Biocatalytic gateway to convert glycerol into 3-hydroxypropionic acid in waste-based biorefineries: Fundamentals, limitations, and potential research strategies. *Biotechnol. Adv.* **2023**, *62*, 108075.
- [26] De Fouchécour, F.; Sánchez-Castañeda, A.-K.; Saulou-Bérion, C.; Spinnler, H. E., Process engineering for microbial production of 3-hydroxypropionic acid. *Biotechnol. Adv.* **2018**, *36*, 1207-1222.
- [27] Pang, X.; Zhuang, X.; Tang, Z.; Chen, X., Polylactic acid (PLA): research, development and industrialization. *Biotechnol. J.* **2010**, *5*, 1125-1136.
- [28] Andreeßen, B.; Steinbüchel, A., Biosynthesis and biodegradation of 3-hydroxypropionate-containing polyesters. *Appl. Environ. Microbiol.* **2010**, *76*, 4919-4925.
- [29] Fan, Y.; Zhou, C.; Zhu, X., Selective catalysis of lactic acid to produce commodity chemicals. *Catal. Rev.* **2009**, *51*, 293-324.
- [30] Pereira, C. S.; Silva, V. M.; Rodrigues, A. E., Ethyl lactate as a solvent: Properties, applications and production processes-a review. *Green Chem.* **2011**, *13*, 2658-2671.
- [31] Valdehuesa, K. N. G.; Liu, H.; Nisola, G. M.; Chung, W.-J.; Lee, S. H.; Park, S. J., Recent advances in the metabolic engineering of microorganisms for the production of 3-hydroxypropionic acid as C₃ platform chemical. *Appl. Microbiol. Biotechnol.* **2013**, *97*, 3309-3321.
- [32] Saxena, R.; Saran, S.; Isar, J.; Kaushik, R., Production and applications of succinic acid. In Current developments in biotechnology and bioengineering, *Elsevier*, **2017**, 601-630.
- [33] Carlson, A.; Coggio, B.; Lau, K.; Mercogliano, C.; Millis, J., Industrial production of succinic acid. *Chemicals and Fuels from Bio-Based Building Blocks* **2016**, 173-190.
- [34] Espro, C.; Paone, E.; Mauriello, F.; Gotti, R.; Uliassi, E.; Bolognesi, M. L.; Rodríguez-Padrón, D.; Luque, R., Sustainable production of pharmaceutical, nutraceutical and bioactive compounds from biomass and waste. *Chem. Soc. Rev.* **2021**, *50*, 11191-11207.

- [35] Mazière, A.; Prinsen, P.; García, A.; Luque, R.; Len, C., A review of progress in (bio) catalytic routes from/to renewable succinic acid. *Biofuels, Bioprod. Biorefin.* **2017**, *11*, 908-931.
- [36] Bechthold, I.; Bretz, K.; Kabasci, S.; Kopitzky, R.; Springer, A., Succinic acid: a new platform chemical for biobased polymers from renewable resources. *Chem. Eng. Technol.: Industrial Chemistry-Plant Equipment-Process Engineering-Biotechnology* **2008**, *31*, 647-654.
- [37] Chimirri, F.; Bosco, F.; Ceccarelli, R.; Venturello, A.; Geobaldo, F., Succinic acid and its derivatives: fermentative production using sustainable industrial agro-food by-products and its applications in the food industry. *Ital. J. Food Sci.* **2010**, *22*, 119-125.
- [38] Kang, S.; Fu, J.; Zhang, G., From lignocellulosic biomass to levulinic acid: A review on acid-catalyzed hydrolysis. *Renew. Sust. Energ.* **2018**, *94*, 340-362.
- [39] Di Bucchianico, D. D. M.; Wang, Y.; Buvat, J.-C.; Pan, Y.; Moreno, V. C.; Leveneur, S., Production of levulinic acid and alkyl levulinates: A process insight. *Green Chem.* **2022**, *24*, 614-646.
- [40] Xu, W. P.; Chen, X. F.; Guo, H. J.; Li, H. L.; Zhang, H. R.; Xiong, L.; Chen, X. D., Conversion of levulinic acid to valuable chemicals: A review. *J. Chem. Technol. Biot.* **2021**, *96*, 3009-3024.
- [41] Yan, L.; Yao, Q.; Fu, Y., Conversion of levulinic acid and alkyl levulinates into biofuels and high-value chemicals. *Green Chem.* **2017**, *19*, 5527-5547.
- [42] Kumar, A.; Shende, D. Z.; Wasewar, K., Production of levulinic acid: A promising building block material for pharmaceutical and food industry. *Mater. Today: Proceedings* **2020**, *29*, 790-793.
- [43] Zhang, M.; Wang, N.; Liu, J.; Wang, C.; Xu, Y.; Ma, L., A review on biomass-derived levulinic acid for application in drug synthesis. *Crit. Rev. Biotechnol.* **2022**, *42*, 220-253.
- [44] Badgujar, K. C.; Badgujar, V. C.; Bhanage, B. M., A review on catalytic synthesis of energy rich fuel additive levulinate compounds from biomass derived levulinic acid. *Fuel Process. Technol.* **2020**, *197*, 106213.

- [45] Hayes, G. C.; Becer, C. R., Levulinic acid: A sustainable platform chemical for novel polymer architectures. *Polym. Chem.* **2020**, *11*, 4068-4077.
- [46] Carnevali, D.; Rigamonti, M. G.; Tabanelli, T.; Patience, G. S.; Cavani, F., Levulinic acid upgrade to succinic acid with hydrogen peroxide. *Appl. Catal. A-Gen.* **2018**, *563*, 98-104.
- [47] Dutta, S.; Iris, K.; Tsang, D. C.; Ng, Y. H.; Ok, Y. S.; Sherwood, J.; Clark, J. H., Green synthesis of gamma-valerolactone (GVL) through hydrogenation of biomass-derived levulinic acid using non-noble metal catalysts: A critical review. *Chem. Eng. J.* **2019**, *372*, 992-1006.
- [48] Kondawar, S.; Rode, C., Ionic liquids for the sustainable transformation of levulinic acid to gamma-valerolactone (GVL). *Curr. Opin. Green Sustain. Chem.* **2022**, *35*, 100607.
- [49] Wright, W. R.; Palkovits, R., Development of heterogeneous catalysts for the conversion of levulinic acid to γ -valerolactone. *ChemSusChem* **2012**, *5*, 1657-1667.
- [50] Marckwordt, A.; El Ouahabi, F.; Amani, H.; Tin, S.; Kalevaru, N. V.; Kamer, P. C.; Wohlrab, S.; de Vries, J. G., Nylon Intermediates from Bio-Based Levulinic Acid. *Angew. Chem. Int. Ed.* **2019**, *131*, 3524-3528.
- [51] Choi, M.; Byun, J.; Park, H.; Jeong, K.; Kim, S. M.; Han, J., Economically-feasible “greener” transformation of gamma-valerolactone to nylon 6,6. *Biomass Bioenergy* **2022**, *162*, 106503.
- [52] Kerkel, F.; Markiewicz, M.; Stolte, S.; Müller, E.; Kunz, W., The green platform molecule gamma-valerolactone-ecotoxicity, biodegradability, solvent properties, and potential applications. *Green Chem.* **2021**, *23*, 2962-2976.
- [53] Xu, C.; Paone, E.; Rodríguez-Padrón, D.; Luque, R.; Mauriello, F., Recent catalytic routes for the preparation and the upgrading of biomass derived furfural and 5-hydroxymethylfurfural. *Chem. Soc. Rev.* **2020**, *49*, 4273-4306.
- [54] Zhang, T.; Li, W.; Xiao, H.; Jin, Y.; Wu, S., Recent progress in direct production of furfural from lignocellulosic residues and hemicellulose. *Bioresour. Technol.* **2022**, *354*, 127126.

- [55] Ricciardi, L.; Verboom, W.; Lange, J.-P.; Huskens, J., Production of furans from C₅ and C₆ sugars in the presence of polar organic solvents. *Sustain. Energy Fuels* **2022**, *6*, 11-28.
- [56] Cousin, E.; Namhaed, K.; Pérès, Y.; Cognet, P.; Delmas, M.; Hermansyah, H.; Gozan, M.; Alaba, P. A.; Aroua, M. K., Towards efficient and greener processes for furfural production from biomass: A review of the recent trends. *Sci. Total Environ.* **2022**, *847*, 157599.
- [57] Kumar, A.; Chauhan, A. S.; Bains, R.; Das, P., Catalytic transformations for agro-waste conversion to 5-hydroxymethylfurfural and furfural: Chemistry and scale-up development. *Green Chem.* **2023**, *25*, 849-870.
- [58] Wang, S.; Zhao, Y.; Lin, H.; Chen, J.; Zhu, L.; Luo, Z., Conversion of C₅ carbohydrates into furfural catalyzed by a Lewis acidic ionic liquid in renewable γ -valerolactone. *Green Chem.* **2017**, *19*, 3869-3879.
- [59] Jiang, S.; Verrier, C.; Ahmar, M.; Lai, J.; Ma, C.; Muller, E.; Queneau, Y.; Pera-Titus, M.; Jérôme, F.; Vigier, K. D. O., Unveiling the role of choline chloride in furfural synthesis from highly concentrated feeds of xylose. *Green Chem.* **2018**, *20*, 5104-5110.
- [60] An, Z.; Li, J., Recent advances in the catalytic transfer hydrogenation of furfural to furfuryl alcohol over heterogeneous catalysts. *Green Chem.* **2022**, *24*, 1780-1808.
- [61] Alonso-Fagúndez, N.; Granados, M. L.; Mariscal, R.; Ojeda, M., Selective conversion of furfural to maleic anhydride and furan with VO_x/Al₂O₃ catalysts. *ChemSusChem* **2012**, *5*, 1984-1990.
- [62] Li, X.; Ko, J.; Zhang, Y., Highly Efficient Gas-Phase Oxidation of Renewable Furfural to Maleic Anhydride over Plate Vanadium Phosphorus Oxide Catalyst. *ChemSusChem* **2018**, *11*, 612-618.
- [63] Lu, G.-H.; Zong, M.-H.; Li, N., Combining Electro-, Photo-, and Biocatalysis for One-Pot Selective Conversion of Furfural into Value-Added C₄ Chemicals. *ACS Catal.* **2023**, *13*, 1371-1380.

- [64] Zhu, W.; Tao, F.; Chen, S.; Li, M.; Yang, Y.; Lv, G., Efficient oxidative transformation of furfural into succinic acid over acidic metal-free graphene oxide. *ACS Sustain. Chem. Eng.* **2018**, *7*, 296-305.
- [65] Palai, Y. N.; Shrotri, A.; Fukuoka, A., Selective oxidation of furfural to succinic acid over Lewis acidic Sn-Beta. *ACS Catal.* **2022**, *12*, 3534-3542.
- [66] Scodeller, I.; Mansouri, S.; Morvan, D.; Muller, E.; de Oliveira Vigier, K.; Wischert, R.; Jérôme, F. Synthesis of Renewable meta-Xylylenediamine from Biomass-Derived Furfural. *Angew. Chem. Int. Ed.* **2018**, *57*, 10510-10514.
- [67] Song, S.; Fung Kin Yuen, V.; Di, L.; Sun, Q.; Zhou, K.; Yan, N., Integrating Biomass into the Organonitrogen Chemical Supply Chain: Production of Pyrrole and D-Proline from Furfural. *Angew. Chem. Int. Ed.* **2020**, *59*, 19846-19850.
- [68] Zhu, L.; Fu, X.; Hu, Y.; Hu, C., Controlling the Reaction Networks for Efficient Conversion of Glucose into 5-Hydroxymethylfurfural. *ChemSusChem* **2020**, *13*, 4812-4832.
- [69] Jiang, Z.; Zeng, Y.; Hu, D.; Guo, R.; Yan, K.; Luque, R., Chemical transformations of 5-hydroxymethylfurfural into highly added value products: present and future. *Green Chem.* **2023**, *25*, 871-892.
- [70] Maitra, S.; Singh, V., A consolidated bioprocess design to produce multiple high-value platform chemicals from lignocellulosic biomass and its techno-economic feasibility. *J. Clean. Prod.* **2022**, *377*, 134383.
- [71] <https://www.linkedin.com/pulse/5-hydroxymethylfurfural-5-hmf-market-share-report>.
- [72] Singhal, S.; Agarwal, S.; Mudoi, M. P.; Singhal, N.; Singh, R., Chemical conversion of furan dicarboxylic acid to environmentally benign polyesters: An overview. *Biomass Convers. Biorefin.* **2023**, *13*, 15619-15636.
- [73] Xu, H.; Wang, C., A Comprehensive Review of 2,5-Dimethylfuran as a Biofuel Candidate. *Biofuels from lignocellulosic biomass: Innovations beyond bioethanol* **2016**, 105-129.

- [74] Moreau, C.; Durand, R.; Razigade, S.; Duhamet, J.; Faugeras, P.; Rivalier, P.; Ros, P.; Avignon, G., Dehydration of fructose to 5-hydroxymethylfurfural over H-mordenites. *Appl. Catal. A-Gen.* **1996**, *145*, 211-224.
- [75] Teong, S. P.; Yi, G.; Zhang, Y., Hydroxymethylfurfural production from bioresources: past, present and future. *Green Chem.* **2014**, *16*, 2015-2026.
- [76] Haworth, W.; Jones, W., The conversion of sucrose into furan compounds. Part I. 5-Hydroxymethylfurfuraldehyde and some derivatives. *Journal of the Chemical Society (Resumed)* **1944**, 667-670.
- [77] Horvat, J.; Klaić, B.; Metelko, B.; Šunjić, V., Mechanism of levulinic acid formation. *Tetrahedron Lett.* **1985**, *26*, 2111-2114.
- [78] Patil, S. K.; Lund, C. R., Formation and growth of humins *via* aldol addition and condensation during acid-catalyzed conversion of 5-hydroxymethylfurfural. *Energy Fuels* **2011**, *25*, 4745-4755.
- [79] Shen, H.; Shan, H.; Liu, L., Evolution Process and Controlled Synthesis of Humins with 5-Hydroxymethylfurfural (HMF) as Model Molecule. *ChemSusChem* **2020**, *13*, 513-519.
- [80] Kang, E.-S.; Kim, B.; Kim, Y. G., Efficient preparation of DHMF and HMFA from biomass-derived HMF *via* a Cannizzaro reaction in ionic liquids. *J. Ind. Eng. Chem.* **2012**, *18*, 174-177.
- [81] Subbiah, S.; Simeonov, S. P.; Esperanca, J. M.; Rebelo, L. P. N.; Afonso, C. A., Direct transformation of 5-hydroxymethylfurfural to the building blocks 2,5-dihydroxymethylfurfural (DHMF) and 5-hydroxymethyl furanoic acid (HMFA) *via* Cannizzaro reaction. *Green Chem.* **2013**, *15*, 2849-2853.
- [82] Krebs, M. L.; Bodach, A.; Wang, C.; Schüth, F., Stabilization of alkaline 5-HMF electrolytes *via* Cannizzaro reaction for the electrochemical oxidation to FDCA. *Green Chem.* **2023**, *25*, 1797-1802.
- [83] Hoang Tran, P., Recent Approaches in the Catalytic Transformation of Biomass-Derived 5-Hydroxymethylfurfural into 2,5-Diformylfuran. *ChemSusChem* **2022**, *15*, e202200220.

- [84] Mascal, M., 5-(Chloromethyl) furfural is the new HMF: functionally equivalent but more practical in terms of its production from biomass. *ChemSusChem* **2015**, 8, 3391-3395.
- [85] Mascal, M., 5-(Chloromethyl) furfural (CMF): a platform for transforming cellulose into commercial products. *ACS Sustain. Chem. Eng.* **2019**, 7, 5588-5601.
- [86] Mascal, M.; Dutta, S., Synthesis of the natural herbicide δ -aminolevulinic acid from cellulose-derived 5-(chloromethyl) furfural. *Green Chem.* **2011**, 13, 40-41.
- [87] Mascal, M.; Dutta, S., Synthesis of ranitidine (Zantac) from cellulose-derived 5-(chloromethyl) furfural. *Green Chem.* **2011**, 13, 3101-3102.
- [88] Castro, G. A. D.; Fernandes, S. A.; de Sousa, R. d. C. S.; Pereira, M. M., Green synthesis of 5-hydroxymethylfurfural and 5-acetoxymethylfurfural using a deep eutectic solvent in a biphasic system assisted by microwaves. *React. Chem. Eng.* **2023**, 8, 1324-1333.
- [89] Bognár, R.; Herczegh, P.; Zsély, M.; Batta, G., Synthesis of 3, 4-dideoxy-dl-hex-3-enopyranosides from 5-hydroxymethyl-2-furaldehyde. *Carbohydr. Res.* **1987**, 164, 465-469.
- [90] Chundury, D.; Szmant, H., Preparation of polymeric building blocks from 5-hydroxymethyl-and 5-chloromethylfurfuraldehyde. *Ind. Eng. Chem. Prod. Res. Develop.* **1981**, 20, 158-163.
- [91] Stanev, N.; Bordado, J. C.; Afonso, C. A.; Simeonov, S. P., Solvent - Free Catalytic Self-Etherification of 5-Hydroxymethyl Furfural. *ChemCatChem* **2018**, 10, 5406-5409.
- [92] Annatelli, M.; Trapasso, G.; Torre, D. D.; Pietrobon, L.; Redolfi-Bristol, D.; Aricò, F., A Green Synthesis of 5,5'-[Oxybis(methylene)]bis-2-Furfural: from By-Product to Attractive Bio-Based Platform Chemical. *Adv. Sustain. Syst.* **2022**, 6, 2200297.
- [93] Mliki, K.; Trabelsi, M., Chemicals from biomass: Efficient and facile synthesis of 5,5'(oxy-bis (methylene))bis-2-furfural from 5-hydroxymethylfurfural. *Ind. Crops Prod.* **2015**, 78, 91-94.

- [94] Zhang, P.; Yang, J.; Hu, H.; Hu, D.; Gan, J.; Zhang, Y.; Chen, C.; Li, X.; Wang, L.; Zhang, J., Catalytic self-etherification of 5-hydroxymethylfurfural to 5,5'(oxy-bis(methylene))bis-2-furfural over zeolite catalysts: effect of pore structure and acidity. *Catal. Sci. Technol.* **2020**, *10*, 4684-4692.
- [95] Yang, J.; Huai, L.; Gan, J.; Hu, H.; Zhou, S.; Zhang, J., Self-Etherification of 5-Hydroxymethylfurfural to 5,5'(Oxy-bis(methylene))bis-2-furfural over Hierarchically Micromesoporous ZSM-5: The Role of Brønsted-and Lewis-Acid Sites. *Ind. Eng. Chem. Res.* **2021**, *61*, 987-994.
- [96] Wang, H.; Wang, Y.; Deng, T.; Chen, C.; Zhu, Y.; Hou, X., Carbocatalyst in biorefinery: Selective etherification of 5-hydroxymethylfurfural to 5,5'(oxy-bis(methylene))bis-2-furfural over graphene oxide. *Catal. Commun.* **2015**, *59*, 127-130.
- [97] Balakrishnan, M.; Sacia, E. R.; Bell, A. T., Etherification and reductive etherification of 5-(hydroxymethyl) furfural: 5-(alkoxymethyl) furfurals and 2,5-bis (alkoxymethyl) furans as potential bio-diesel candidates. *Green Chem.* **2012**, *14*, 1626-1634.
- [98] Shinde, S.; Rode, C., Cascade Reductive Etherification of Bioderived Aldehydes over Zr-Based Catalysts. *ChemSusChem* **2017**, *10*, 4090-4101.
- [99] Xiang, Y.; Wen, S.; Tian, Y.; Zhao, K.; Guo, D.; Cheng, F.; Xu, Q.; Liu, X.; Yin, D., Efficient synthesis of 5-ethoxymethylfurfural from biomass-derived 5-hydroxymethylfurfural over sulfonated organic polymer catalyst. *RSC Adv.* **2021**, *11*, 3585-3595.
- [100] He, A.; Gu, Q.; Shen, X.; Zheng, J.; Hu, L.; Wang, X.; Jiang, Y.; Wu, Z.; Xu, J.; Song, J., One-pot reductive etherification of biomass-derived 5-hydroxymethylfurfural to 2,5-bis (isopropoxymethyl) furan over a sulfonic acid-functionalized zirconium-based coordination catalyst. *Green Chem.* **2023**, *25*, 2349-2360.
- [101] Li, H.; Saravanamurugan, S.; Yang, S.; Riisager, A., Direct transformation of carbohydrates to the biofuel 5-ethoxymethylfurfural by solid acid catalysts. *Green Chem.* **2016**, *18*, 726-734.

- [102] Yang, F.; Tang, J.; Ou, R.; Guo, Z.; Gao, S.; Wang, Y.; Wang, X.; Chen, L.; Yuan, A., Fully catalytic upgrading synthesis of 5-Ethoxymethylfurfural from biomass-derived 5-Hydroxymethylfurfural over recyclable layered-niobium-molybdate solid acid. *Appl. Catal. B-Environ.* **2019**, *256*, 117786.
- [103] Arias, K.; Al-Resayes, S. I.; Climent, M. J.; Corma, A.; Iborra, S., From Biomass to Chemicals: Synthesis of Precursors of Biodegradable Surfactants from 5-Hydroxymethylfurfural. *ChemSusChem* **2013**, *6*, 123-131.
- [104] Arias, K. S.; Climent, M. J.; Corma, A.; Iborra, S., Biomass-Derived Chemicals: Synthesis of Biodegradable Surfactant Ether Molecules from Hydroxymethylfurfural. *ChemSusChem* **2014**, *7*, 210-220.
- [105] Garcia-Ortiz, A.; Arias, K. S.; Climent, M. J.; Corma, A.; Iborra, S., One-Pot Synthesis of Biomass-Derived Surfactants by Reacting Hydroxymethylfurfural, Glycerol, and Fatty Alcohols on Solid Acid Catalysts. *ChemSusChem* **2018**, *11*, 2870-2880.
- [106] Tšupova, S.; Rominger, F.; Rudolph, M.; Hashmi, A. S. K., Synthesis of phenols from hydroxymethylfurfural (HMF). *Green Chem.* **2016**, *18*, 5800-5805.
- [107] Grossmann, A.; Bartlett, S.; Janecek, M.; Hodgkinson, J. T.; Spring, D. R., Diversity-oriented synthesis of drug-like macrocyclic scaffolds using an orthogonal organo-and metal catalysis strategy. *Angew. Chem. Int. Ed.* **2014**, *126*, 13309-13313.
- [108] Viil, I.; Bredihhin, A.; Mäeorg, U.; Vares, L., Preparation of potential biofuel 5-ethoxymethylfurfural and other 5-alkoxymethylfurfurals in the presence of oil shale ash. *RSC Adv.* **2014**, *4*, 5689-5693.
- [109] Liu, F.; Audemar, M.; De Oliveira Vigier, K.; Clacens, J. M.; De Campo, F.; Jérôme, F., Palladium/carbon dioxide cooperative catalysis for the production of diketone derivatives from carbohydrates. *ChemSusChem* **2014**, *7*, 2089-2093.
- [110] Wozniak, B.; Spannenberg, A.; Li, Y.; Hinze, S.; de Vries, J. G., Cyclopentanone Derivatives from 5-Hydroxymethylfurfural via 1-Hydroxyhexane-2,5-dione as Intermediate. *ChemSusChem* **2018**, *11*, 356-359.

- [111] Ohyama, J.; Kanao, R.; Esaki, A.; Satsuma, A., Conversion of 5-hydroxymethylfurfural to a cyclopentanone derivative by ring rearrangement over supported Au nanoparticles. *ChemComm.* **2014**, *50*, 5633-5636.
- [112] Dutta, S.; Bhat, N. S., Catalytic Transformation of Biomass-Derived Furfurals to Cyclopentanones and Their Derivatives: A Review. *ACS omega* **2021**, *6*, 35145-35172.
- [113] Kumalaputri, A. J.; Randolph, C.; Otten, E.; Heeres, H. J.; Deuss, P. J., Lewis acid catalyzed conversion of 5-hydroxymethylfurfural to 1, 2, 4-benzenetriol, an overlooked biobased compound. *ACS Sustain. Chem. Eng.* **2018**, *6*, 3419-3425.
- [114] Amarasekara, A. S.; Okorie, N. C., 1-(Alkylsulfonic)-3-methylimidazolium chloride Brönsted acidic ionic liquid catalyzed hydrogen peroxide oxidations of biomass derived furan aldehydes. *Catal. Commun.* **2018**, *108*, 108-112.
- [115] Gomes, R. F.; Coelho, J. A.; Afonso, C. A., Direct Conversion of Activated 5-Hydroxymethylfurfural into δ -Lactone-Fused Cyclopentenones. *ChemSusChem* **2019**, *12*, 420-425.
- [116] Yang, Y.; Wang, Y.; Li, S.; Shen, X.; Chen, B.; Liu, H.; Han, B., Selective hydrogenation of aromatic furfurals into aliphatic tetrahydrofurfural derivatives. *Green Chem.* **2020**, *22*, 4937-4942.
- [117] Jia, W.; Sun, Y.; Zuo, M.; Feng, Y.; Tang, X.; Zeng, X.; Lin, L., One-Pot Synthesis of Renewable Phthalic Anhydride from 5-Hydroxymethylfurfural by using $\text{MoO}_3/\text{Cu}(\text{NO}_3)_2$ as Catalyst. *ChemSusChem* **2020**, *13*, 640-646.
- [118] Cioc, R. C.; Lutz, M.; Pidko, E. A.; Crockatt, M.; Van Der Waal, J. C.; Bruijninx, P. C., Direct Diels-Alder reactions of furfural derivatives with maleimides. *Green Chem.* **2021**, *23*, 367-373.
- [119] Tao, L.; Yan, T.-H.; Li, W.; Zhao, Y.; Zhang, Q.; Liu, Y.-M.; Wright, M. M.; Li, Z.-H.; He, H.-Y.; Cao, Y., Toward an integrated conversion of 5-hydroxymethylfurfural and ethylene for the production of renewable *p*-xylene. *Chem.* **2018**, *4*, 2212-2227.
- [120] Wan, Y.; Lee, J. M., Recent Advances in Reductive Upgrading of 5-Hydroxymethylfurfural via Heterogeneous Thermocatalysis. *ChemSusChem* **2022**, *15*, e202102041.

- [121] Hu, Q.; Jiang, S.; Wu, Y.; Xu, H.; Li, G.; Zhou, Y.; Wang, J., Ambient-Temperature Reductive Amination of 5-Hydroxymethylfurfural Over Al₂O₃-Supported Carbon-Doped Nickel Catalyst. *ChemSusChem* **2022**, *15*, e202200192.
- [122] Xie, C.; Song, J.; Hua, M.; Hu, Y.; Huang, X.; Wu, H.; Yang, G.; Han, B., Ambient-temperature synthesis of primary amines *via* reductive amination of carbonyl compounds. *ACS Catal.* **2020**, *10*, 7763-7772.
- [123] Karve, V. V.; Sun, D. T.; Trukhina, O.; Yang, S.; Oveisi, E.; Luterbacher, J.; Queen, W. L., Efficient reductive amination of HMF with well dispersed Pd nanoparticles immobilized in a porous MOF/polymer composite. *Green Chem.* **2020**, *22*, 368-378.
- [124] Seitkalieva, M. M.; Vavina, A. V.; Posvyatenko, A. V.; Egorova, K. S.; Kashin, A. S.; Gordeev, E. G.; Strukova, E. N.; Romashov, L. V.; Ananikov, V. P., Biomass-derived ionic liquids based on a 5-HMF platform chemical: Synthesis, characterization, biological activity, and tunable interactions at the molecular level. *ACS Sustain. Chem. Eng.* **2021**, *9*, 3552-3570.
- [125] Li, X.; Ma, J.; Jia, X.; Xia, F.; Huang, Y.; Xu, Y.; Xu, J., Al-doping promoted aerobic amidation of 5-hydroxymethylfurfural to 2, 5-furandicarboxamide over cryptomelane. *ACS Sustain. Chem. Eng.* **2018**, *6*, 8048-8054.
- [126] Ramdani, W.; González, I. R.; Benbakoura, N.; Ahmar, M.; Verrier, C.; Queneau, Y.; Pera-Titus, M.; Jérôme, F.; de Oliveira Vigier, K., Catalytic Aldol Condensation of 5-Hydroxymethylfurfural and its Synthesis from Concentrated Feed of Carbohydrates. *ChemCatChem* **2023**, *15*, e202300044.
- [127] Romani, F.; Corrieri, R.; Braga, V.; Ciardelli, F.; Ju, Y.; Varma, R.; Ansari, A.; Ali, A.; Asif, M.; Eftekhari-Sis, B., Exploration of the role of double schiff bases as catalytic intermediates in the knoevenagel reaction of furanic aldehydes: mechanistic considerations. *Synlett* **2018**, *29*, 1983-1988.
- [128] Mancipe, S.; Castillo, J.-C.; Brijaldo, M. a. H.; López, V. P.; Rojas, H.; Macías, M. A.; Portilla, J.; Romanelli, G. P.; Martínez, J. J.; Luque, R., B-Containing hydrotalcites effectively catalyzed synthesis of 3-(Furan-2-yl) acrylonitrile derivatives *via* the Knoevenagel condensation. *ACS Sustain. Chem. Eng.* **2022**, *10*, 12602-12612.

- [129] Arias, K. S.; Garcia-Ortiz, A.; Climent, M. J.; Corma, A.; Iborra, S., Mutual valorization of 5-hydroxymethylfurfural and glycerol into valuable diol monomers with solid acid catalysts. *ACS Sustain. Chem. Eng.* **2018**, *6*, 4239-4245.
- [130] Yu, C.; Liu, B.; Hu, L., Efficient Baylis-Hillman reaction using stoichiometric base catalyst and an aqueous medium. *J. Org. Chem.* **2001**, *66*, 5413-5418.
- [131] Tan, J.-N.; Ahmar, M.; Queneau, Y., Bio-based solvents for the Baylis-Hillman reaction of HMF. *RSC Adv.* **2015**, *5*, 69238-69242.
- [132] Wang, L.; Tan, J.-N.; Ahmar, M.; Queneau, Y., New functionalized scaffolds from hydroxymethylfurfural and glucosyloxymethylfurfural by Morita-Baylis-Hillman reaction with cycloalkenones. *C.R. Chim.* **2019**, *22*, 615-620.
- [133] Ontiveros, J. s. F.; Wang, L.; Chatel, K.; Yue, X.; Tan, J.-N.; Ali-Rachedi, F.; Ahmar, M.; Verrier, C.; Fusina, A.; Nardello-Rataj, V., Design and properties of a novel family of nonionic biobased furanic hydroxyester and amide surfactants. *ACS Sustain. Chem. Eng.* **2021**, *9*, 16977-16988.
- [134] Domling, A.; Wang, W.; Wang, K., Chemistry and biology of multicomponent reactions. *Chem. Rev.* **2012**, *112*, 3083-3135.
- [135] Fan, W.; Queneau, Y.; Popowycz, F., HMF in multicomponent reactions: utilization of 5-hydroxymethylfurfural (HMF) in the Biginelli reaction. *Green Chem.* **2018**, *20*, 485-492.
- [136] Afradi, N.; Foroughifar, N.; Pasdar, H.; Qomi, M., Aspartic-acid-loaded starch-functionalized Mn-Fe-Ca ferrite magnetic nanoparticles as novel green heterogeneous nanomagnetic catalyst for solvent-free synthesis of dihydropyrimidine derivatives as potent antibacterial agents. *Res. Chem. Intermed.* **2019**, *45*, 3251-3271.
- [137] Fan, W.; Queneau, Y.; Popowycz, F., The synthesis of HMF-based α -amino phosphonates *via* one-pot Kabachnik-Fields reaction. *RSC Adv.* **2018**, *8*, 31496-31501.
- [138] Wang, L.; Verrier, C.; Ahmar, M.; Queneau, Y., Dipolar cycloadditions of HMF-based nitrones: Stepwise and multicomponent reactions, stereochemical outcome and structural scope. *Green Chem.* **2020**, *22*, 7907-7912.

- [139] Cristóbal, C.; Corral, C.; Carretero, J. C.; Ribagorda, M.; Adrio, J., Enantioselective transformations of 5-hydroxymethylfurfural *via* catalytic asymmetric 1, 3-dipolar cycloaddition of azomethine ylides. *ChemComm.* **2023**, *59*, 4336-4339.
- [140] Wu, Q.; Chen, J.; Guo, X.; Xu, Y., Copper (I)-Catalyzed Four - Component Coupling Using Renewable Building Blocks of CO₂ and Biomass-Based Aldehydes. *Eur. J. Org. Chem.* **2018**, *2018*, 3105-3113.
- [141] Sabahi-Agabager, L.; Nasiri, F., One-pot, solvent-free facile stereoselective synthesis of rhodanine–furan hybrids from renewable resources. *J. Sulfur Chem.* **2020**, *41*, 170-181.
- [142] de la Sovera, V.; López, G. V.; Porcal, W., Synthetic Study of 5-Hydroxymethylfurfural in Groebke-Blackburn-Bienaymé Reaction. *Eur. J. Org. Chem.* **2022**, *2022*, e202101369.
- [143] Yang, H.-B.; Wang, Z.-H.; Li, J.-M.; Wu, C., Modular synthesis of α -aryl β -perfluoroalkyl ketones *via* *N*-heterocyclic carbene catalysis. *ChemComm.* **2020**, *56*, 3801-3804.
- [144] Li, S.-S.; Qin, Q.; Qi, Z.; Yang, L.-M.; Kang, Y.; Zhang, X.-Z.; Ma, A.-J.; Peng, J.-B., Synthesis of disubstituted γ -butyrolactones and spirocyclopropanes *via* a multicomponent reaction of aldehydes, Meldrum's acid and sulfoxonium ylides. *Org. Chem. Front.* **2021**, *8*, 3069-3075.
- [145] Benasi, G.; Guidi, J.; Offidani, E.; Balon, R.; Rickels, K.; Fava, G. A., Benzodiazepines as a monotherapy in depressive disorders: a systematic review. *Psychother. Psychosom.* **2018**, *87*, 65-74.
- [146] Arora, N.; Dhiman, P.; Kumar, S.; Singh, G.; Monga, V., Recent advances in synthesis and medicinal chemistry of benzodiazepines. *Bioorg. Chem.* **2020**, *97*, 103668.
- [147] Archer, G. A.; Sternbach, L. H., Chemistry of benzodiazepines. *Chem. Rev.* **1968**, *68*, 747-784.
- [148] Sankar, R., GABA_A receptor physiology and its relationship to the mechanism of action of the 1, 5-benzodiazepine clobazam. *CNS drugs* **2012**, *26*, 229-244.

- [149] Finar, I., The preparation and properties of some 2:3-benzo-1:4-diazepines. *Journal of the Chemical Society (Resumed)* **1958**, 4094-4097.
- [150] Bariwal, J. B.; Upadhyay, K. D.; Manvar, A. T.; Trivedi, J. C.; Singh, J. S.; Jain, K. S.; Shah, A. K., 1,5-Benzothiazepine, a versatile pharmacophore: a review. *Eur. J. Med. Chem.* **2008**, *43*, 2279-2290.
- [151] Shorvon, S. D., The use of clobazam, midazolam, and nitrazepam in epilepsy. *Epilepsia* **1998**, *39*, 15-23.
- [152] Görlitzer, K.; Wilpert, C.; Rübsamen-Waigmann, H.; Suhartono, H.; Wang, L.; Immelmann, A., Pyrido (3,2-e)(1,4) diazepines--synthesis and testing of anti-HIV-1 activity. *Arch. Pharm.* **1995**, *328*, 247-255.
- [153] Baldessarini, R. J.; Frankenburg, F. R., Clozapine: a novel antipsychotic agent. *N. Engl. J. Med.* **1991**, *324*, 746-754.
- [154] Mueller, E., Benzodiazepine receptor interactions of arfendazam, a novel 1,5-benzodiazepine. *Pharmacopsychiatry* **1985**, *18*, 10-11.
- [155] Gauthier, A. C.; Mattson, R. H., Clobazam: a safe, efficacious, and newly rediscovered therapeutic for epilepsy. *CNS Neurosci. Ther.* **2015**, *21*, 543-548.
- [156] Aastha, P.; Navneet, K.; Anshu, A.; Pratima, S.; Dharma, K., 1,5 Benzodiazepines: overview of properties and synthetic aspects. *Res. J. Chem. Sci.* **2013**, *2231*, 606X.
- [157] Gawandi, S. J.; Desai, V. G.; Joshi, S.; Shingade, S.; Pissurlenkar, R. R., Assessment of elementary derivatives of 1,5-benzodiazepine as anticancer agents with synergy potential. *Bioorg. Chem.* **2021**, *117*, 105331.
- [158] Singh, R. K.; Sharda, S.; Sharma, S.; Kumar, S.; Prasad, D. N., Multicomponent catalytic synthesis of 1,5-benzodiazepines: an update. *Mini-Rev. Org. Chem.* **2020**, *17*, 465-484.
- [159] Teli, S.; Teli, P.; Soni, S.; Sahiba, N.; Agarwal, S., Synthetic aspects of 1,4-and 1,5-benzodiazepines using *o*-phenylenediamine: A study of past quinquennial. *RSC Adv.* **2023**, *13*, 3694-3714.

- [160] Maleki, A.; Kamalzare, M., An efficient synthesis of benzodiazepine derivatives *via* a one-pot, three-component reaction accelerated by a chitosan-supported superparamagnetic iron oxide nanocomposite. *Tetrahedron Lett.* **2014**, *55*, 6931-6934.
- [161] Sibous, S.; Ghailane, T.; Houda, S.; Ghailane, R.; Boukhris, S.; Souizi, A., Green and efficient method for the synthesis of 1,5-benzodiazepines using phosphate fertilizers as catalysts under free solvent. *Mediterr. J. Chem.* **2017**, *6*, 53-59.
- [162] Maleki, A.; Firouzi-Haji, R.; Farahani, P., Green multicomponent synthesis of benzodiazepines in the presence of CuFe₂O₄ as an efficient magnetically recyclable nanocatalyst under solvent-free ball-milling conditions at room temperature. *Org. Chem. Res.* **2018**, *4*, 86-94.
- [163] Sun, Y.-W.; Wang, L.-Z., One-pot synthesis of novel functionalized benzodiazepines *via* three-component or domino reactions. *New J. Chem.* **2018**, *42*, 20032-20040.
- [164] Zhou, L.; Wang, M.; Wang, K.; Wen, T.; Wang, L., Fe₃O₄@SiO₂-CeCl₃ Catalyzed Chemoselective Synthesis of Functionalized 3-Substituted-1,5-Benzodiazepines *via* One-pot Multicomponent and Domino Reactions. *Appl. Organomet. Chem.* **2020**, *34*, e5707.
- [165] Wu, H.-t.; Wang, L.-z., Expedient green-chemistry approaches for a one-pot synthesis of two series of novel 1,5-benzodiazepines *via* domino reactions. *New J. Chem.* **2020**, *44*, 10428-10440.
- [166] Siddiqui, S.; Siddiqui, Z. N., Synthesis and catalytic evaluation of PVP-CeO₂/rGO as a highly efficient and recyclable heterogeneous catalyst for multicomponent reactions in water. *Nanoscale Adv.* **2020**, *2*, 4639-4651.
- [167] Yin, L.; Wang, L., Chemo-/regio-selective synthesis of 2-aryl-3-acetyl-2, 4-dihydro-1H-5H-1,5-benzodiazepines using Lewis acid, CeCl₃·7H₂O. *Tetrahedron Lett.* **2016**, *57*, 5935-5940.
- [168] An, X.; Gao, L.; Wang, M.; Wu, H.; Wang, L., One-pot synthesis of 1,5-benzodiazepine-2,3-dicarboxylates *via* three-component domino reactions in the presence of γ-Fe₂O₃@SiO₂/Ce(OTf)₃. *Chem. Heterocycl. Compd.* **2021**, *57*, 806-816.

- [169] Maury, S. K.; Kumar, D.; Kamal, A.; Singh, H. K.; Kumari, S.; Singh, S., A facile and efficient multicomponent ultrasound-assisted “on water” synthesis of benzodiazepine ring. *Mol. divers.* **2021**, *25*, 131-142.
- [170] Zhang, K.; Li, J.; Wang, K.; An, X.; Wang, L., Atom-economical Approaches to 1,5-Benzodiazepines Containing Indole Ring via Fe₃O₄@SiO₂-PTSA-catalyzed Multicomponent Domino Reactions. *ChemistrySelect* **2020**, *5*, 14056-14061.
- [171] Sun, Y.-W.; Bei, Y.-M.; Wang, L.-Z., A catalyst-free four-component domino reaction for the synthesis of functionalized 3-acyl-1,5-benzodiazepines. *Org. Biomol. Chem.* **2019**, *17*, 930-938.
- [172] Qian, J.; Liu, Y.; Cui, J.; Xu, Z., Gold (I)-catalyzed synthesis of 1,5-benzodiazepines directly from o-phenylenediamines and alkynes. *J. Org. Chem.* **2012**, *77*, 4484-4490.
- [173] Mishra, R.; Sharma, A. K.; Kumar, R.; Baweja, V.; Mothsra, P.; Singh, M. K.; Yadav, S. B., Solid support based synthesis of 1,5-benzodiazepines: A mini review. *Synthetic Commun.* **2022**, *52*, 481-503.
- [174] Farhid, H.; Khodkari, V.; Nazeri, M. T.; Javanbakht, S.; Shaabani, A., Multicomponent reactions as a potent tool for the synthesis of benzodiazepines. *Org. Biomol. Chem.* **2021**, *19*, 3318-3358.
- [175] Zhao, Y.; Sharma, S.; Huang, M.; Sandhar, A.; Singh, R. K.; Ma, Y., Investigation of Various Organocatalysts for Improved and Efficient One Pot Synthesis of 2,3-Dihydro-1*H*-1,5-benzodiazepines Under Solvent-Free Condition. *Asian J. Chem.* **2014**, *26*, 5116.
- [176] Sarhandi, S.; Fekri, L. Z.; Vessaly, I., Ultrasound assisted 1,4-diazabicyclo [2.2.2] octaniumdiacetate multicomponent synthesis of benzodiazepines: A novel, highly efficient and green protocol. *Acta Chim. Slov.* **2018**, *65*, 246-252.
- [177] Pozarentzi, M.; Stephanidou-Stephanatou, J.; Tsoleridis, C. A., An efficient method for the synthesis of 1,5-benzodiazepine derivatives under microwave irradiation without solvent. *Tetrahedron Lett.* **2002**, *43*, 1755-1758.
- [178] Sun, P.; Hu, Z., The convenient synthesis of benzimidazole derivatives catalyzed by I₂ in aqueous media. *J. Heterocycl. Chem.* **2006**, *43*, 773-775.

- [179] Azarifar, D.; Pirhayati, M.; Maleki, B.; Sanginabadi, M.; Yami, N. R., Acetic acid-promoted condensation of *o*-phenylenediamine with aldehydes into 2-aryl-1-(arylmethyl)-1*H*-benzimidazoles under microwave irradiation. *J. Serbian Chem. Soc.* **2010**, *75*, 1181-1189.
- [180] Chandrashekhar, V. G.; Natte, K.; Alenad, A. M.; Alshammari, A. S.; Kreyenschulte, C.; Jagadeesh, R. V., Reductive Amination, Hydrogenation and Hydrodeoxygenation of 5-Hydroxymethylfurfural using Silica-supported Cobalt-Nanoparticles. *ChemCatChem* **2022**, *14*, e202101234.
- [181] Maruani, V.; Framery, E.; Andrioletti, B., Influence of the ammonium salts used in the Brønsted acid catalyzed hydrothermal decomposition of D-glucose towards 5-HMF. *New J. Chem.* **2020**, *44*, 4171-4176.
- [182] de Haro, T.; Nevado, C., Gold-catalyzed ethynylation of arenes. *J. Am. Chem. Soc.* **2010**, *132*, 1512-1513.
- [183] Chassaing, S.; Kueny - Stotz, M.; Isorez, G.; Brouillard, R., Rapid preparation of 3-deoxyanthocyanidins and novel dicationic derivatives: New insight into an old procedure. *Eur. J. Org. Chem.* **2007**, *2007*, 2438-2448.
- [184] Ieronimo, G.; Palmisano, G.; Maspero, A.; Marzorati, A.; Scapinello, L.; Masciocchi, N.; Cravotto, G.; Barge, A.; Simonetti, M.; Ameta, K. L., A novel synthesis of *N*-hydroxy-3-aryloxyindoles and 3-aryloxyindoles. *Org. Biomol. Chem.* **2018**, *16*, 6853-6859.
- [185] Peil, S.; Guthertz, A.; Biberger, T.; Fürstner, A., Hydrogenative cyclopropanation and hydrogenative metathesis. *Angew. Chem. Int. Ed.* **2019**, *58*, 8851-8856.
- [186] Tan, H.-b.; Wang, Y.-f.; Xu, J.; Hu, C.-s., One-pot, multi-component synthesis of ethyl (*E*)-1-(3-ethoxy-3-oxoprop-1-en-1-yl)-2-aryl-2,5-dihydro-1*H*-benzo[*b*][1,4]diazepine-3-carboxylate derivatives. *Tetrahedron Lett.* **2020**, *61*, 151604.
- [187] Xu, G. G.; Pagare, P. P.; Ghatge, M. S.; Safo, R. P.; Gazi, A.; Chen, Q.; David, T.; Alabbas, A. B.; Musayev, F. N.; Venitz, J. r., Design, synthesis, and biological evaluation of ester and ether derivatives of antisickling agent 5-HMF for the treatment of sickle cell disease. *Mol. Pharm.* **2017**, *14*, 3499-3511.

- [188] Koh, P.-F.; Loh, T.-P., Synthesis of biologically active natural products, aspergillides A and B, entirely from biomass derived platform chemicals. *Green Chem.* **2015**, *17*, 3746-3750.
- [189] Pezzetta, C.; Veiros, L. F.; Oble, J.; Poli, G., Murai reaction on furfural derivatives enabled by removable *N, N'*-Bidentate directing groups. *Chem. Eur. J.* **2017**, *23*, 8385-8389.
- [190] Zhou, X.; Rauchfuss, T. B., Production of hybrid diesel fuel precursors from carbohydrates and petrochemicals using formic acid as a reactive solvent. *ChemSusChem* **2013**, *6*, 383-388.
- [191] Hantzsch, A., Condensationsprodukte aus Aldehydammoniak und ketonartigen Verbindungen. *Ber. Dtsch. Chem. Ges.* **1881**, *14*, 1637-1638.
- [192] Loev, B.; Goodman, M. M.; Snader, K. M.; Tedeschi, R.; Macko, E., Hantzsch-type dihydropyridine hypotensive agents. *J. Med. Chem.* **1974**, *17*, 956-965.
- [193] Bossert, F.; Horstmann, H.; Meyer, H.; Vater, W., The influence of the ester function on the vasodilating activity of 1,4-dihydro-2,6-dimethyl-4-nitrophenyl-pyridine-3,5-dicarboxylates (author's transl). *Arzneimittel-forsch.* **1979**, *29*, 226-229.
- [194] Triggle, D. J., The 1,4-dihydropyridine nucleus: a pharmacophoric template part 1. Actions at ion channels. *Mini. Rev. Med. Chem.* **2003**, *3*, 215-223.
- [195] Bossert, F.; Vater, W., 1, 4 - Dihydropyridines-a basis for developing new drugs. *Med. Res. Rev.* **1989**, *9*, 291-324.
- [196] Carosati, E.; Ioan, P.; Micucci, M.; Broccatelli, F.; Cruciani, G.; Zhorov, B.; Chiarini, A.; Budriesi, R., 1,4-Dihydropyridine scaffold in medicinal chemistry, the story so far and perspectives (part 2): action in other targets and antitargets. *Curr. Med. Chem.* **2012**, *19*, 4306-4323.
- [197] Vijesh, A.; Isloor, A. M.; Peethambar, S.; Shivananda, K.; Arulmoli, T.; Isloor, N. A., Hantzsch reaction: synthesis and characterization of some new 1,4-dihydropyridine derivatives as potent antimicrobial and antioxidant agents. *Eur. J. Med. Chem.* **2011**, *46*, 5591-5597.

- [198] Praveenkumar, E.; Gurrapu, N.; Kolluri, P. K.; Yerragunta, V.; Kunduru, B. R.; Subhashini, N., Synthesis, anti-diabetic evaluation and molecular docking studies of 4-(1-aryl-1*H*-1,2,3-triazol-4-yl)-1,4-dihydropyridine derivatives as novel 11- β hydroxysteroid dehydrogenase-1 (11 β -HSD1) inhibitors. *Bioorg. Chem.* **2019**, *90*, 103056.
- [199] Liu, G.; Zhang, Q.; Li, Y.; Wang, X.; Wu, H.; Wei, Y.; Zeng, Y.; Tao, L., High-throughput preparation of antibacterial polymers from natural product derivatives via the Hantzsch reaction. *Iscience* **2020**, *23*.
- [200] Kumar, A.; Sharma, S.; Tripathi, V. D.; Maurya, R. A.; Srivastava, S. P.; Bhatia, G.; Tamrakar, A.; Srivastava, A. K., Design and synthesis of 2,4-disubstituted polyhydroquinolines as prospective antihyperglycemic and lipid modulating agents. *Bioorg. Med. Chem.* **2010**, *18*, 4138-4148.
- [201] Yousuf, H.; Shamim, S.; Khan, K. M.; Chigurupati, S.; Hameed, S.; Khan, M. N.; Taha, M.; Arfeen, M., Dihydropyridines as potential α -amylase and α -glucosidase inhibitors: synthesis, in vitro and in silico studies. *Bioorg. Chem.* **2020**, *96*, 103581.
- [202] Simon, C.; Constantieux, T.; Rodriguez, J., Utilisation of 1, 3-dicarbonyl derivatives in multicomponent reactions. *Eur. J. Org. Chem.* **2004**, *2004*, 4957-4980.
- [203] Saini, K. K.; Rani, R.; Khanna, N.; Mehta, B.; Kumar, R., An Overview of Recent Advances in Hantzsch's Multicomponent Synthesis of 1,4-Dihydropyridines: A Class of Prominent Calcium Channel Blockers. *Curr. Org. Chem.* **2023**, *27*, 119-129.
- [204] Wan, J.-P.; Liu, Y., Recent advances in new multicomponent synthesis of structurally diversified 1,4-dihydropyridines. *RSC Adv.* **2012**, *2*, 9763-9777.
- [205] Sohal, H. S., A review on recent trends in synthesis and applications of 1,4-dihydropyridines. *Mater. Today: Proceedings* **2022**, *48*, 1163-1170.
- [206] Alvim, H. G.; da Silva Júnior, E. N.; Neto, B. A., What do we know about multicomponent reactions? Mechanisms and trends for the Biginelli, Hantzsch, Mannich, Passerini and Ugi MCRs. *Rsc Adv.* **2014**, *4*, 54282-54299.
- [207] Saini, A.; Kumar, S.; Sandhu, J. S., Hantzsch reaction: Recent advances in Hantzsch 1,4-dihydropyridines. *J. Sci. Ind. Res.* **2008**, *67*, 95-111.

- [208] Pajuste, K.; Plotniece, A., Ionic liquids, metal oxide nanoparticles, and enzymes in synthesis of 1,4-dihydropyridines (microreview). *Chem. Heterocycl. Compd.* **2016**, *52*, 538-540.
- [209] Sonali Anantha, I. S.; Kerru, N.; Maddila, S.; Jonnalagadda, S. B., Recent progresses in the multicomponent synthesis of dihydropyridines by applying sustainable catalysts under green conditions. *Front. Chem.* **2021**, *9*, 800236.
- [210] Mathur, R.; Negi, K. S.; Shrivastava, R.; Nair, R., Recent developments in the nanomaterial-catalyzed green synthesis of structurally diverse 1,4-dihydropyridines. *RSC Adv.* **2021**, *11*, 1376-1393.
- [211] Calvino-Casilda, V.; Martín-Aranda, R. M., Ordered mesoporous molecular sieves as active catalysts for the synthesis of 1,4-dihydropyridine derivatives. *Catal. Today* **2020**, *354*, 44-50.
- [212] Undale, K.; Shaikh, T.; Gaikwad, D.; Pore, D., One-pot multi-component synthesis of polyhydroquinolines at ambient temperature. *C. R. Chim.* **2011**, *14*, 511-515.
- [213] Das, S.; Santra, S.; Roy, A.; Urinda, S.; Majee, A.; Hajra, A., One-pot multicomponent synthesis of polyhydroquinolines under catalyst and solvent-free conditions. *Green. Chem. Lett. Rev.* **2012**, *5*, 97-100.
- [214] Lu, L.; Xu, H.; Zhou, P.; Yu, F., Progress in Synthesis of 1,4-Dihydropyridines. *Chinese J. Org. Chem.* **2016**, *36*, 2858.
- [215] Tamaddon, F.; Ghazi, S., Urease: a highly biocompatible catalyst for switchable Biginelli reaction and synthesis of 1,4-dihydropyridines from the in situ formed ammonia. *Catal. Commun.* **2015**, *72*, 63-67.
- [216] Nguyen, H. T.; Truong, V. A.; Tran, P. H., Synthesis of polyhydroquinolines and propargylamines through one-pot multicomponent reactions using an acidic ionic liquid immobilized onto magnetic Fe₃O₄ as an efficient heterogeneous catalyst under solvent-free sonication. *RSC Adv.* **2020**, *10*, 25358-25363.
- [217] Nguyen, V. T.; Nguyen, H. T.; Tran, P. H., One-pot three-component synthesis of 1-amidoalkyl naphthols and polyhydroquinolines using a deep eutectic solvent: A green method and mechanistic insight. *New J. Chem.* **2021**, *45*, 2053-2059.

- [218] Huang, X.; Liu, S.; Liu, G.; Tao, Y.; Wang, C.; Zhang, Y.; Li, Z.; Wang, H.; Zhou, Z.; Shen, G., An Unprecedented 2-fold interpenetrated 1vt open framework built from Zn_6 ring seamed trivacant polyoxotungstates used for photocatalytic synthesis of pyridine derivatives. *Appl. Catal. B-Environ.* **2023**, *323*, 122134.
- [219] Bhat, N. S.; Kumari, M.; Naik C, P.; Mal, S. S.; Dutta, S., Synthesis of novel Biginelli and Hantzsch products from biorenewable furfurals using 1,4-diazabicyclo[2.2.2]octanium diacetate as a Brønsted acidic ionic liquid catalyst. *ChemistrySelect* **2023**, *8*, e202301782.
- [220] Zhu, S.; Tu, S.; Gao, Y.; Miao, C.; Li, T.; Zhang, X.; Fang, F.; Shi, D., Synthesis of Bis-1,4-Dihydropyridine Derivatives. *Synthetic Commun.* **2005**, *35*, 1011-1015.



FOLIO ADMINISTRATIF

THESE DE L'INSA LYON, MEMBRE DE L'UNIVERSITE DE LYON

NOM : JIANG

DATE de SOUTENANCE : 03 Avril 2024

Prénoms : Jingjing

TITRE : 5-Hydroxyméthylfurfural (HMF) en chimie fine: réactions multicomposantes vers les 1,5-benzodiazépines et les 1,4-dihydropyridines

NATURE : Doctorat

Numéro d'ordre : 2024ISAL0026

Ecole doctorale : ED de Chimie

Spécialité : Chimie

RESUME :

Parmi les molécules de la plateforme furannique renouvelable biosourcée, le 5-hydroxyméthylfurfural a retenu notre attention en raison de sa riche réactivité chimique et de sa facile disponibilité à partir des sucres. Dans cette thèse, je me suis concentrée sur l'utilisation de molécules de plateforme furaniques issues de la biomasse, en particulier le 5-HMF, pour construire des hétérocycles azotés, par le biais de réactions à plusieurs composants qui présentent une économie d'atome avantageuse.

Une première approche a été l'application d'une cycloaddition multicomposante [4+2+1] dans la construction des 1,5-benzodiazépines cycliques. Utilisant de nouvelles conditions réactionnelles, cette réaction économe en atome combine le 5-HMF (ou ses dérivés) avec des o-phénylènediamines et des alcynones en présence d'acétate d'ammonium. L'application de ce protocole à un large éventail de substrats a conduit à une bibliothèque de benzodiazépines diversement substituées qui sont désormais disponibles pour être intégrées dans la chimiothèque de l'ICBMS pour de futures évaluations biologiques et biochimiques.

La deuxième partie de cette thèse a concerné l'utilisation du 5-HMF dans la synthèse de dihydropyridine de Hantzsch. NH_4OAc à la fois comme source d'azote et comme promoteur doux. Tout d'abord, des 1,4-dihydropyridines symétriques ont été préparées par réaction de 5-HMF, de deux molécules de β -cétoesters/ β -dicétones et d'acétate d'ammonium dans des conditions sans solvant avec d'excellents rendements. Par la suite, nous avons étudié une version à quatre composants visant la formation sélective d'1,4-dihydropyridines dissymétriques, en remplaçant les 2 équivalents de β -cétoester par 1 équivalent de β -cétoester et un équivalent de 5,5-diméthyl-1,3-cyclohexanedione. Ce processus s'est révélé efficace soit sans solvant soit dans l'éthanol. Ainsi, l'application de cette réaction à divers substrats a conduit à une série de nouvelles 1,4-dihydropyridines symétriques ou dissymétriques comportant une entité furyl comme substituant qui seront intégrées dans des évaluations biologiques et biochimiques dans le cadre des projets développés par la chimiothèque de l'ICBMS.

MOTS-CLÉS : biomasse, 5-hydroxyméthylfurfural (5-HMF), réaction multi-composants (MCR), hétérocycle azoté, acétate d'ammonium, cycloaddition [4+2+1], 1,5-benzodiazépines réaction de Hantzsch dihydropyridine.

Laboratoire (s) de recherche : ICBMS

Directeur de thèse: Dr. QUENEAU Yves, Prof. POPOWYCZ Florence

Président de jury : Prof. BONNEVIOT Laurent

Composition du jury :

M. BONNEVIOT Laurent, Professeur des Universités, Ecole Normale Supérieure de Lyon, Président

Mme LUBIN-GERMAIN Nadège, Professeure des Universités, CY Cergy Paris Université, Rapporteure

Mme DE OLIVEIRA VIGIER Karine, Professeure des Universités, Université de Poitiers, Rapporteure

M. XAVIER Nuno Manuel, Assistant Professor, Université de Lisbonne, Examinateur

M. QUENEAU Yves, Directeur de Recherche au CNRS, Université de Lyon, Directeur de thèse

Mme POPOWYCZ Florence, Professeure des Universités, INSA-Lyon, Co-directrice de thèse